1-1-2004

Recycling thermosets : the use of high-pressure high-temperature sintering (HPHTS) and degraded material as means of producing new products.

Drew E. Williams
University of Massachusetts Amherst

RECYCLING THERMOSETS: THE USE OF HIGH-PRESSURE HIGH-TEMPERATURE SINTERING (HPHTS) AND DEGRADED MATERIAL AS MEANS OF PRODUCING NEW PRODUCTS

A Dissertation Presented

by

DREW E. WILLIAMS

Submitted to the Graduate School of the
University of Massachusetts Amherst in partial fulfillment
of the requirements for the degree of

DOCTOR OF PHILOSOPHY

September 2004

Polymer Science and Engineering

RECYCLING THERMOSETS: THE USE OF HIGH-PRESSURE HIGH-TEMPERATURE SINTERING (HPHTS) AND DEGRADED MATERIAL AS MEANS OF PRODUCING NEW PRODUCTS

A Dissertation Presented

by

DREW E. WILLIAMS

Approved as to style and content by:

Richard J. Farris, Chair

William J. MacKnight, Member

James A. Donovan, Member

Shaw Ling Hsu, Department Head
Polymer Science and Engineering

DEDICATION

To the loving memories of James Curtis Williams and Kelly Jean Doherty.

ACKNOWLEDGMENTS

I would like to thank my advisor Professor Richard J. Farris for his guidance and support during my tenure at the University of Massachusetts Amherst. I am also indebted to Professors William J. MacKnight and James A. Donovan for their efforts as committee members. Without these three individuals, I would not be where I am today.

I would like to extend a thank you to all of the members of the Farris Research Group (past and present) for their help and guidance along my journey through graduate school. A special thank you goes to Dr. Amiya Tripathy and Dr. Jeremy Morin for their collaborative efforts in the areas of High-Pressure High-Temperature Sintering (HPHTS) and Degraded/Devulcanized Rubber. I would like to thank the Environmental Protection Agency's Science to Achieve Results (STAR) Program for the funding they provided during my last year at the University of Massachusetts. In addition, I would like to acknowledge my appreciation of other funding agencies for their financial support of this project. These agencies include the Center for University of Massachusetts Industrial Research on Polymers (CUMIRP), the National Environmental Technology Institute (NETI), and the Chelsea Center for Recycling and Economic Development.

I would like to thank my parents and all of my friends for their encouragement and support during these past 5 years at the University of Massachusetts. Finally, I would like to say a special thank you to Jen for all of the love and support she has given to me in and out of school to help me make this thesis a reality.

ABSTRACT

RECYCLING THERMOSETS: THE USE OF HIGH-PRESSURE HIGH-TEMPERATURE SINTERING (HPHTS) AND DEGRADED MATERIAL AS MEANS OF PRODUCING NEW PRODUCTS

SEPTEMBER 2004

DREW E. WILLIAMS, B.A., COLGATE UNIVERSITY

M.S., UNIVERSITY OF MASSACHUSETTS AMHERST

Ph.D., UNIVERSITY OF MASSACHUSETTS AMHERST

Directed by: Professor Richard J. Farris

Thermosetting materials have long been considered impossible to reuse since they do not melt or dissolve. Few technologies have been developed to recycle waste thermosets compared to those available for the recycling of metals, glasses, and thermoplastics (meltable polymers). As rubbers are a sub-category of thermosetting materials, they also suffer from these limitations to recycling. Currently, scrap rubber tires and waste polyurethanes represent two of the largest recycling dilemmas facing our society. The work herein offers two potential solutions to this problem of recycling thermosets.

The first technique, High-Pressure High-Temperature Sintering (HPHTS), allows parts to be produced from 100% recycled material (current techniques typically use less than 10% recycled content). Several thermosetting systems were investigated in efforts to understand why certain thermosets are more recyclable via HPHTS than others. The goal of this work was to understand the mechanism of HPHTS and design and/or synthesize thermosets that are more easily recycled when they reach the waste stream. During this study, it was realized that Chemical Stress Relaxation (CSR)

techniques offered excellent insight into the HPHTS process. As such, a section of the thesis is focused on Chemical Stress Relaxation and its correlation with HPHTS. The last sections devoted to HPHTS involve the utilization of additives in the HPHTS process as a means of increasing mechanical properties and engineering the backbone of thermosets in efforts to enhance recyclability. These chapters target the end uses of these materials; their purpose being to increase properties so that the materials can be utilized for real world products.

The second technique, degradation/devulcanization of thermosets (specifically rubber), is carried out at high temperatures (>280°C) under a variety of conditions (in a melt press while under pressure, in a Parr-reactor, etc). The resulting viscous liquid-like material has numerous uses that include revulcanization, asphalt modification, and oil replacement in the compounding and molding of virgin rubber. Many of these uses not only increased the amount of rubber recycled, but also offered potential improvements over prior art. Materials incorporating over 35% recycled content were produced and maintained all of the original mechanical properties of the control (oil compounded) specimen.

TABLE OF CONTENTS

LIST OF TABLES

LIST OF FIGURES

CHAPTER 1

INTRODUCTION TO THERMOSET RECYCLING

1.1 Background

As the tonnage of polymers produced has reached historical proportions in recent years, the practice of recycling polymeric materials has become an important industry. For thermoplastic polymers such as polyethylene (PE) and polystyrene (PS) recycling of the polymer is a simple endeavor. Once the polymer has been taken above its crystal melting temperature (PE) or its glass transition temperature (PS), it flows readily and can be reformed into new products. The main challenge is acquiring the waste polymer, as it requires collection from the end user of products such as milk jugs and soda bottles, as well as sorting and cleaning the different types of polymers once they are obtained.

On the contrary, thermosetting materials face a different challenge. Collection of rubber and polyurethanes, for example, is simpler as they are often present in large quantities (tire piles, car seat foam, etc.) and are readily accessible. However, thermosetting materials have long been considered impossible to remold since they do not melt or dissolve. Few technologies have been developed to recycle waste thermosets (epoxies, polyurethanes, etc.) compared to those available for the recycling of metals, glasses, and thermoplastics. Since rubbers are a sub-category of thermosetting materials, they also suffer from these limitations to recycling. Scrap rubber tires and waste polyurethanes currently represent two of the largest recycling dilemmas for our society. The focus of this thesis is to explore two solutions to the problem of recycling waste thermosets. The first involves sintering thermoset powders at high pressures and

temperatures to produce new parts. The second involves degrading/devulcanizing the thermosets to viscous liquids, which can then be used in a variety of applications.

1.2 History

The first mention of thermosetting materials is found in scientific literature between 1843 and 1844 in patents by Charles Goodyear, Thomas Hancock, and Nathaniel Hayward wherein they describe the vulcanization of rubber.[1,2,3,4,5] Although the earliest claim of vulcanization is found in Hancock's 1843 patent (one month earlier than Goodyear's), Hancock in his 1856 autobiography credits the invention to Goodyear.[6] In particular, he tells a story of a friend, William Brockendon that brought him samples of American rubber that had been altered with sulfur and how they showed a remarkable improvement in mechanical properties over unmodified rubber. He also mentions that it was Brockendon that nicknamed the process "vulcanization" after the mythological Roman god (of fire and craftsmanship) named Vulcan.

The most important claim however is found in Goodyear's 1844 patent, where he states:[4]

- "No degree of heat, without blaze, can melt it {rubber}..."
- "It resists the most powerful chemical reagents: Aquafortis (nitric acid), sulfuric acid, essential and common oils, turpentine and other solvents..."

With these patents and much of the work that followed, Goodyear and others created one of the most useful materials of the modern era and helped to spawn the industrial revolution. Unfortunately, they also created one of the most difficult recycling problems ever encountered.

1.3 Motivation

Due to enormous demand and the inability for economic recycling, rubber (especially rubber tires) has become a significant waste problem during the last century. Studies estimate that approximately 300 million scrap tires exist currently in U.S. landfills, with over 281 million additional tires reaching the waste stream each year.[7] This equates to approximately 5.7 million tons of waste per year or an astonishing 360 pounds of rubber reaching the waste stream per second! Of these 281 million tires, about 115 million are burned for fuel, 96 million are incorporated into a variety of uses (civil engineering ~ 40 million, ground rubber ~ 33 million, exported ~ 15 million, etc.), with the remaining 60 million ending up in landfills.[7] Once in landfills, tires are enormous fire hazards, as well as breeding grounds for disease carrying pests such as mosquitoes and rodents.

Similarly, polyurethanes rival rubber tires in quantity of waste disposed. As of 1998, 5.8 billion pounds of polyurethanes were produced annually in the United States and Canada with this number expected to exceed 6 billion by 2004.[8] Of this only a small fraction is reused.

1.4 Prior Art

In the 160 years since Goodyear's patent, numerous ideas have been formulated to combat the problem of recycling thermosets, all with varying degrees of success. Interestingly, Goodyear recognized the need for rubber reuse methods, and in 1853 he patented a rubber recycling process.[9] He obtained ground rubber powder by shredding

scrap rubber and mixed the resulting powdered rubber with virgin uncrosslinked rubber prior to vulcanization. This process, termed regrind blending, is commonly used today.

In 1855, Charles Morey[10] patented a process he described as, "*Forming or molding scrapings, filings, dust, powder, or sheets of hard vulcanized India-rubber into a compact solid mass by means of a high degree of heat and pressure...*" This concept was revisited in 1981, when Accetta and Vergnaud[11,12] molded ground rubber (procured from car tires) at high temperatures and pressures while incorporating additional vulcanizing agents, such as sulfur. Phadke and De[13,14] vulcanized cryoground reclaimed rubber (CGR), and blended CGR with virgin rubber. Law et al.[15] described a proprietary method of molding polyurethane powders into films. James[16] employed compression molding at high temperatures to recycle urethanes, but the poor mechanical properties obtained were likely due to the excessively high temperature conditions used. Corbett and Wadie[17] discussed a similar technique to produce solid sheets from polyurethane foam as a mechanical testing technique, but failed to realize its potential application for recycling. Arastoopour et al.[18] have received a patent for "processing recycled rubber." The document, however, contains little mechanical data, and the majority of the patent is focused on rubber grinding. Adhikari et al.[19] offer an excellent review of the past and present techniques for rubber recycling, and list numerous references for further study. The previous references highlight works that complement and yield insight into the development of High-Pressure High-Temperature Sintering (HPHTS), the focus of this thesis.

Currently, thermosetting materials are recycled and/or reused in only a few low technology applications. Some specific applications of recycled thermosets include:[15,20,21]

- Oil spill absorbing media (rubber powder)
- Synthetic turf for athletic uses (rubber powder with a binder)
- Asphalt/concrete and virgin rubber goods additive (rubber powder as a filler)
- Retread industry (tire carcass reused)
- Artificial ocean reefs/highway crash barriers/erosion control (whole tires bundled together)
- Additive to car seat foams (polyurethane powders)
- Chemical recovery (polyurethanes, chemically decomposed to recover raw materials)
- Carpet underlay industry (polyurethane foams)

While these approaches to recycling thermosets make headway, there is still a large discrepancy between the supply of waste materials and viable uses. Despite the enormous amount of time and money devoted to recycling thermosets, no significant advancement has been made to reduce the amount of material reaching the waste stream.

1.5 Dissertation Overview

Figure 1.1 diagrams the different approaches formulated in efforts to close the recycling circle of thermosetting materials. Chapter 2 focuses on the High-Pressure High-Temperature Sintering (HPHTS) process as a means of using powderized waste

thermosets to create new products. The main advantage of this process is that it utilizes 100% recycled material, thus significantly increasing the usage of waste and scrap material. A discussion of the HPHTS results for natural rubber, styrene-butadiene rubber, polysulfide rubber and polyurethane, along with the benefits of the process and its limitations are detailed.

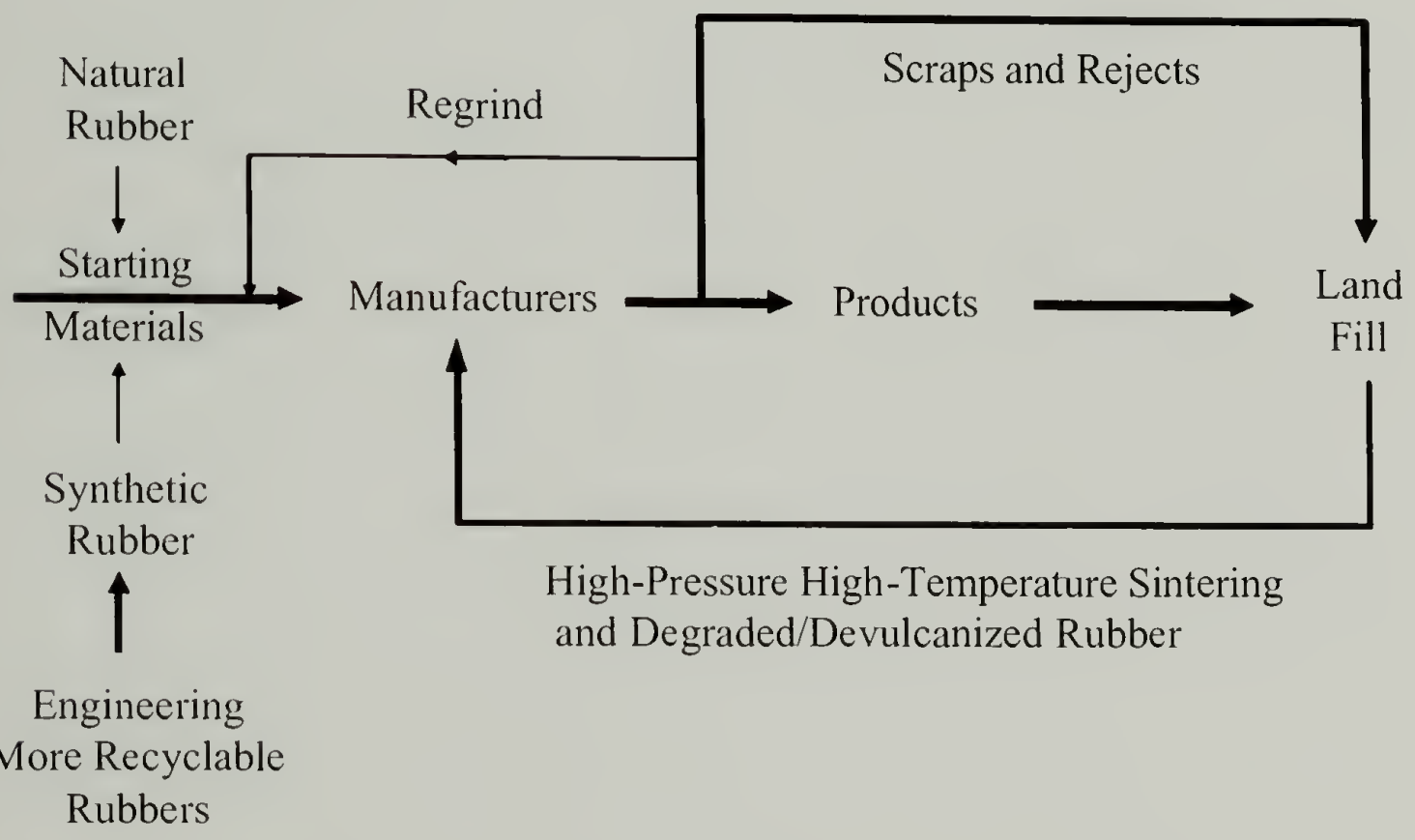

Figure 1.1. Methods for closing the recycling loop of thermosets.

Chapter 3 explores Chemical Stress Relaxation (CSR) as an investigative technique and how it can be used to understand the mechanism of the HPHTS process. Chapter 4 continues this work by correlating the CSR findings of Chapter 3 with the HPHTS results of Chapter 2 and includes the development of a model aimed at predicting optimum sintering conditions and mechanical property retention. Chapter 5 shifts the focus to the use of additives in the HPHTS process and how additives can improve

mechanical properties of sintered thermosets. Chapter 6 investigates the influence of rubber backbone on recyclability and includes HPHTS and CSR studies on several hybrid rubbers of styrene, isoprene and butadiene. Finally, Chapter 7 investigates the use of degraded/devulcanized material as a replacement for oil in typical rubber compounding.

CHAPTER 2

HIGH-PRESSURE HIGH TEMPERATURE SINTERING (HPHTS)

2.1 Background

Numerous ideas have been developed over the years in efforts to reduce the impact of thermoset waste on our environment. Unfortunately, there have been few techniques mentioned in the literature where new thermoset products are produced solely from waste materials. Ideally, a method accomplishing this task would have a large impact on the environment. As highlighted in Chapter 1 there is a large annual tonnage of thermosets ending up in the waste stream in the United States, and abroad. While much of this waste is recycled as filler or burned for fuel, these low technology alternatives to land filling cannot keep up with the waste demand. Furthermore, they add no value to the waste material. However, a method incorporating 100% waste thermoset would greatly increase the amount of recycled material used. Additionally, as the new products would be produced from 100% recycled material, the demand for raw materials necessary to produce new products would diminish, further preserving our natural resources.

High-Pressure High-Temperature Sintering (HPHTS) is a technique that takes 100% waste thermoset and produces new thermoset materials. To accomplish this, recycled thermosets are first ground (cryo or ambient conditions) into fine powders. The powders are then placed in a mold and subjected to high temperatures (> 200°C) and high pressures (>8 MPa). The extreme temperature incites chemical interchange reactions that allow the crosslinked network of the thermoset to rupture and reform in the new, molded

configuration. Pressure is required to force all of the particle interfaces into direct contact and thus alleviate void formation.[22]

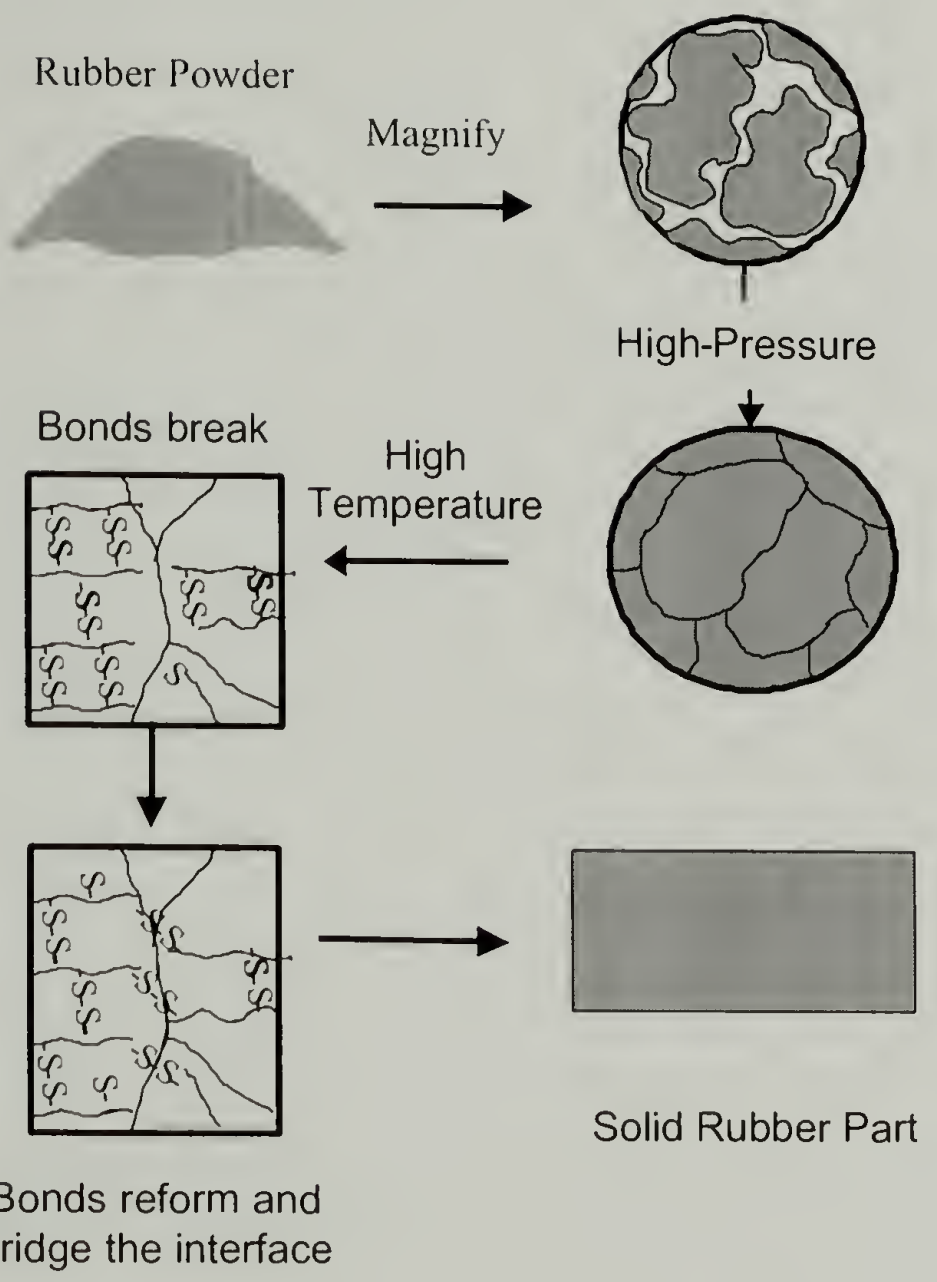

Figure 2.1. Schematic of the High-Pressure High-Temperature Sintering (HPHTS) process.

The mechanical properties of the parts produced correlate to the time, temperature and pressure of the molding stage, as well as the type of starting rubber used and the rubber particle size. Furthermore, the time between grinding and molding is important, as shorter times between processes yield better mechanical properties. Finally, the initial

mechanical properties dictate the recycled properties, as better starting materials retain higher recycled properties.

2.2 Experimental Techniques

2.2.1 Vulcanization of Rubbers

Optimum cure times of unvulcanized rubbers were determined by measuring the t-90 (time at 90% of maximum torque) with a Rheometrics rheometer at 160°C. Subsequent molding was carried out on a Carver model C press in a 100 x 100 x 2 mm^3 mold at 160°C for the predetermined t-90 times. Upon curing, samples were allowed to sit for 2 days before heat treatment, mechanical testing, or grinding and sintering occurred.

2.2.2 Thermoset Grinding

Powdered samples were obtained by grinding approximately 6 x 6 x 2 mm^3 pieces of vulcanized rubber or thermoset polyurethane in a Spex CertiPrep 6800 cryogenic grinder for 6 cycles of 5 minute grind and 4 minute cool, with a pre-cool time of 15 minutes. The cryogenic grinder uses a bath of liquid nitrogen in order to take the thermoset material (housed in polycarbonate tubes) below its glass transition temperature. During the grinding step, an oscillating magnetic field is applied over the tube causing a metal bar inside the tube to move back and forth between the two heavy metal end caps that enclose the thermoset. As the thermoset material is below its glass transition, it is extremely brittle, and subsequently fractures upon impact with the metal bar and the metal end caps. The resulting powder has been characterized (via mesh screens) to be

between 40 and 20 mesh in particle size (400-800 μm), with slight variations to larger and smaller sizes depending on the specific material being ground, the related glass transition temperature, and the times employed for grinding.

2.2.3 Sintering of Powders

High-Pressure High-Temperature Sintered (HPHTS) sheets of each thermoset powder were obtained by placing approximately 30 g of the powder in a 100 x 100 x 2 mm^3 mold for 1 hr, and 8.6 MPa pressure at the temperatures shown in the figures. Upon cooling to temperatures below 60°C, the pressure is released and the part is extracted from the mold. The purpose of this cooling was to allow dissolved gases to slowly diffuse out of the thermoset. This cooling prevents blistering of the material surface that occurred if pressure was released at elevated temperatures.

2.2.4 Heat-Treated Sheets

Heat treated sheets of the different thermosets were obtained by placing 100 x 100 mm^2 sections of the vulcanized sheets in a 100 x 100 x 2 mm^3 mold for 1 hr, at 8.6 MPa pressure at the temperatures depicted in the figures. Again, the parts are cooled to below 60°C before they are removed from the mold. The heat treated sheets were used to determine the changes in mechanical properties that ungrounded thermosets would experience when subjected to the severe temperatures required by HPHTS.

2.2.5 Mechanical Testing

Stress-strain curves were obtained on ring samples with average diameters of 22.2 mm, 2.5 mm in thickness and 2 mm in width, at room temperature, using an Instron 4468 at a test rate of 10 mm/min following ASTM D 412.

2.3 Molding Parameters

2.3.1 Pressure

Work by Morin[22,23] regarding the pressure influence on HPHTS noted that increasing the pressure of the sintering conditions from 2 to 8 MPa, while maintaining constant time and temperature, resulted in a slight increase in mechanical properties of the sintered part (roughly 5-10%). To date, no definite conclusions have been drawn for this occurrence, although higher pressure leading to less void formation might be one possibility. Morin also notes that this pressure is well above the pressure needed for intimate contact of the particles (~0.7 MPa[23]). For the studies herein, a pressure of 8.6 MPa was applied.

2.3.2 Time

Initial work carried out by Morin[22,23] shows that increasing the molding time in HPHTS, while maintaining a constant temperature and pressure, results in a logarithmic increase in mechanical properties. From these studies it has been garnered that above 1 hour of molding time at constant temperature and pressure, no advantageous increase in mechanical properties is obtained.

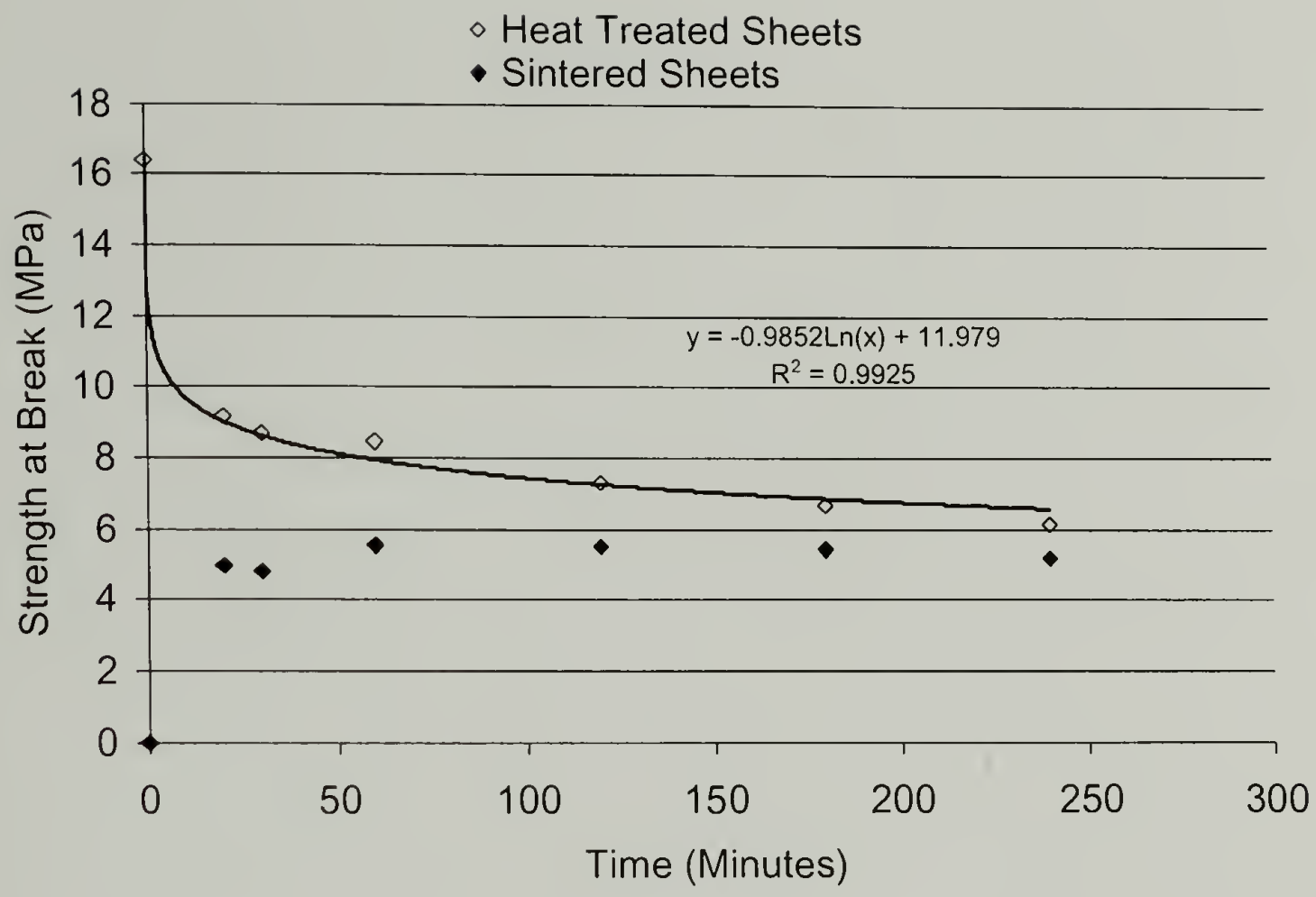

Figure 2.2. HPHTS results of strength at break vs. time for carbon black-filled NR sintered at 200°C and at 8.6 MPa.

Figure 2.2 and Figure 2.3 further substantiate the logarithmic dependence of strength and elongation at break, respectively, on time for carbon black-filled natural rubber (NR). Figure 2.4 illustrates the change in modulus with time, also for carbon black-filled NR. Figure 2.2 and Figure 2.3 reinforce Morin's conclusion that after 1 hour of molding time, no substantial improvement of mechanical properties occurs. Thus for all the following studies of HPHTS, 1 hour was chosen as the sintering time.

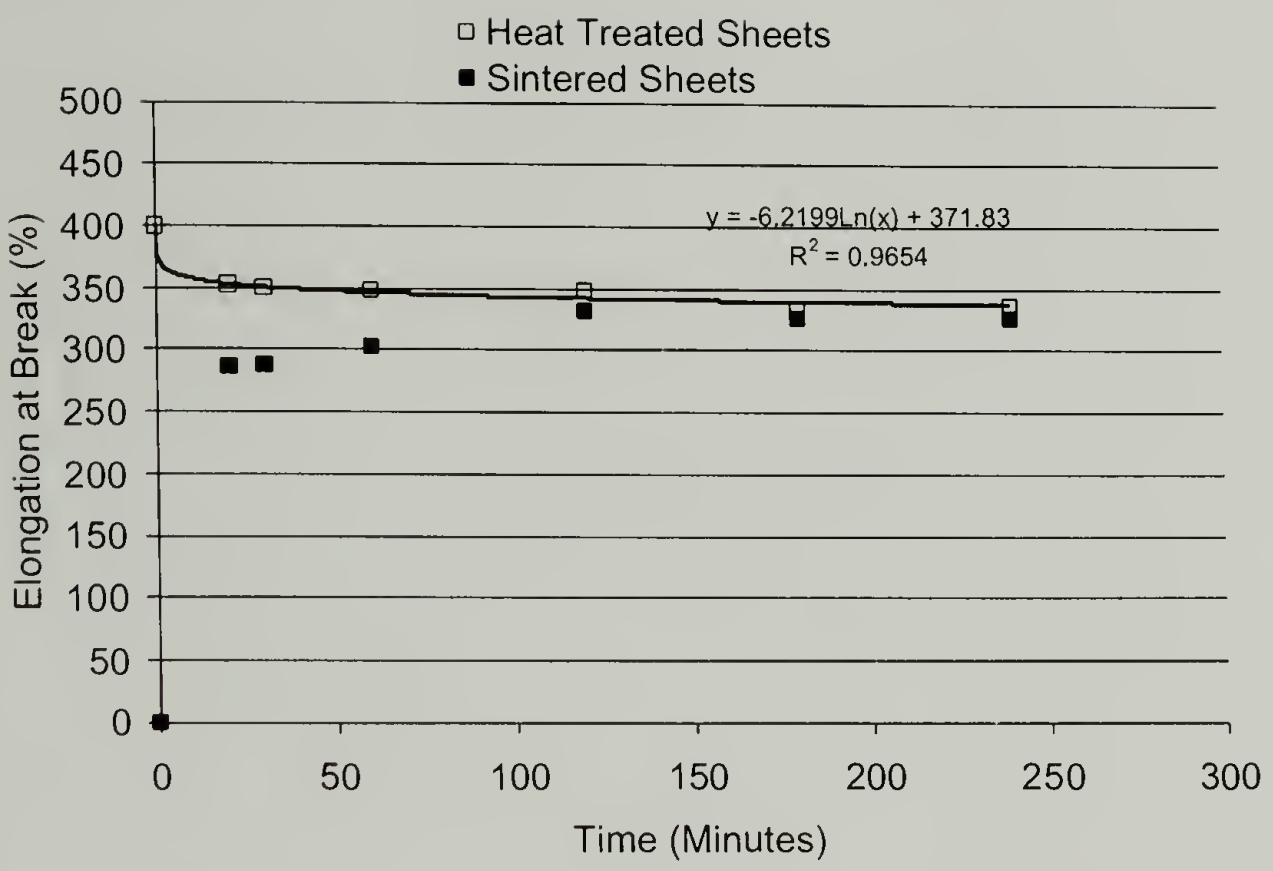

Figure 2.3. HPHTS results of elongation at break vs. time for carbon black-filled NR sintered at 200°C and at 8.6 MPa.

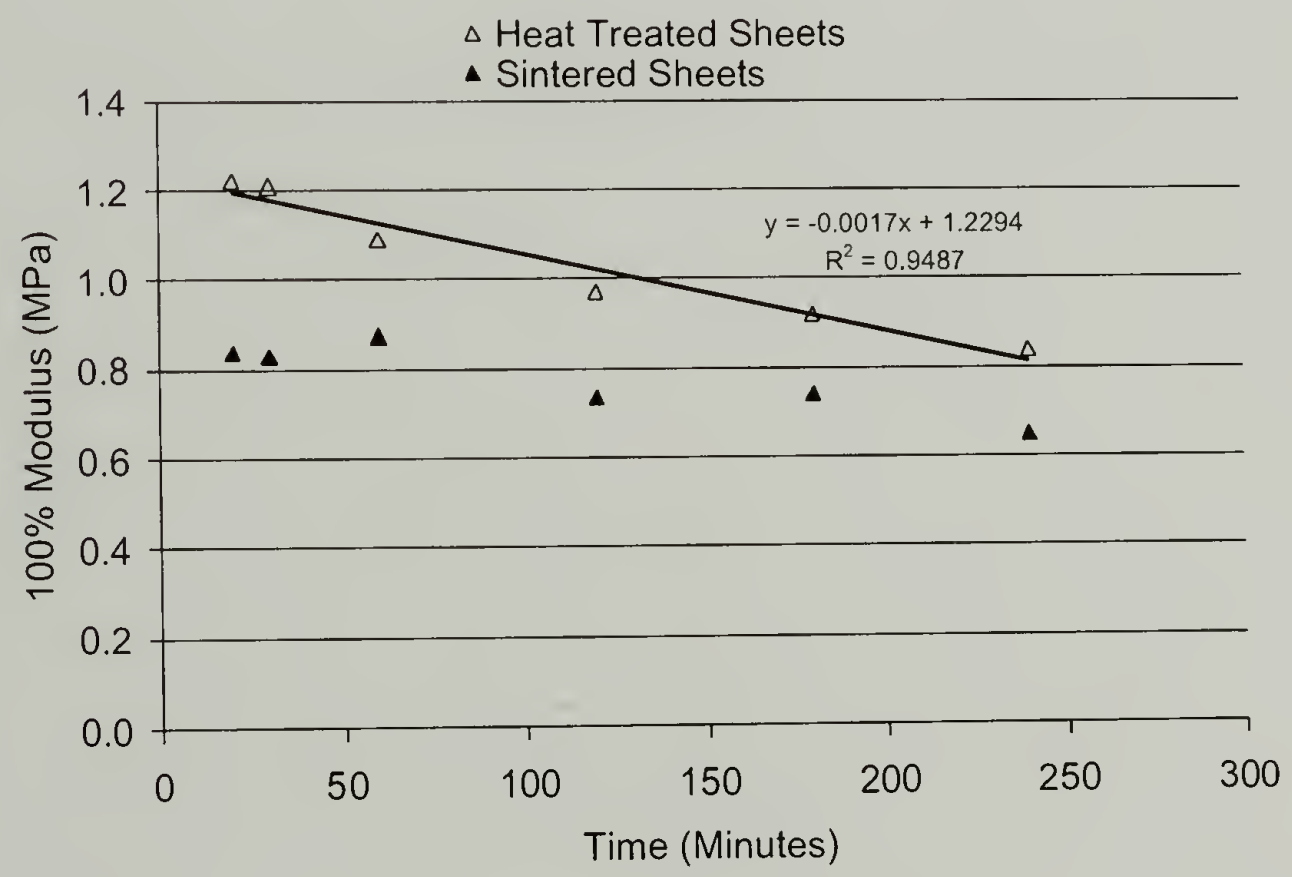

Figure 2.4. HPHTS results of 100% modulus vs. time for carbon black-filled NR sintered at 200°C and at 8.6 MPa.

2.3.3 Temperature

The most critical parameter to the HPHTS process and the one most readily controlled is temperature. Morin[23] noted an increasing linear correlation between molding temperature and the mechanical properties of sintered parts produced at constant time and pressure. Morin also noted a critical temperature above which the mechanical properties of the sintered parts no longer increased. For the present studies, temperature will be the key variable explored as the time and pressure variables will be held constant.

2.3.4 Powder Particle Size

Figure 2.5, Figure 2.6 and Figure 2.7 show the influence of particle size on strength at break, elongation at break, and 100% modulus, respectively, for sintered sheets of natural rubber. These results indicate that the smaller the particle size of the starting powder, the higher the mechanical properties obtained when the particles are sintered. Over a 2-3 MPa gain in strength is observed for the smaller starting particle sized material, along with an almost 50% gain in elongation at break. Interestingly, however, the moduli of materials made from the two different particle sizes are identical.

The observation that finer particles produce superior mechanical properties is consistent with all that is known about the influence of particle size on properties of composite materials and Farris et al.[24] note that similar observations are found in the sintering of metals. Kraus discusses how reinforcing rubber with smaller particles yields higher mechanical properties in comparison to a similar loading of larger particles.[25] The above results are also in agreement with literature data regarding the sintering of polyurethane powders and other adhesion research.[26,27]

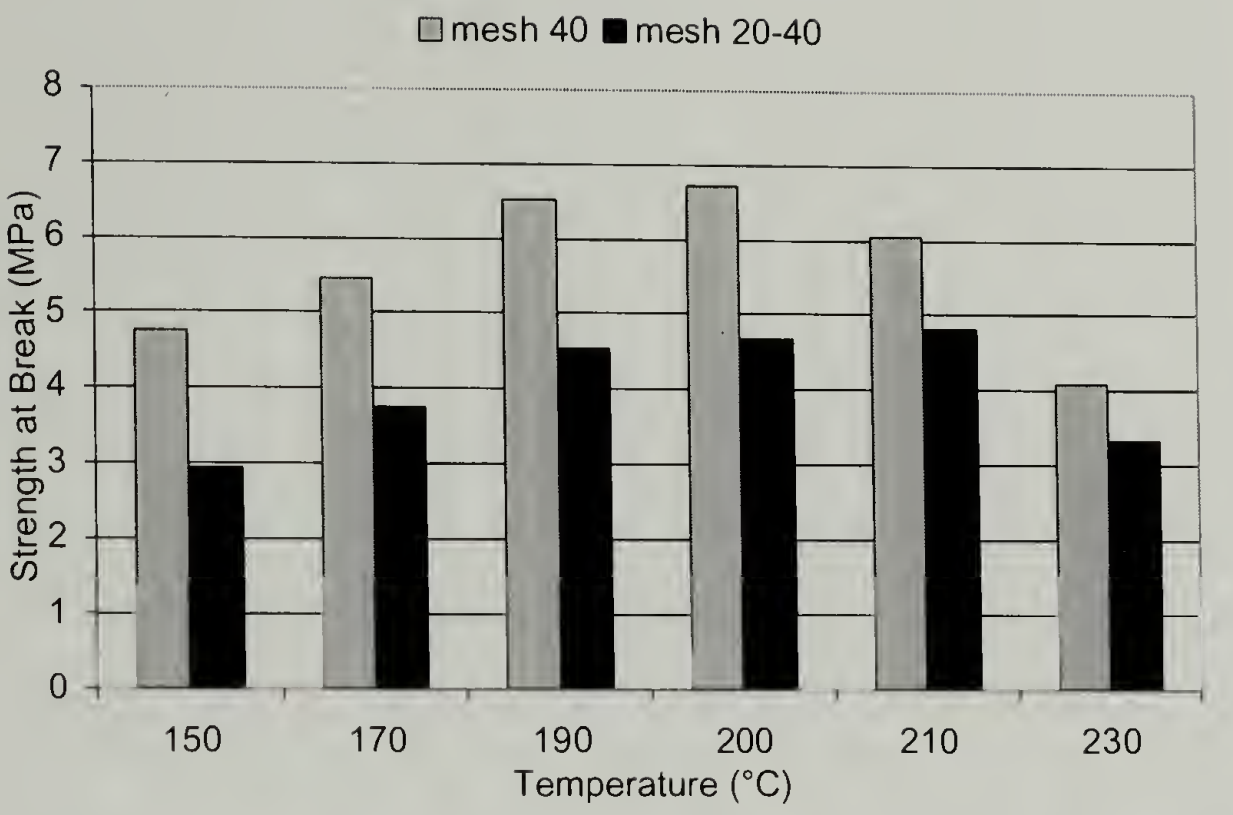

Figure 2.5. Influence of particle size on the strength at break of HPHTS sheets of carbon black-filled NR sintered at 200°C and at 8.6 MPa.

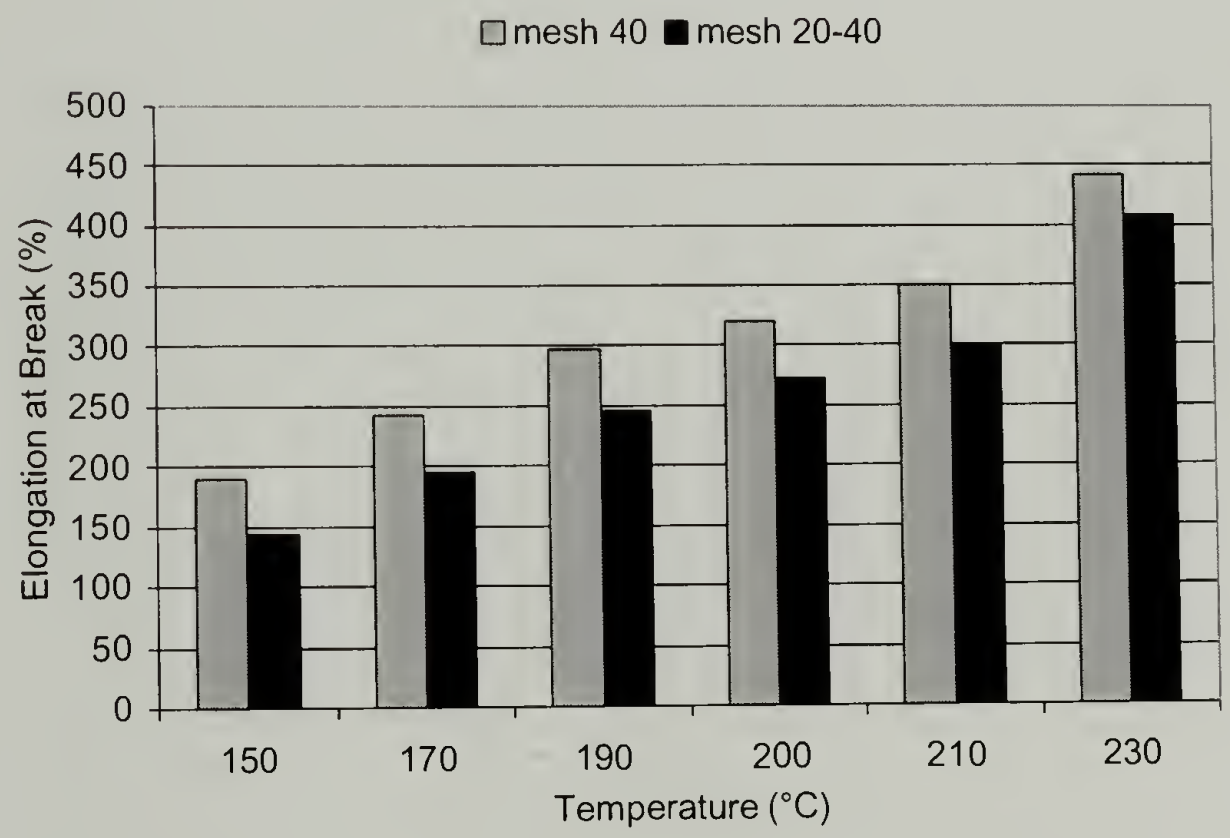

Figure 2.6. Influence of particle size on the elongation at break of HPHTS sheets of carbon black-filled NR sintered at 200°C and at 8.6 MPa.

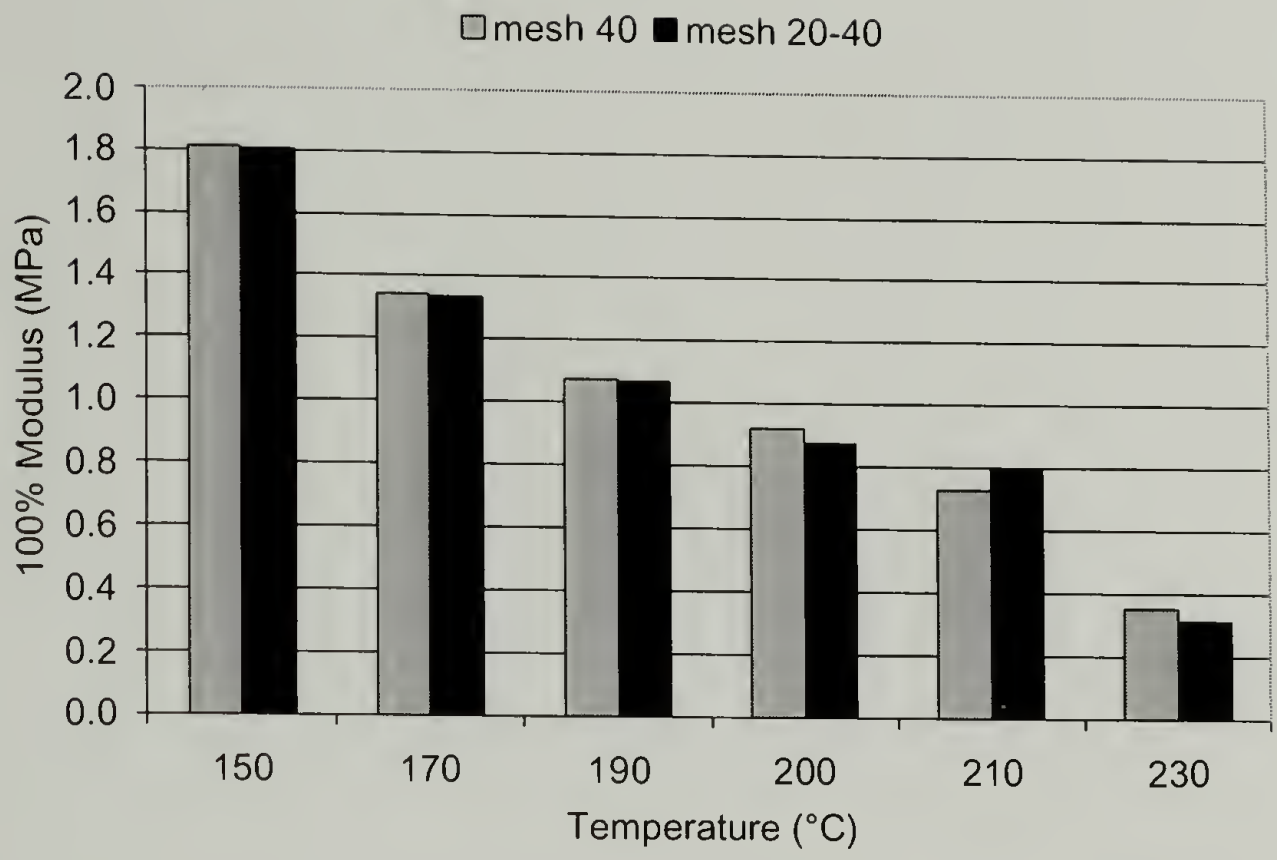

Figure 2.7. Influence of particle size on the 100% modulus of HPHTS sheets of carbon black-filled NR sintered at 200°C and at 8.6 MPa.

2.3.5 Time Between Grinding and Molding

During the initial investigations of HPHTS, it was noted that rubber powders molded under identical conditions from a batch of grounded rubber did not always display identical mechanical properties. Through further studies, it was realized that rubber that was ground to a powder and molded immediately yielded better mechanical properties than one with time between the grinding and molding steps. While the difference was not drastic (5-10% difference), it was significant enough to skew some initial conclusions. As such, for all of the studies herein, the time between grinding and molding was carefully controlled in efforts to eliminate discrepancies in the data. Specifically, powders to be sintered were ground approximately 2 days prior to HPHTS.

2.4 HPHTS of Natural Rubber

Figure 2.8 shows how heat-treating vulcanized sheets (i.e., exposing vulcanized sheets to the conditions used in sintering, in effect a form of accelerated aging) of NR between 140°C and 230°C causes a linear decay in the strength at break. Figure 2.9 illustrates the change in the elongation at break for NR for heat-treated sheets. In contrast, increasing the molding temperature during HPHTS of NR powder raises the resulting strength and elongation for temperatures up to 210°C as is shown in Figure 2.8 and Figure 2.9. However, beyond this point, no further increase is observed and HPHTS sheets molded at temperatures higher than 210°C appear to be mechanically identical to the heat-treated sheets of the same temperature range. Therefore, for this NR system, 210°C is the critical temperature as defined by Morin (the temperature at which the heat-treated sheets and sintered sheets begin to overlap).[23] The critical temperature is also the temperature above which the sintered sheets no longer display an increase in strength at break.

Figure 2.10 shows the 100 % modulus data versus temperature for the heat-treated and HPHTS sheets. Ahagon showed that the 100 % modulus is proportional to crosslink density, with higher modulus values indicating higher crosslink density and lower modulus values indicating lower crosslink density.[28] As one can see from the data in Figure 2.10, NR incurs crosslink breakdown (reversion) over the entire temperature range as its 100% modulus decreases with increasing temperature. This further verifies work by Morin and others, and concludes that having the isoprene repeat unit along the backbone causes crosslink breakdown (reversion) when the rubber is exposed to the high temperatures associated with HPHTS.[23]

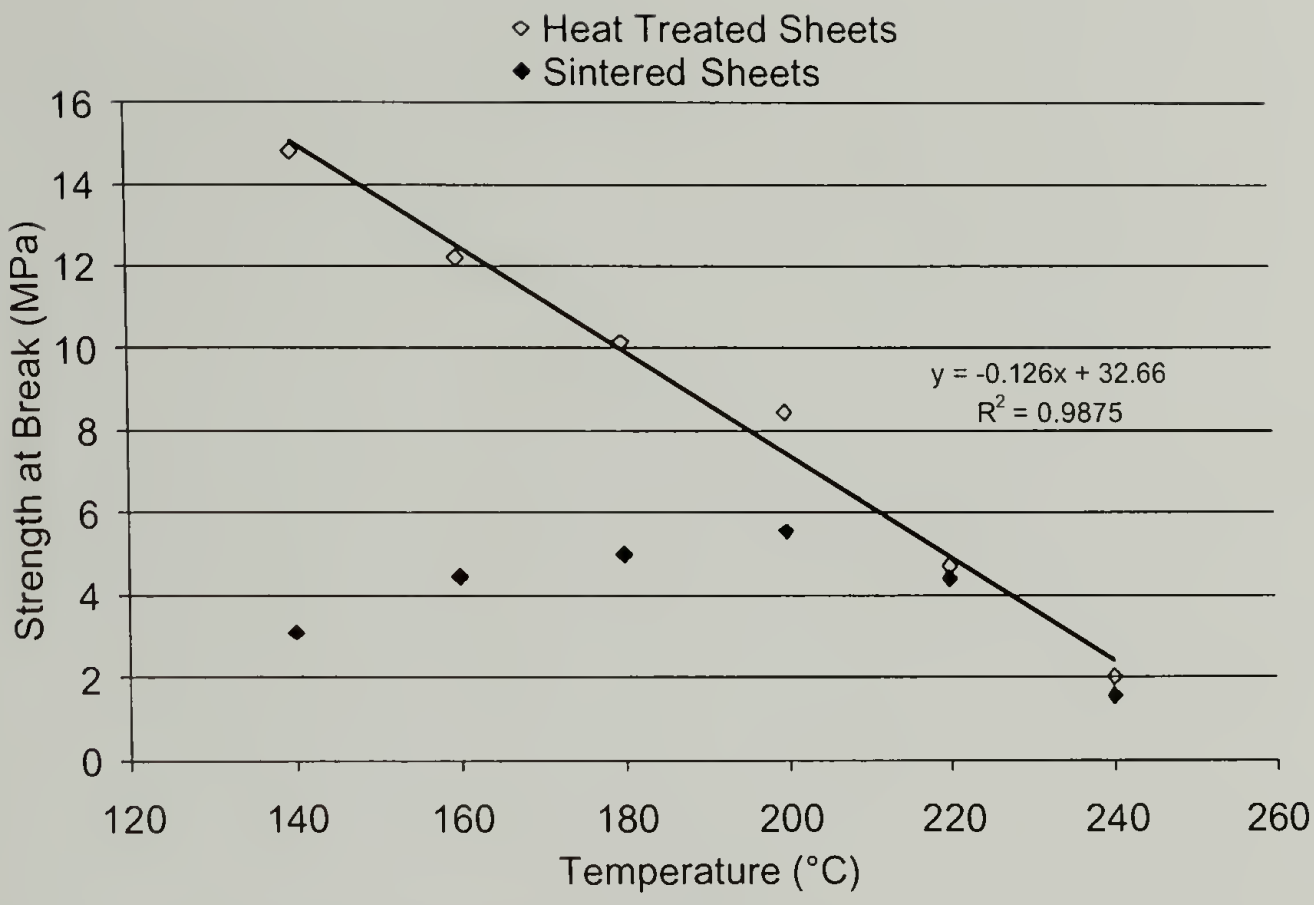

Figure 2.8. HPHTS results of strength at break vs. temperature for carbon black-filled NR sintered at 8.6 MPa for 1 hour.

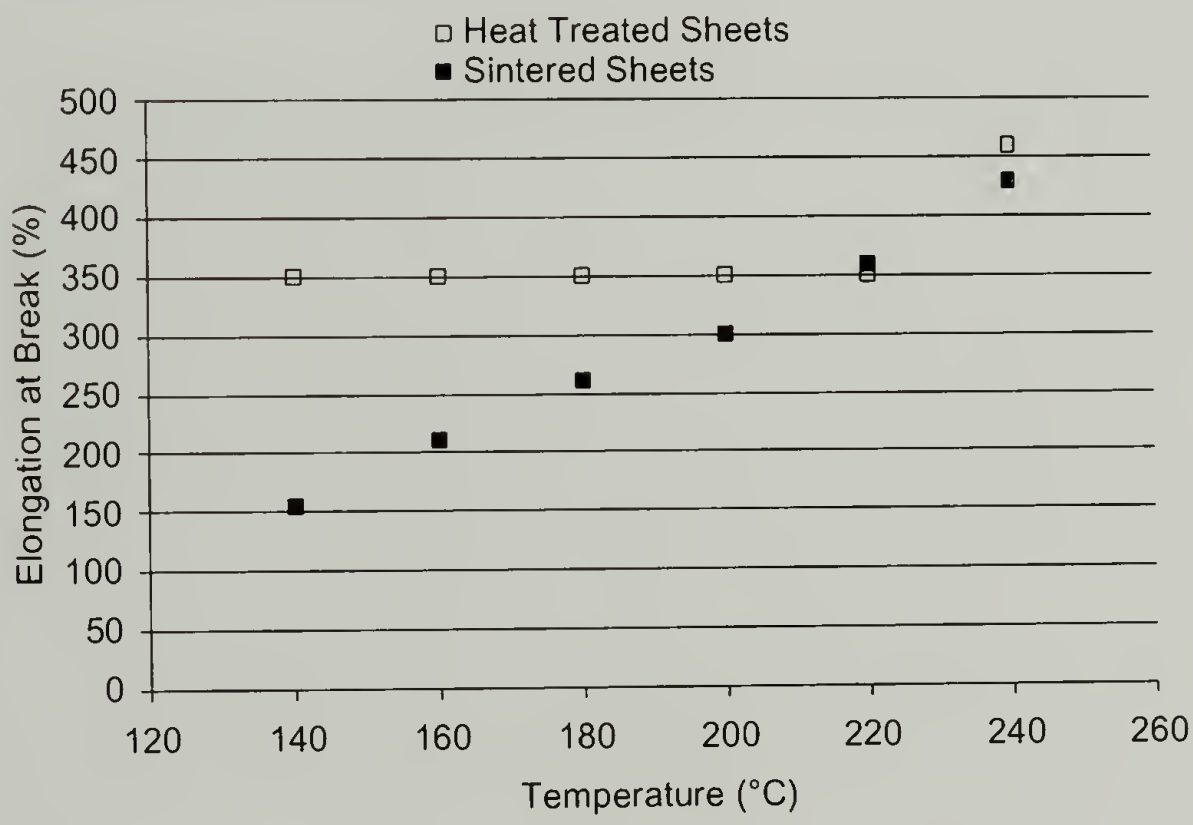

Figure 2.9. HPHTS results of elongation at break vs. temperature for carbon black-filled NR sintered at 8.6 MPa for 1 hour.

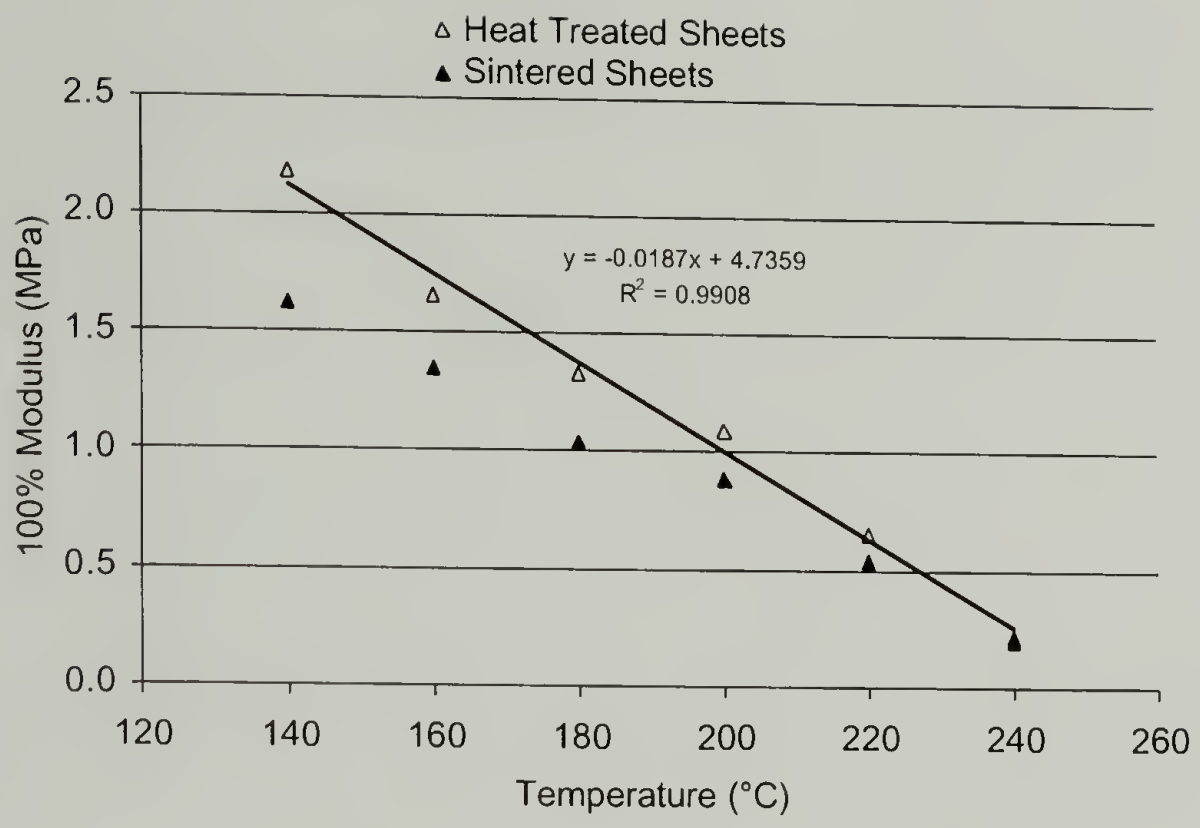

Figure 2.10. HPHTS results of 100% modulus vs. temperature for carbon black-filled NR sintered at 8.6 MPa for 1 hour.

2.5 HPHTS of Styrene-Butadiene Rubber

Figure 2.11 and Figure 2.12 show how heat-treating vulcanized sheets of sulfur-cured black-filled SBR at 8.6 MPa pressure and 1 hour between 160°C and 280°C causes a linear decay in the properties of strength and elongation at break, respectively. This is similar, but not identical to heat-treating sheets of NR. A difference is noted between Figure 2.9 and Figure 2.12 as the heat-treated sheets of NR show an increase in elongation at break with increasing temperature, while the heat-treated sheets of SBR show a diminishing elongation with increasing temperature. Figure 2.11 and Figure 2.12 illustrate that between 180°C and 250°C the mechanical properties of the sintered sheets of SBR show an upward trend, until no further increase above 250°C is observed and the eventual decay of mechanical properties above ~250°C occurs. Therefore, the critical

temperature for SBR is ~250°C, substantially higher than that observed with the NR system.

Figure 2.13 shows the 100 % modulus data for both the heat-treated and sintered sheets of SBR over the described temperature range. Figure 2.13 illustrates that above 220°C, the SBR system increases in crosslink density. This contrasts with the previous data from the NR system, where the 100% modulus data indicated that crosslink breakdown (reversion), was occurring. This fundamental difference in behavior underscores how SBR and NR react to the extreme temperatures of sintering differently, and the results are congruent to previous work in the over cure region.[29]

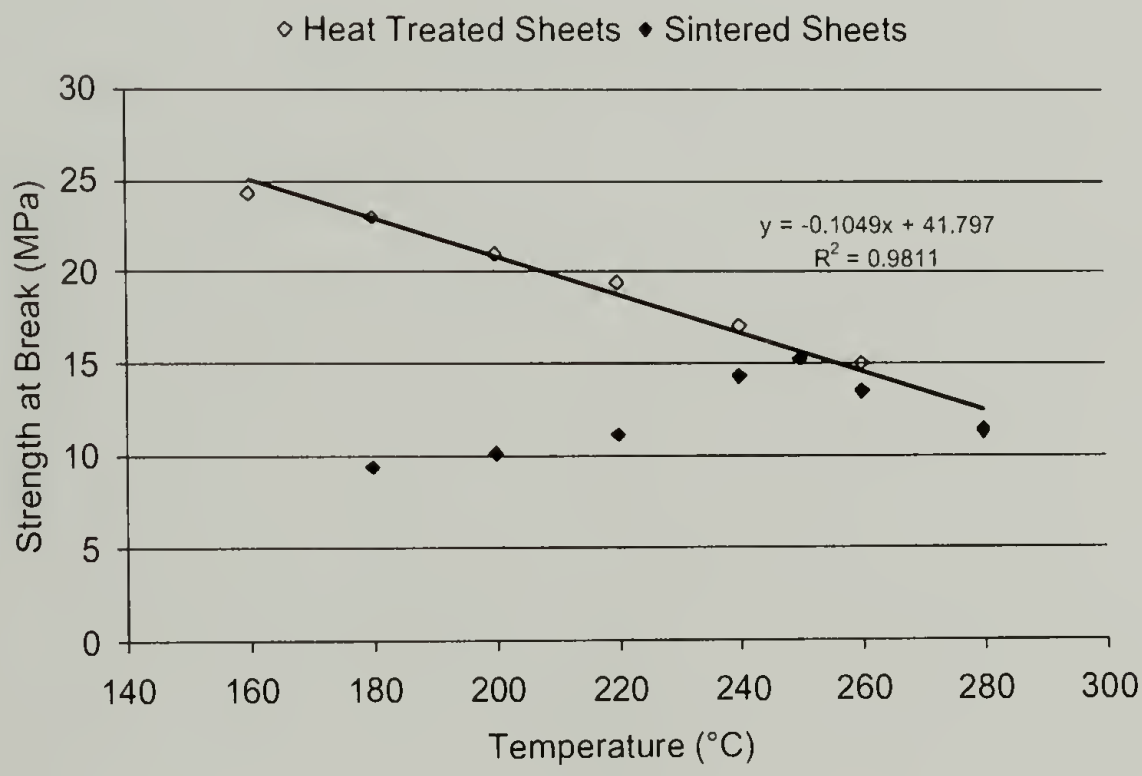

Figure 2.11. HPHTS results of strength at break vs. temperature for carbon black-filled SBR sintered at 8.6 MPa for 1 hour.

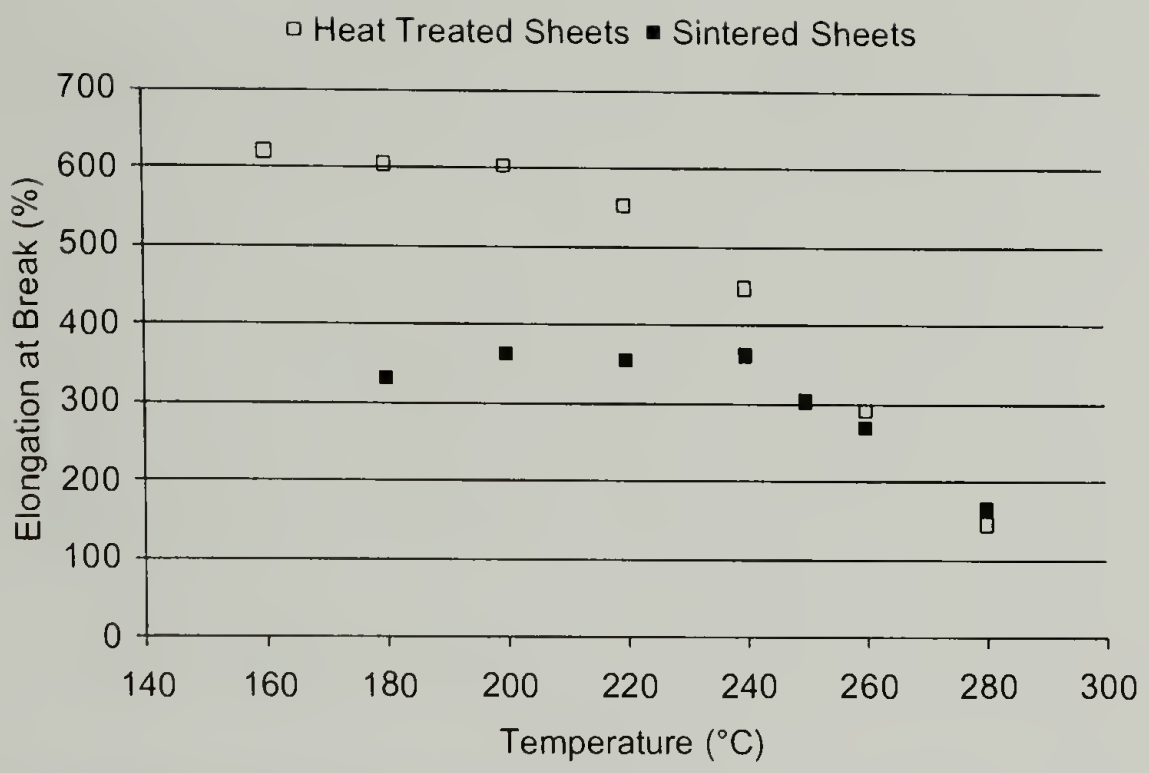

Figure 2.12. HPHTS results of elongation at break vs. temperature for carbon black-filled SBR sintered at 8.6 MPa for 1 hour.

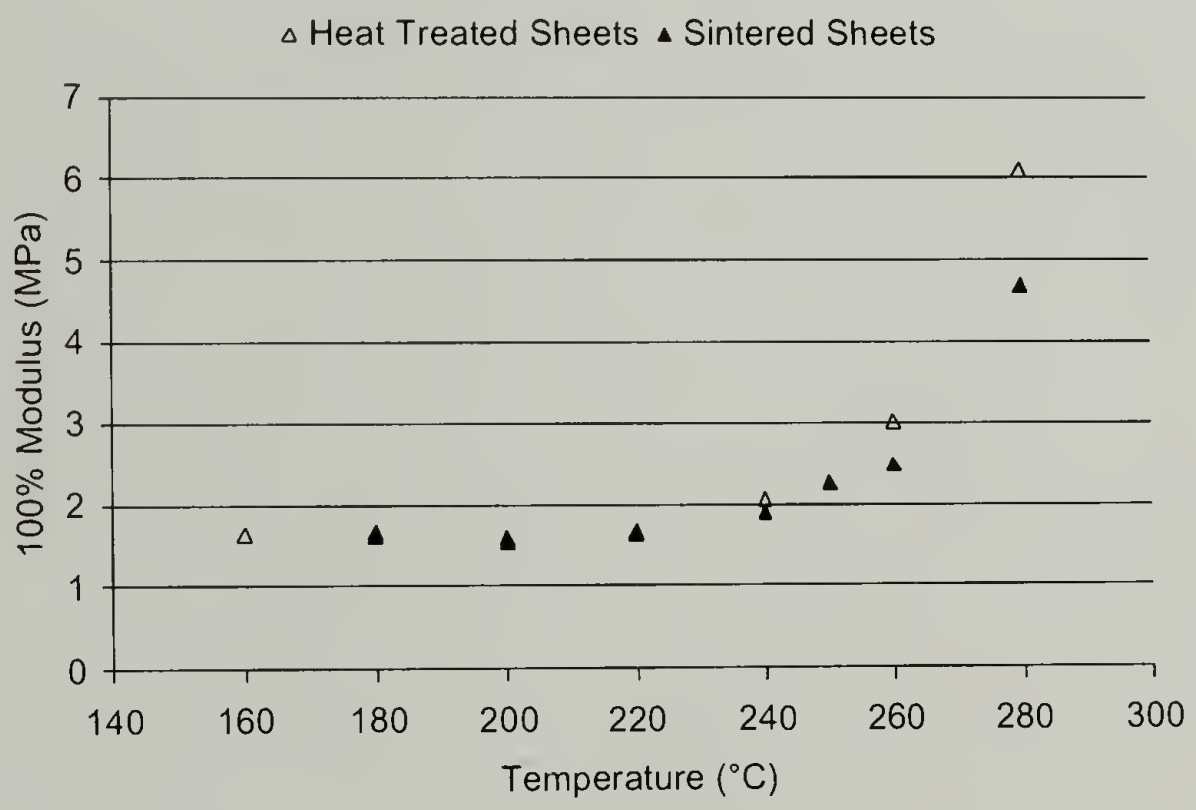

Figure 2.13. HPHTS results of 100% modulus vs. temperature for carbon black-filled SBR sintered at 8.6 MPa for 1 hour.

2.6 HPHTS of Polysulfide Rubber

Figure 2.14 and Figure 2.15 show the effect of temperature on the mechanical properties of strength and elongation at break, respectively, for heat-treated and sintered sheets of polysulfide rubber (TR). Heat-treated sheets of TR maintain their properties up to temperatures of about 140°C. Above this temperature TR begins to act like natural rubber, displaying decreasing mechanical properties. This loss in mechanical integrity (similar to NR) is further illustrated in the 100% modulus data shown in Figure 2.16. A slight loss in modulus is registered in the low temperature range, while a large loss in modulus (i.e. crosslink density) is not seen until above 160°C. Unlike NR and SBR however, sintered sheets of TR can retain 100% of their original mechanical properties during sintering. This results from the fact that the critical temperature of TR is below the temperature at which reversion (or with SBR, overcrosslinking) takes place.

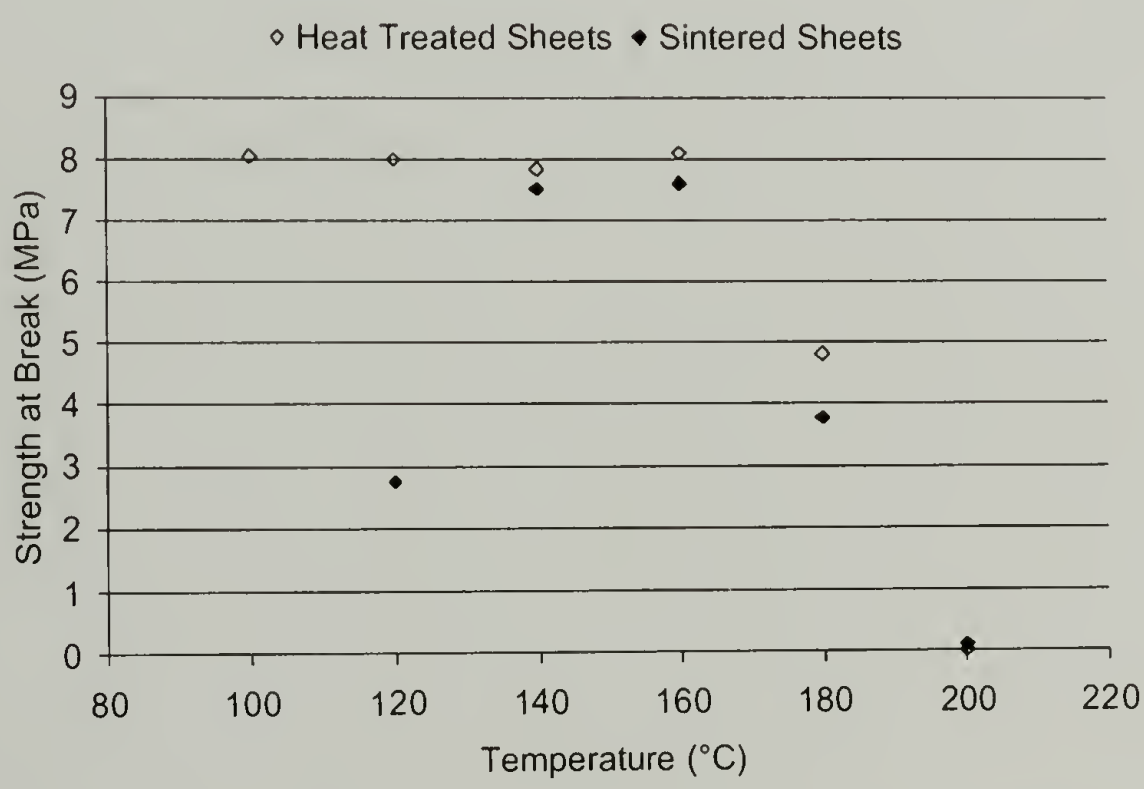

Figure 2.14. HPHTS results of strength at break vs. temperature for silica filled polysulfide rubber sintered at 8.6 MPa for 1 hour.

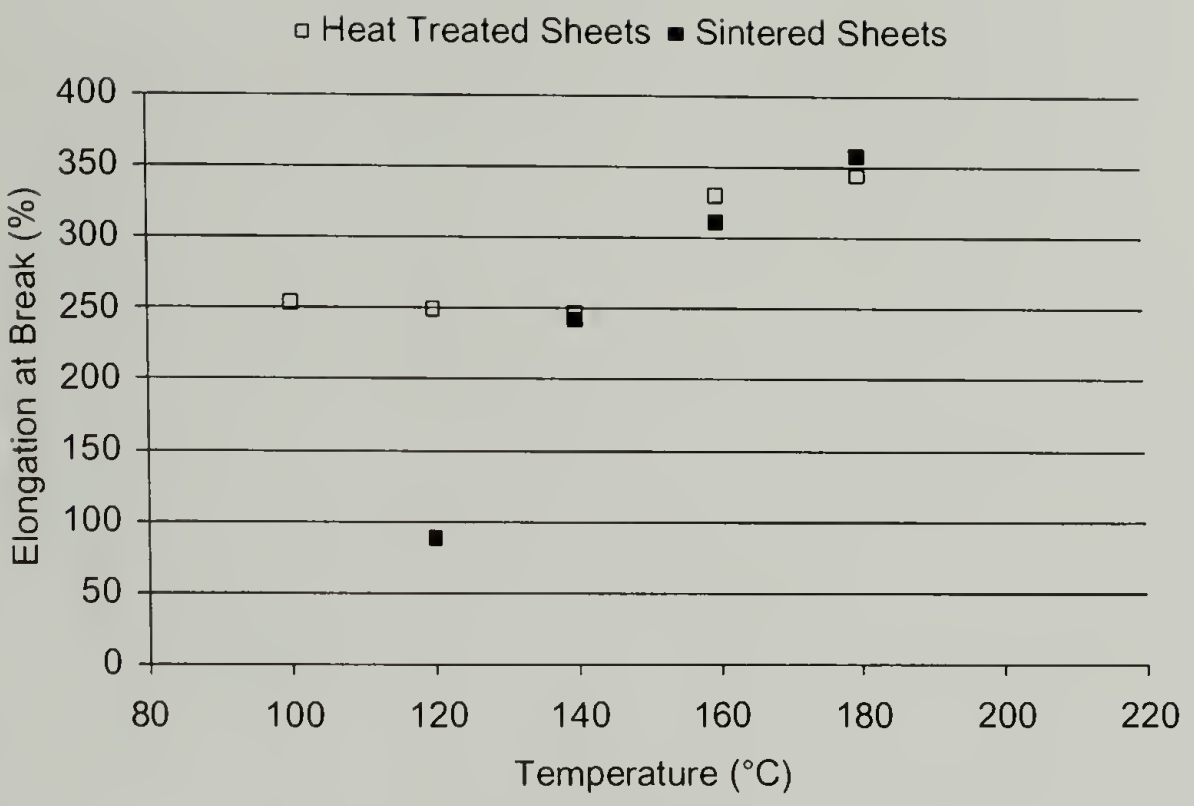

Figure 2.15. HPHTS results of elongation at break vs. temperature for silica filled polysulfide rubber sintered at 8.6 MPa for 1 hour.

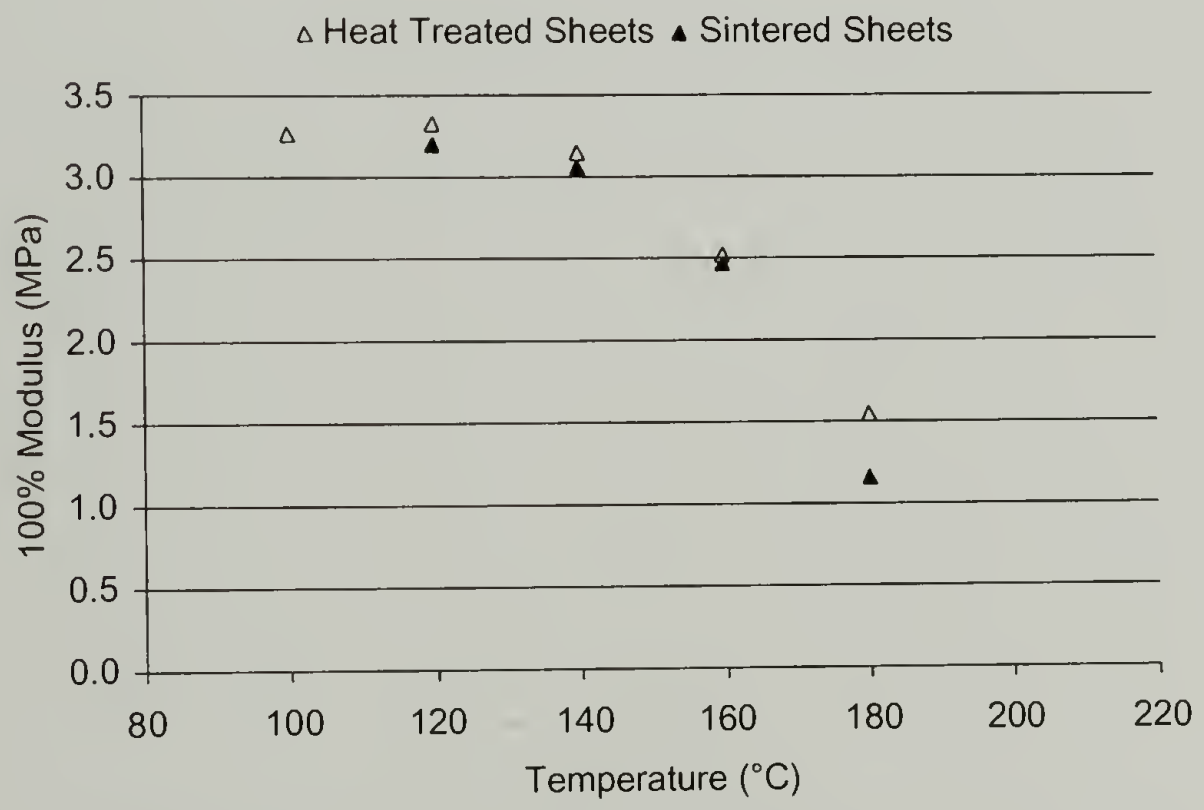

Figure 2.16. HPHTS results of 100% modulus vs. temperature for silica filled polysulfide rubber sintered at 8.6 MPa for 1 hour.

2.7 HPHTS of Polyurethane

Figure 2.17 shows the strength at break of sintered thermoset polyurethane tape. For these experiments, the starting material was not ground into a powder. Instead, the tape-like material was wrapped around itself and placed in the melt press for 1 hour and at 8.6 MPa for the temperatures described in Figure 2.17. With the polyurethane, the strength at break increases linearly up to ~ 160°C, after which a decrease in strength is noted. It appears that 160°C is the critical temperature for polyurethane, and this value is much closer to the critical temperature of the polysulfide than the critical temperatures of either the NR or SBR. This is to be expected as many of the bonds of the polyurethane are known to be weaker than those found in NR and SBR and are of similar strength as those found in polysulfides. While the elongation and 100% modulus data are not shown (the samples experienced grip slip, as they were tested in dogbone form, not ring form), the polyurethane appears to be undergoing reversion as the material, especially at the higher molding temperatures, was softer than the original in hardness tests. It is interesting to note that the strength of the sintered polyurethane was remarkably high (almost 30 MPa). Overall, this is the second time a polyurethane was successfully recycled by HPHTS, and the results appear consistent with the original results from Morin.[23]

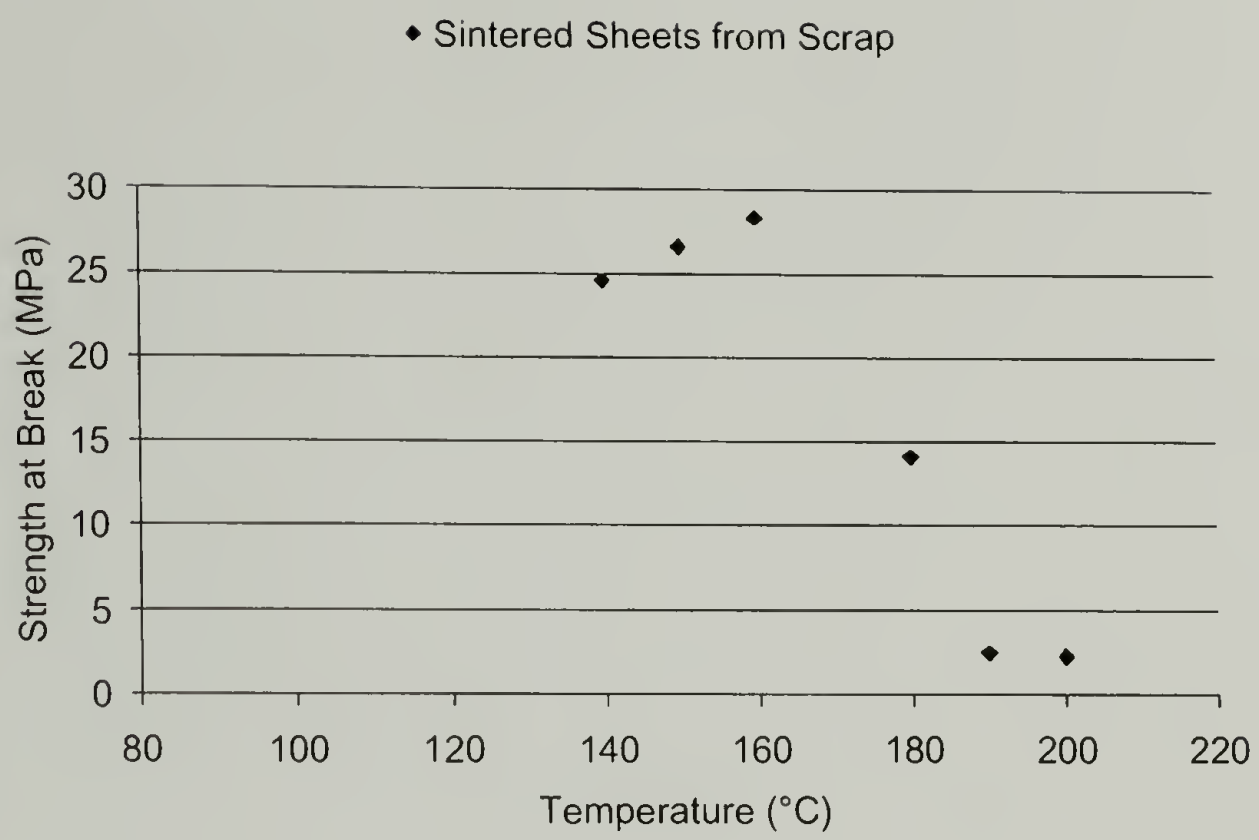

Figure 2.17. HPHTS results of strength at break vs. temperature for a thermoset polyurethane sintered at 8.6 MPa for 1 hour.

2.8 HPHTS Conclusions

The previous sections on HPHTS have given significant insight into how several thermoset systems behave differently during the sintering process. From this work, it appears that the amount of change that the crosslink density of the material undergoes during sintering determines how well the material will maintain its original mechanical properties. Specifically, thermosets that exhibit very little change in crosslink density during sintering near their critical temperature (polysulfide and polyurethane) retain the greatest percentage of original mechanical properties. Thermosets exhibiting an increase or decrease in crosslink density near their critical temperature show diminished mechanical properties when sintered.

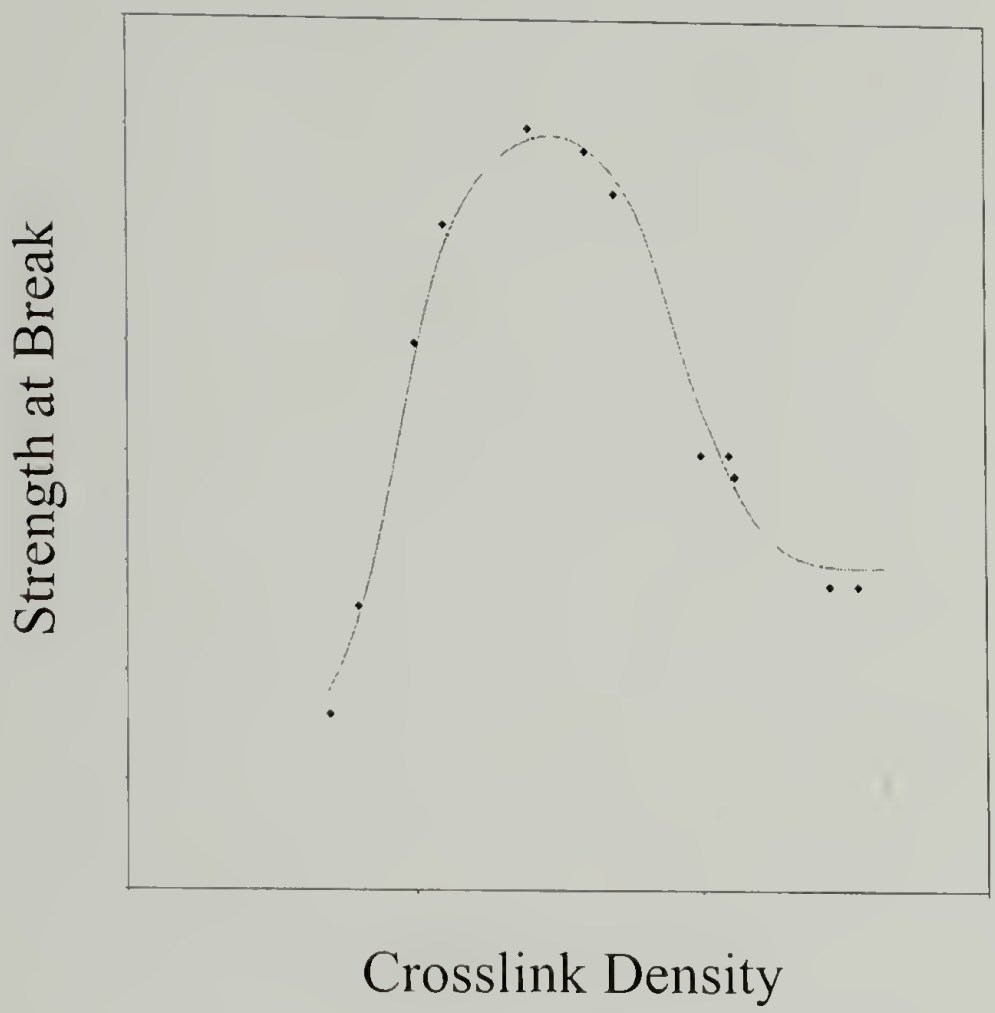

Figure 2.18. Strength at break vs. crosslink density of a typical rubber.[30]

The information gathered is very important and can be correlated to work conducted by A.N. Gent.[30] Gent formulated that a parabolic-like correlation of strength and crosslink density exists (see Figure 2.18). As most thermosets are formulated to yield the maximum obtainable strength when originally molded, any altering of the crosslink density during HPHTS would result in a decrease in mechanical properties. Since the modulus yields information about the crosslink density of the overall rubber network, the work presented previously illustrates that each system is undergoing a different change in crosslink density. The NR and SBR systems do not retain 100% of their original properties as they incur a decrease and an increase in crosslink density, respectively, and thus move away from the peak of the parabola. TR, however, is able to

retain its properties during sintering, as it is not subjected to a change in crosslink density. More details about these trends are found in Williams et al.[35]

Although no 100% modulus data was obtained for the HPHTS of polyurethane, a qualitative look at the produced parts indicated that parts sintered below 160°C incurred little change in hardness and thus likely retained a constant crosslink density. Parts sintered at temperatures above 160°C, however were much softer than the original material. Thus it appears that polyurethane exhibits behavior similar to that of TR as it maintains a constant crosslink density when sintered near its critical temperature.

In summary, studies of thermoset systems have shown that thermosets with good mechanical properties can be obtained from waste and scrap material. The retention of properties differs, however, for each type of thermoset. It appears that property retentions are dependent upon many different factors including molding conditions, particle size, and especially the chemical structure of the thermoset. The next few chapters further explore the differences between the various thermosets and the development of techniques to better understand the reasons for their behavior.

CHAPTER 3

CHEMICAL STRESS RELAXATION (CSR)

3.1 Background

To understand the mechanism of HPHTS we must take a closer look at what is taking place inside the mold. The high temperatures and pressures involved in the sintering process cause the breaking and reformation of chemical bonds. As can be envisioned, when bonds at the surface of a particle break and subsequently reform between two particles, the interface between the particles will begin to disappear. However, from earlier HPHTS studies it appears that the mechanism of bond breakage and reformation is different for each type of thermoset system, and thus no general mechanistic scheme can be drawn. However, some insight into how the different systems work has been achieved during these studies. For example, it is known that the overall crosslink density in sulfur cured natural rubber (sulfur-sulfur and carbon-sulfur bonds), as well as the chemical backbone (carbon-carbon bonds), breakdown at the temperatures employed in the sintering process. This breakdown is apparent from the decrease in the 100% modulus during sintering, and leads to a decrease in the maximum obtainable strength as predicted from Gent's data. In contrast, sulfur-cured SBR systems exhibit overcrosslinking that eventually results in lower mechanical property retention. The most important finding, however, is that the polysulfide rubber maintains a constant crosslink density during sintering while recovering 100% of its starting mechanical properties. This result has made polysulfide a focal point for determining the characteristics that an ideal rubber should have. Further insight into these different behaviors is available from chemical stress relaxation experiments. To this end, a discussion of the behavior of the

aforementioned rubbers (NR, SBR and TR) during chemical stress relaxation experiments is presented.

Chemical stress relaxation, or the relaxation of mechanical stress through chemical means, was discovered by Tobolsky in the 1940's in an investigation of crosslinked (vulcanized) rubbers.[31] Despite the fact that the rubbers were crosslinked and should have shown virtually no stress relaxation at elevated temperatures, Tobolsky discovered that above 100°C the rubbers exhibited a fairly rapid decay to zero stress when held at a constant strain. Tobolsky attributed this stress decay to chemical (bond) rupture of the network. Tobolsky further noted that during the chemical stress relaxation experiments some rubbers (NR and butyl) became progressively softer, while other rubbers (SBR) became harder even though the stress in all rubbers was diminishing. This led him to theorize that at elevated temperatures, two processes must be occurring: chemical bond scission and additional crosslinking.[31]

When a rubber is held at a constant length, the scission of the original chemical network leads to the stress relaxation (bonds holding stress break, thereby relieving the stress). Furthermore, additional crosslinking does not affect the stress of the sample held at constant length, unless there is sufficient crosslinking occurring such that a significant volume change occurs (this has not been found). In other words, the new network is formed in a relaxed state and therefore will not contribute to the measured stress value of the experiment. In order to separate the two reactions (chemical scission and additional crosslinking), Tobolsky developed two stress relaxation tests. He coined the terms "Continuous" and "Intermittent", respectively, for these two stress relaxation methods.[31]

3.1.1 Continuous Stress Relaxation

Continuous chemical stress relaxation provides information on the breakdown (or scission) of network crosslinks. In order to measure the impact of network scission (bond breakage), a material is deformed to a fixed elongation at a given temperature and the stress is measured as a function of time (see Figure 3.1 and Figure 3.2). At elevated temperatures, the network will undergo chain scission and subsequent recrosslinking. However, the new bonds will form in the relaxed state, thereby orienting in such a manner that they provide no new stress onto the system. As a result, the measured stress of the material will decay as a function of time as bonds capable of sustaining stress are broken. Continuous stress relaxation provides an excellent means for determining how efficiently the old network will be eradicated during sintering. The ideal material for HPHTS will have a fast decay time to zero stress as elimination of the old network is a necessary step for new network formation.

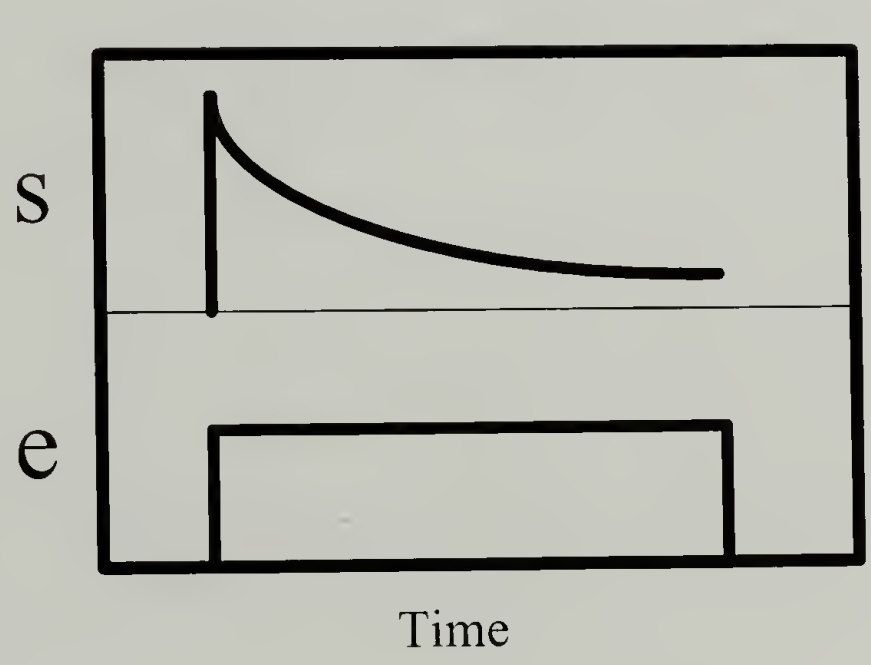

Figure 3.1. Stress (s) response for an imposed strain (?) in a continuous stress relaxation experiment.

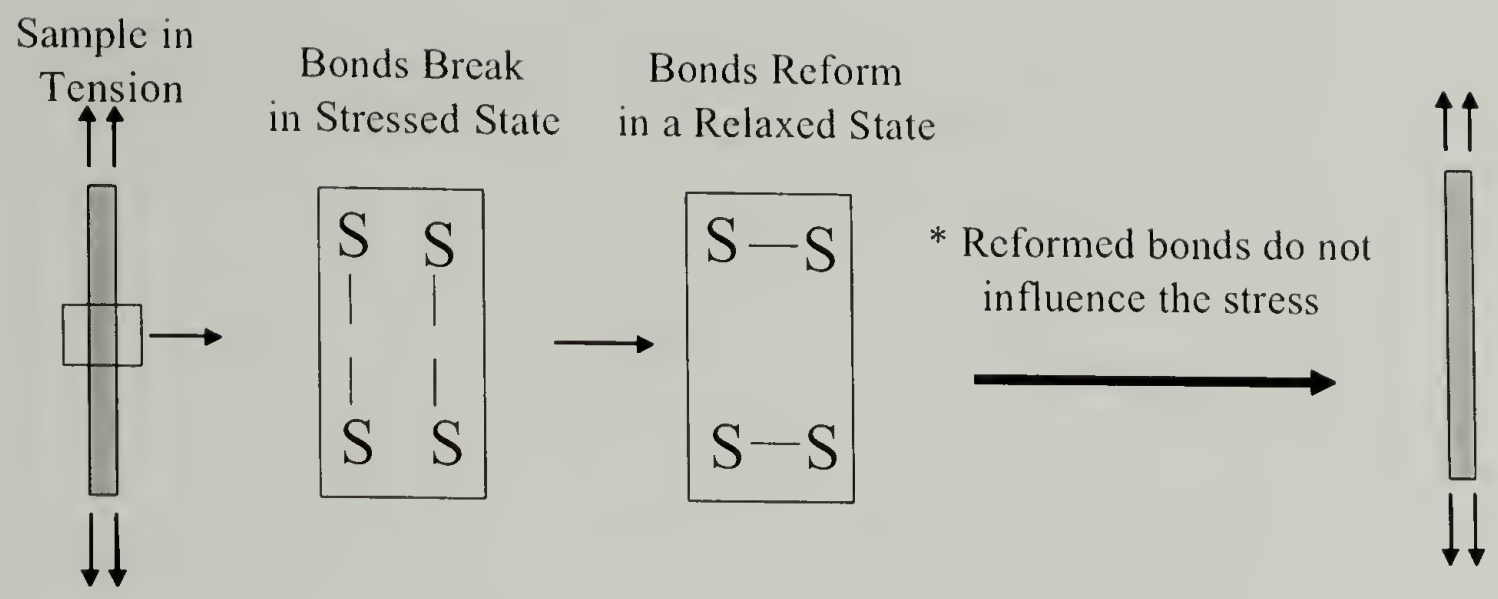

Figure 3.2. Influence of bond breakage in a continuous stress relaxation experiment.

To fully characterize a material, experiments are run at several different test temperatures (strain does not significantly influence CSR results[36] as the data is normalized by dividing the measured force at time t {f(t)} by the initial force {f(0)} to allow for comparison between different samples). As expected, with increasing testing temperature, materials exhibit faster continuous stress relaxation as the kinetics of the bond breaking reactions are increased. Furthermore, Tobolsky[31] notes the presence of a time-temperature superposition for the experiments. This finding will be exploited later to create "master" curves of superimposed data that will help predict HPHTS results from CSR data.

3.1.2 Intermittent Stress Relaxation

Intermittent stress relaxation provides information on the formation of new bonds within the network during sintering. During intermittent stress relaxation experiments, a material is kept in a relaxed state at a set temperature (see Figure 3.3 and Figure 3.4). At various timed intervals, the material is stretched rapidly (or compressed/sheared) to a

fixed elongation and the stress at equilibrium is measured. The material is then returned to its original relaxed state. As almost all network breakdown and subsequent recrosslinking processes occur while the material is in the relaxed state, this method provides a measurement of the total crosslink density, a result of both the scission of network bonds and formation of new bonds via crosslink reactions. In essence, intermittent stress relaxation experiments are providing instantaneous measurements of the modulus of the network (again the data f(t) is normalized by the initial force f(0), thus a value of one is indicative of no change in crosslink density). Ahagon notes that the modulus of a network directly correlates to the crosslink density.[32] Therefore, intermittent stress relaxation is a measure of how a material's crosslink density will change during sintering.

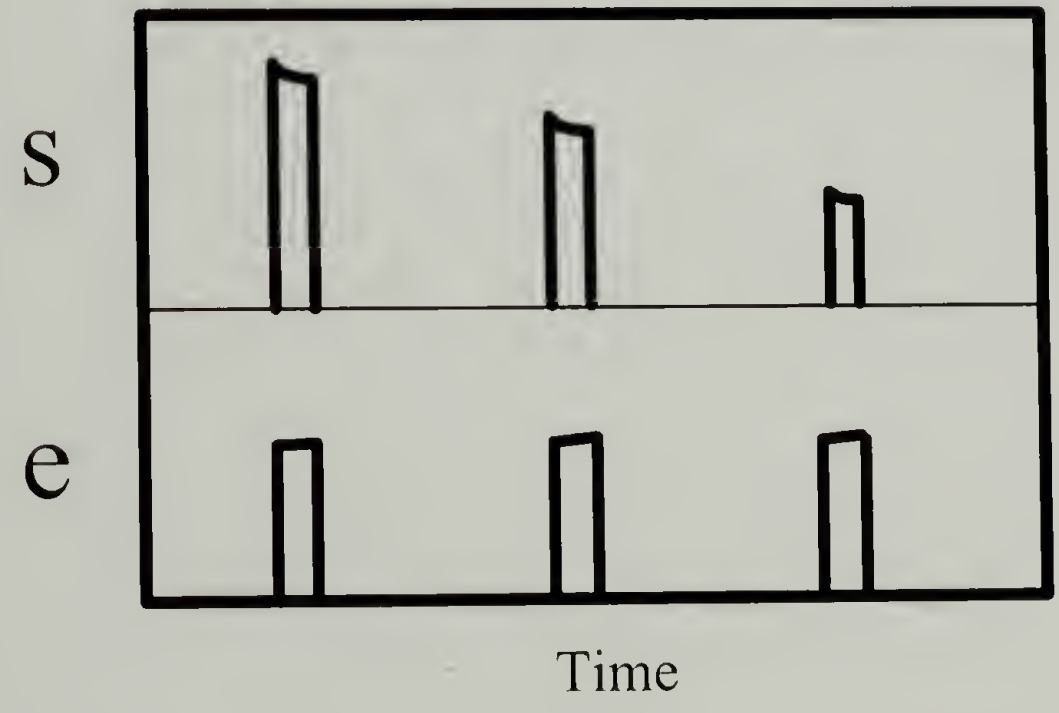

Figure 3.3. Stress (s) response to imposed strain (?) for an intermittent stress relaxation experiment.

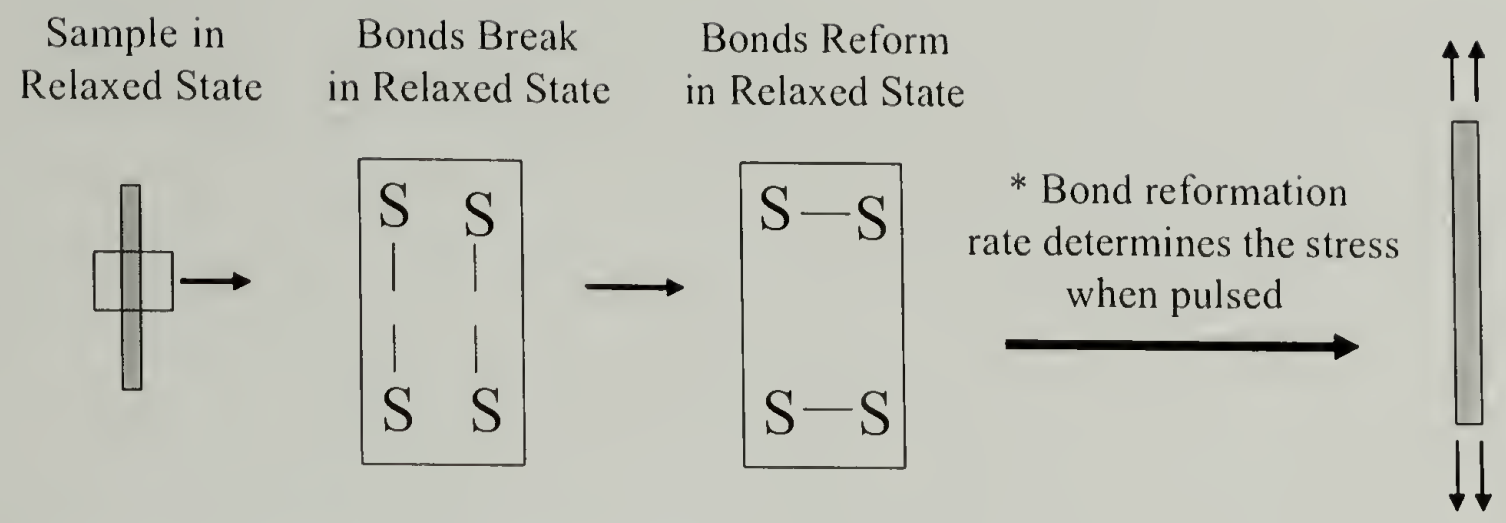

Figure 3.4. Influence of bond breakage in an intermittent stress relaxation experiment.

As illustrated by Gent's work, understanding changes in the network's crosslink density is essential for ensuring good mechanical property retention when employing HPHTS. Therefore, evaluating thermosets via intermittent stress relaxation experiments appears to be an excellent method for understanding how well they will perform after sintering.

3.2 Experimental Techniques

3.2.1 Rheometer – Stress Relaxation Experiments

Stress relaxation experiments were conducted on 25.4 mm diameter and 3 mm thick samples. The experiments were performed on a Rheometrics rheometer and both continuous and intermittent stress relaxation experiments were attempted individually and simultaneously. The Rheometrics rheometer allowed for controlled temperature conditions up to 300°C and thus covered the entire range of sintering conditions currently used.

Decker et al.[33] have shown oscillating disk rheometers to be useful devices for vulcanization studies and it was believed that this technique would be valid for stress

relaxation measurements. S.A. Eller[34] and Armah et al.[35] discussed stress relaxation under compression and concluded it to be a valid technique. All previous work suggests a rheometers stress relaxation experiment to be a valid testing technique despite no prior attempts in the literature to do so.

Unfortunately, problems arose in utilizing the Rheometrics rheometer for chemical stress relaxation studies. The main problem was the slippage of the thermoset from the parallel plates caused by a relaxation of the normal force initially applied by the plates on the thermoset. As other methods became available, this technique was not further pursued, although it is likely that the slippage problem might be overcome by affixing the rubber directly to the plates.

3.2.2 Instron – Stress Relaxation in Tension

An Instron 5564 instrument was used to conduct stress relaxation experiments under tension. Unfortunately, the oven apparatus available could only reach a temperature of 120°C without modification. These limitations inhibited meaningful data from being obtained, as the region of interest for comparison to sintering is around 200°C. As such, very few attempts of CSR data collection were made via this technique.

3.2.3 Instron – Stress Relaxation in Compression

An Instron 5564 instrument was utilized in order to perform stress relaxation experiments under compression. As diagrammed in Figure 3.5, a heating platen, similar to those used for sintering, was placed at the bottom of the load frame. A compression attachment was fitted to the load cell and moveable part of the frame. The platen was

allowed to reach temperature, and the thermoset material (25.4 mm diameter and 12 mm thick) was subsequently placed between the platen and the compression plate. Continuous relaxation experiments were conducted by compressing the rubber to a fixed negative elongation and recording the diminishing stress value.

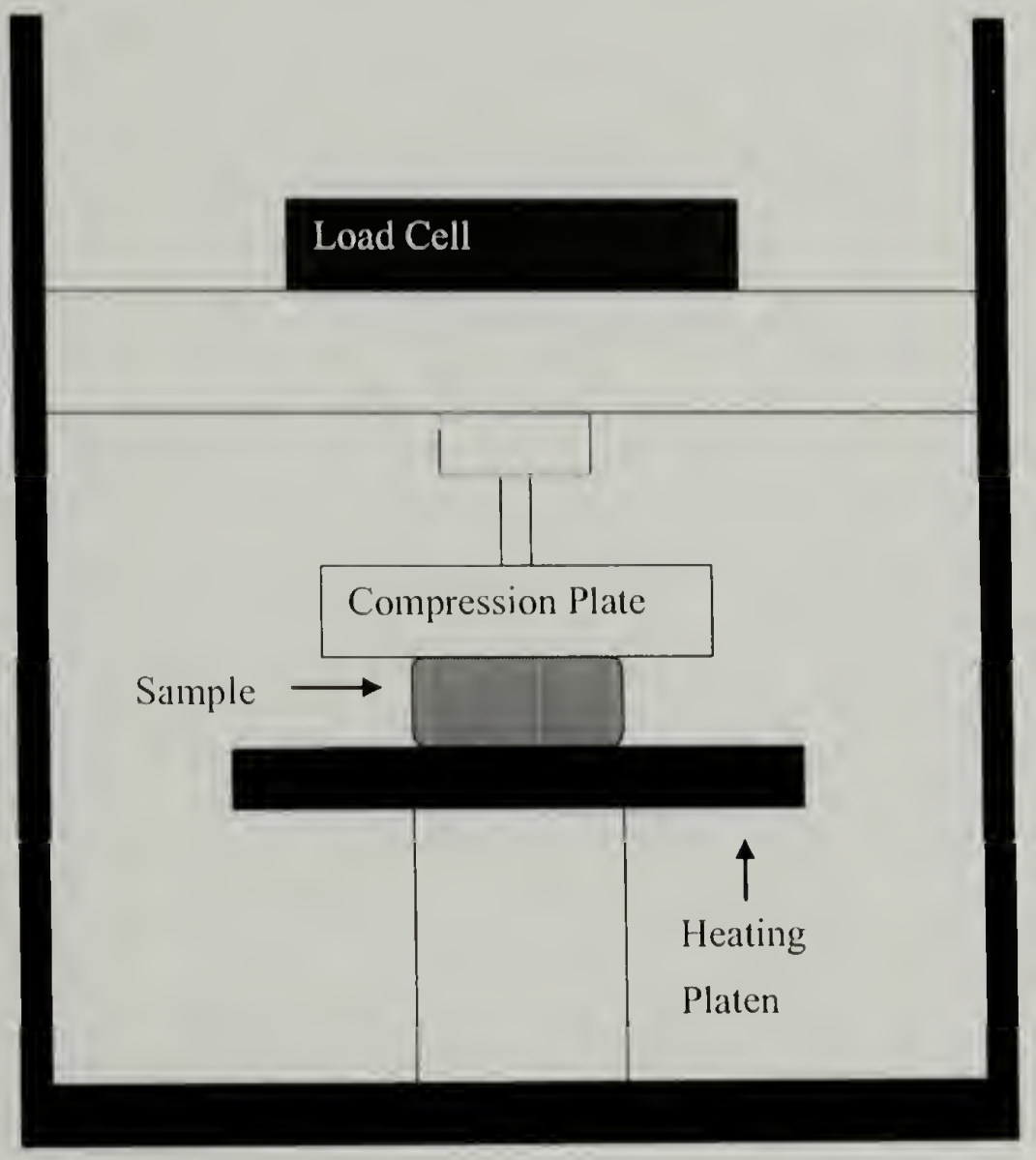

Figure 3.5. Schematic of Instron compression stress relaxation experiment.

Intermittent measurements were made by periodically compressing the rubber to a fixed negative elongation and measuring the stress. This technique became the main method of CSR data collection as it did not present any significant engineering problems.

As such, the majority of the data collected in subsequent chapters was obtained using this technique.

3.3 CSR of Polysulfide Rubber

The stress relaxation data used for the investigation of polysulfide rubber was taken from Stern and Tobolsky.[36] Their study focused on Thiokol ST (polydiethylformal disulfide) and is equivalent to the rubber used in the earlier HPHTS of polysulfide. Figure 3.6 shows the continuous stress relaxation at several different testing temperatures for the Thiokol ST. As is evident, the rate of relaxation increases significantly at higher testing temperatures. In order to perform a time-temperature superposition, Stern and Tobolsky take the following steps. First a line is drawn across the data at the value where $F(t)/F(0) = e^{-1} = 0.368$. The time values where the individual stress relaxation curves intersect the line are then calculated and tabulated. Next Equation 3.1 is reduced as per Equation 3.2 allowing for a superposition constant k' to come out as per the time of the intersection with the line of e^{-1} (Equation 3.3). A tabulation of Stern and Tobolsky's data for Thiokol ST appears in Table 3.1.

$$\frac{f(t)}{f(0)} = 0.368 = e^{-k't}$$

Equation 3.1

$$\ln(0.368) = \ln(e^{-k't})$$

Equation 3.2

$$k' = \frac{1}{t}$$

Equation 3.3

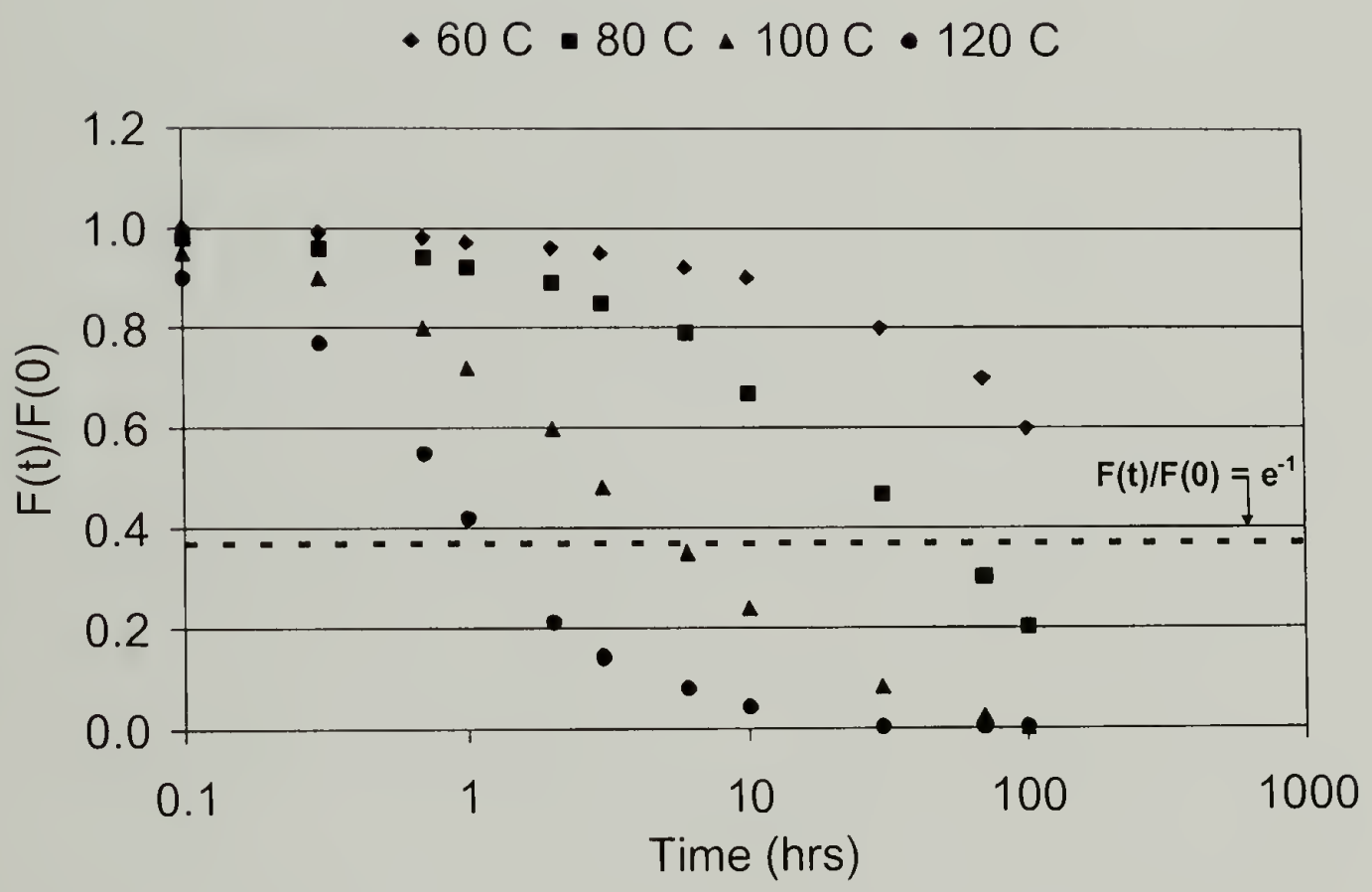

Figure 3.6. Continuous stress relaxation results for Thiokol ST (polysulfide rubber) as performed by Tobolsky et al.[36]

Table 3.1. Superposition calculations for Thiokol ST (polysulfide rubber).

Time (hrs)	k'	Temp C	1/T*10^3
500	0.002	60	3.00
200	0.005	70	2.92
50	0.020	80	2.83
20	0.050	90	2.75
6.0	0.167	100	2.68
2.5	0.400	110	2.61
1.1	0.909	120	2.54

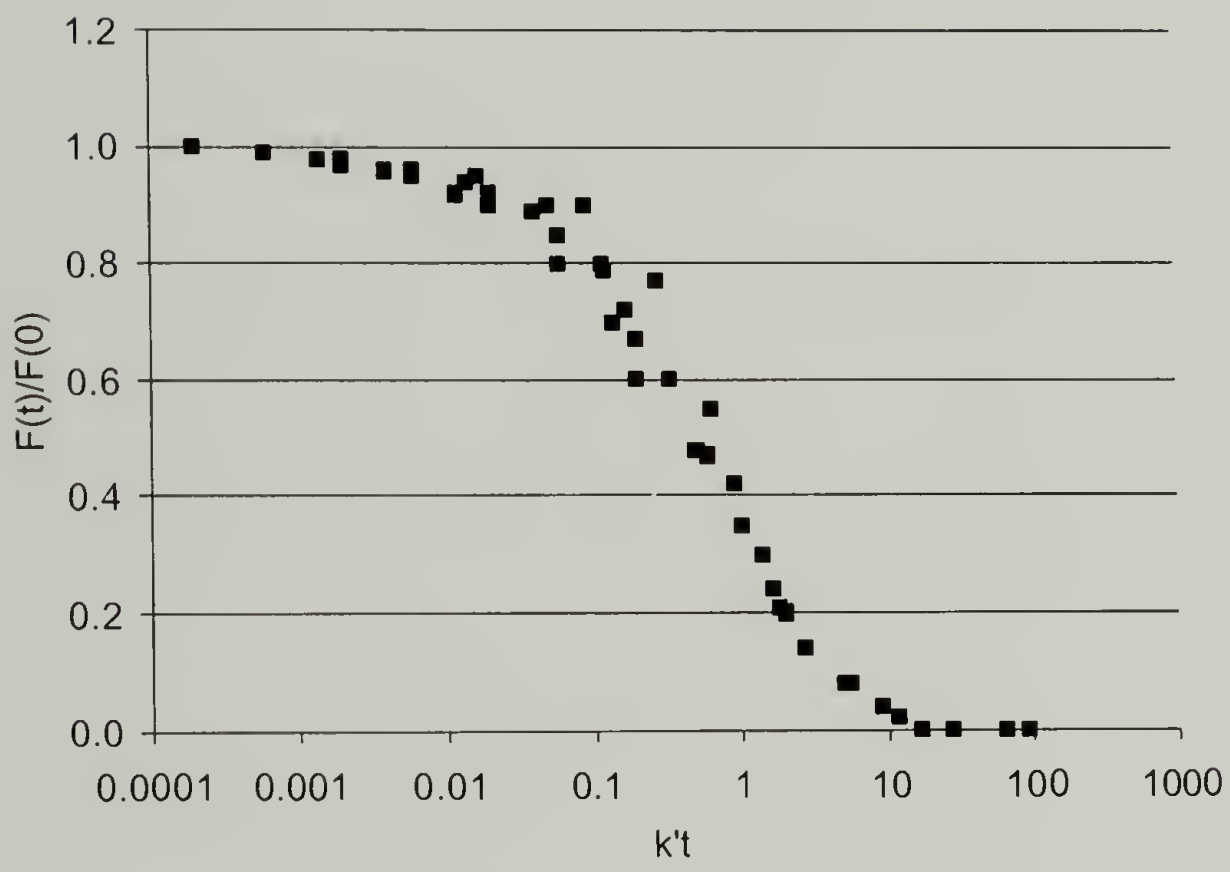

Figure 3.7. Superimposed continuous stress relaxation results for Thiokol ST (polysulfide rubber).

To complete the superposition shift, the time values of the original data are multiplied by the k' value corresponding to the temperature of the experiment. Figure 3.7 illustrates how applying this technique allows Stern and Tobolsky to obtain a universal continuous stress relaxation curve for polysulfide rubber. Along with these results, Stern and Tobolsky[36] report that the intermittent stress relaxation of polysulfide remains

constant (F(t)/F(0) = 1) over the entire temperature range investigated. These results will be used in the next chapter in order to understand the correlation between CSR and HPHTS for polysulfide rubber.

3.4 CSR of Natural Rubber

Early work by Tobolsky[31] indicated that NR would behave significantly different than polysulfide rubbers during chemical stress relaxation experiments. Figure 3.8 shows the continuous stress relaxation results for a carbon black-filled NR utilizing the Instron compression stress relaxation apparatus (Figure 3.5). As is evident, the continuous stress relaxation results for NR are very similar to polysulfide, albeit at higher temperatures. Again, as the testing temperature is increased, an increase in the rate of relaxation is observed.

To achieve superposition, a line was drawn at F(t)/F(0) = 0.5 in contrast to the 0.368 used with the polysulfide data. The reason for the change in this case is that not all of the data reaches the 0.368 line and therefore a higher value was chosen. This changes the superposition calculation slightly as Equation 3.1, Equation 3.2 and Equation 3.3 are transformed into Equation 3.4, Equation 3.5 and Equation 3.6.

$$\frac{f(t)}{f(0)} = 0.500 = e^{-k't}$$

Equation 3.4

$$\ln(0.500) = \ln(e^{-k't})$$

Equation 3.5

$$k' = \frac{0.693}{t}$$

Equation 3.6

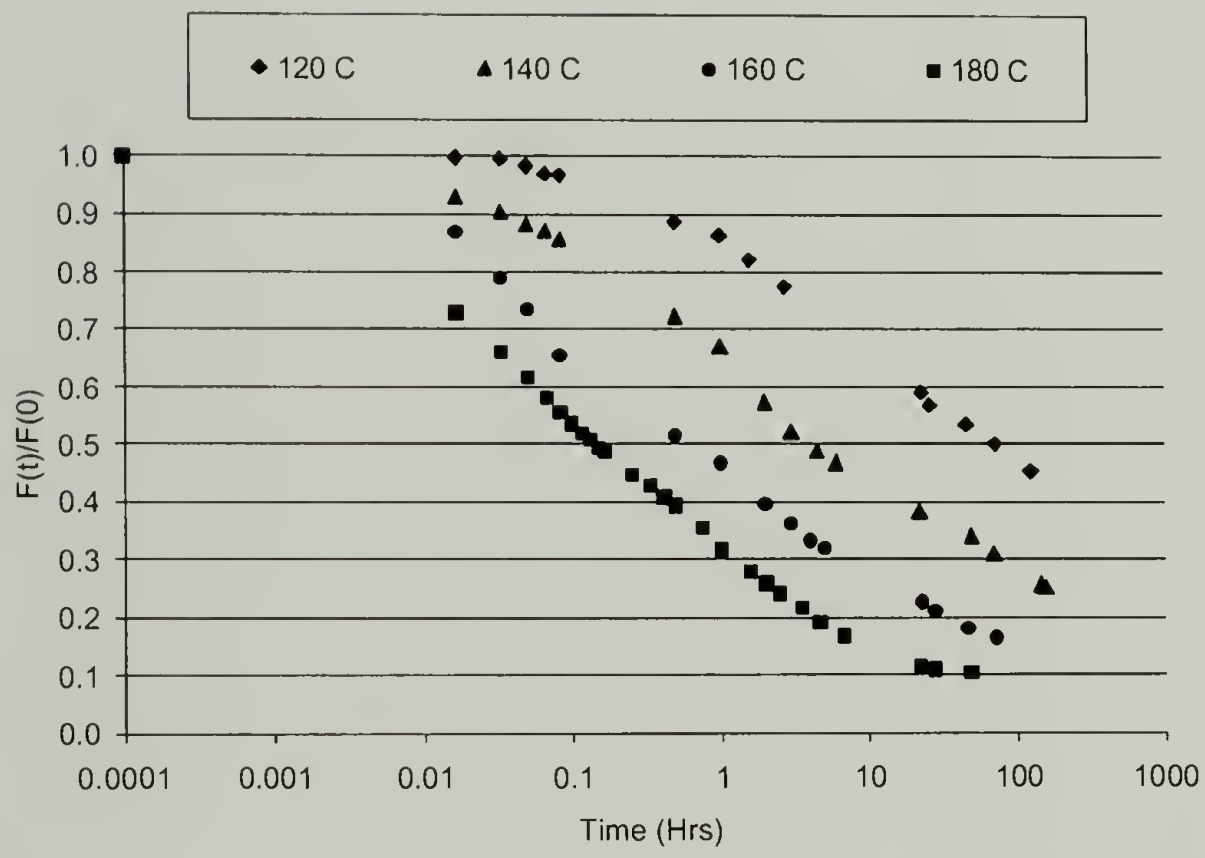

Figure 3.8. Continuous stress relaxation results for sulfur cured, carbon black-filled NR.

Table 3.2. Superposition calculations for sulfur cured, carbon black-filled NR.

Time (hrs)	K'	Temp C	(1/T)*10^3
72	0.01	120	2.54
4.0	0.17	145	2.39
0.65	1.07	160	2.31
0.14	4.95	180	2.21

As with the polysulfide, the time values are multiplied by their respective k' value in order to shift all of the data onto a universal axis. The result is shown in Figure 3.9. Similar to the polysulfide data, the various NR continuous stress relaxation experiments superimpose well and follow a similar pattern as described by Tobolsky.[31]

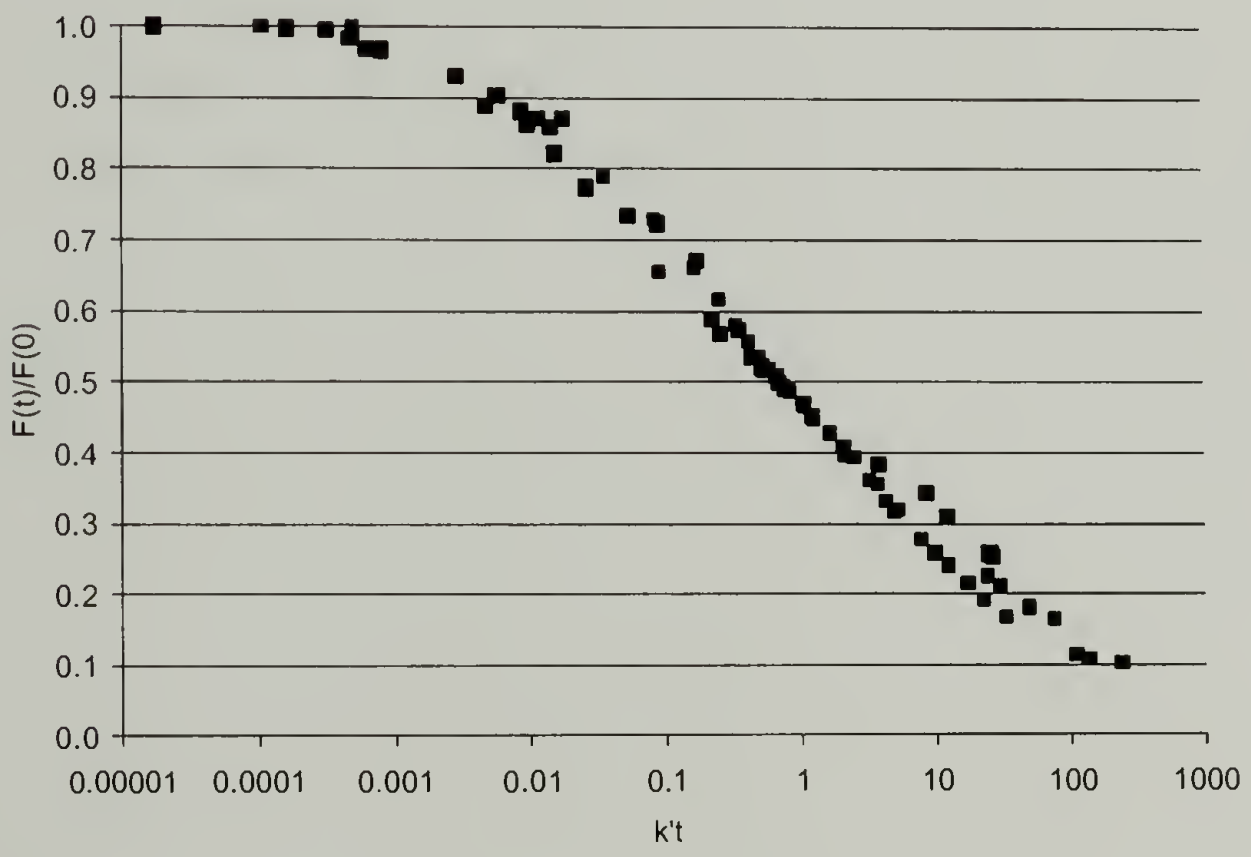

Figure 3.9. Superimposed continuous stress relaxation results for sulfur cured, carbon black-filled NR.

The next step in the stress relaxation investigation of NR was to explore the influence of temperature on the intermittent stress relaxation. Unlike the polysulfide rubber that exhibits a constant intermittent stress relaxation, Tobolsky's early work suggested that the intermittent stress relaxation of NR would be less at high temperatures and longer times.[31] Data obtained from the intermittent stress relaxation of carbon black-filled NR (same NR as used in the continuous and HPHTS studies) is shown in Figure 3.10, again utilizing the Instron compression relaxation apparatus of Figure 3.5. Similar to the continuous data, as the temperature of the experiment is increased, the intermittent stress relaxation value diminishes faster. This is indicative of network breakdown, or reversion, and is consistent with the data obtained in the HPHTS section on NR.

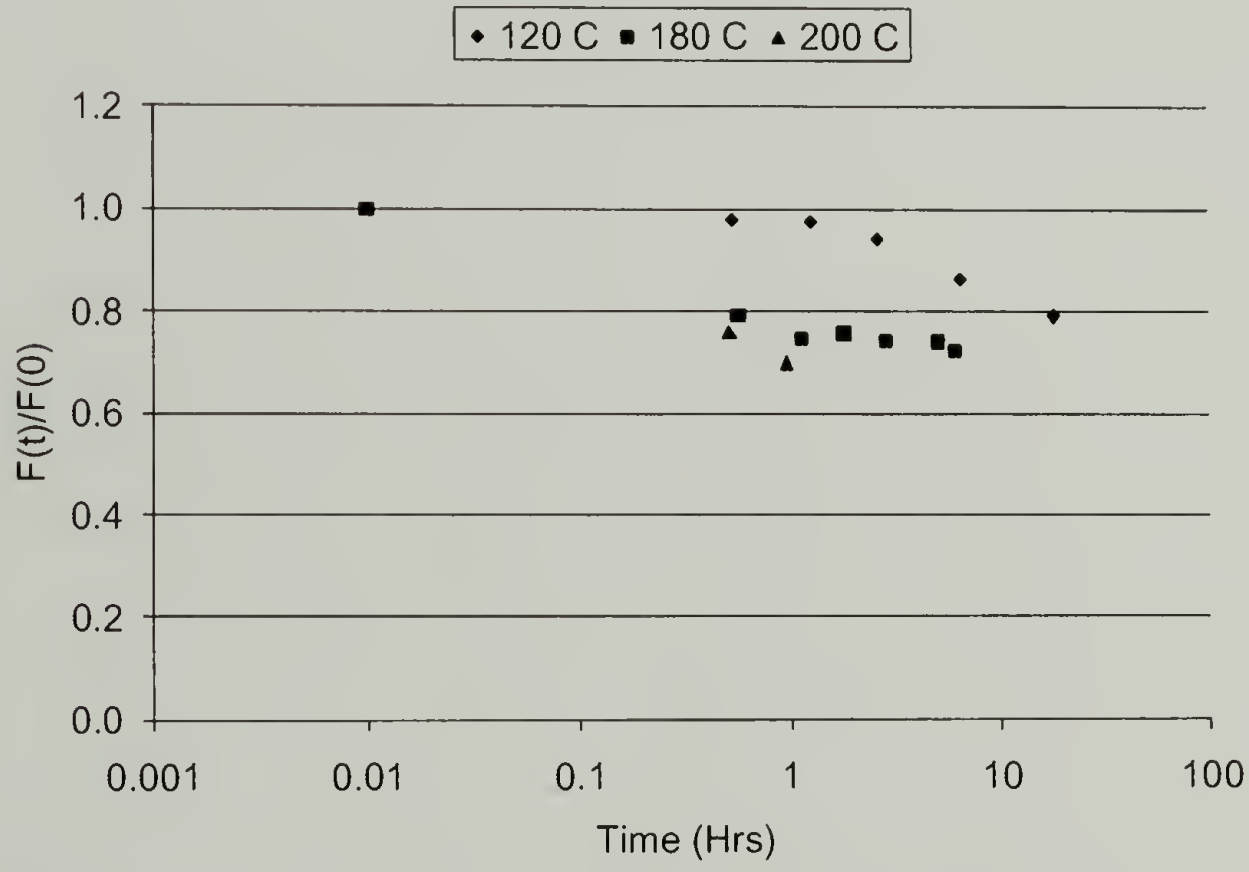

Figure 3.10. Intermittent stress relaxation results for sulfur cured, carbon black-filled NR.

Again, it is possible to superimpose the data through a time-temperature superposition. Following the results from the continuous stress relaxation of NR, Figure 3.11 shows the superimposed intermittent stress relaxation data for NR. This graph clearly illustrates how the NR is losing crosslink density when exposed to the extreme temperatures that are utilized in HPHTS. Although the figure shows some slight variance (likely due in part to oxidation during the CSR experiments) in the results of the superposition, the data overlaps fairly well. As with the polysulfide rubber, the continuous and intermittent stress relaxation results will be used in Chapter 4 to form a correlation between CSR and HPHTS.

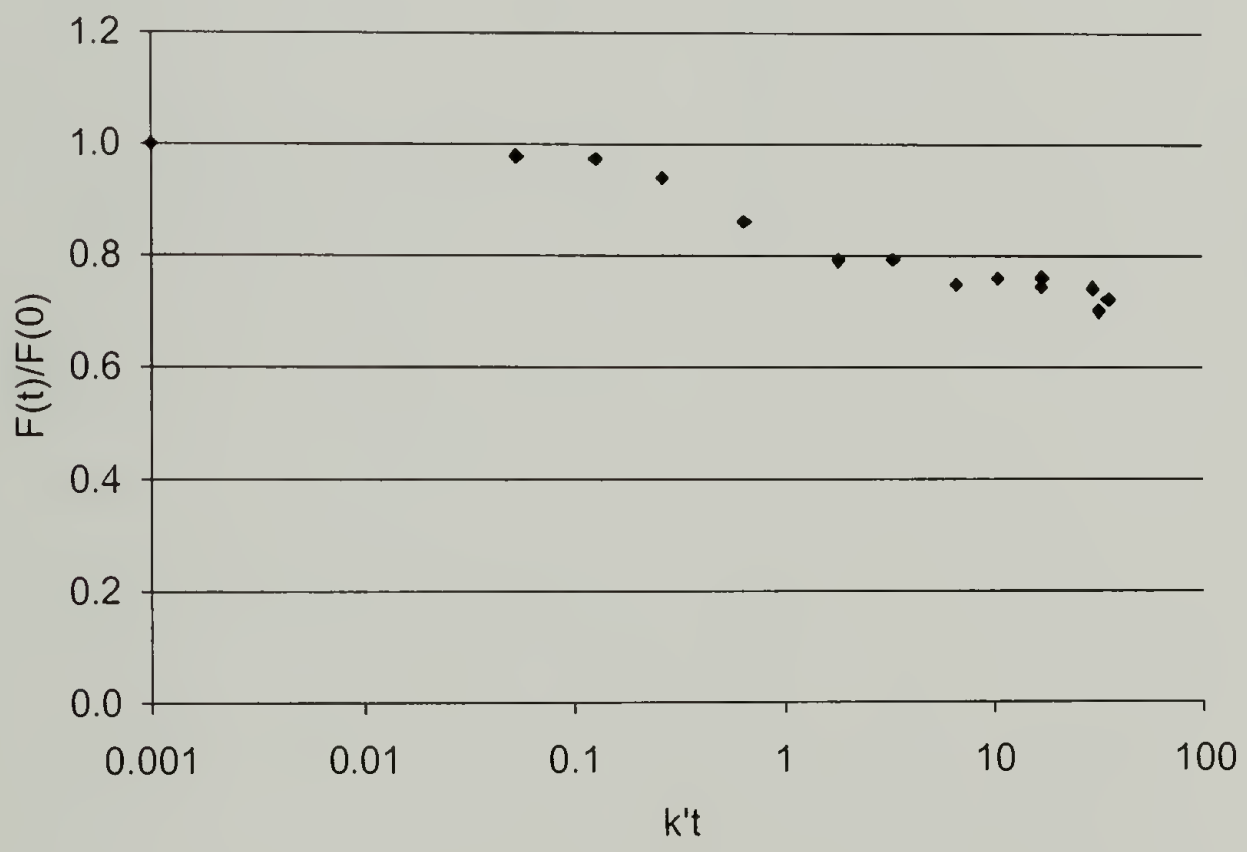

Figure 3.11. Superimposed intermittent stress relaxation results for sulfur cured, carbon black-filled NR.

3.5 CSR of Styrene-Butadiene Rubber

As with NR, work by Tobolsky[31] indicated that SBR would behave significantly differently than polysulfide rubbers during chemical stress relaxation experiments. Figure 3.12 shows the continuous stress relaxation results for a carbon black-filled SBR utilizing the Instron compression stress relaxation apparatus from Figure 3.5. As is clear, the continuous stress relaxation results for SBR are similar to polysulfide and NR, although they are shifted to even higher temperatures than either of the previous two rubbers. Again, however, as the testing temperature is increased, an increase in the rate of relaxation is observed.

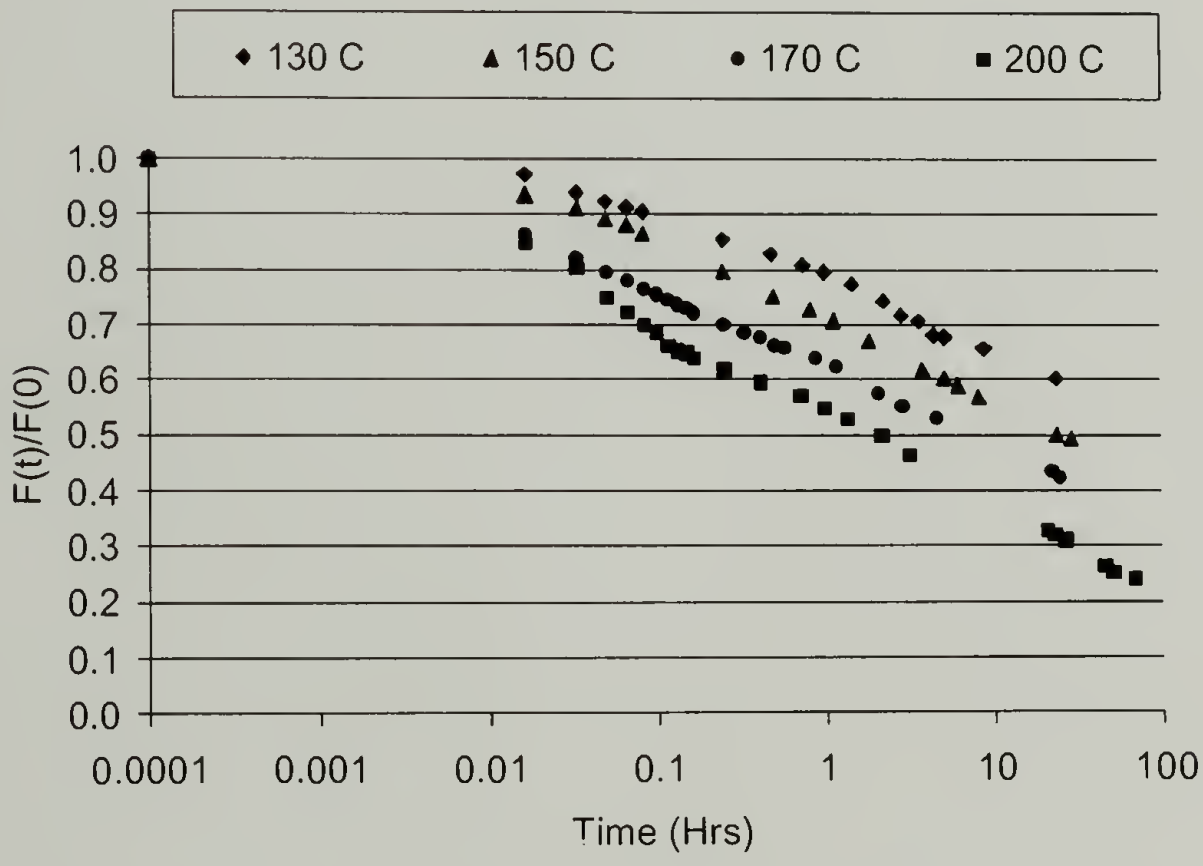

Figure 3.12. Continuous stress relaxation results for sulfur cured, carbon black-filled SBR.

To achieve superposition with SBR CSR data, a line was drawn at F(t)/F(0) = 0.6, in contrast to the 0.368 line used with the polysulfide data and the 0.5 line for the NR. The reason for the change was again that not all of the data reached 0.368 or 0.5.

Table 3.3. Superposition calculations for sulfur cured, carbon black-filled SBR.

Time (hrs)	K'	Temp C	(1/T)*10^3
23.7	0.02	130	2.48
5.15	0.10	150	2.36
1.95	0.26	170	2.26
0.42	1.23	200	2.11

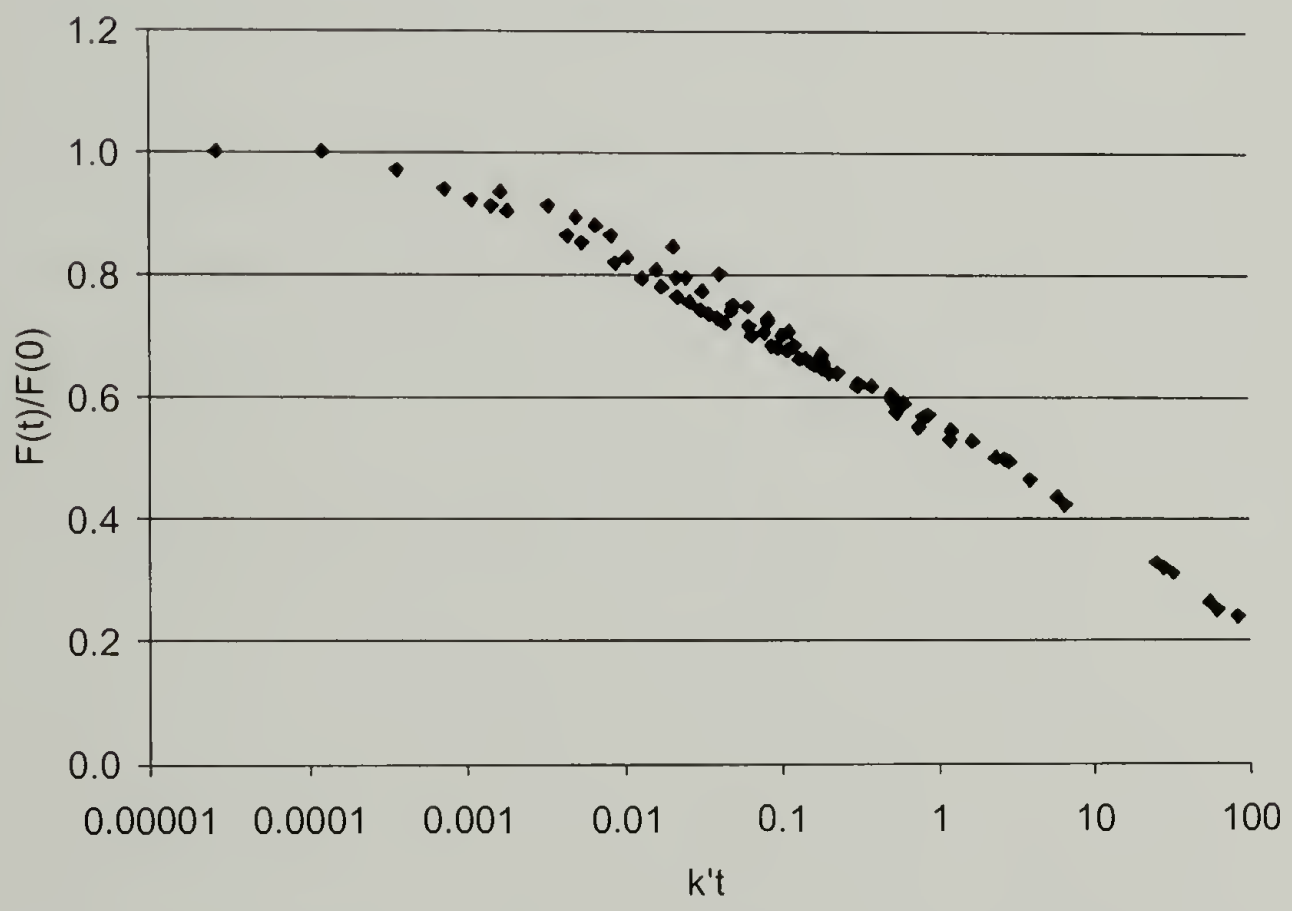

Figure 3.13. Superimposed continuous stress relaxation results for sulfur cured, carbon black-filled SBR.

As with the polysulfide, the time values are multiplied by their respective k' value in order to shift all of the data onto a universal axis. The result is shown in Figure 3.13. Similar to the polysulfide and NR data, the various SBR continuous stress relaxation experiments superimpose well.

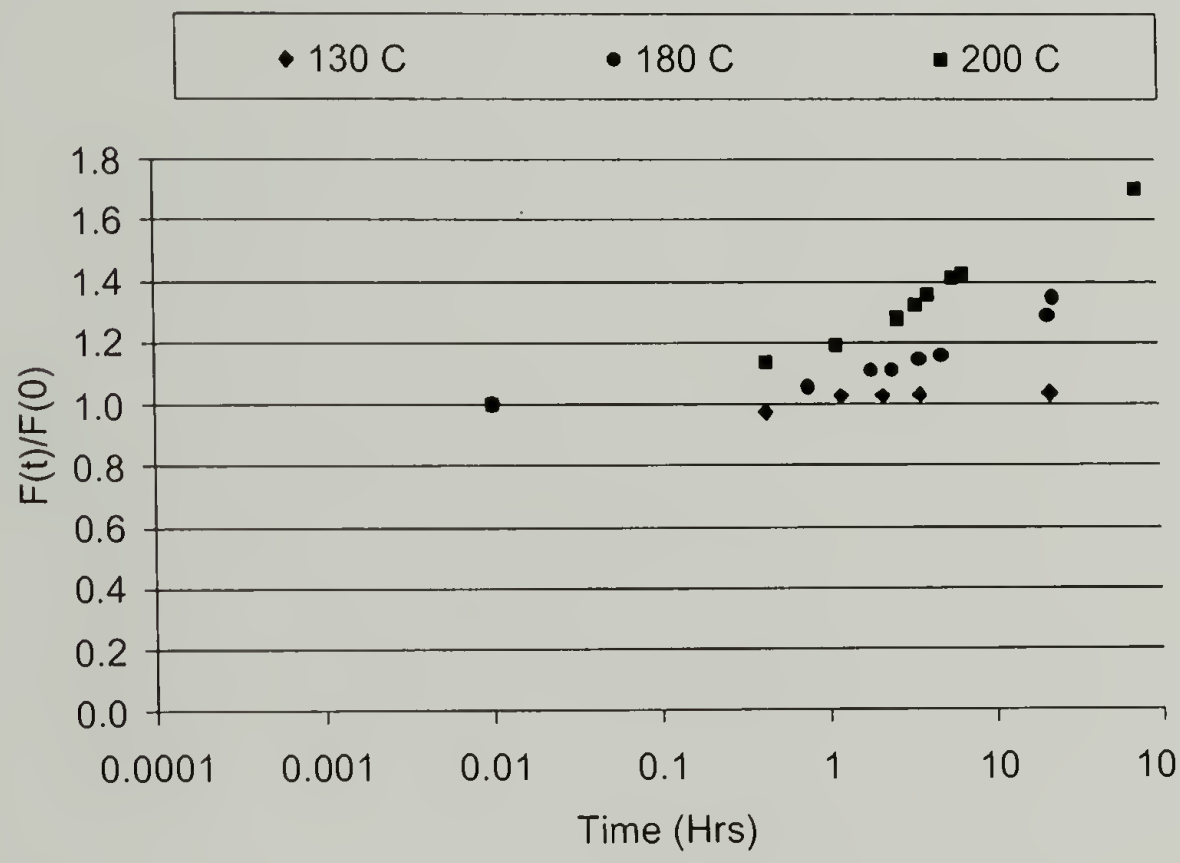

Figure 3.14. Intermittent stress relaxation results for sulfur cured, carbon black-filled NR.

Continuing the stress relaxation investigation of SBR, the influence of temperature on the intermittent stress relaxation was measured. Unlike the polysulfide rubber that exhibits a constant intermittent stress relaxation, Tobolsky's early work suggested that the intermittent stress relaxation of SBR would be greater than one at higher temperatures and longer times, indicating extensive overcrosslinking.[31] Data obtained from the intermittent stress relaxation of carbon black-filled SBR is shown in

Figure 3.14, again utilizing the Instron compression relaxation apparatus of Figure 3.5. Contrary to the continuous data, as the temperature of the experiment is increased, the intermittent stress relaxation value becomes greater than 1. This is indicative of overcrosslinking and is consistent with the data obtained in the HPHTS section on SBR and Tobolsky's work on the CSR of SBR.[31]

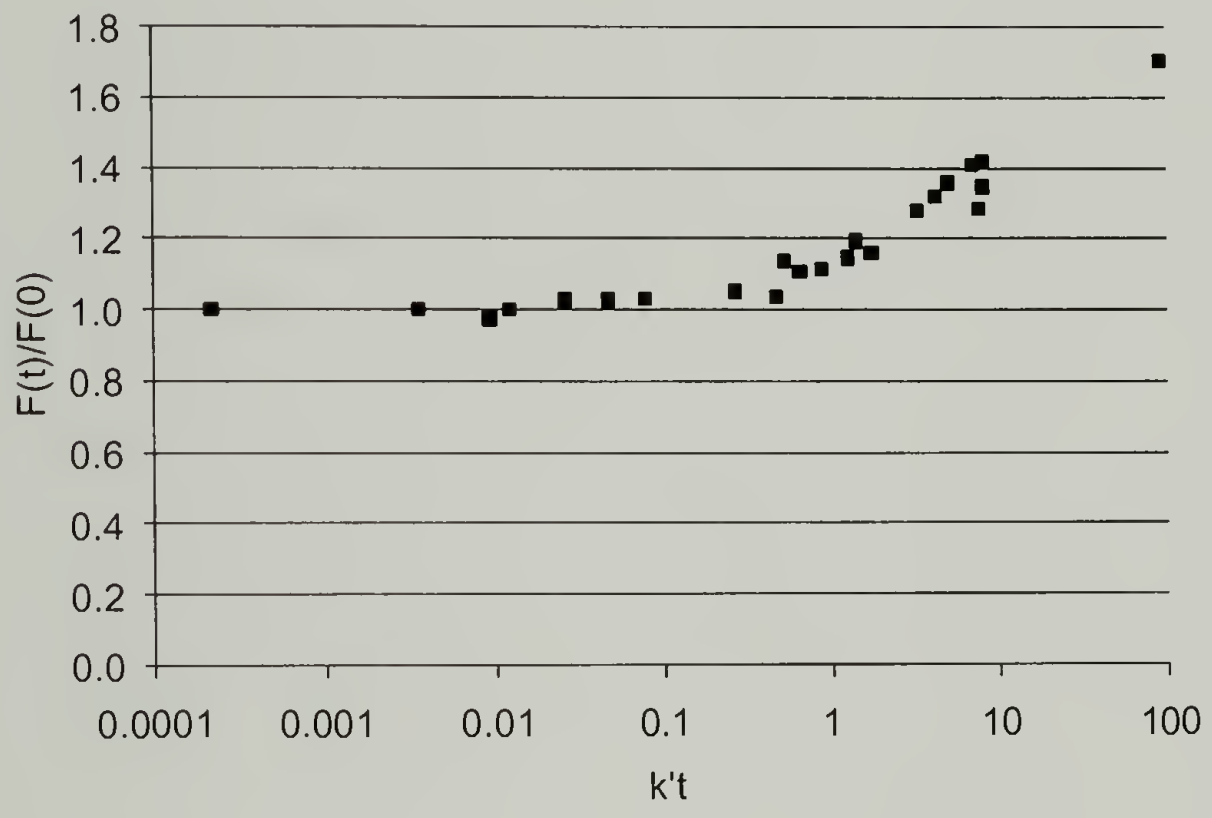

Figure 3.15. Superimposed intermittent stress relaxation results for sulfur cured, carbon black-filled NR.

Superposition of the data through the time-temperature superposition described in the continuous section for SBR is shown in Figure 3.15. This graph illustrates how the SBR is gaining crosslink density when exposed to the extreme temperatures that are utilized in HPHTS. As with the polysulfide rubber and NR, the continuous and

intermittent stress relaxation results will be used in Chapter 4 to form a correlation between CSR and HPHTS.

3.6 CSR of Polyurethanes

The last thermoset investigated was a polyurethane similar in structure to the scrap polyurethane used in the HPHTS section. The data below has been interpreted from Tobolsky.[37] Figure 3.16 shows the continuous stress relaxation at several different temperatures. As with the rubber samples above, the thermoset polyurethane experiences increased continuous stress relaxation rates at higher temperatures. Similarly, a time-temperature superposition is possible and the continuous stress relaxation overlaps well as shown in Figure 3.17.

Figure 3.18 shows the intermittent stress relaxation results as a function of time for polyurethane. The intermittent stress relaxation for polyurethane looks similar in nature to the NR data reported above. At lower times or temperatures the material behaves like the polysulfide, losing little of the chemically crosslinked network. However, at higher temperatures and times, the network begins to breakdown and it appears that polyurethane reverts. This is further verified by the findings in the HPHTS section of polyurethanes where reversion is observed at high temperatures.

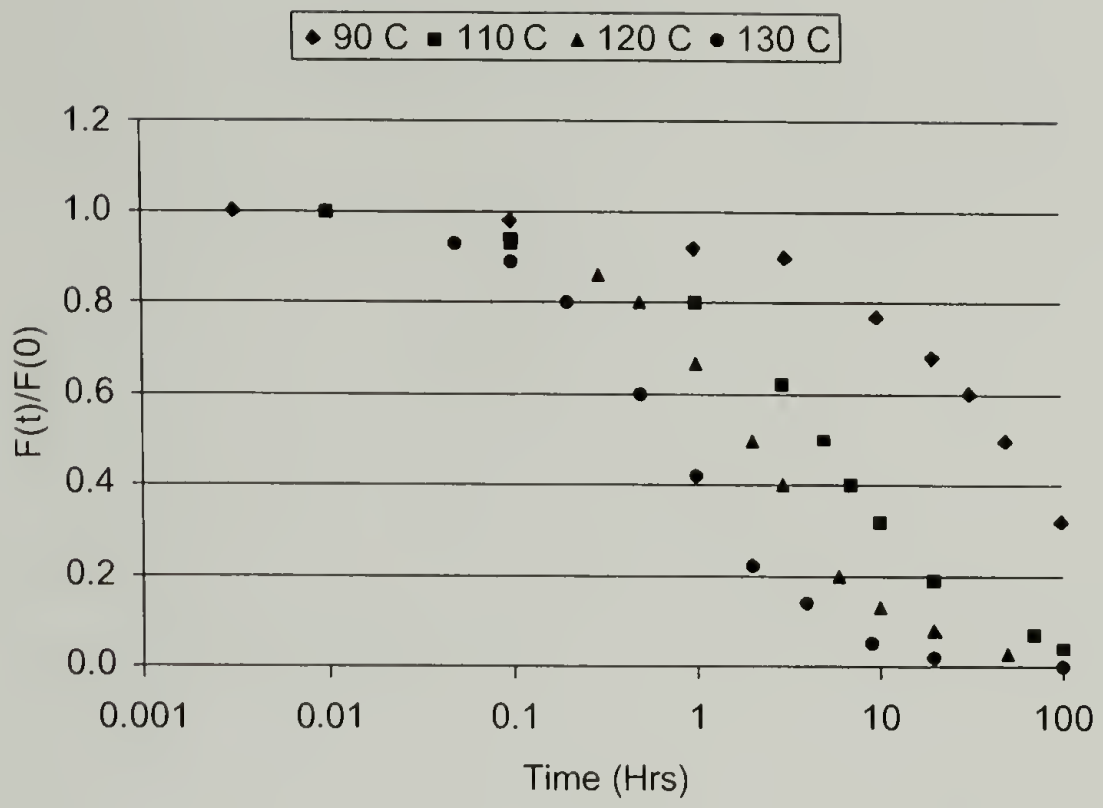

Figure 3.16. Continuous stress relaxation results for polyurethane as performed by Tobolsky et al.[37]

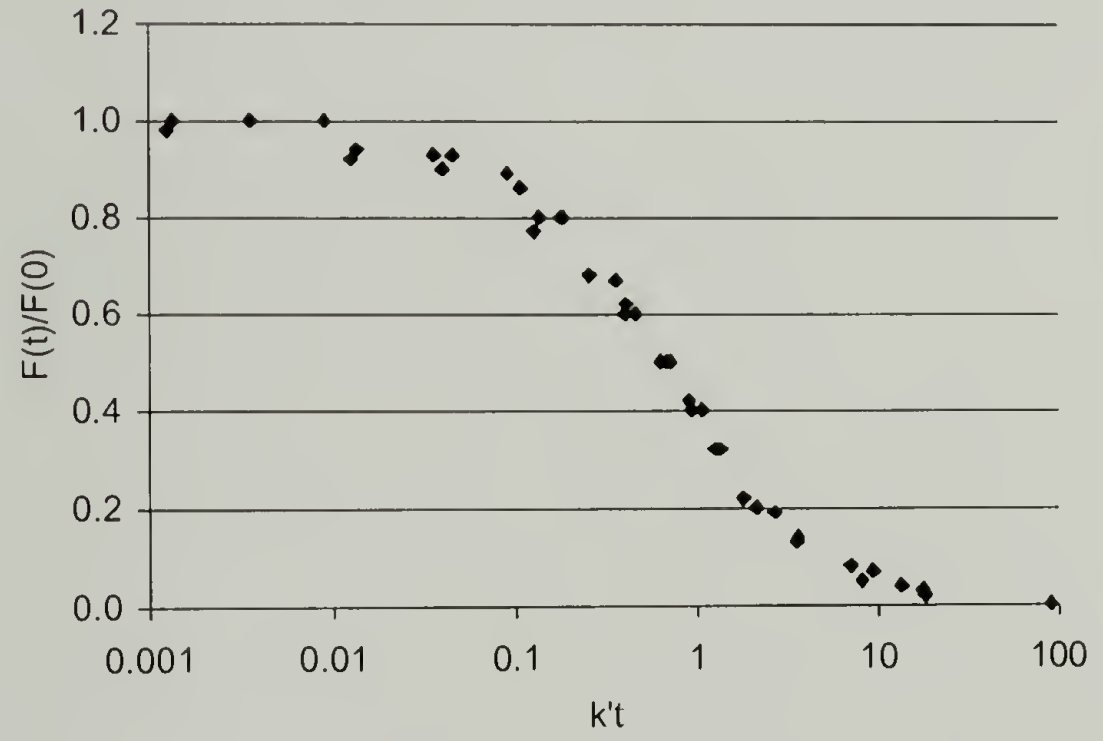

Figure 3.17. Superimposed continuous stress relaxation results for polyurethane.

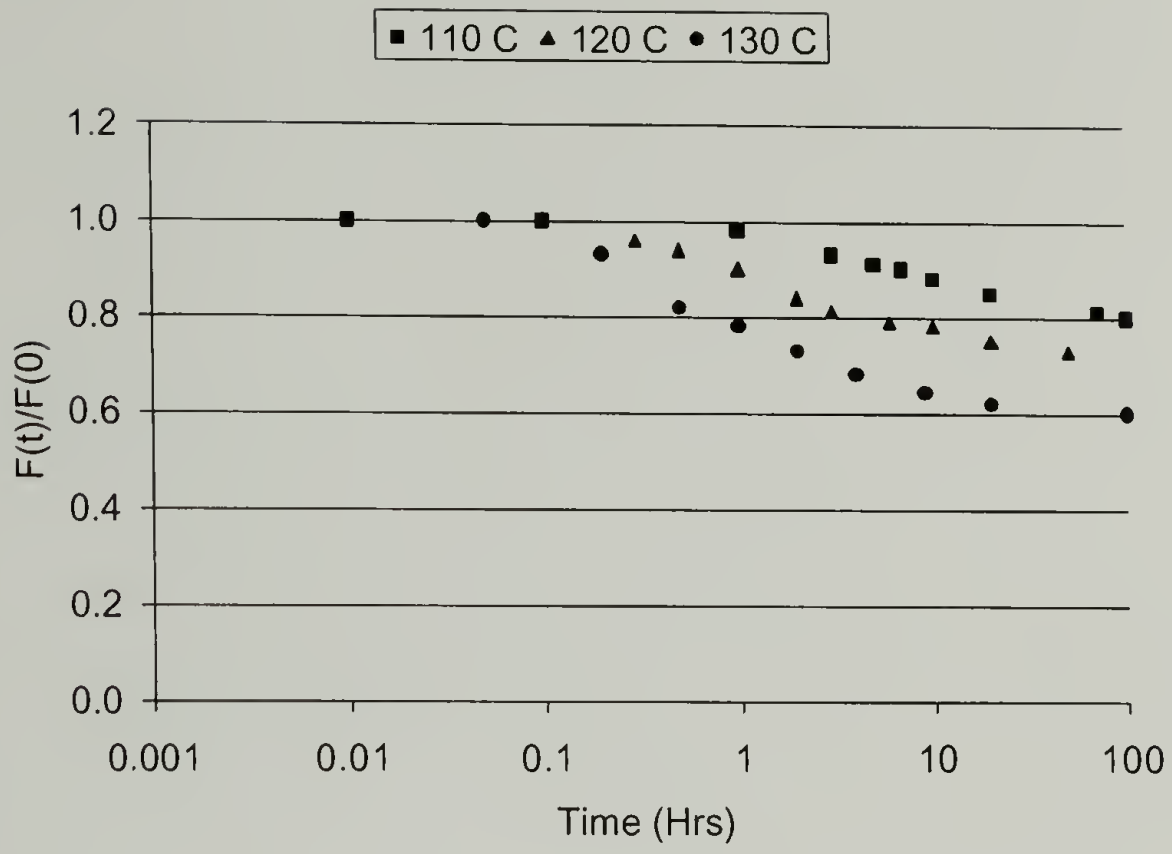

Figure 3.18. Intermittent stress relaxation results for polyurethane as performed by Tobolsky et al.[37]

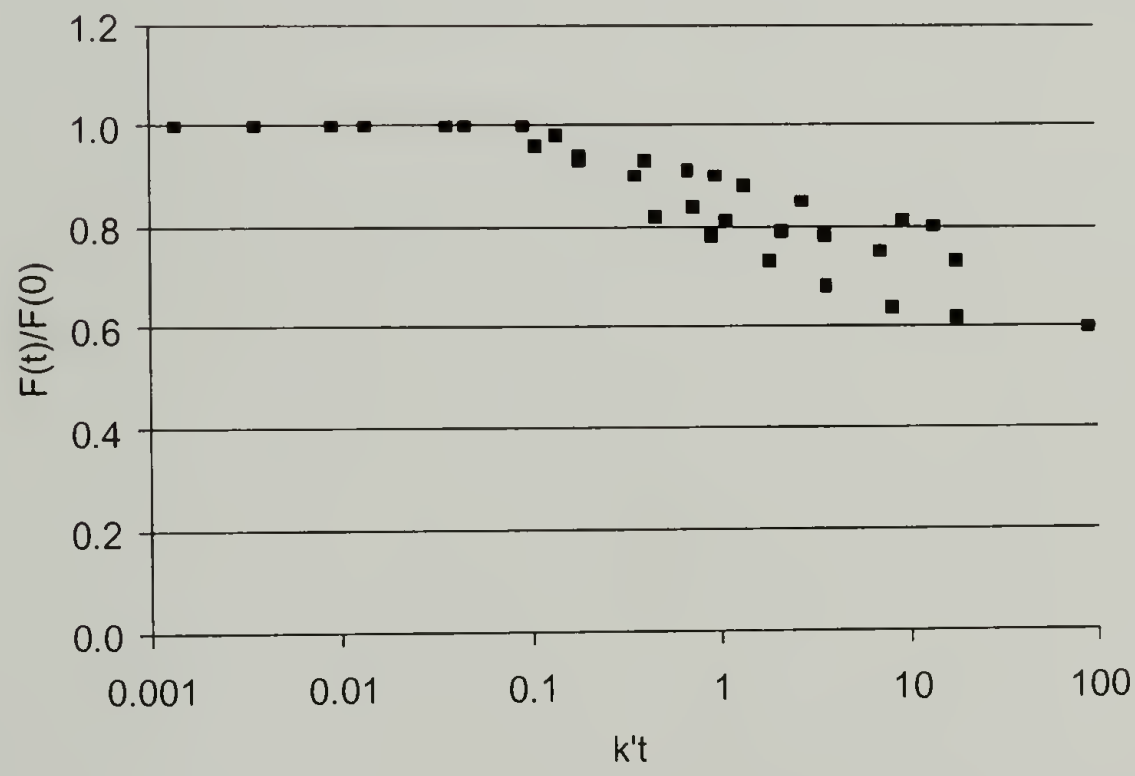

Figure 3.19. Superimposed intermittent stress relaxation results for polyurethane.

Figure 3.19 shows the time-temperature superposition of the data. As is clear, the superposition is not perfect and some variation results. However, the trend of reversion is apparent, and stress relaxation results will be used in Chapter 4 to form a correlation between CSR and HPHTS.

3.7 CSR Conclusions

The chemical stress relaxation results for the various thermosets offer a unique look into the mechanism of HPHTS. The polysulfide system investigated by Tobolsky shows a very fast continuous relaxation to zero at relatively low temperatures. This is indicative of bond breakage within the original network, and is a necessary requirement for subsequent bond reformation. The intermittent relaxation of polysulfide remains constant (I=1), illustrating how once bonds break in a polysulfide network, new ones are immediately formed, with the number reforming being equivalent to the number originally broken. Following the work in the HPHTS section regarding Gent's work on strength and crosslink density, it appears from CSR that polysulfide would be an ideal rubber for the HPHTS process. From the earlier results of the HPHTS of polysulfide, it is apparent that this hypothesis holds true.

The NR and SBR results offer similar insight into their mechanistic behavior during HPHTS. NR also incurs a fairly quick continuous relaxation to zero, albeit at slightly higher temperatures than that of the polysulfide. However, the intermittent stress relaxation is significantly different from the polysulfide, as it falls below 1. This indicates that as bonds break in NR, not all are recombining to form new stress-bearing bonds. This is clearly the case in the HPHTS of NR as a decrease in the 100% modulus

is reported, indicating lower crosslink densities at higher sintering temperatures. Applying Gent's work of strength and crosslink density, it appears that NR will suffer lower mechanical properties during sintering as a result of this loss in crosslink density.

Similar to NR, SBR also incurs a quick continuous relaxation to zero. However, its intermittent stress relaxation indicates that the rubber is incurring extra crosslinking reactions. As predicted from Gent's work, this extra crosslinking is causing a reduction in the measured strength for HPHTS parts of SBR.

The final case of the thermoset polyurethane illustrates that CSR does not just apply to chemically crosslinked rubbers, but works for other thermoset networks as well. The polyurethane data from Tobolsky follows the NR data in a very similar manner. The continuous relaxation appears to go to zero at a faster rate, while the intermittent data diminishes slower and is scattered more than the NR data. However, it again appears that reversion is the main cause for lower mechanical property retention as the intermittent relaxation of polyurethane ($I<1$) indicates that not all bonds that are broken are reforming.

Overall, CSR has provided a useful technique for the investigation of the mechanism of HPHTS. From the results it appears that a fast continuous relaxation is necessary to allow for breakage of the old network. However, and more importantly, it is a constant intermittent stress relaxation, indicative of consistent bond reformation (one and only one bond forming for each bond breaking) that appears to make a thermoset sinter well. This investigation of CSR has provided a solid foundation for understanding the process of HPHTS. Work in Chapter 4 will take this knowledge and attempt to apply it in the form of a predicative model of HPHTS based on CSR results.

CHAPTER 4

CORRELATION OF CSR AND HPHTS RESULTS

4.1 New Bond Formation Theory

The previous chapter illustrated how CSR can be used to better understand the HPHTS process. Specifically, by investigating both the continuous and intermittent stress relaxation of various thermosets, it appears possible to understand how thermosets will behave during HPHTS. Expanding on this idea, it was decided that a theory could be developed in efforts to model the HPHTS process.

Equation 4.1 and Equation 4.2 highlight the stress at time 0 and t respectively during a continuous or intermittent experiment (N = number of chains per unit volume, R = universal gas constant, T = temperature (K) and ? = extension). Normalizing the stress at time t by the original stress at time t = 0, one obtains Equation 4.3. Therefore, although the normalized continuous and intermittent stress relaxations do not give exact bond numbers, the number of bonds at time t can be calculated if the original number of bonds is known. Herein, however, only proportional values of bonds will be dealt with and specific bond numbers will not be calculated.

$$\sigma(0) = N(0)RT\left(\lambda - \frac{1}{\lambda^2}\right)$$

Equation 4.1

$$\sigma(t) = N(t)RT\left(\lambda - \frac{1}{\lambda^2}\right)$$

Equation 4.2

$$\frac{\sigma(t)}{\sigma(0)} = \frac{N(t)}{N(0)}$$

Equation 4.3

Mathematically, it is possible to use a combination of continuous and intermittent stress relaxation experiments to determine the relative number of new bonds formed during sintering. For example, continuous stress relaxation yields information about the breaking of the original network's bonds. Therefore, the normalized {fcont(t)/f(0)} continuous stress relaxation term can be considered to be proportional to one (representing the total starting crosslinks in the system) minus the fraction of total crosslinks that have been broken (these are reactive sites capable of forming new crosslinks), or the amount of original crosslinks remaining.

Furthermore, it was stated that the intermittent stress relaxation experiments yield information about the reformation of bonds from the "broken" network. Specifically, the normalized {fint(t)/f(0)} intermittent stress relaxation value yields the percentage of original crosslinks remaining at time t, in addition to the amount of newly formed crosslinks. Thus, by subtracting the normalized continuous stress relaxation value (the amount of original crosslinks left) from the normalized intermittent stress relaxation

value (the percentage of original crosslink plus the newly formed crosslinks) one is left with the percentage of newly formed crosslinks.

Simplifying particle sintering, one can examine the case of two particles being sintered together. As bonds of the original network (within the particles) are broken, there are reactive sites that become available. Since no bonds are present at the interface of the two particles, it is likely that bonds will form across the interface. Mechanically speaking, the weak portion of this now joined system would be the interface between the two particles as this is the area with the least amount of bonds capable of holding stress. Therefore, the mechanical integrity of this two particle system should be proportional to the number of bonds at the interface between the particles.

Applying this understanding to HPHTS, one can expand the idea and state that the difference between the intermittent and continuous stress relaxation values should be proportional to the mechanical integrity (i.e. strength) of parts produced via HPHTS. This was first alluded to in Equation 4.4 from Morin[23], where I is the intermittent stress relaxation value at time t, C is the continuous relaxation value at time t, and N is the amount of newly formed bonds at time t.

$$N(t) = I(t) - C(t)$$

Equation 4.4. New bond formation as a function of time and normalized intermittent and continuous stress relaxation values.

4.2 Polysulfide Rubber

To calculate the amount of new bond formation for polysulfide rubber, we must re-examine Tobolsky's CSR data from Chapter 3. As Tobolsky states, the intermittent stress relaxation of polysulfide is constant, and therefore the *I(t)* for Equation 4.4 is equal to one. This dictates that the new bond formation curve will be a mirror image of the continuous stress relaxation. Figure 4.1 illustrates the new bond formation percentage versus the reduced time axis for Tobolsky's polysulfide (Thiokol ST). One can predict the maximum mechanical properties from Figure 4.1 by looking at the number of new bonds formed at a given k't value. For example, at a k't value of 1, the corresponding new bond percentage is 60%. This indicates that only 40% of the original network remains, while 60% of that original network has reformed in the "new" state. This is in essence saying that 60% of the original network is capable of sustaining stress in the newly formed state. One would predict this value of k't should equate to HPHTS part strength equal to 60% of the original mechanical strength.

All of the experiments in the HPHTS section were conducted for one hour. Therefore, the time value t for them is 1. Thus, temperature's relationship with k' will dictate where along the x-axis of Figure 4.1 the specific sintering conditions will fall. Figure 4.2 illustrates the relationship between k' and temperature, where temperature is in Kelvin and k' is calculated as in Chapter 3. Table 4.1 summarizes the data from Chapter 3, along with extrapolations to higher temperatures (shown in italics) following the equation in Figure 4.2. By taking the k' value from Table 4.1 and evaluating the new bond percentage in Figure 4.1 corresponding to this value, one is able to predict the

amount of original mechanical properties a part sintered at the temperature associated with a specific k' will recover.

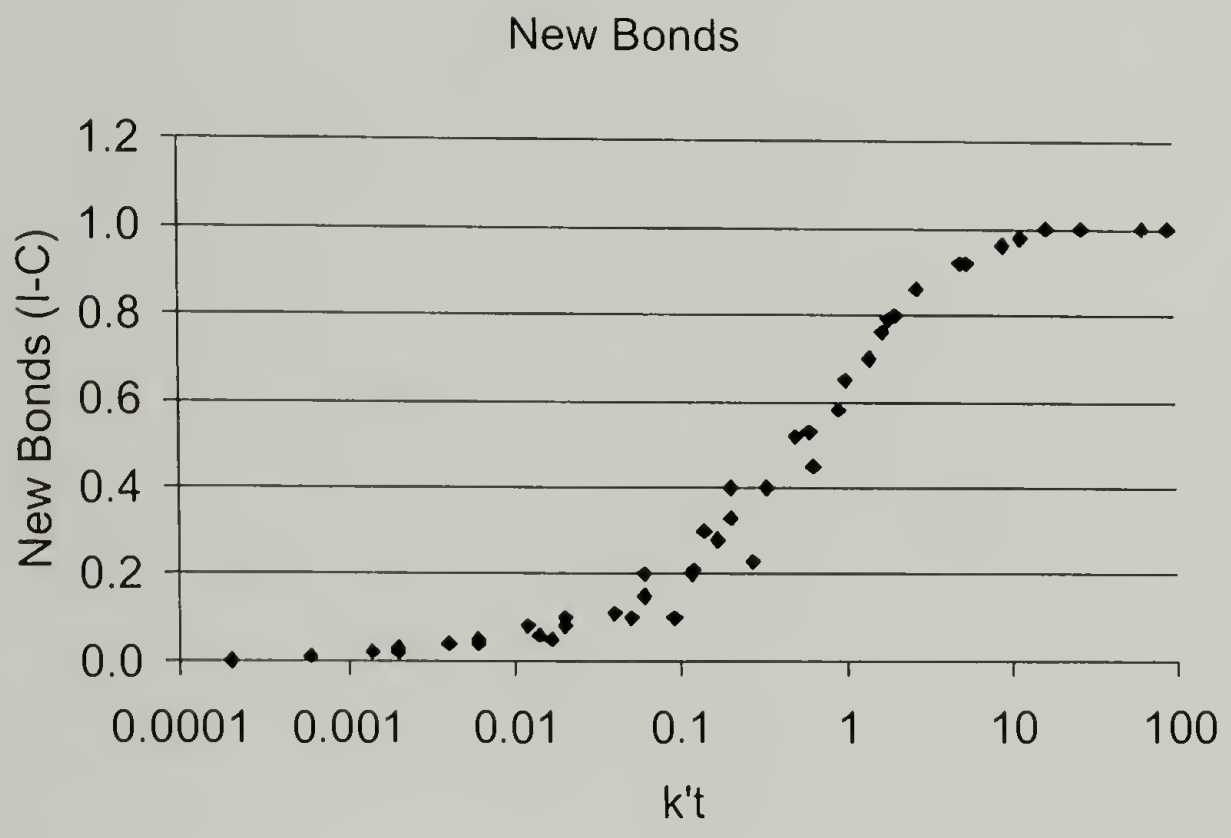

Figure 4.1. New bond formation for Thiokol ST (polysulfide rubber) vs. reduced time.

Table 4.1. Extrapolation of shift factor correlation with temperature for Thiokol ST (polysulfide rubber).

Time (hrs)	k'	Temp	1/T*10^3
500	0.00	60	3.00
200	0.01	70	2.92
50	0.02	80	2.83
20	0.05	90	2.75
6	0.17	100	2.68
2.5	0.40	110	2.61
1.1	0.91	120	2.54
	5	*140*	*2.42*
	25	*160*	*2.31*

Table 4.2 shows the predieted HPHTS strengths for polysulfide rubber using CSR experiments and the new bond formation theory. The results are very similar within experimental error and up to temperatures of 160°C. Above this temperature deviation is noted as the polysulfide rubber incurs degradation and reversion that is not aeeounted for in Tobolsky's intermittent data that did not go to these extreme temperatures (due to degradation, I values would be <1). However, it is elear in Figure 2.16 from Chapter 2 that the 100% modulus of polysulfide diminishes at high temperatures indicating network breakdown. Therefore, this is the reason for deviation at temperatures over 160°C.

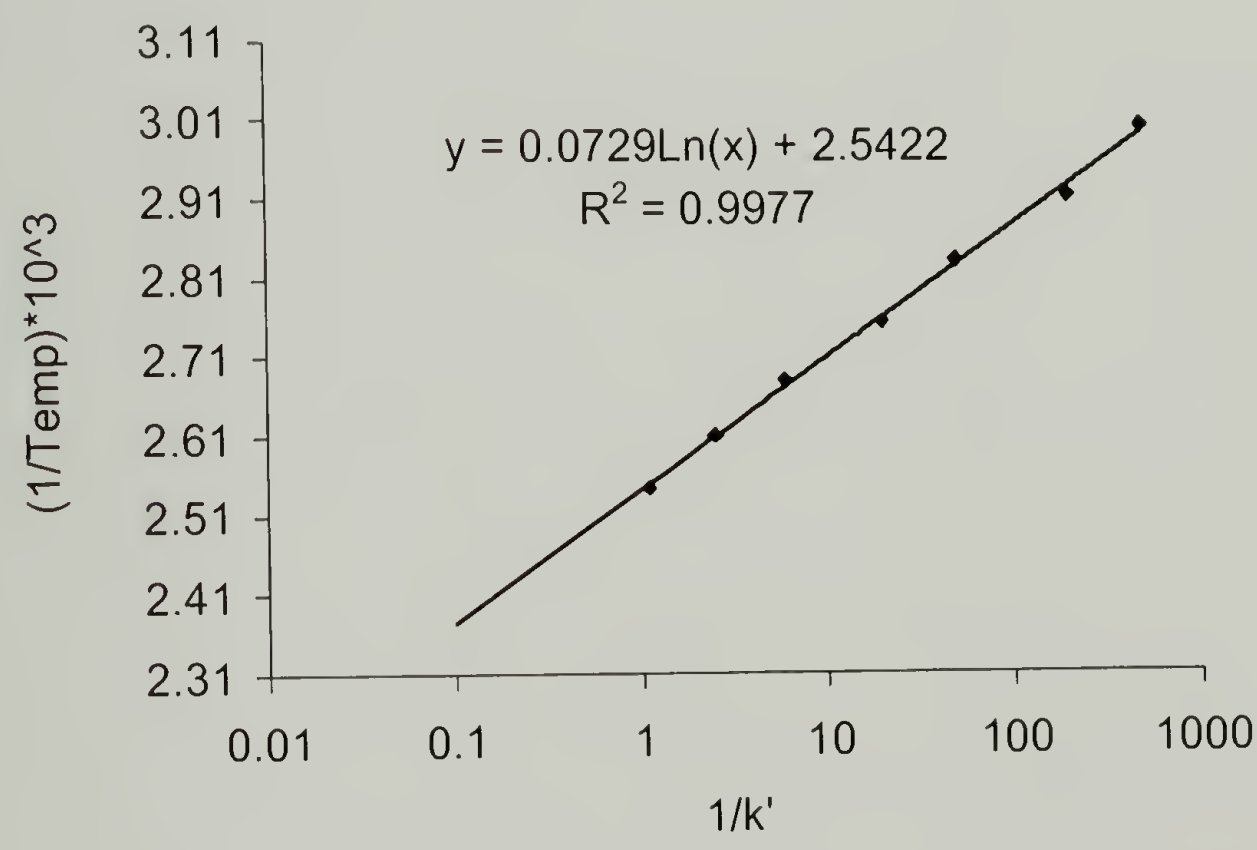

Figure 4.2. Relationship of temperature to shift factor k' for Thiokol ST (polysulfide rubber) with correlation equation.

Table 4.2. Strength % retention predicted by new bond formation theory and actual HPHTS strength retention results (from Chapter 2) as a function of temperature for Thiokol ST (polysulfide rubber).

k'	Temp	% Predicted	HPHTS Actual
0.40	110	30	N/A
0.91	120	45	40
5	*140*	*90*	95
25	*160*	*100*	100
95	*180*	*100*	50
375	*200*	*100*	0

4.3 Natural Rubber

A similar treatment can be conducted on the CSR data of NR from Chapter 3. Superimposing Figure 3.9 and Figure 3.11, and using Equation 4.4, one obtains Figure 4.3. It is apparent that the diminishing intermittent stress relaxation is directly responsible for the new bond formation curve not reaching 100%. In fact, as a result of a decreasing intermittent curve, the highest new bond formation potential generated from the CSR data is 55%. Thus, the CSR of NR predicts less than 60% retention of mechanical strength during sintering.

Table 4.3. Extrapolation of shift factor correlation with temperature for NR.

Time (hrs)	K'	Temp C	(1/T)*10^3
72	0.01	120	2.54
4	0.10	140	2.42
0.65	0.79	160	2.31
0.14	5.81	180	2.21
	33.83	*200*	*2.11*
	170.66	*220*	*2.03*
	758.80	*240*	*1.95*

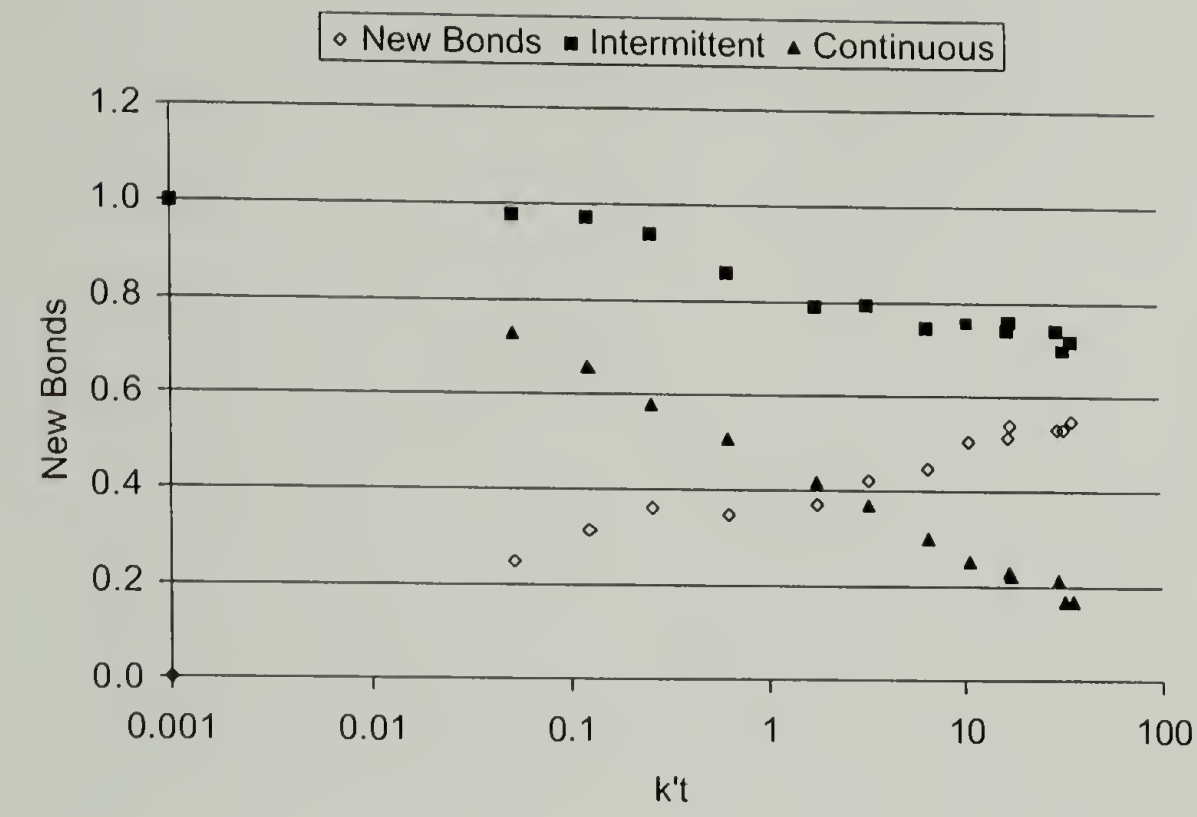

Figure 4.3. Superimposed continuous and intermittent stress relaxation results and calculated new bond formation for NR.

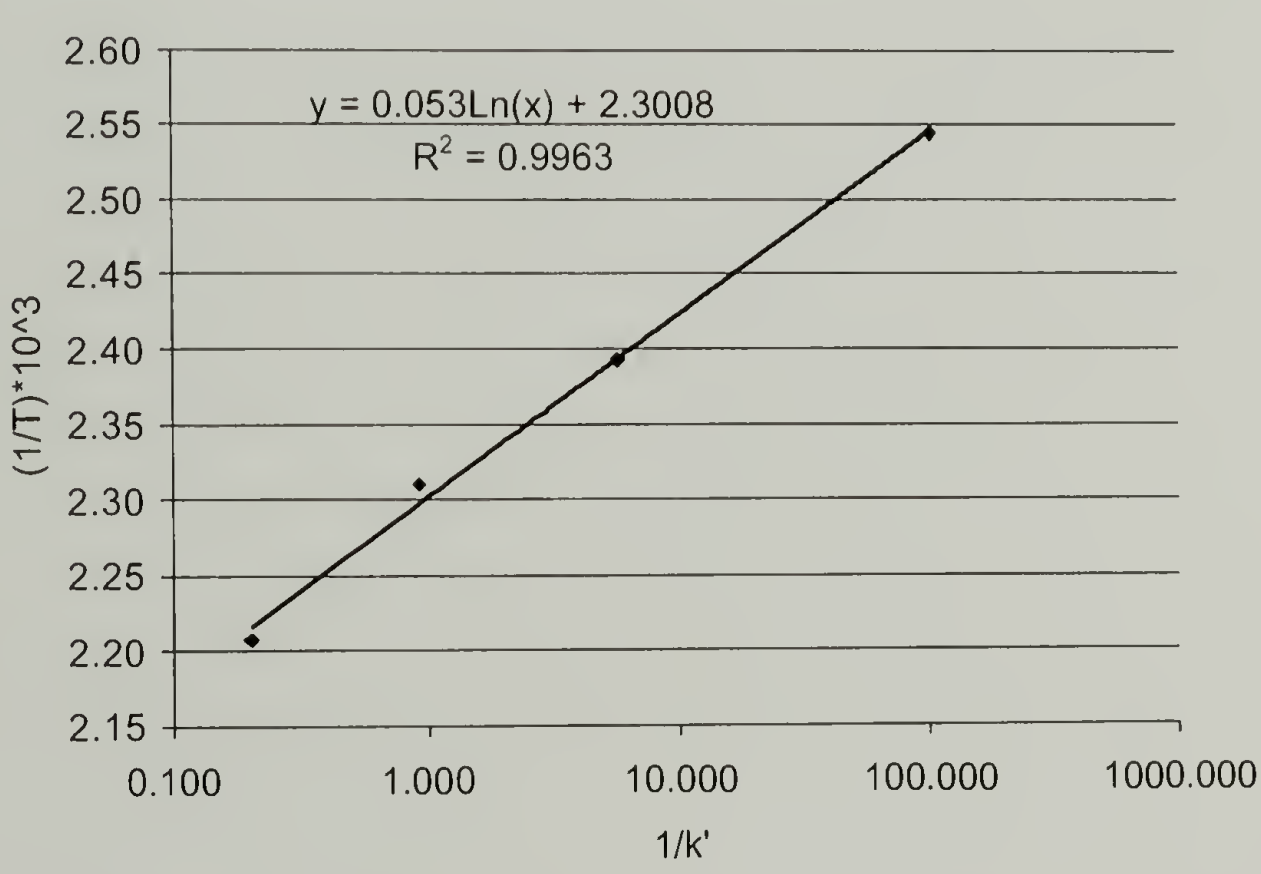

Figure 4.4. Relationship of temperature to shift factor k' for NR (with correlation equation).

Table 4.3 shows the corresponding k' values for temperature from the NR CSR data in Chapter 3. Figure 4.4 highlights the extrapolation equation necessary to get values of k' at temperatures beyond those of CSR experiments. Again using the value of 1 for time (as all HPHTS experiments were conducted for 1 hour), one is able to generate the predicted retention of sintering values for NR from Figure 4.3 by using the k' values of Table 4.3.

Table 4.4. Strength % retention predicted by new bond formation theory and actual HPHTS strength retention results (from Chapter 2) as a function of temperature for NR.

K'	Temp C	% Predicted	HPHTS Actual
0.01	120	<10	10
0.10	140	25	20
0.79	160	35	30
5.81	180	45	35
33.83	200	50	40
170.66	220	55	30
758.80	240	N/A	10

Table 4.4 summarizes the predicted results, along with showing the actual HPHTS retention data from Figure 2.8. As is evident in Table 4.4, the predicted results for NR are slightly higher than those achieved by HPHTS. One potential explanation for this is the intermittent stress relaxation data for NR from Chapter 3 is slightly skewed at higher k't values. In comparison to other literature data on the intermittent stress relaxation of NR, the data appears to be slightly higher.[31] It is possible that oxidation (due to the experimental technique) could be causing a higher value to be recorded than is actually exhibited during HPHTS. A slightly lower intermittent value would move the predicted

and actual HPHTS data into almost perfect agreement. As it is however, the agreement between predicted and actual HPHTS results appears favorable.

4.4 Polyurethane

Although the polyurethane system investigated by Tobolsky in Chapter 3 is different than the polyurethane used for HPHTS in Chapter 2 a comparison and prediction was still conducted. Following the work with polysulfide and NR,

Table 4.5 summarizes the k' values for polyurethane at a variety of experimental and extrapolated (in italics) temperatures. Again, all HPHTS experiments were conducted for 1 hour and as such, the k' value of the corresponding temperature yields the expected retention value. Substituting the k' values into Figure 4.5 one can summarize the expected retention of mechanical properties for the various temperatures as per Table 4.6. The 40 MPa and 45 MPa value are estimates to the starting strength of the polyurethane of the HPHTS experiments in Chapter 2. No initial starting strength was available as the shape of the scrap material did not make tensile testing a viable technique. These estimates of strength are based on literature values of comparable polyurethanes and qualitative strength tests (manual breaking of the material).

As is shown in Table 4.6, the CSR predicted values are very similar to the actual HPHTS results. It appears that the fast decay to zero stress of the continuous stress relaxation, along with a slowly diminishing intermittent curve (as with polysulfide rubber) allows for a significant retention of mechanical strength. Again, as with the polysulfide rubber, it is the eventual lowering of the intermittent stress relaxation curve that leads to lower strength retention after some critical temperature. From Figure 4.5,

this temperature is approximately 170-180°C for polyurethane. This is in excellent agreement with the data from HPHTS of polyurethane in Figure 2.17.

Table 4.5. Extrapolation of shift factor correlation with temperature for polyurethane.

Time (hrs)	k'	1/k'	Temp	1/T*10^3
79	0.01	79.00	90	2.75
7.4	0.14	7.40	110	2.61
2.8	0.36	2.80	120	2.54
1.1	0.91	1.10	130	2.48
0.17	*5.87*	*0.17*	*150*	*2.36*
0.07	*13.94*	*0.07*	*160*	*2.31*
0.03	*31.84*	*0.03*	*170*	*2.26*

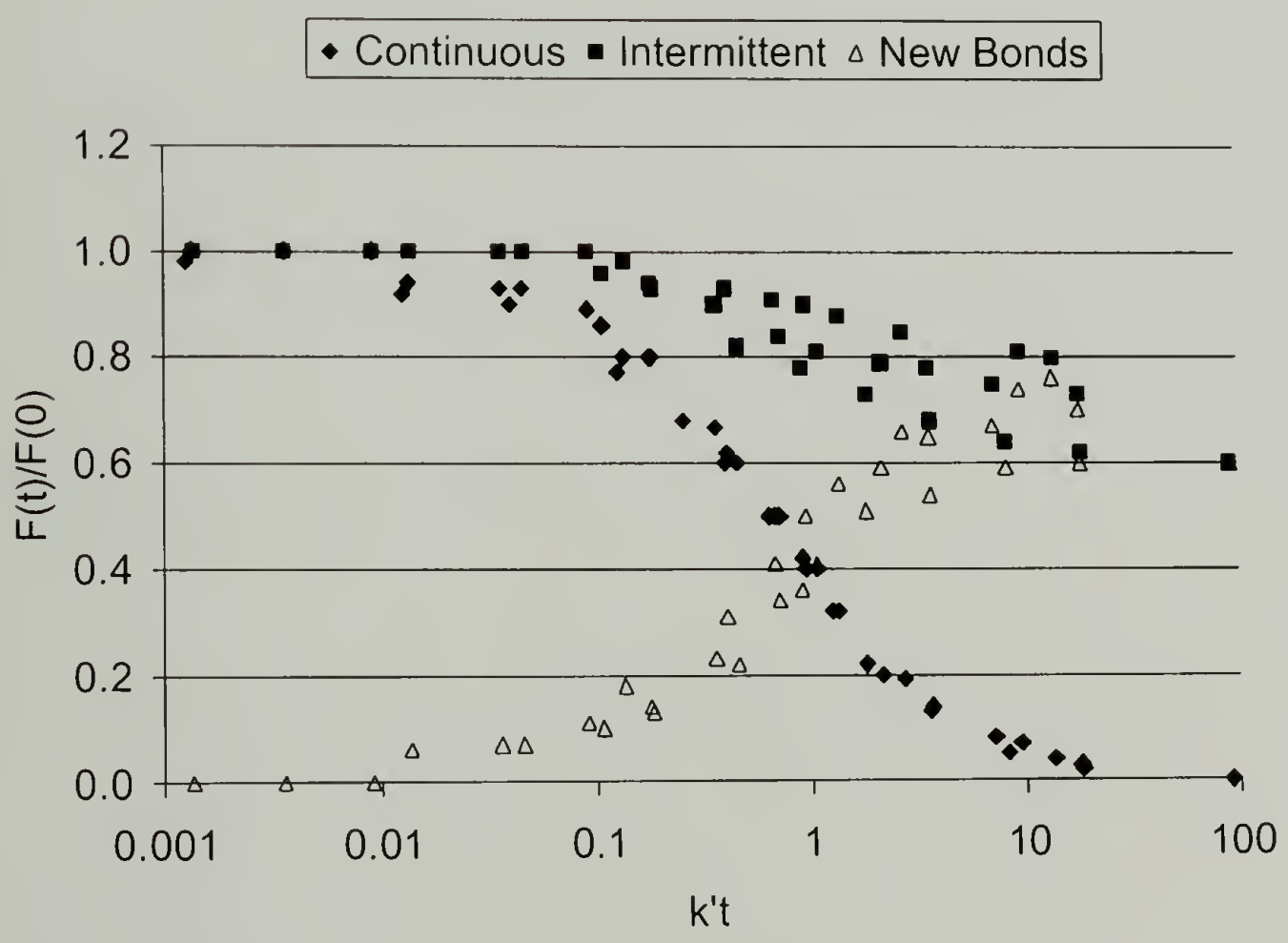

Figure 4.5. Superimposed continuous and intermittent stress relaxation results and calculated new bond formation for polyurethane.

Table 4.6. Strength % retention predicted by new bond formation theory and actual HPHTS strength retention results (from Chapter 2, assuming two different starting strengths) as a function of temperature for polyurethane.

K'	Temp C	% Predicted	HPHTS Actual (40 MPa)	HPHTS Actual (45 MPa)
0.91	130	35	N/A	N/A
2.37	140	60	62	55
5.87	150	65	68	60
13.94	160	75	75	68
31.84	170	70	N/A	N/A
70.13	180	<60	38	30

4.5 Styrene-Butadiene Rubber

Unfortunately, Equation 4.4 is not valid for rubbers that have intermittent values that exceed one during sintering. For example, as shown previously, styrene-butadiene rubber (SBR) overcrosslinks, and therefore its intermittent stress relaxation value is greater than 1 (more bonds form than are broken). Equation 4.4 does not take overcrosslinking into account as a mechanism of strength loss for sintered parts, and therefore cannot be applied in overcrosslinking situations as it predicts N values greater than 1 (or mechanical properties of sintered parts being higher than the virgin properties).

In efforts to predict SBR HPHTS data from CSR a modified new bond formation theory is presented. As Gent's work highlights, strength and crosslink density form a parabolic-like relationship (Figure 2.18). Thus it can be envisioned that overcrosslinking has a similar effect on strength as reversion does. Therefore, by reflecting the intermittent data through I=1, it is hoped that the intermittent stress relaxation data can be converted into a useable form. Figure 4.6 shows this result for the SBR intermittent stress relaxation data.

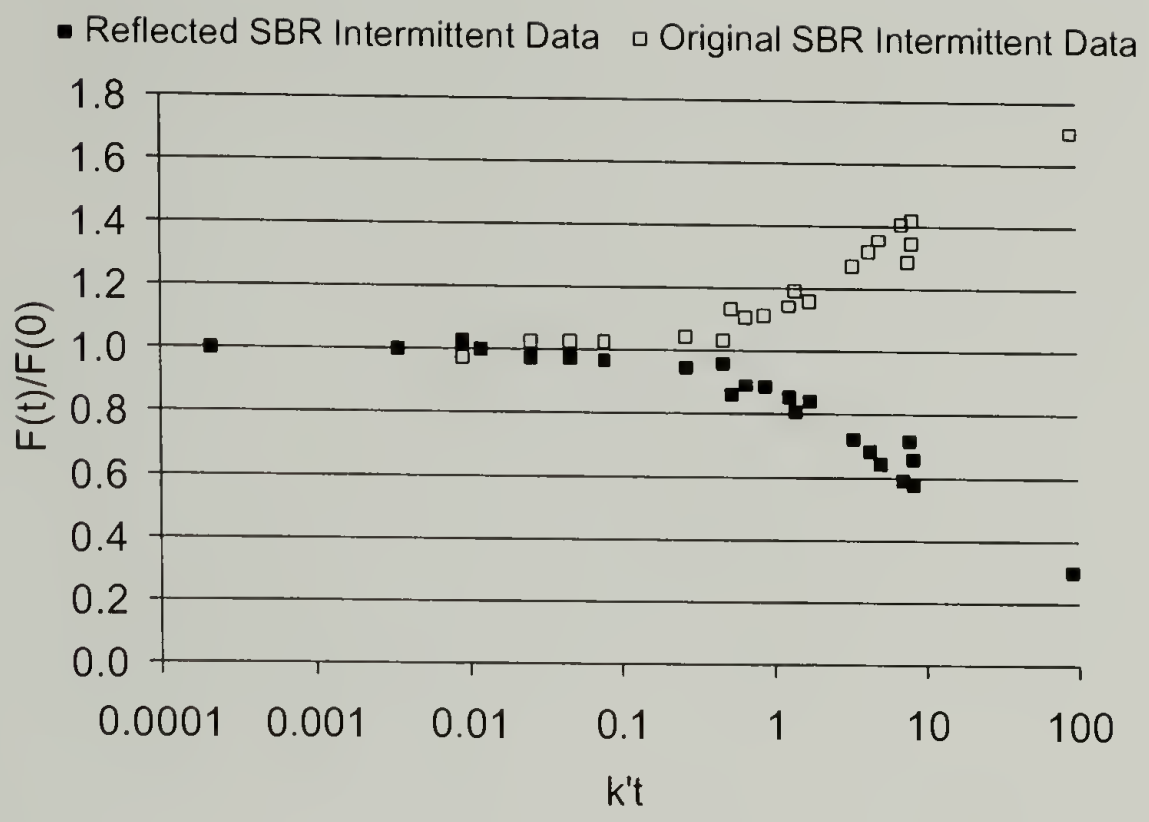

Figure 4.6. Absolute value calculation for SBR intermittent data.

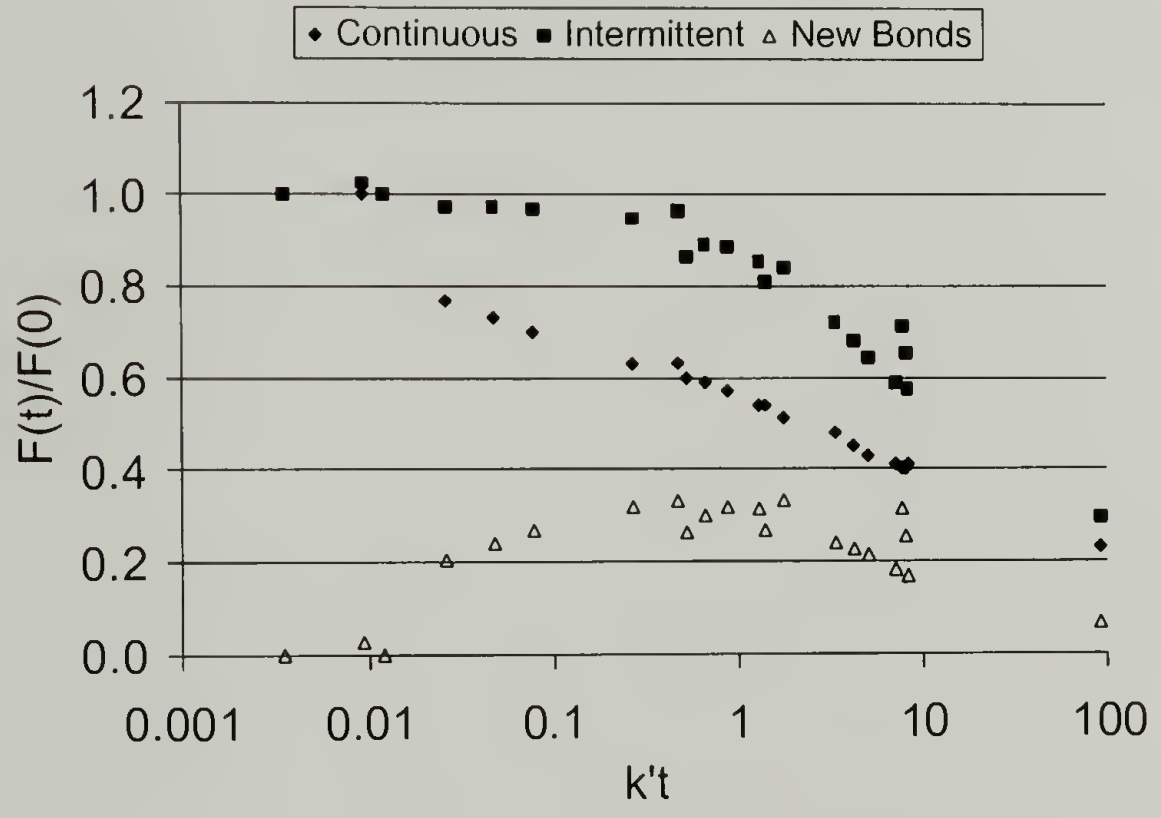

Figure 4.7. Superimposed continuous and intermittent stress relaxation results and calculated new bond formation for SBR.

Table 4.7. Strength % retention predicted by modified new bond formation theory and actual HPHTS strength retention results (from Chapter 2) as a function of temperature for SBR.

K'	Temp C	% Predicted	HPHTS Actual
0.029	180	<10	35
1.225	200	30	40
3.25	220	25	45
7.69	240	25	50
17.05	260	20	50

Figure 4.7 displays the continuous and modified intermittent stress relaxation results and the subsequent predicted new bond formation. Table 4.7 summarizes the predicted and actual HPHTS results for SBR. Unfortunately the new bond formation theory for SBR appears to underestimate property retention. This may have to do with the manner in which the intermittent stress relaxation data was modified to fit the new bond formation equation. To date no conclusions have been drawn for this result.

4.6 New Bond Formation Theory Conclusions

Overall, New Bond Formation Theory appears to be successful in correlating Chemical Stress Relaxation with HPHTS results. The theory clearly illustrates why thermosets that maintain constant crosslink densities during sintering retain the largest percentage of original mechanical properties. The data presented also highlights how CSR is able to predict the recyclability and optimum temperature for sintering for most thermosets. This is very useful as it eliminates the trial and error associated with grinding and molding numerous parts in order to obtain a thermosets critical temperature.

CHAPTER 5

ADDITIVES AND HPHTS

5.1 Background

The previous chapters helped formulate a mechanistic understanding of the HPHTS process and how each type of thermoset behaves differently under the extreme temperature conditions of sintering. The goal of this chapter is to apply this knowledge in efforts to increase mechanical property retention through the use of additives. Gent's[30] work highlighted how thermosets often have maximum strength at one crosslink density. Altering the crosslink density from this maximum strength crosslink density to either higher or lower values lowers the strength of the thermoset. As the previous CSR work demonstrated, the conditions needed for HPHTS can change the crosslink density of the sintered thermosets; it is believed that this is the reason they exhibit lower mechanical properties than the original starting thermosets. It was hoped that chemical additives could reduce reversion and overcrosslinking, and maintain a constant crosslink density and therefore improve mechanical properties.

5.2 Reversion

Reversion is a term used in the rubber industry to describe decreases in the mechanical properties (namely modulus, elongation, and strength) at the end of the curing period or during service.[38] Although the complete mechanistic formulation of reversion is still debated, most prominent scientists in this field conclude that reversion results from a degradation of load bearing sulfur crosslinks along the backbone of the rubber main chain. It is also known that certain rubbers (isoprene containing rubbers such as NR) are

more susceptible to reversion reactions than are other rubbers (SBR, nitrile, etc.). It has recently been demonstrated that zinc complexes have the ability to catalyze reversion reactions, and thus after curing can lower the obtained properties. Unfortunately, zinc is used in almost all sulfur cured rubber systems due to its ability to dramatically increase cure rate, and thus it is not likely to be eliminated from vulcanization packages any time soon. In several papers, Nieuwenhuizen, et al.[38,39,40] demonstrate the role of zinc complexes in reversion reactions, and show (through model reactions) their influence on the main rubber backbone. The conclusion from the work is that zinc complexes accelerate the breakdown of sulfur crosslinks, resulting in the formation of cyclic sulfur, and diene and triene structures along the backbone of the rubber where the sulfur crosslinks had previously been (see Figure 5.1).

Nieuwenhuizen, et al. continued their work by developing two logical strategies to counteract the reversion phenomenon.[38] First, they proposed deactivation of the zinc complex, and thus elimination of its catalytic activity promoting reversion, and second, the use of anti-reversion additives such as biscitraconimides. The role of the biscitraconimides is to replace broken sulfur cross-links with new more thermally stable carbon crosslinks (see Figure 5.2). It is believed that the biscitraconimides react through a Diels-Alder type mechanism to reattach the chains where crosslinks previously had been, thus eliminating the loss of mechanical properties normally observed when reversion occurs.[40,41,42,43]

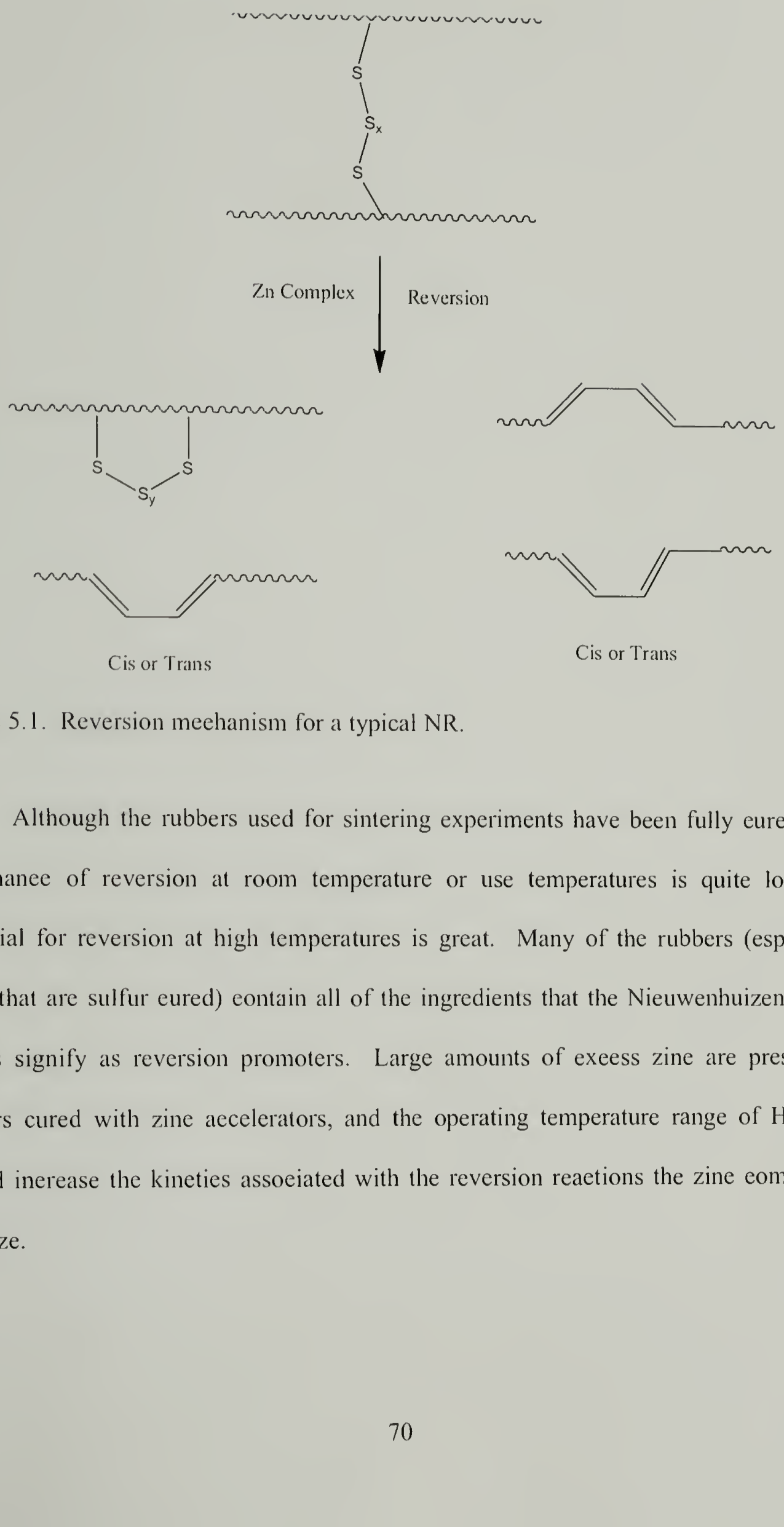

Figure 5.1. Reversion meehanism for a typical NR.

Although the rubbers used for sintering experiments have been fully eured, and the chanee of reversion at room temperature or use temperatures is quite low, the potential for reversion at high temperatures is great. Many of the rubbers (especially those that are sulfur eured) eontain all of the ingredients that the Nieuwenhuizen, et al. papers signify as reversion promoters. Large amounts of exeess zine are present in rubbers cured with zine aeeelerators, and the operating temperature range of HPHTS should inerease the kineties assoeiated with the reversion reaetions the zine eomplexes eatalyze.

Tripathy added organic acids (retarders in typical vulcanization packages) to a NR powder sample prior to HPHTS.[44] It is believed that the acids react with, and neutralize, common accelerators such as 2-mercaptobenzothiazole (MBT), and help slow the formation of the zinc complex [$Zn(MBT)_2$] believed to be the main accelerator in crosslink formation during vulcanization. Interestingly, most of the employed organic acids showed an increase in mechanical properties (modulus, strength, and elongation) obtained for the sintered natural rubber system investigated. Furthermore, Morin concluded that chemicals used for rubber acceleration (MBT, ZnO, etc.) often lowered HPHTS property retention, while chemicals typically termed "retarders" or vulcanization inhibitors, generally improved HPHTS property retention.[23]

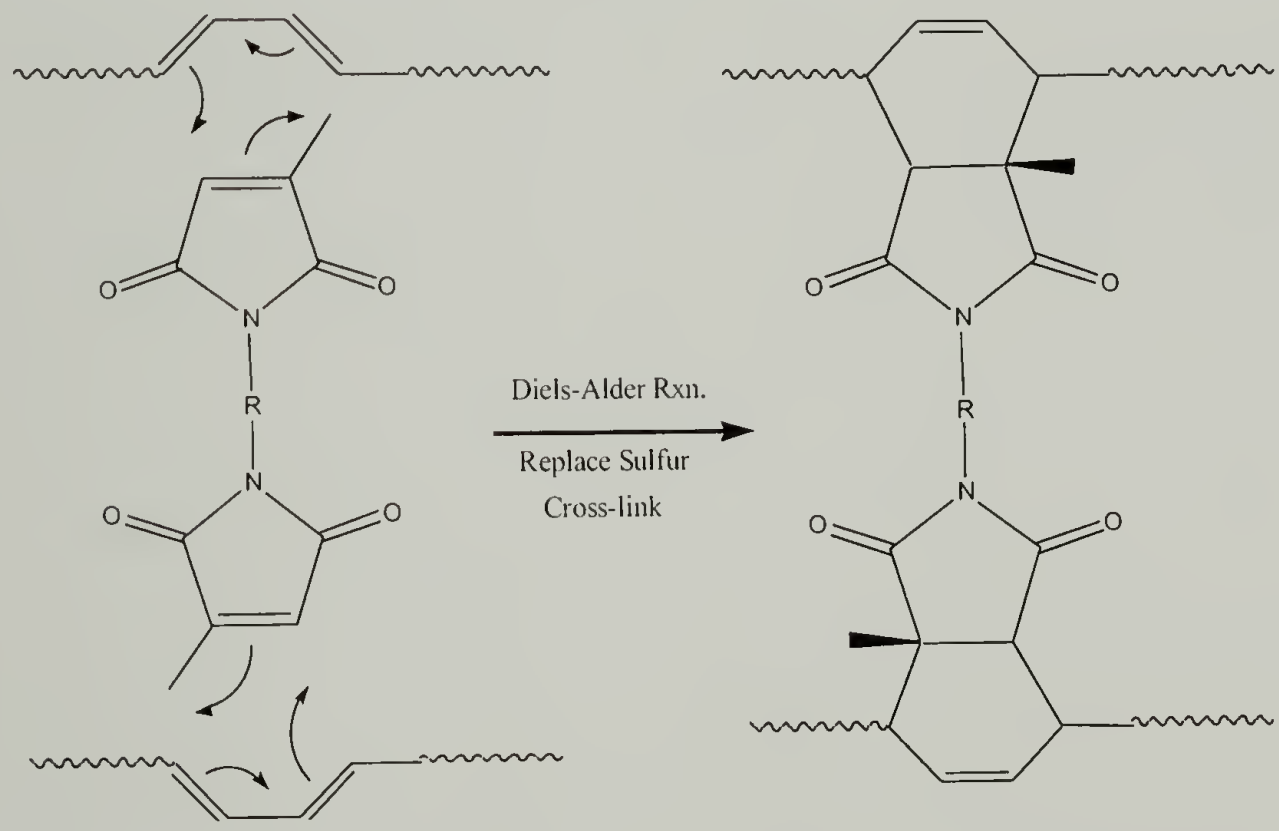

Figure 5.2. Proposed mechanism for anti-reversion behavior of biscitraconimides.

The current understanding is that these additives may be reducing the amount of the zinc complex present, thus limiting reversion as suggested by Nieuwenhuizen, et al. In addition, acids that contained a double bond showed the largest increase in properties. It is likely that this double bond may be able to bridge a broken crosslink in a similar to, yet mechanistically different manner than the biscitraconimides. Figure 5.3 depicts a potential mechanism for maleic anhydride.

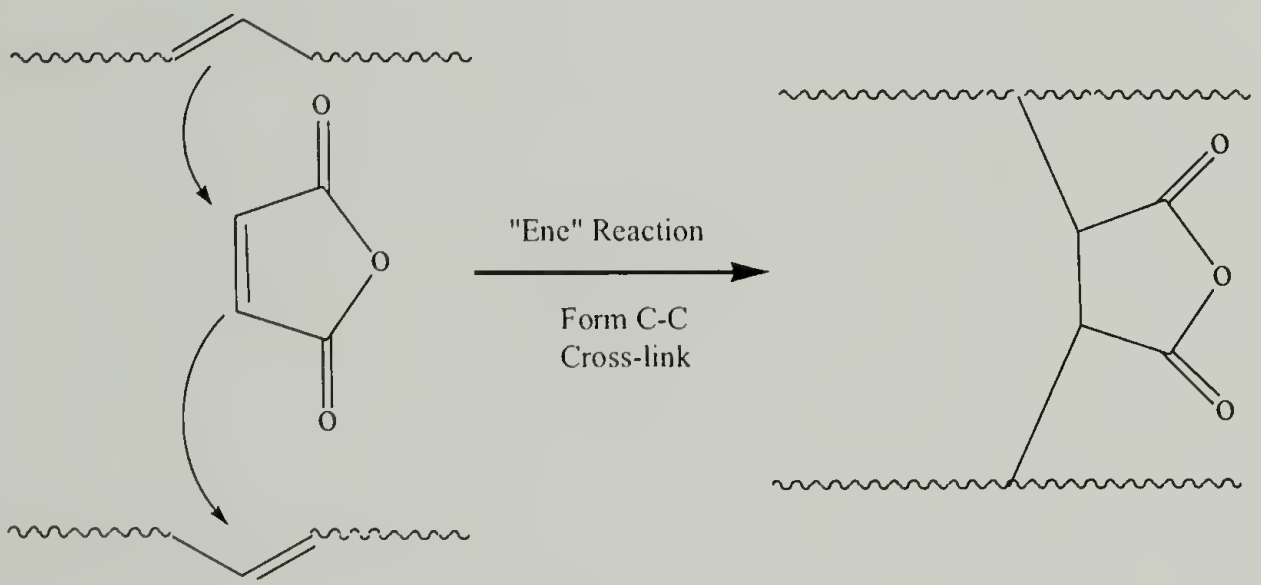

Figure 5.3. Proposed mechanism for "ene" reaction of maleic anhydride with a double bond.

5.2.1 Experimental and Materials

Materials:

Stearic acid (98%, Aldrich), molecular sulfur (Flexsys), zinc oxide (99%, powder, <1μm, Aldrich), N-cyclohexyl-2-benzothiazole sulfenamide (Santocure CBS, Flexsys) were used without further purification. Dipolarophiles and dienophiles: benzoic acid (99%, Aldrich), salicylic acid (99%, Aldrich), maleic acid (99%, Aldrich), phthalic acid (98%, Aldrich), adipic acid (98%, Aldrich), maleic anhydride (99%, Fluka), phthalic anhydride (99%, Aldrich), phthalimide (99%, Aldrich), N-methylphthalimide (98%,

Aldrich) were used as received. Sulfur vulcanized styrene-butadiene rubber (silica and carbon black-filled) obtained from the Bayer Corporation and carbon black-filled natural rubber procured from Trico Products were used as received.

Cryo-grinding, HPHTS and Mechanical Testing:

Vulcanized rubber (SBR and NR) was converted to a powder as described in Chapter 2. Sintering was conduced by first powder mixing the chemicals and the rubber powder and then subjecting the mixture to 200°C and 8.5 MPa using compression molding for one hour as described in Chapter 2. The mechanical behavior of the vulcanized and sintered samples was calculated as per Chapter 2.

5.2.2 Organic Acids and NR

Tripathy et al. and Morin highlight the results of the addition of organic acids to natural rubber.[23,44] The overall results are summarized in Table 5.1. As is evident, organic acids significantly increase property retention for natural rubber. The 100% modulus data also illustrates that double bond containing molecules likely induce additional crosslinking since both the maleic acid and maleic anhydride 100% modulus results are significantly higher than the original rubber and that of the HPHTS part with no additives. Tripathy provides further data supporting the idea of the organic acid molecules inhibiting reversion reactions during sintering and delves into a potential mechanism[44] It was with this knowledge that the work was expanded to other thermoset systems.

Table 5.1. HPHTS results for NR powder mixed with various additives prior to sintering (% indicates loading percentage).

Additive (loading in parentheses)	Strength at Break (MPa)	Elongation at Break (%)	100% Modulus (MPa)
NR Original	14.5	420	1.8
NR Sintered	5.3	520	0.9
Phthalic Anhydride (2%)	8.9	500	1.1
Maleic Acid (6%)	8.3	580	2.8
Maleic Anhydride (6%)	8.1	560	2.8
Phthalimide (4%)	9.6	540	1.4

5.2.3 Organic Acids and Carbon Black-Filled SBR

Figure 5.4 highlights the chemicals used in the study on carbon black-filled styrene butadiene rubber (SBR). The phthalimide, N-methylphthalimide, phthalic anhydride and 3,3',4,4'-benzophenonetetracarboxylic dianhydride are all organic acid derived molecules used previously to complex with the ZnMBT complex. While these compounds appear to reduce reversion in the HPHTS of NR, their incorporation here is aimed at stopping the overcrosslinking reactions that occur when SBR is sintered at high temperatures. 1,3 Biscitraconimidomethyl benzene (Perkalink) is an anti-reversion agent and was introduced into the study before the overcrosslinking mechanism of SBR during HPHTS was well understood. Finally, the maleic anhydride is a combination molecule as it can act as an organic acid as well as an extra crosslinker due to its double bond.

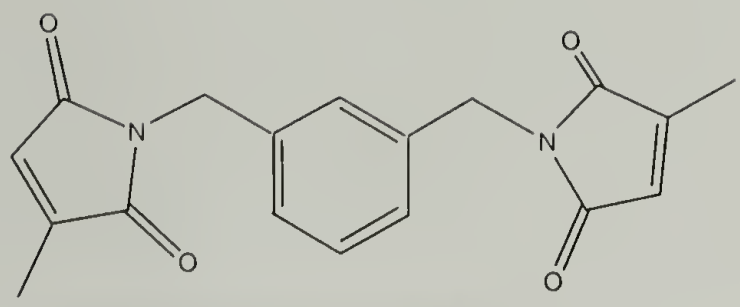

1,3-Biscitraconimidomethyl Benzene (Perkalink)

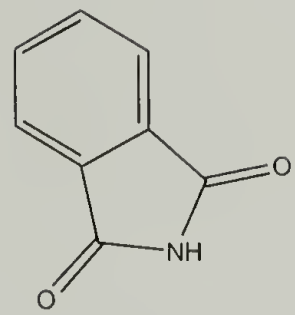

Phthalimide

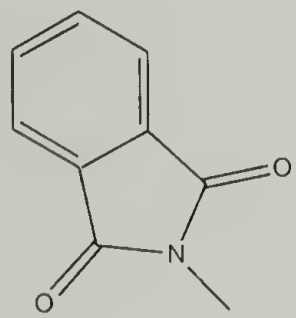

N-Methylphthalimide

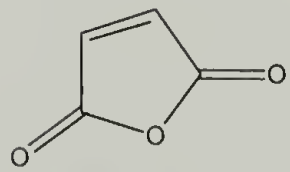

Maleic Anhydride

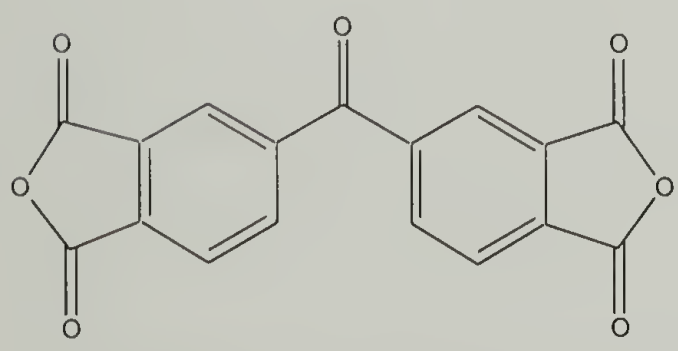

3,3',4,4'-Benzophenonetetracarboxylic dianhydride

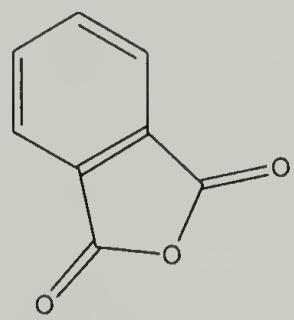

Phthalic Anhydride

Figure 5.4. Chemical illustrations of several additives used.

Figure 5.5, Figure 5.6, and Figure 5.7 show the strength at break, elongation at break, and 100% modulus results, respectively, for the HPHTS of carbon black-filled SBR with a variety of additives, along with the HPHTS sheet with no additives (sintered powder) and an original vulcanized sheet (original). As the figures show, none of the additives significantly increase the mechanical properties of the HPHTS parts. Perkalink and sulfur improve the strength at break of the HPHTS parts, however both lower the

elongation at break and significantly increase the 100% modulus (indicating extreme overcrosslinking is occurring). Phthalimide and N-methylphthalimide appear to have no effect on the mechanical properties. The rest of the compounds employed appear to lower the mechanical properties. It is also clear from the 100% modulus data that maleic anhydride does not induce as much extra crosslinking as with the natural rubber system.

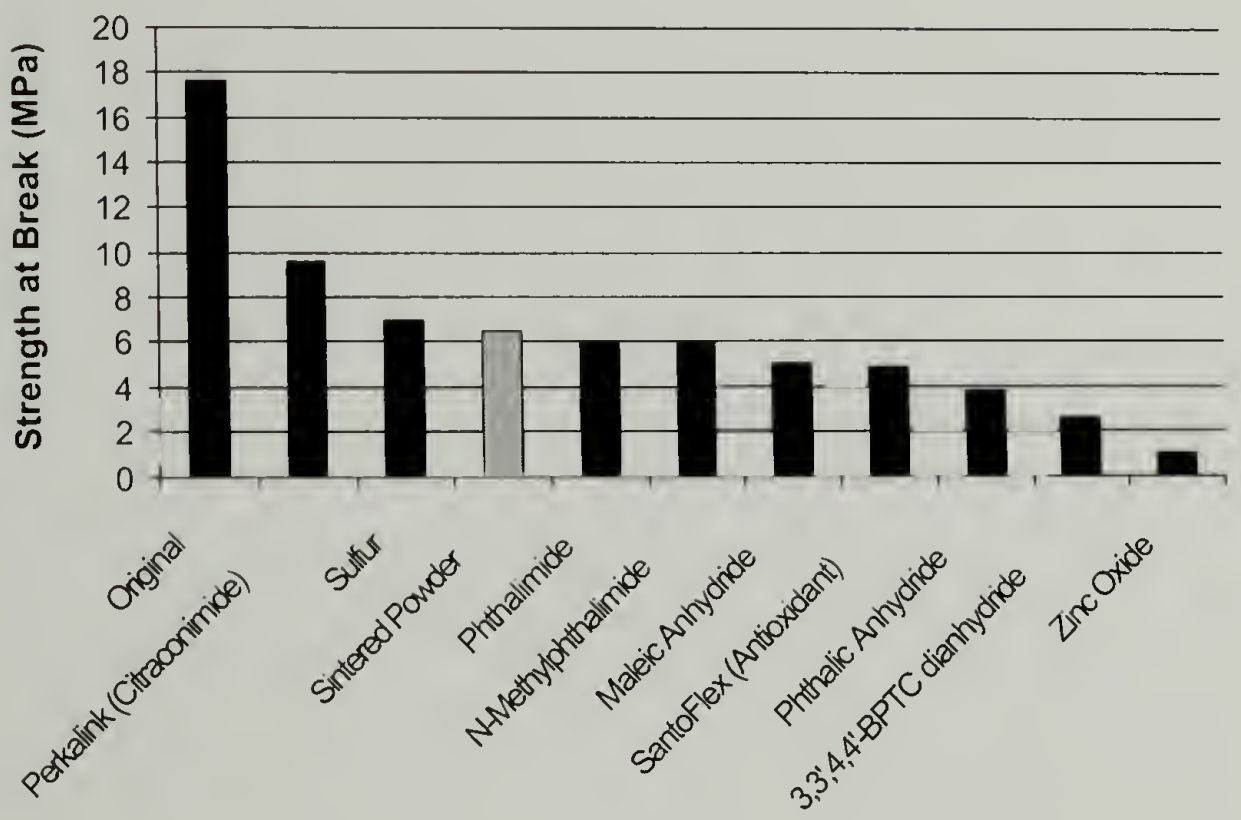

Figure 5.5. Strength at break vs. additive (3% loading) for carbon black-filled SBR sintered at 200°C and 8.6 MPa for 1 hour.

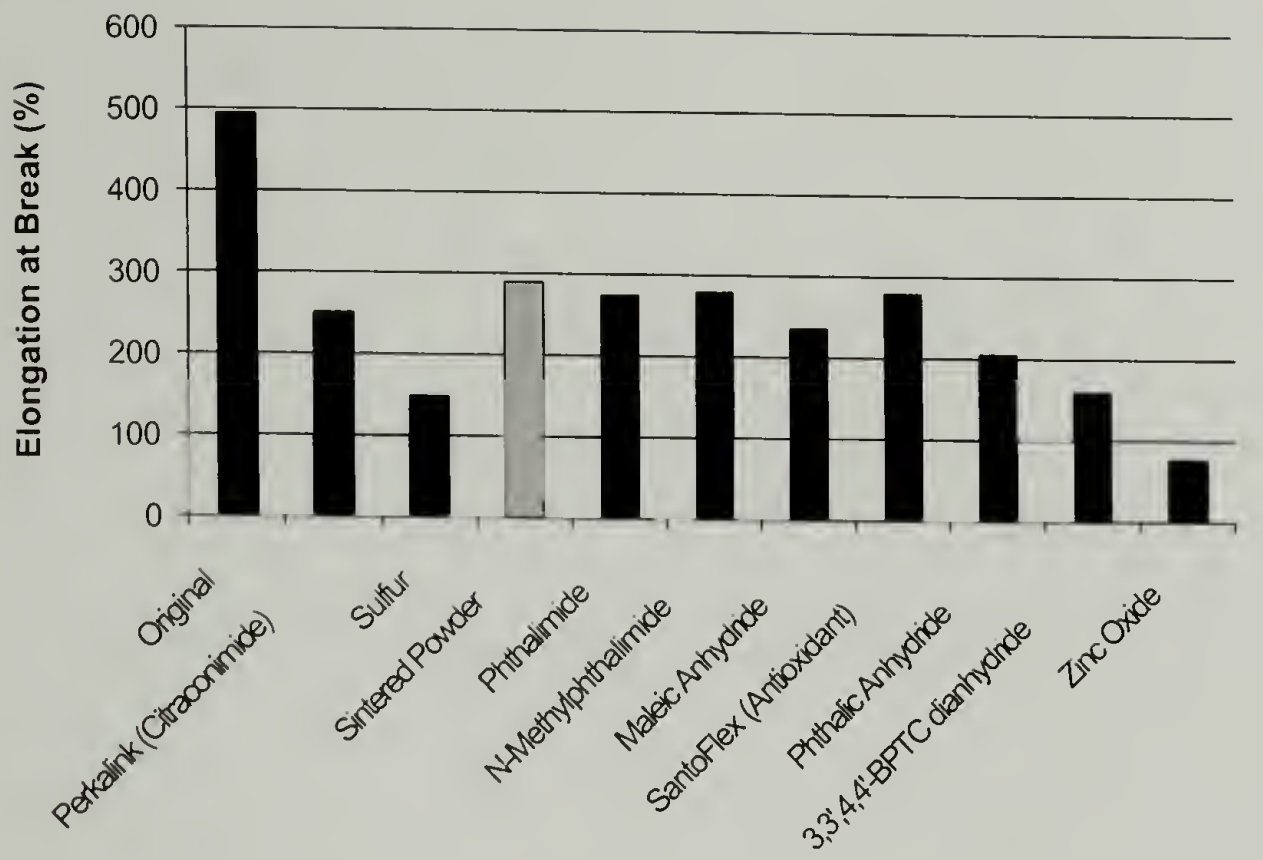

Figure 5.6. Elongation at break vs. additive (3% loading) for carbon black-filled SBR sintered at 200°C and 8.6 MPa for 1 hour.

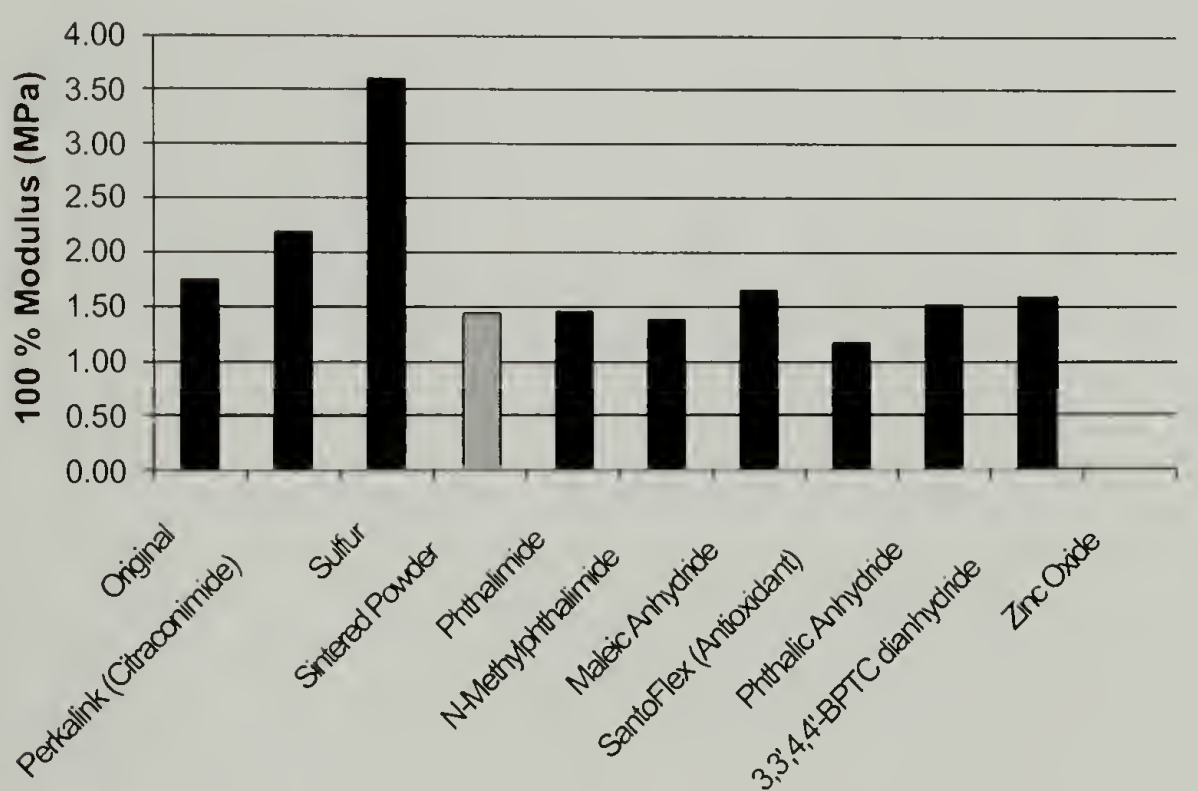

Figure 5.7. 100% modulus vs. additive (3% loading) for carbon black-filled SBR sintered at 200°C and 8.6 MPa for 1 hour.

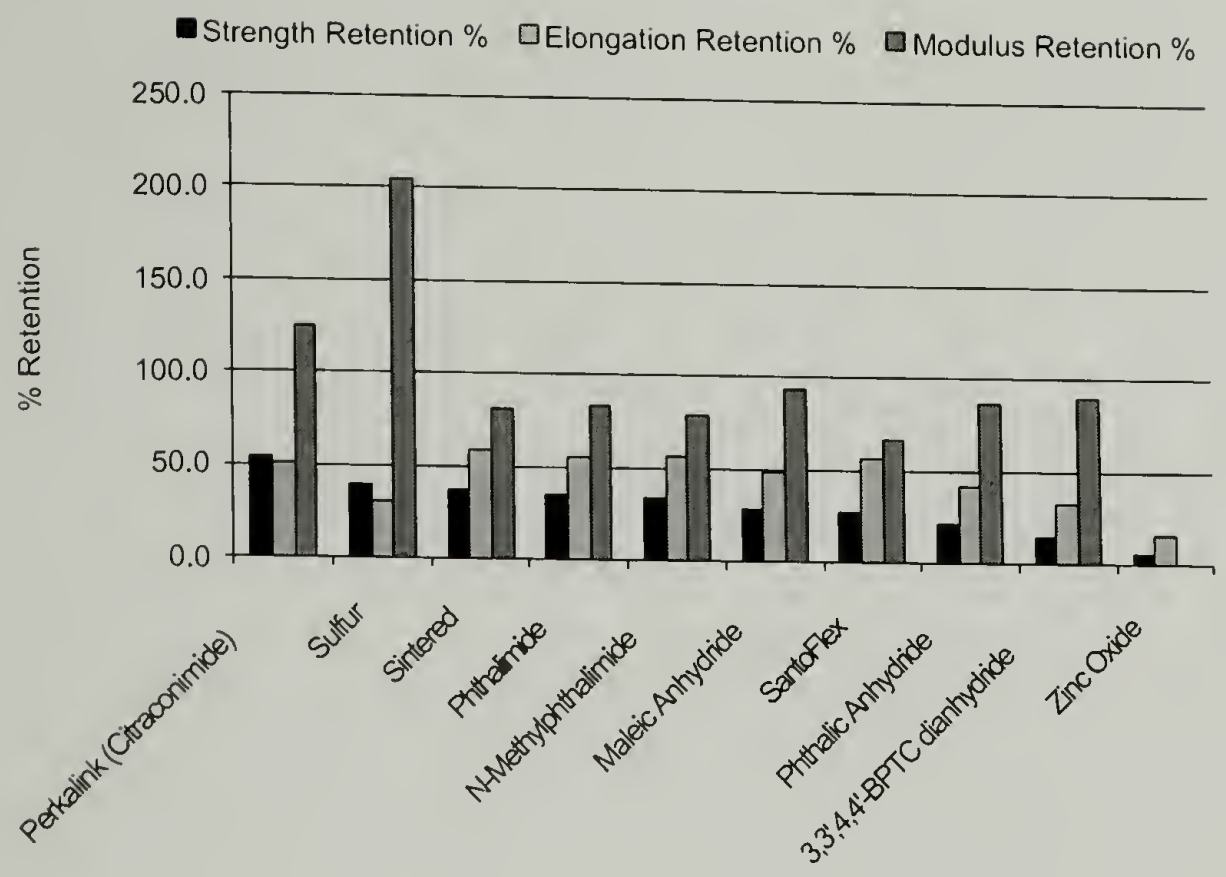

Figure 5.8. Summary of the mechanical property retention for the various additives employed in the carbon black-filled SBR study.

Figure 5.8 summarizes the retention data for all of the additives employed. Perkalink appears to be the only additive offering an increase in properties. The majority of the additives has little to no effect on the mechanical properties and actually lowered the retention of mechanical properties compared to the sintered part with no additives. Evaluating Perkalink's retention values in comparison to SBR sintered at different temperatures, it appears that incorporating 3% Perkalink and sintering at 200°C yields a part comparable to one sintered at 250°C with no additives. As 250°C is the optimum temperature for HPHTS of SBR, it does appear that Perkalink offers a slight benefit (a lower mold temperature) if one is able to deal with the increase in 100% modulus. Overall, however, the results of adding organic acids and anti-reversion agents to carbon black-filled SBR do not approach those obtained with NR.

5.2.4 Organic Acids and Silica-Filled SBR

Figure 5.9, Figure 5.10 and Figure 5.11 show the strength at break, elongation at break and 100% modulus results, respectively, for the addition of organic acids to silica-filled SBR along with the HPHTS sheet with no additives (sintered) and an original vulcanized sheet (original). Similar to the work on carbon black-filled SBR, the organic acids do not significantly increase the strength at break or elongation at break results with silica-filled SBR. Perkalink, does appear to increase the strength at break and allows for over 75% retention of the original strength. This is the highest value obtained for a SBR system. However, it does appear that Perkalink lowers the elongation at break (in comparison to the HPHTS sample with no additives), and also results in overcrosslinking (100% modulus higher than original).

Figure 5.12 summarizes the retention percentages for silica-filled SBR. The results are very similar to those obtained for the carbon black-filled SBR. Perkalink appears to be the only additive that increases mechanical properties. However, the addition of Perkalink results in an overcrosslinking of the rubber that raises the 100% modulus value above the original. The other organic acid additives appear to offer little improvement in mechanical properties.

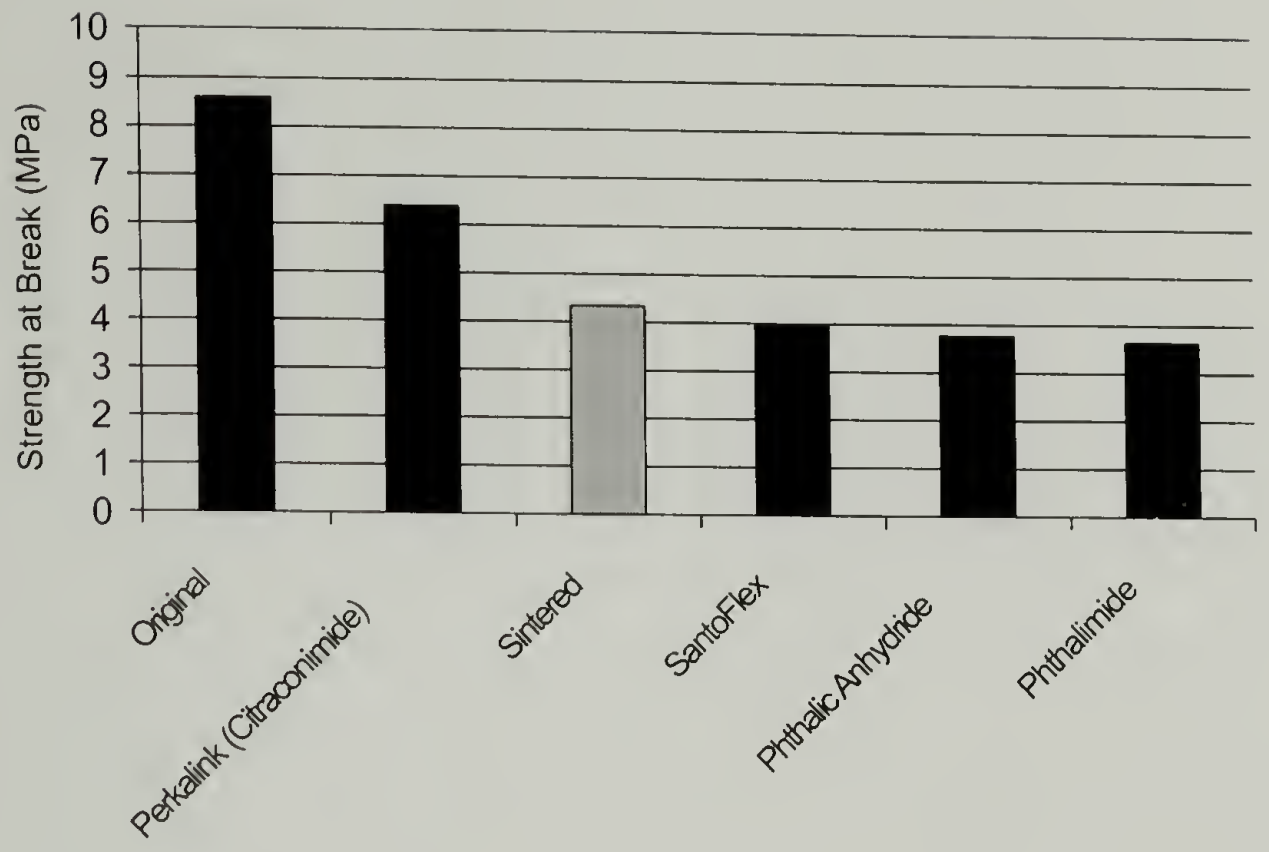

Figure 5.9. Strength at break vs. additive (3% loading) for silica-filled SBR sintered at 200°C and 8.6 MPa for 1 hour.

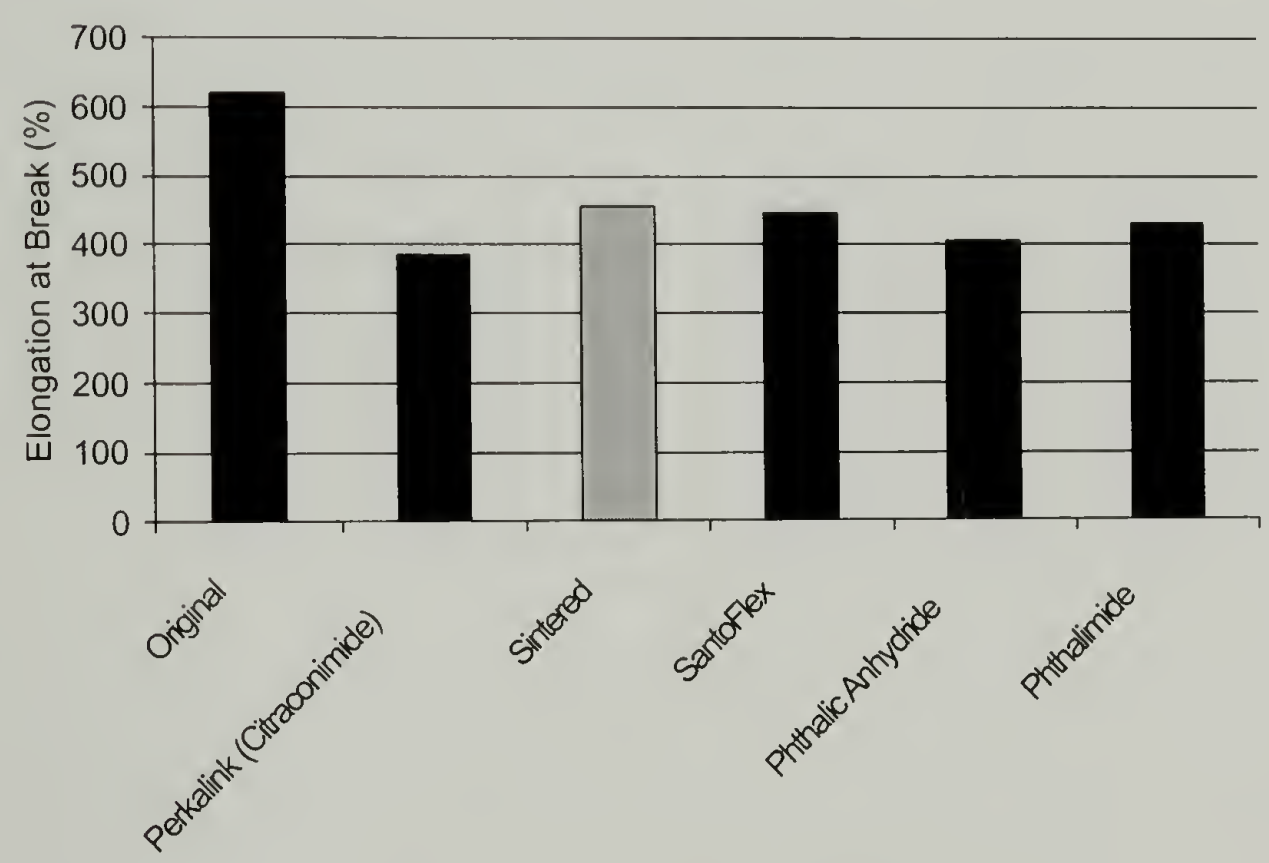

Figure 5.10. Elongation at break vs. additive (3% loading) for silica-filled SBR sintered at 200°C and 8.6 MPa for 1 hour.

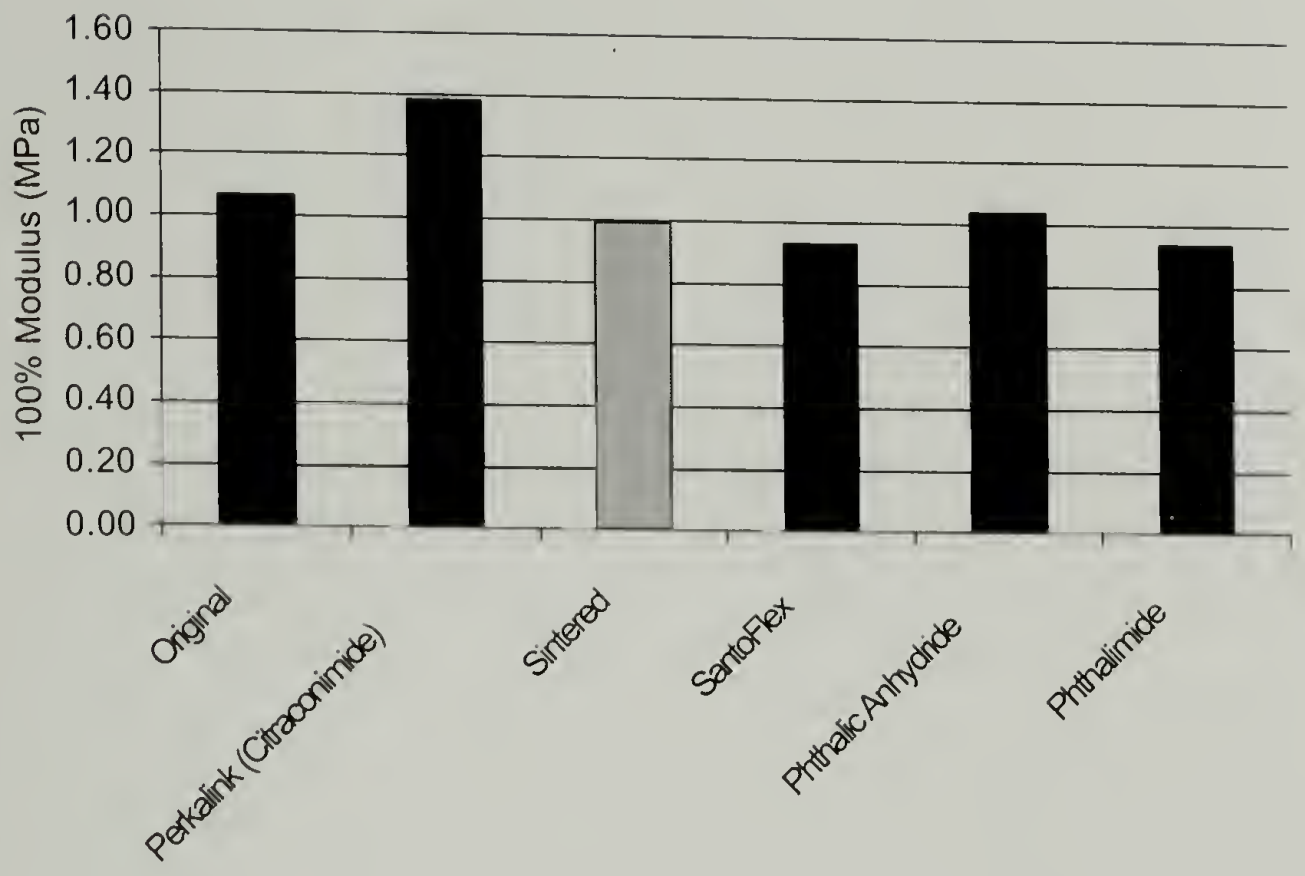

Figure 5.11. Strength at break vs. additive (3% loading) for silica-filled SBR sintered at 200°C and 8.6 MPa for 1 hour.

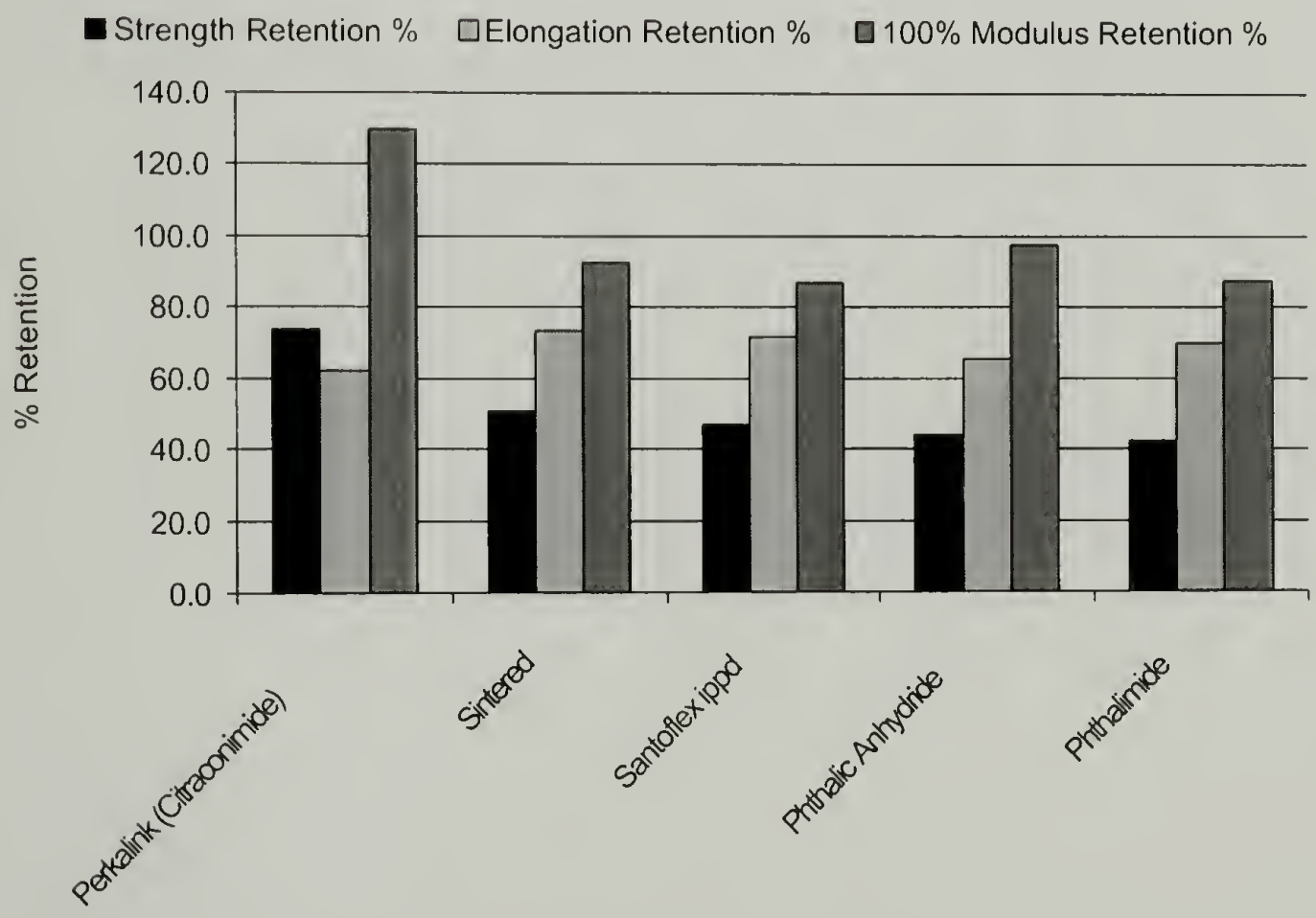

Figure 5.12. Summary of the mechanical property retention for the various additives employed in the silica-fille SBR study.

5.2.5 Anti-Reversion Agents and NR

After the initial studies on organic acids, an in-depth survey of the anti-reversion agent Perkalink was conducted. The purpose of Perkalink is to replace sulfur crosslinks that break after initial vulcanization. As shown previously, Perkalink conducts a Diels-Alder type reaction with conjugated dienes from broken crosslinks and thus builds back crosslink density. As NR showed crosslink loss during HPHTS and CSR experiments, Perkalink appeared to be an ideal additive to counteract crosslink loss and thus potentially improve mechanical properties.

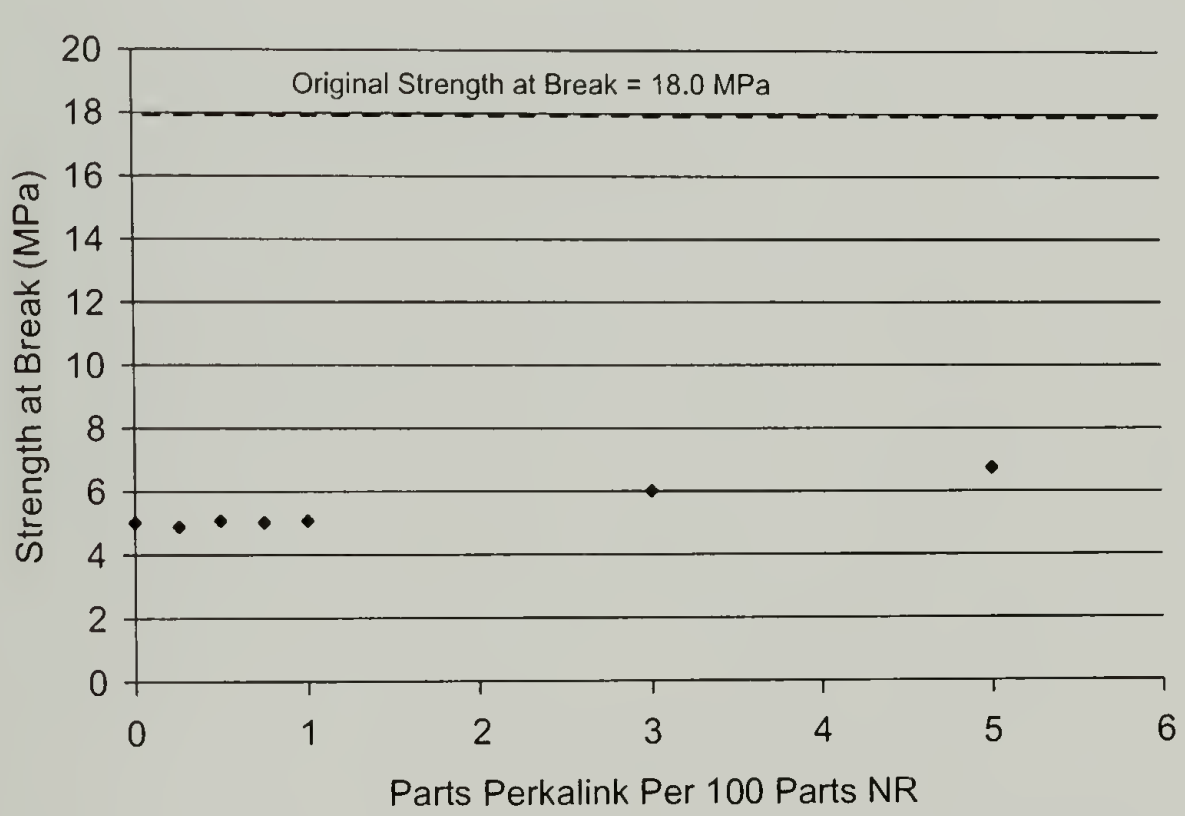

Figure 5.13. Strength at break vs. parts Perkalink per 100 parts rubber for carbon black-filled NR sintered at 200°C and 8.6 MPa for 1 hour.

Figure 5.13 shows the HPHTS strength at break results as one increases the loading of Perkalink in NR (original vulcanized properties of NR shown with dashed line). It appears that at low loadings, no beneficial effect is evidenced. Increasing the

loading to 3 and 5 phr, however, does increase the strength at break retention. In this specific example, the retention was raised by more that 15% at a 5 phr loading. However, Figure 5.14 shows the loading effect on the elongation at break. Addition of Perkalink causes a pronounced lowering of the elongation at break, suggesting additional crosslinking is occurring. This extra crosslinking is evidenced in the 100% modulus results of Perkalink addition in Figure 5.15. Here, as the loading of Perkalink is increased, a linear increase in the 100% modulus (crosslink density) is observed. It is also noted that above 1 phr loading, the 100% modulus values exceed the original 100% modulus, indicating that the rubber has incurred excessive crosslinking.

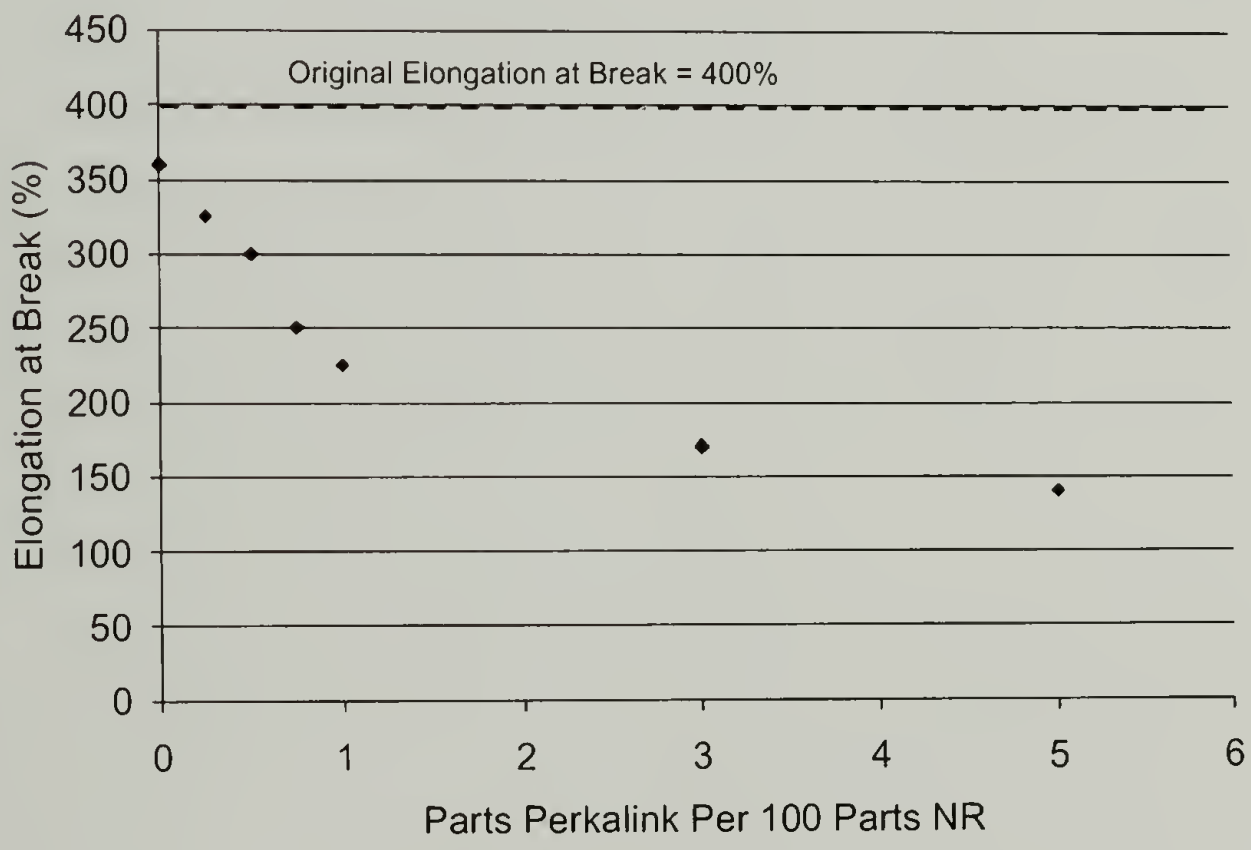

Figure 5.14. Elongation at break vs. parts Perkalink per 100 parts rubber for carbon black-filled NR sintered at 200°C and 8.6 MPa for 1 hour.

Overall, the results suggest that in this NR system, addition of Perkalink (an anti-reversion agent) does not increase the retention of properties during HPHTS. Although slight increases in strength at break are observed, these increases are more than offset by losses in the elongation at break, and excess increases in the 100% modulus, signifying overcrosslinking.

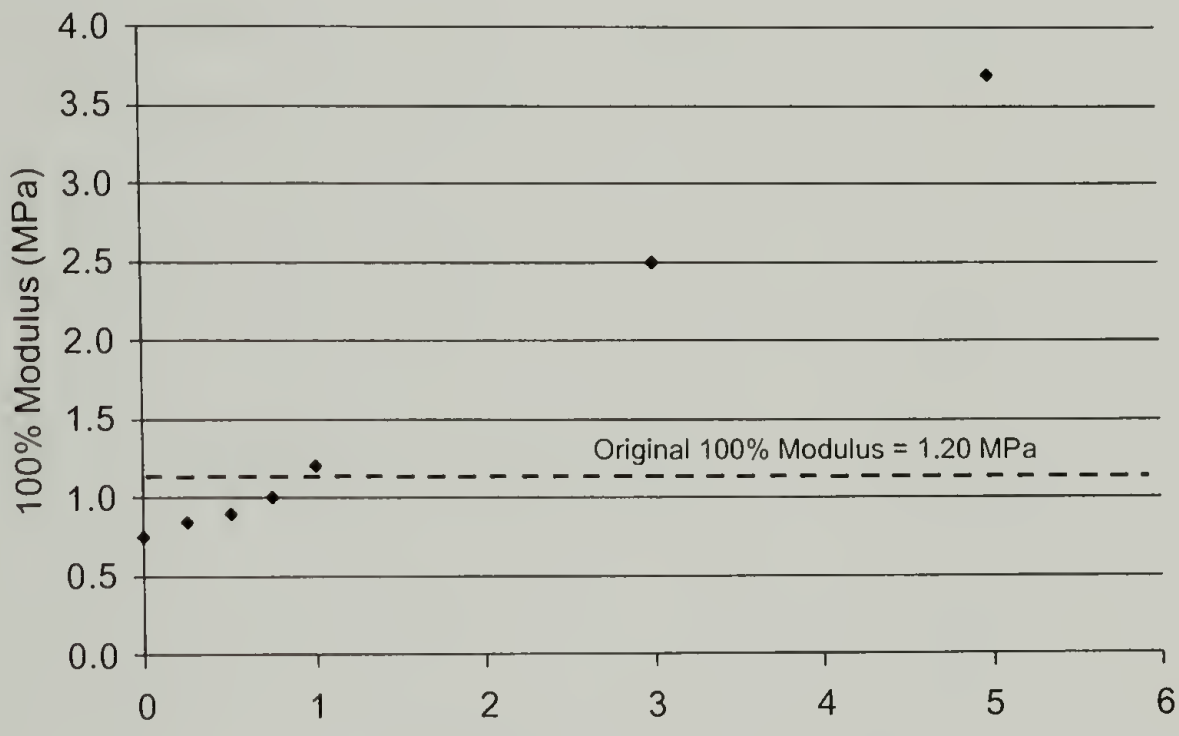

Figure 5.15. 100% Modulus vs. parts Perkalink per 100 parts rubber for carbon black-filled NR sintered at 200°C and 8.6 MPa for 1 hour.

5.2.6 Anti-Reversion Agents and Carbon Black-Filled SBR

As shown earlier, the anti-reversion agent Perkalink increased property retention when added to a carbon black-filled SBR. To better understand the effect of Perkalink, a study was conducted whereby the loading of Perkalink was varied over a wide range (initial work done only at 3 phr loading). Figure 5.16, Figure 5.17 and Figure 5.18 show the strength at break, elongation at break and 100% modulus data, respectively, for HPHTS parts produced with a variety of Perkalink loadings (original vulcanized

properties shown with dashed line). From the figures, it appears that the initial loading investigated (3 phr) offers the best property retention. Above this loading condition, the strength at break is lowered and the 100% modulus begins to flatten. Over all loadings, the elongation at break diminishes, although it also appears to flatten at very high loadings of Perkalink.

Overall, the results initially follow the expected trend of higher strength at break and 100% modulus with a lower elongation at break. However, the data from the large loadings of Perkalink does not seem to follow. It may be possible that extra Perkalink (not reacting) is acting as a plasticizer in the rubber, thus accounting for the lower observed properties, however, this was not observed in the NR system at high loadings and thus is just speculation.

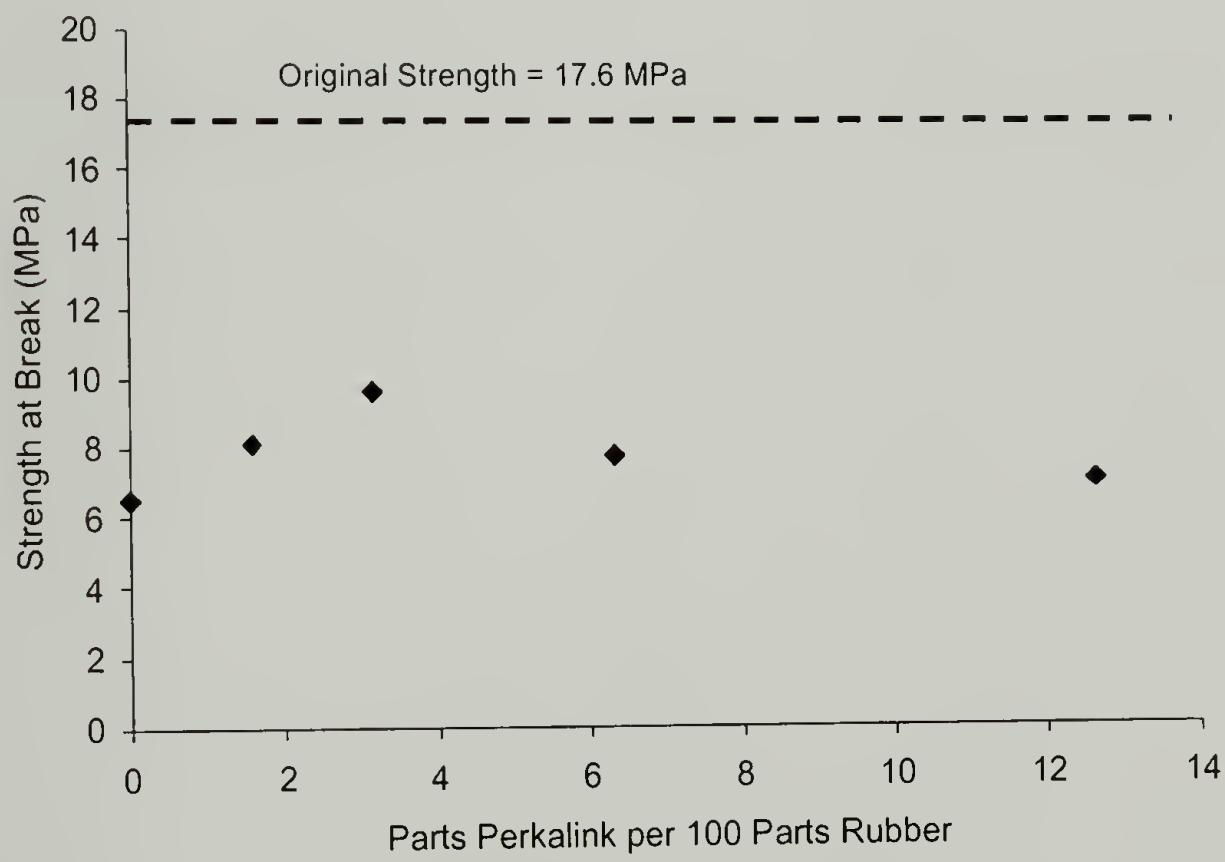

Figure 5.16. Strength at break vs. parts Perkalink per 100 parts rubber for carbon black-filled SBR sintered at 200°C and 8.6 MPa for 1 hour.

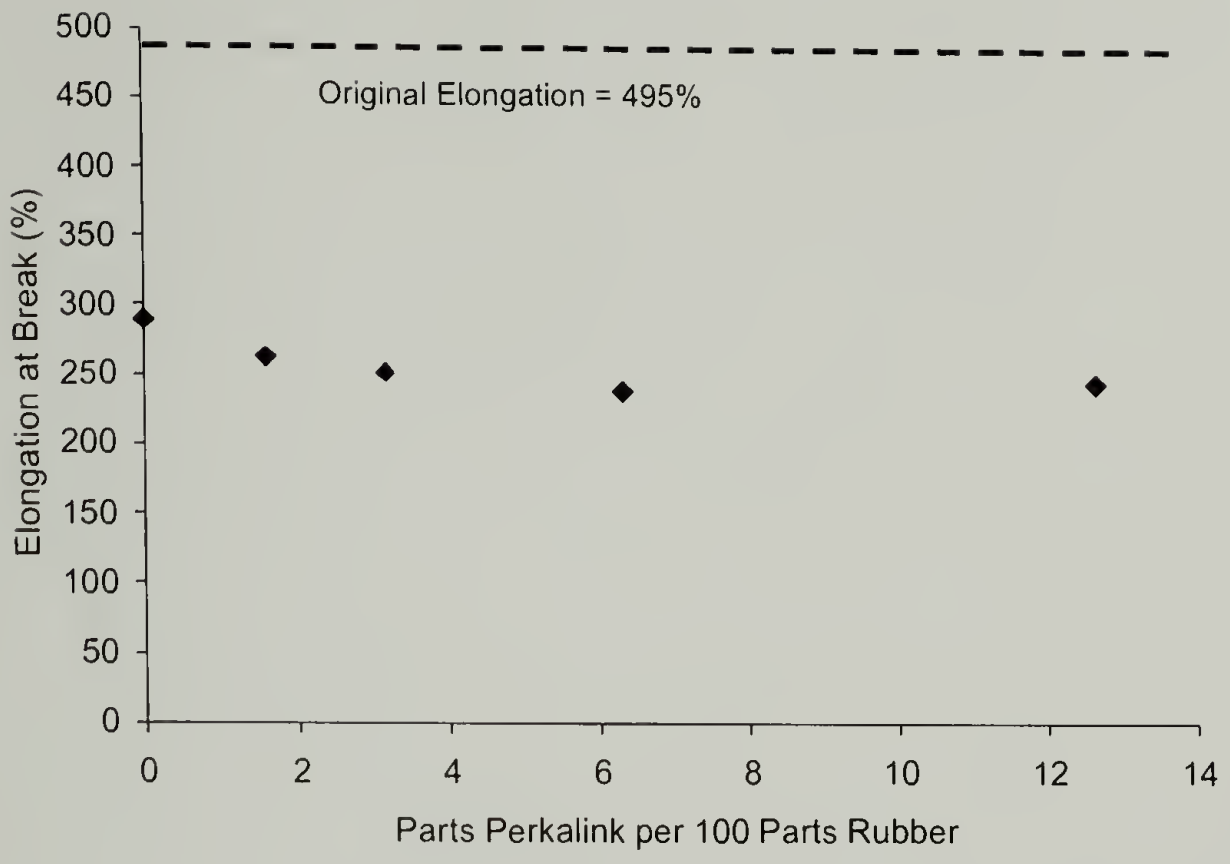

Figure 5.17. Elongation at break vs. parts Perkalink per 100 parts rubber for carbon black-filled SBR sintered at 200°C and 8.6 MPa for 1 hour.

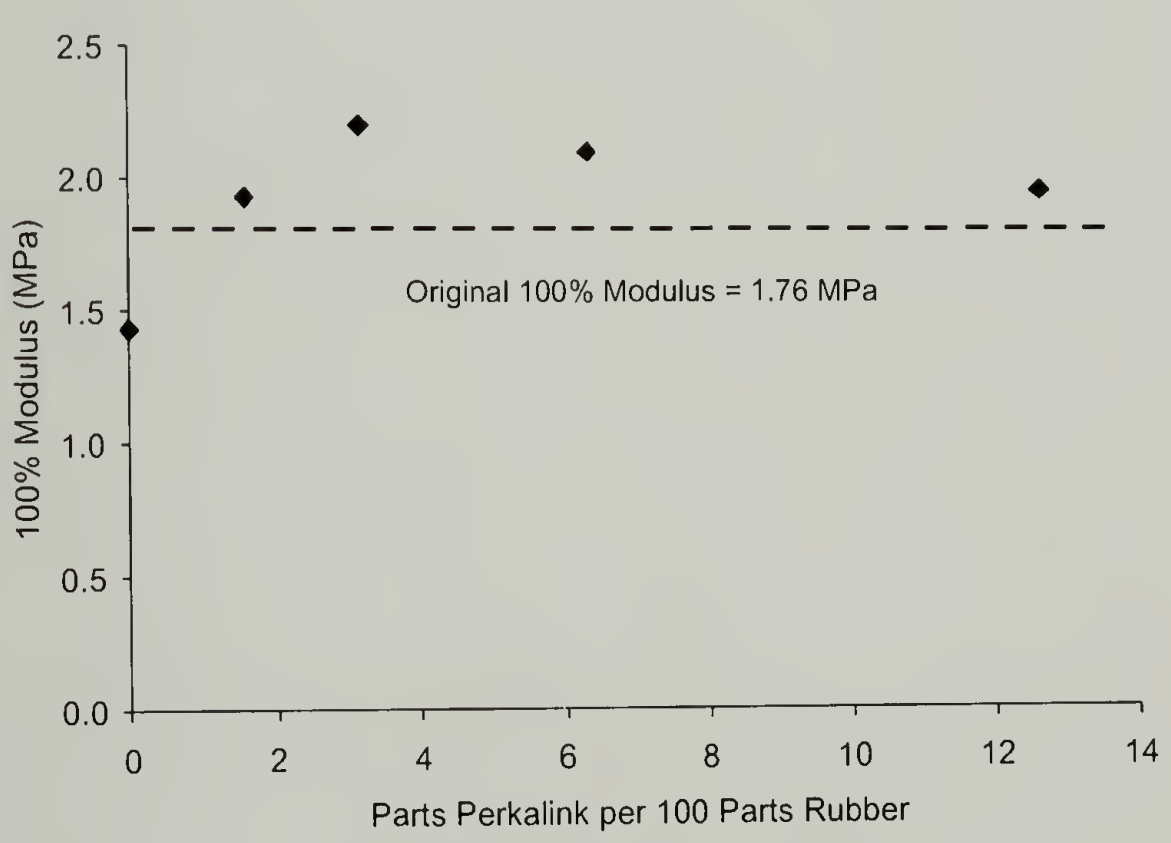

Figure 5.18. 100% Modulus vs. parts Perkalink per 100 parts rubber for carbon black-filled SBR sintered at 200°C and 8.6 MPa for 1 hour.

Overcrosslinking

To date, no additives have been found that eliminate the overcrosslinking phenomenon associated with SBR rubber. The ideal additive for SBR would be able to break crosslinks or quench reactive sites during the sintering process to minimize the overcrosslinking that occurs. However, as this is not a large problem in the rubber industry (unlike reversion), very little work was conducted in efforts to solve the overcrosslinking problem. Instead, the focus shifted to the work in Chapter 6, in which blends of rubbers were procured in efforts to minimize crosslink changes and increase property retention.

CHAPTER 6

BACKBONE ENGINEERING OF THERMOSETS

6.1 Background

Chemical stress relaxation and HPHTS have demonstrated that a thermoset that maintains a constant crosslink density when exposed to high temperatures is likely to retain a large percentage of its original mechanical properties. The main problem of the HPHTS process is that the high temperatures employed often change the crosslink density of the thermoset being sintered and thus maintaining a constant crosslink density is not a simple matter. As has been discussed previously, the two most commonly used rubbers, NR and SBR, behave remarkably different during HPHTS in terms of crosslink density change. NR incurs reversion and thus a lowering of crosslink density is observed. On the contrary, SBR exhibits overcrosslinking. The ideal material is one that maintains a constant crosslink density (i.e. polysulfide). It is possible that such a rubber might be produced by co-polymerizing isoprene [decreasing intermittent relaxation curve] and butadiene [increasing intermittent relaxation curve]. McGrath et al.[45] talks about the chemical stress relaxation of butadiene and isoprene blends and how copolymers (random and block) often fall in between the two homopolymers in terms of chemical stress relaxation.

To study such materials, several rubbers were obtained from the Goodyear Tire and Rubber Company. These included a terpolymer of styrene (25%), isoprene (50%) and butadiene (25%), as well as physical blends of natural rubber and styrene-butadiene rubber. The first rubber incorporates the overcrosslinking and reverting sections into the backbone of the rubber (chemically bonded), while the physical blend has regions that

will overcrosslink (SBR) and others that will revert (NR), but the regions are not chemically bonded. The following sections highlight the HPHTS results and the chemical stress relaxation data obtained for these rubber blends.

6.2 Styrene-Isoprene-Butadiene Rubber

Styrene-isoprene-butadiene rubber (SIBR) is a terpolymer of styrene (25%), isoprene (50%) and butadiene (25%) produced by the Goodyear Tire and Rubber Company. HPHTS and CSR studies were conducted on SIBR in efforts to see if a beneficial increase in property retention arises. As was demonstrated by the polysulfide rubber in Chapters 2 and 3, a thermoset not changing in crosslink density at its critical temperature retains 100% of its original mechanical properties when sintered. Adding isoprene in a random fashion to styrene-butadiene should help prevent over-crosslinking from occurring as isoprene rubbers do not undergo overcrosslinking.

6.2.1 HPHTS Results

HPHTS was performed on cryogenically ground SIBR as per Chapter 2. Figure 6.1, Figure 6.2 and Figure 6.3 highlight the HPHTS results of strength at break, elongation at break and 100% modulus, respectively. It appears that the SIBR's critical temperature is between that of NR (200°C) and SBR (250°C) at 220°C. Examining the elongation at break and 100% modulus data, SIBR rubber is behaving similar to NR as it shows reversion type behavior indicated by a lower 100% modulus and thus retains a lower crosslink density after sintering.

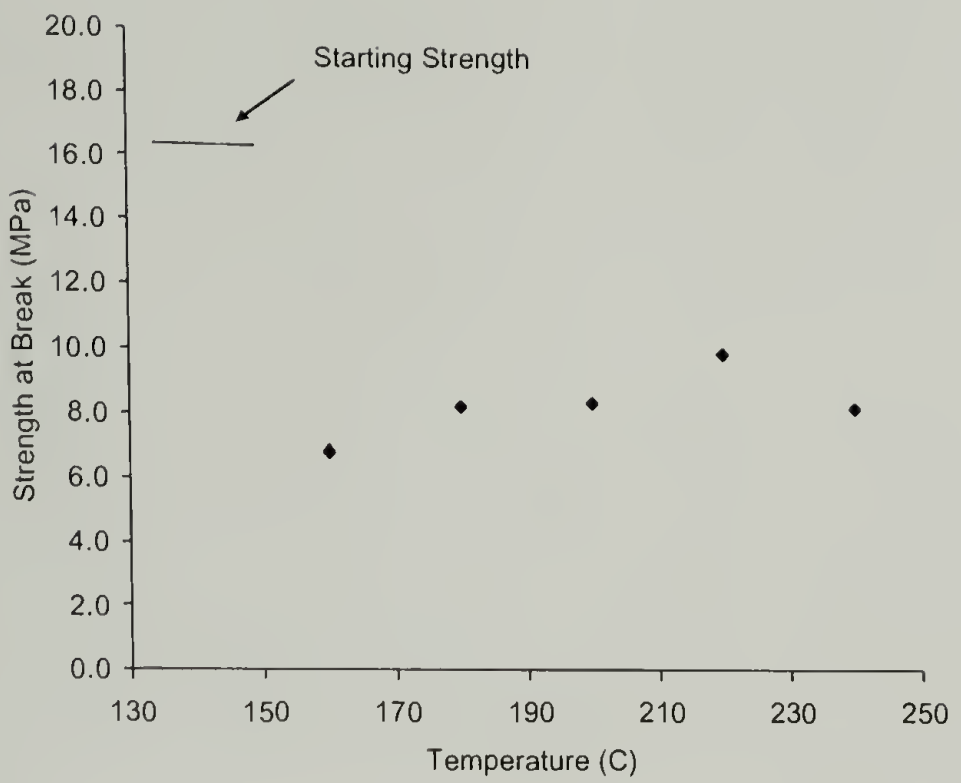

Figure 6.1. HPHTS results of strength at break vs. temperature for carbon black-filled SIBR sintered at 8.6 MPa for 1 hour.

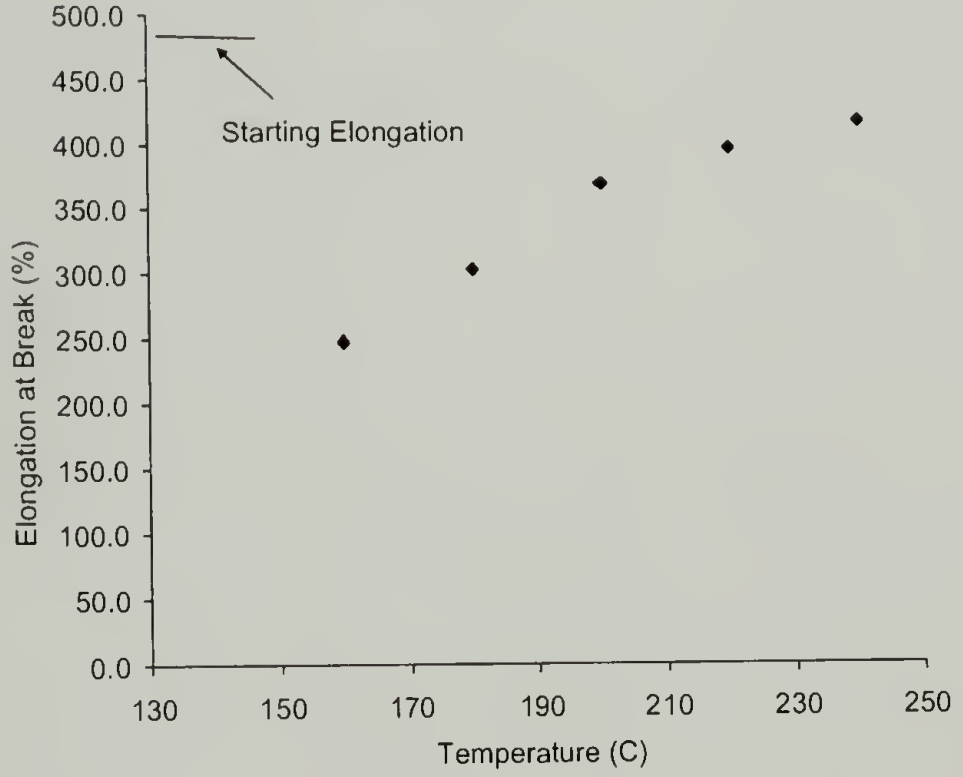

Figure 6.2. HPHTS results of elongation at break vs. temperature for carbon black-filled SIBR sintered at 8.6 MPa for 1 hour.

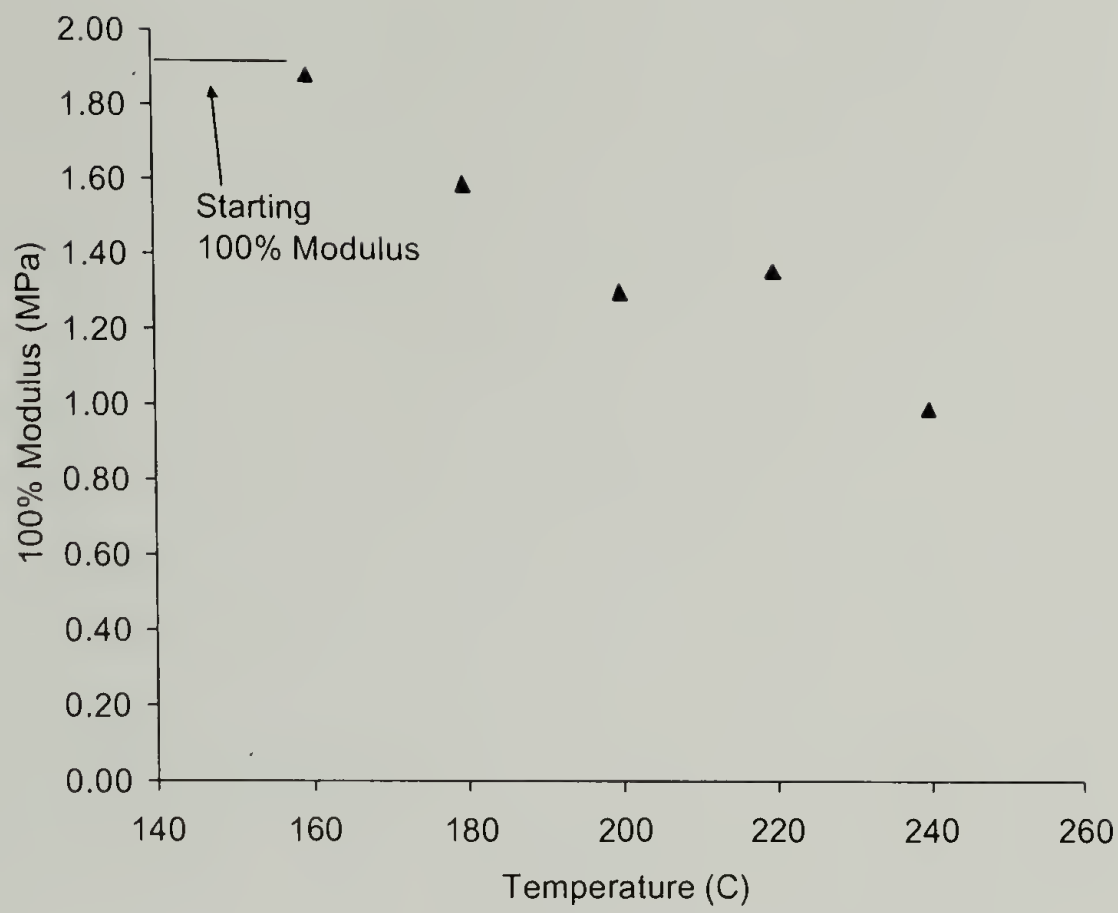

Figure 6.3. HPHTS results of 100% modulus vs. temperature for carbon black-filled SIBR sintered at 8.6 MPa for 1 hour.

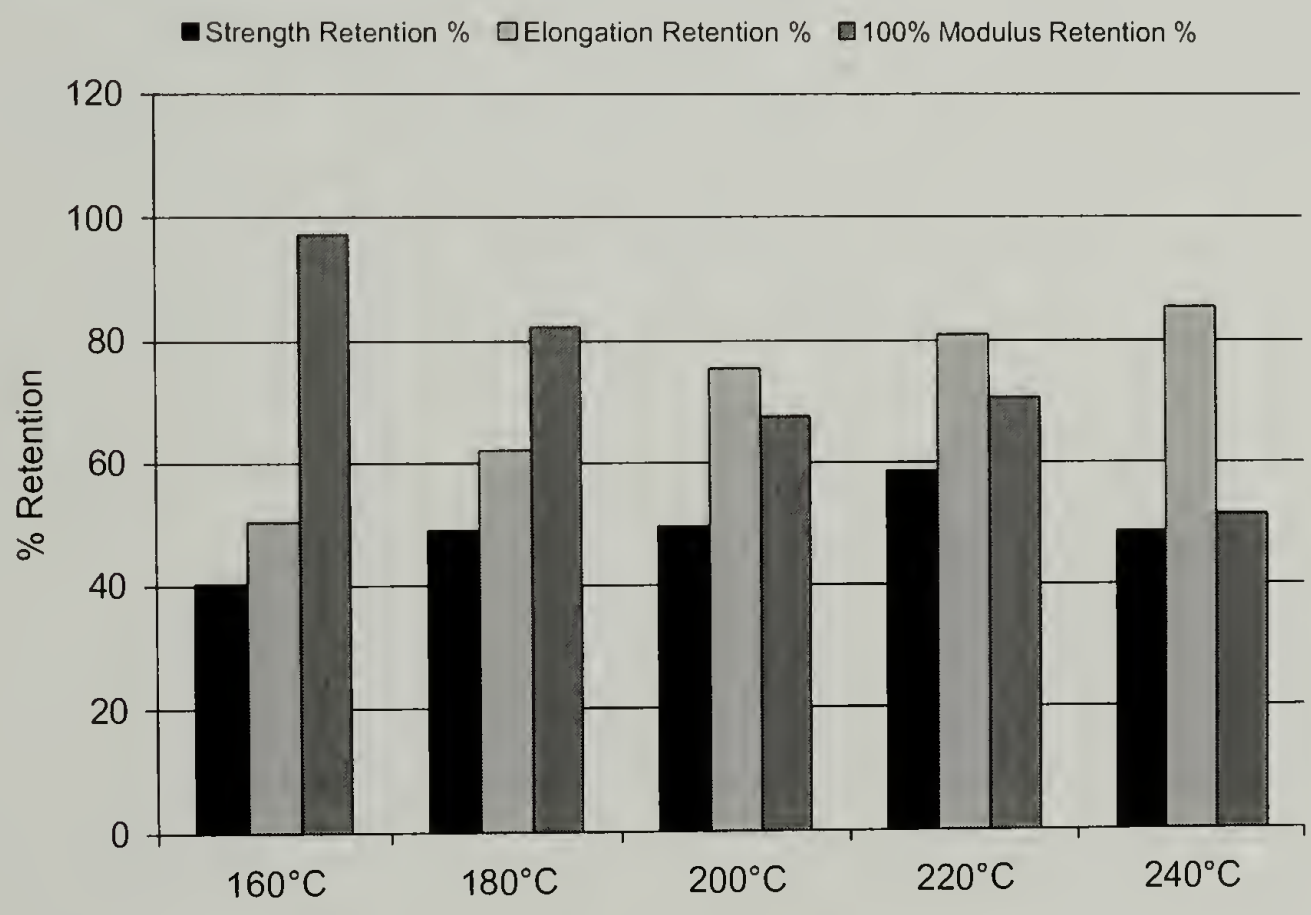

Figure 6.4. Mechanical property retention summary for carbon black-filled SIBR sintered at 8.6 MPa for 1 hour.

Figure 6.4 shows the retention percentages of the HPHTS sheets in comparison to the original mechanical properties of vulcanized SIBR. One interesting note is that the maximum strength retention is greater (~60%) than that of NR, despite SIBR behaving in a similar manner (reverting). At its critical temperature, SIBR also maintains a higher percentage of its starting modulus (70%) than NR does at its critical temperature (40%).

Overall, the HPHTS data for SIBR indicates that while SIBR maintains a greater percentage of the original crosslink density (100% modulus data) than NR, SIBR does incur a loss in properties due to reversion (similar to NR). However, this loss is not as great as with NR, and the possibility exists that the percentages of styrene, isoprene, and butadiene may be manipulated to eliminate this occurrence. To data this has not been attempted.

6.2.2 CSR Results

Work by McGrath[45] on isoprene/butadiene systems suggested that blends of NR and SBR would behave differently than NR or SBR homopolymers during chemical stress relaxation experiments. Figure 6.5 shows the continuous stress relaxation results for a carbon black-filled SIBR utilizing the Instron compression stress relaxation apparatus from Figure 3.5. The continuous stress relaxation results for SIBR are similar to polysulfide, NR, and SBR. As the testing temperature is increased, an increase in the rate of relaxation is observed.

To achieve superposition with SIBR CSR data, a line was drawn at $F(t)/F(0) = 0.6$, in contrast to the 0.368 line used with the polysulfide data and the 0.5 line for the NR. This changes the superposition calculation slightly as Equation 3.1, Equation 3.2

and Equation 3.3 are transformed into Equation 6.1, Equation 6.2 and Equation 6.3. As highlighted in Chapter 3, the time values are multiplied by their respective k' value in order to shift all of the data onto a universal axis. The result is shown in Figure 6.6. Similar to the previous relaxation data, the various SIBR continuous stress relaxation experiments superimpose well, with some slight deviation recorded at early times. The deviation likely results from the curves not adhering to a strictly exponential decay. This could result from more complex reactions taking place than those highlighted by Tobolsky. To date, no characterization of these additional reactions has taken place.

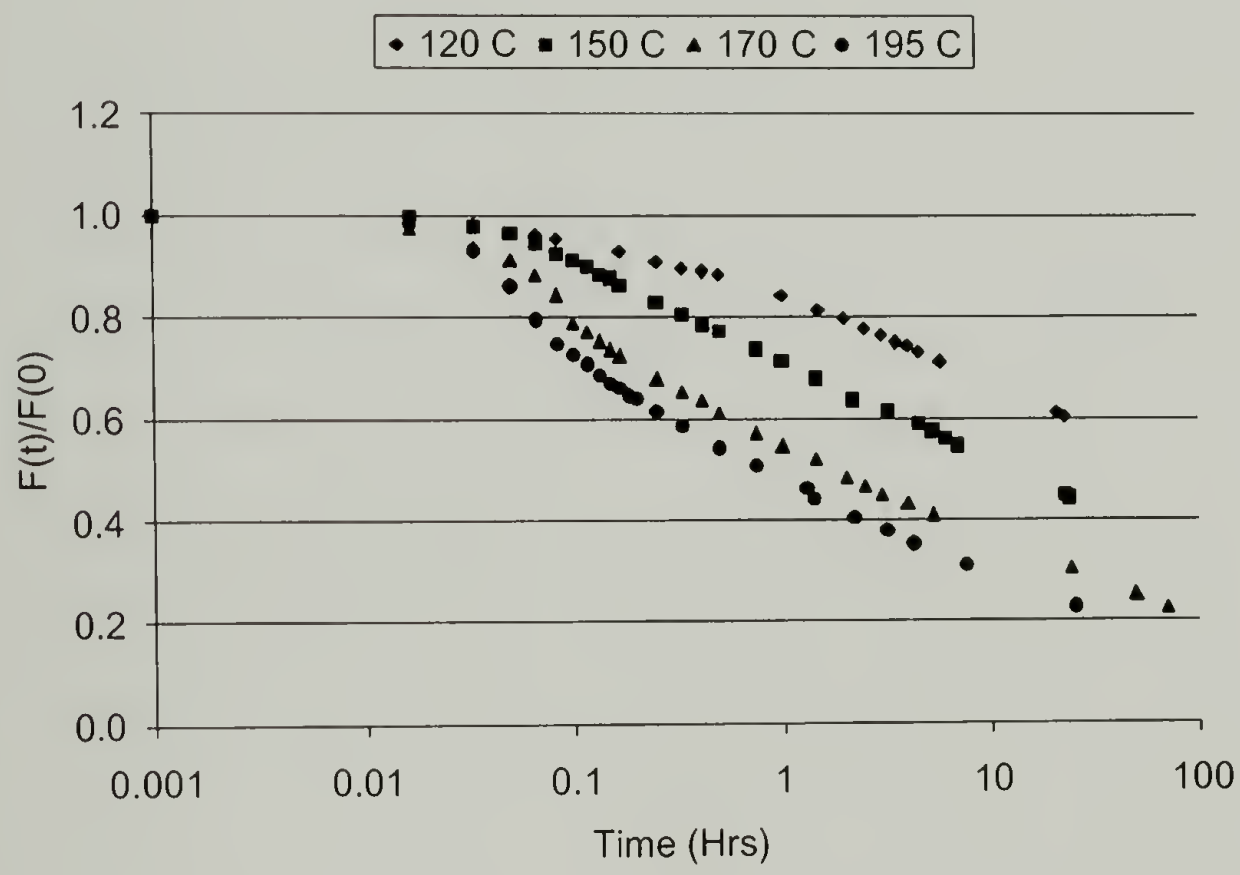

Figure 6.5. Continuous stress relaxation results for sulfur cured, carbon black-filled SIBR.

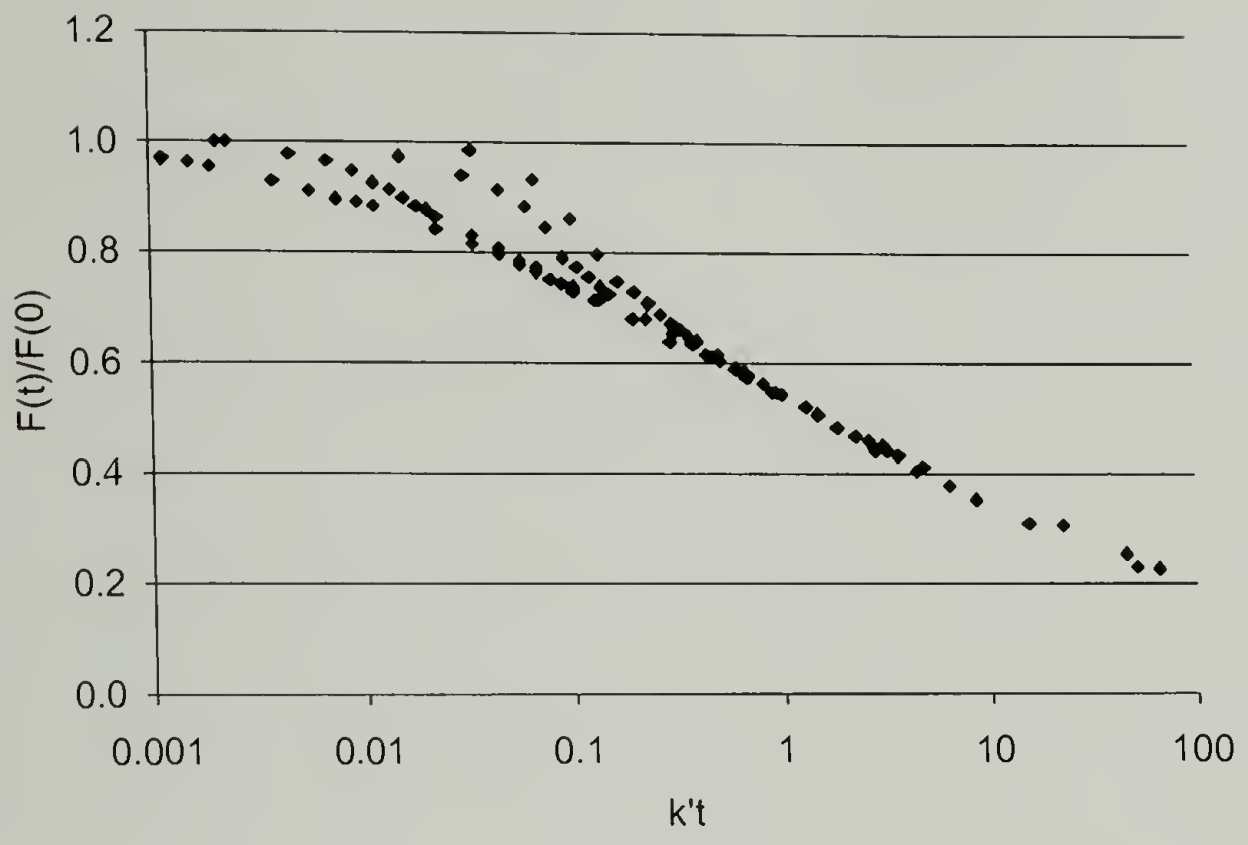

Figure 6.6. Superimposed continuous stress relaxation results for sulfur cured, carbon black-filled SIBR.

$$\frac{f(t)}{f(0)} = 0.600 = e^{-k't}$$

Equation 6.1

$$\ln(0.600) = \ln(e^{-k't})$$

Equation 6.2

$$k' = \frac{0.5108}{t}$$

Equation 6.3

Continuing the stress relaxation investigation of SIBR, the influence of temperature on the intermittent stress relaxation was measured. Data obtained from the intermittent stress relaxation of carbon black-filled SIBR is shown in Figure 6.7 again utilizing the Instron compression relaxation apparatus of Figure 3.5. Similar to NR, as the temperature of the experiment is increased, the intermittent stress relaxation value becomes less than 1. This is indicative of reversion and is consistent with the data obtained in the HPHTS section on SIBR.

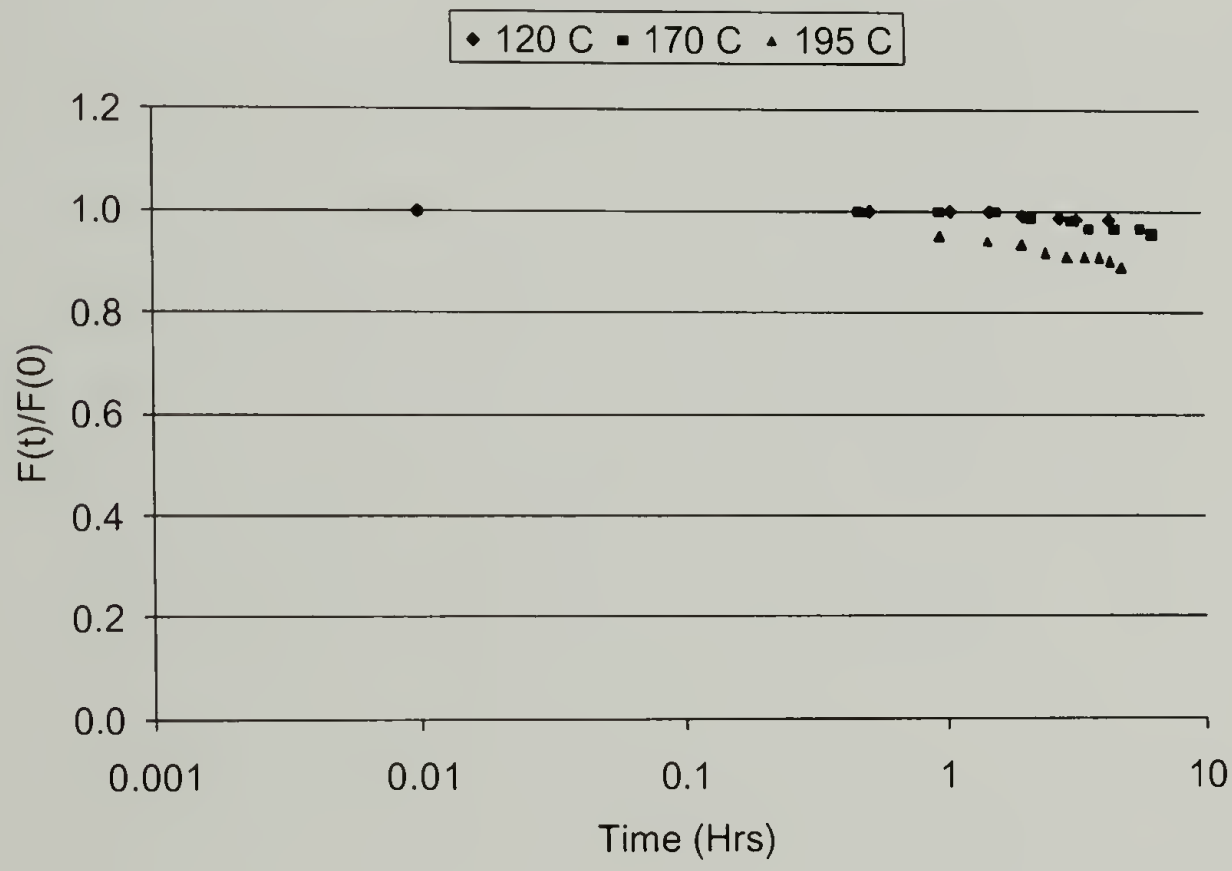

Figure 6.7. Intermittent stress relaxation results for sulfur cured, carbon black-filled SIBR.

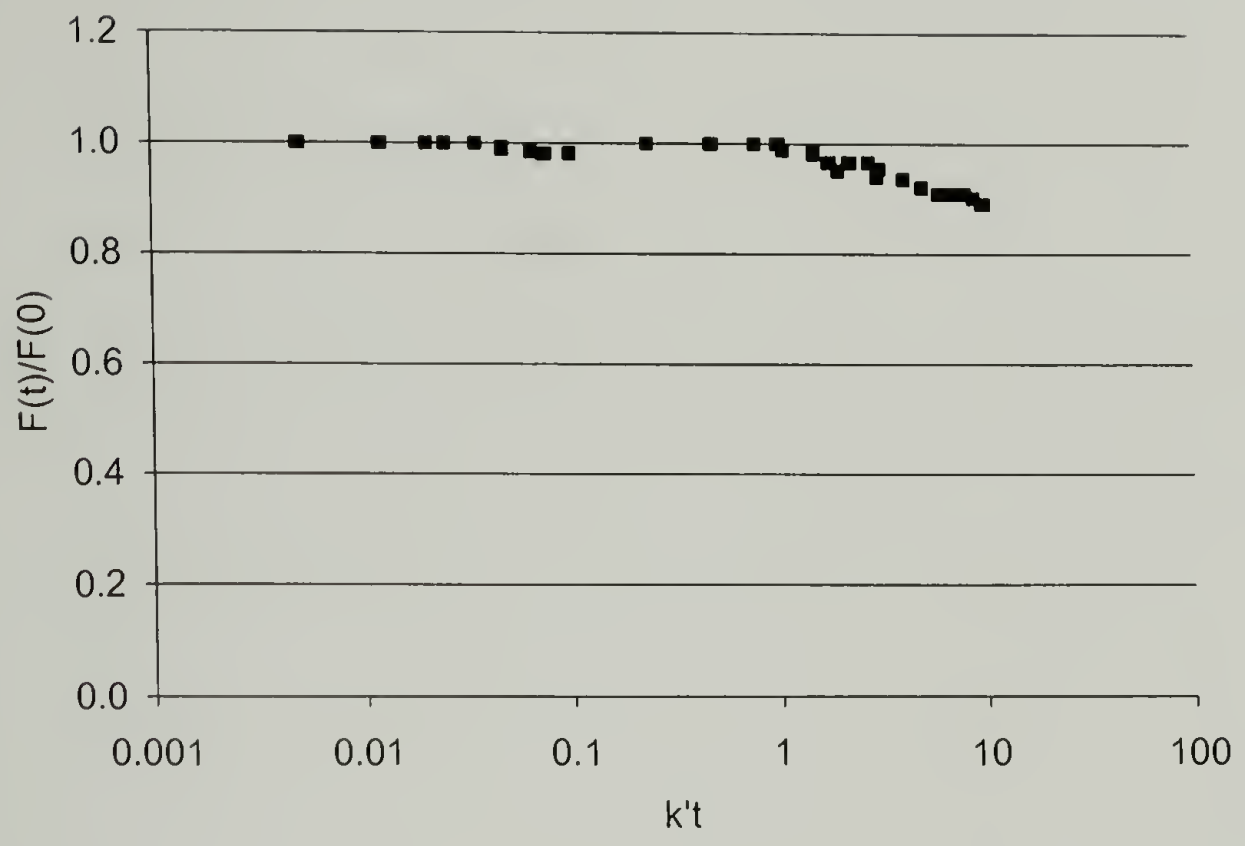

Figure 6.8. Superimposed intermittent stress relaxation results for sulfur cured, carbon black-filled SIBR.

Superposition of the data through the time-temperature superposition described in the continuous section for SBR is shown for the intermittent stress relaxation in Figure 6.8. This graph illustrates how the SIBR is losing crosslink density when exposed to the extreme temperatures of HPHTS. As with the polysulfide rubber, NR and SBR, the continuous and intermittent stress relaxation results can be used to predict HPHTS results.

A similar treatment can be conducted on the CSR data to calculate the new bond formation of SIBR as with the CSR data in Chapter 4. Superimposing Figure 6.6 and Figure 6.8, and using Equation 4.4 (new bond formation theory), one obtains Figure 6.9. It is apparent that the diminishing intermittent stress relaxation is directly responsible for the new bond formation curve not reaching 100%. In fact, as a result of the decreasing

intermittent curve, the highest new bond formation potential generated from the CSR data of SIBR is 60%.

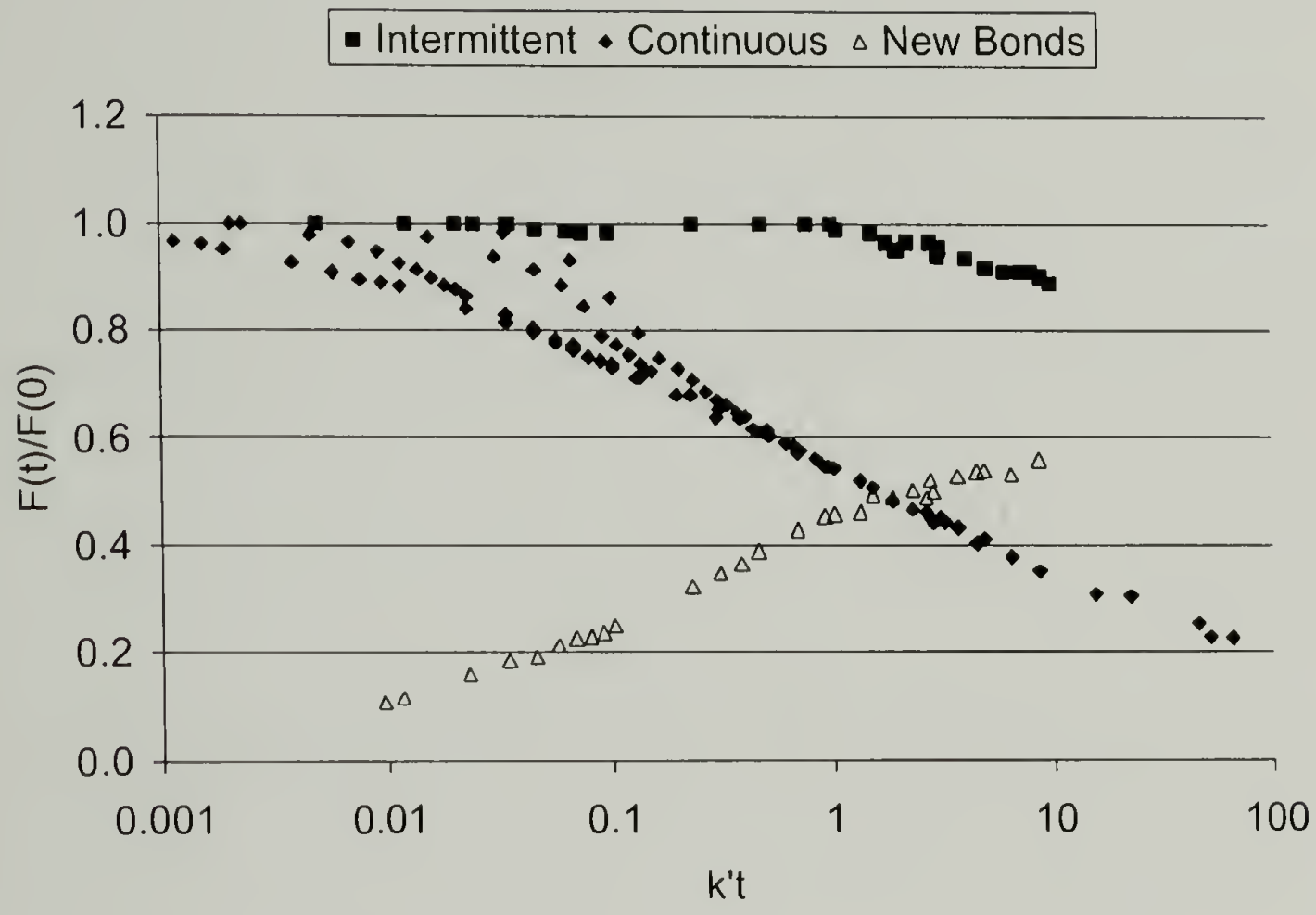

Figure 6.9. Superimposed continuous and intermittent stress relaxation results and calculated new bond formation for SIBR.

Table 6.1. Extrapolation of shift factor correlation with temperature for SIBR.

Time (hrs)	K'	1/k'	Temp C	(1/T)*10^3
22.60	0.02	44.24	120	2.54
3.70	0.14	7.24	145	2.39
0.55	0.93	1.08	170	2.26
0.25	2.04	0.49	195	2.14
	9.42	0.11	220	2.03
	23.56	0.04	240	1.95
	55.00	0.02	260	1.88

Table 6.1 shows the corresponding k' values for temperature from the SIBR CSR. Figure 6.10 highlights the extrapolation equation necessary to get values of k' at temperatures beyond those of CSR experiments. Again using the value of 1 for time (as all HPHTS experiments were conducted at 1 hour), one is able to generate the predicted retention of sintering values for SIBR from Figure 6.9 by using the k' values of Table 6.1. Table 6.2 summarizes these results, along with showing the actual HPHTS retention data from Figure 6.4. As is evident in Table 6.2, the predicted values and the actual HPHTS are in very good agreement.

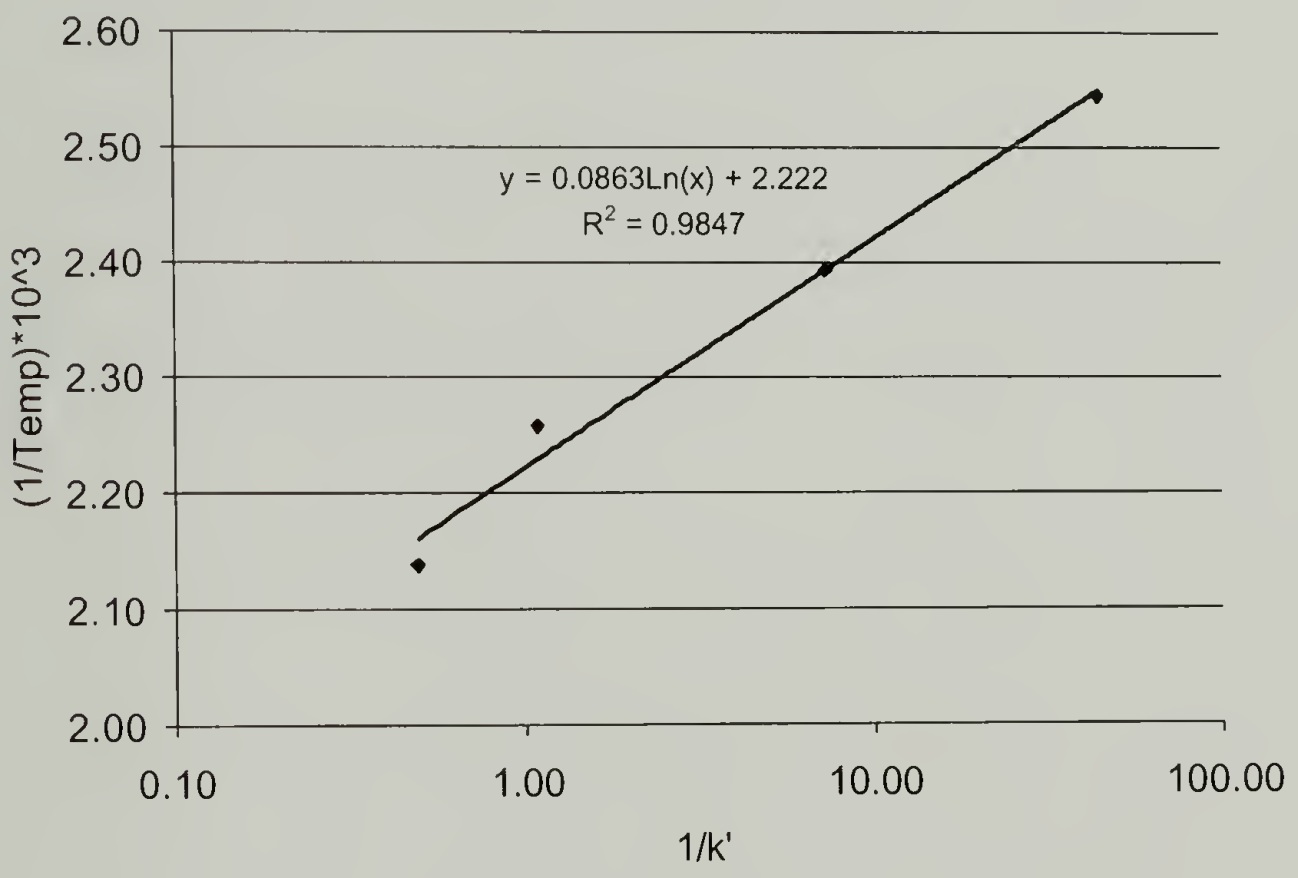

Figure 6.10. Relationship of temperature to shift factor k' for SIBR (with correlation equation).

Table 6.2. Strength % retention predicted by new bond formation theory and actual HPHTS strength retention results as a function of temperature for SIBR.

K'	Temp C	% Predicted	HPHTS Actual
0.49	120	<15	N/A
0.10	140	25	N/A
0.36	160	35	40
1.18	180	45	50
3.49	200	50	50
9.42	220	57	60
23.56	240	55	50

6.3 Natural Rubber/ Solution-Styrene-Butadiene Rubber Blends

The next rubber attempted was a 50/50 physical blend of natural rubber and solution polymerized styrene-butadiene rubber (S-SBR). Again, it was believed that such a rubber might exhibit the properties in-between those of NR and SBR. As such, it was hoped that the blend would exhibit a constant crosslink density during sintering as part of the rubber would be overcrosslinking, while the other half would be reverting. The main concern here, however, was that the blend would have localized sections of NR and SBR with low and high crosslink densities, respectively. Again, HPHTS and CSR experiments were conducted in efforts to understand the recyclability of such a blend.

6.3.1 HPHTS Results

HPHTS was performed on cryogenically ground NR/S-SBR blend as per chapter 2. Figure 6.11, Figure 6.12 and Figure 6.13 highlight the strength at break, elongation at break and 100% modulus HPHTS results, respectively, for the NR/S-SBR blend. As with the SIBR, the blend of NR and SBR has a critical temperature around 220°C, again in-

between the values of NR and SBR. However, from the elongation at break and 100% modulus results, the NR/S-SBR physical blend is incurring more overcrosslinking than reversion, especially at temperatures above its critical temperature of 220°C. This is evidenced by the sharp upturn in the 100% modulus, and a likewise diminishing of elongation at break. Figure 6.14 summarizes the HPHTS retentions of the original mechanical properties for the various molding temperatures. Overall, the retention values of the physical blend do not appear to be as favorable as the chemical co-polymer blend.

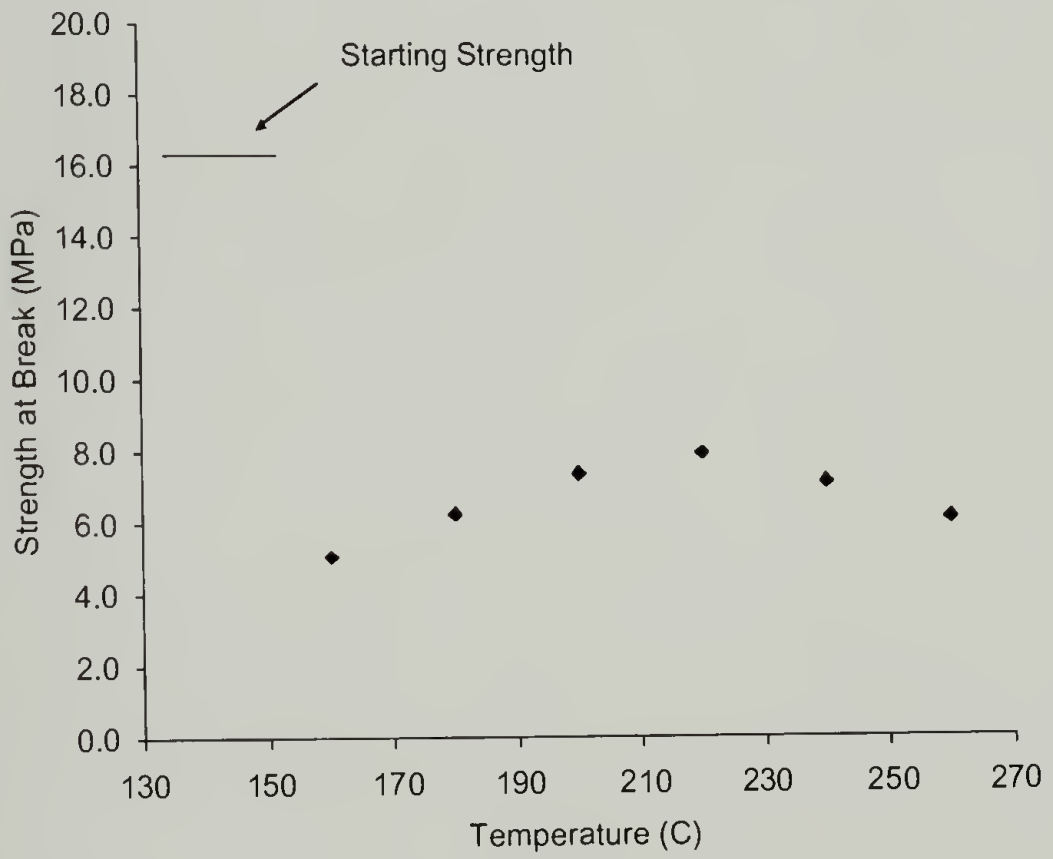

Figure 6.11. HPHTS results of strength at break vs. temperature for carbon black-filled NR/S-SBR sintered at 8.6 MPa for 1 hour.

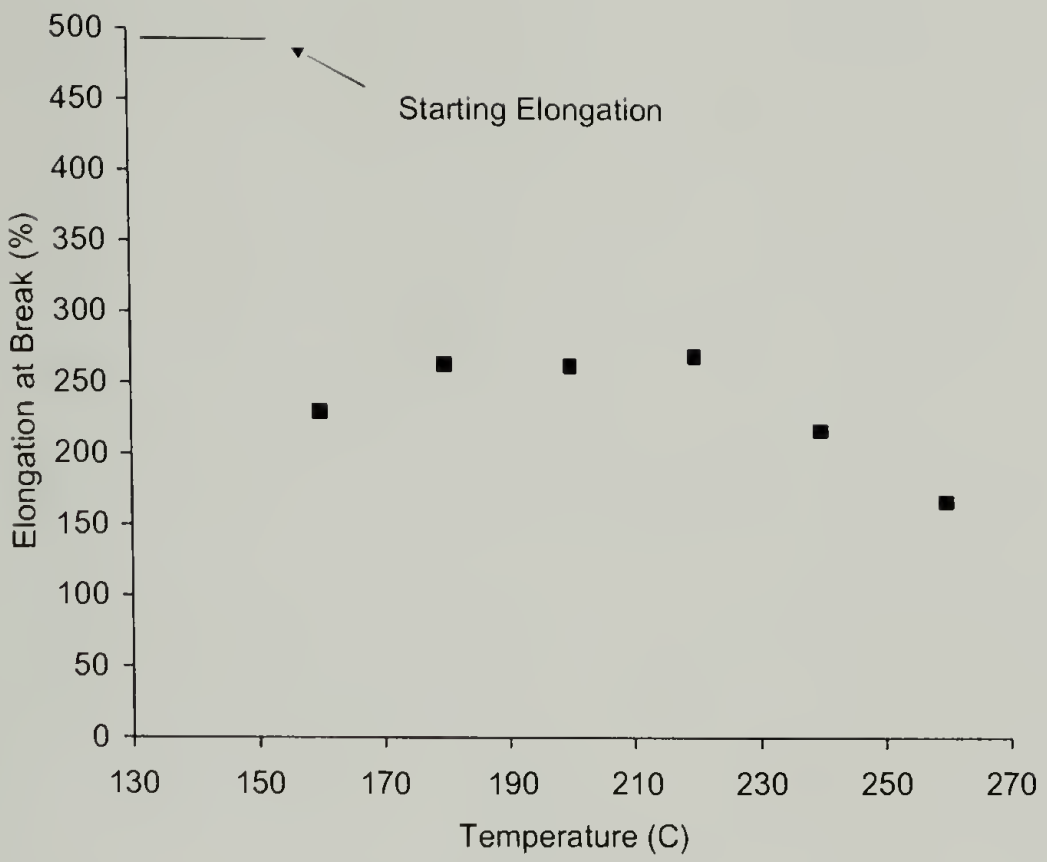

Figure 6.12. HPHTS results of elongation at break vs. temperature for carbon black-filled NR/S-SBR sintered at 8.6 MPa for 1 hour.

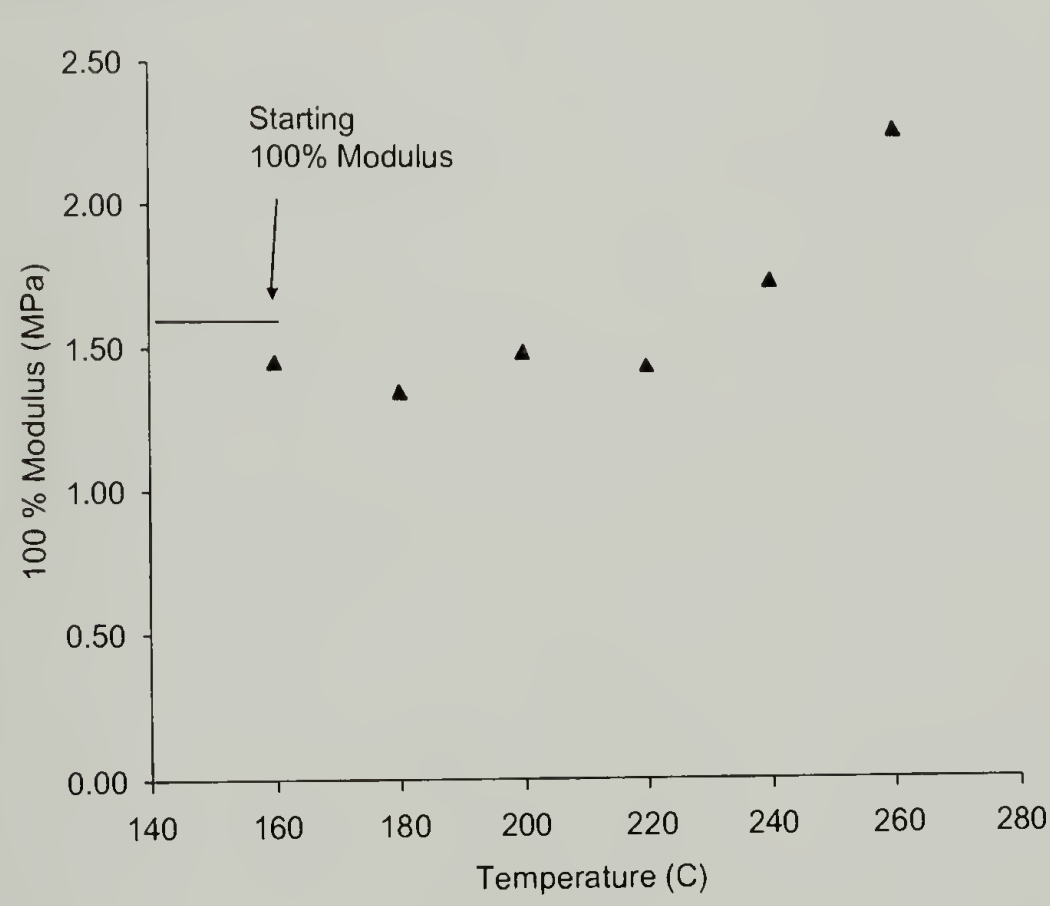

Figure 6.13. HPHTS results of 100% modulus vs. temperature for carbon black-filled NR/S-SBR sintered at 8.6 MPa for 1 hour.

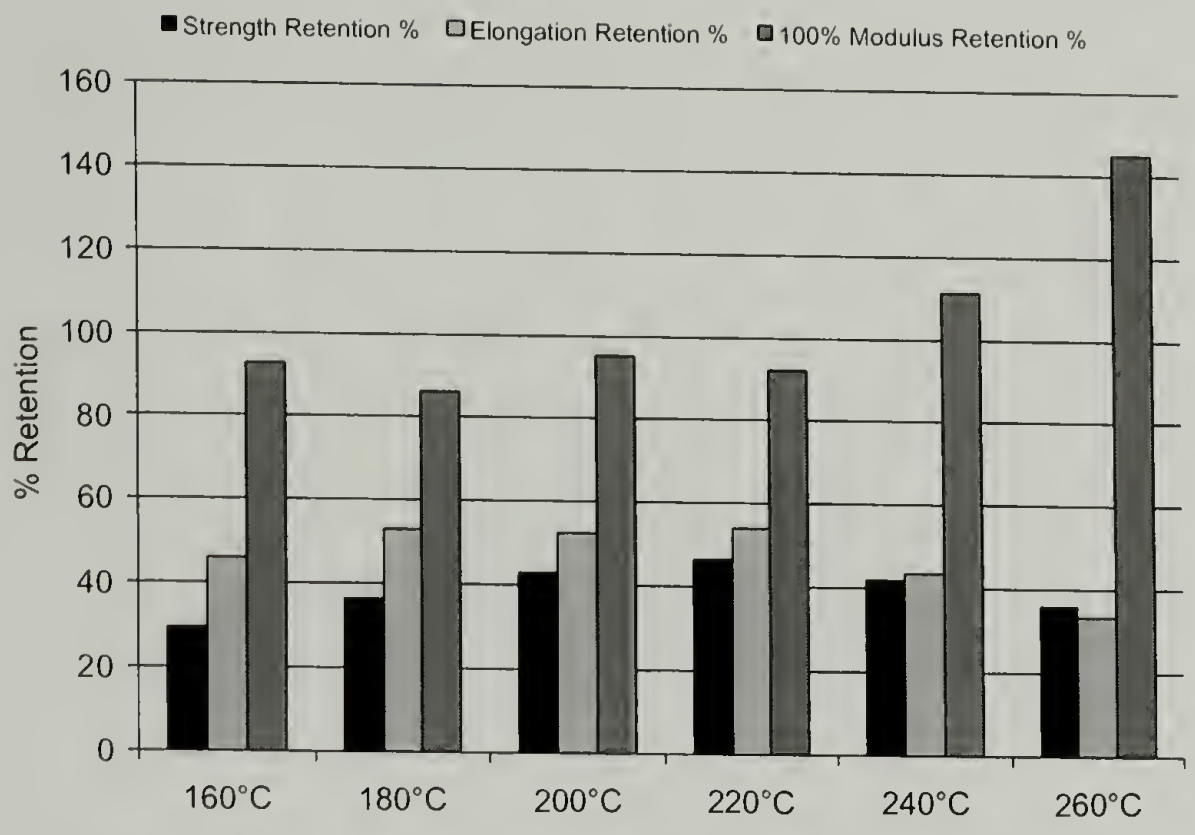

Figure 6.14. Mechanical property retention summary for carbon black-filled NR/S-SBR sintered at 8.6 MPa for 1 hour.

6.3.2 CSR Results

Figure 6.15 shows the continuous stress relaxation results for a carbon black-filled NR/S-SBR blend utilizing the Instron compression stress relaxation apparatus from Figure 3.5. The continuous stress relaxation results for NR/S-SBR are similar to polysulfide, NR, SBR and SIBR. Again, as the testing temperature is increased, an increase in the rate of relaxation is observed.

To achieve superposition with NR/S-SBR CSR data, a line was drawn at F(t)/F(0) = 0.4 (see Table 6.3). This changes the superposition calculation as Equation 3.1, Equation 3.2 and Equation 3.3 are transformed into Equation 6.4, Equation 6.5 and Equation 6.6. The superimposed result is shown in Figure 6.16. Similar to the previous relaxation data, the various NR/S-SBR continuous stress relaxation experiments superimpose well.

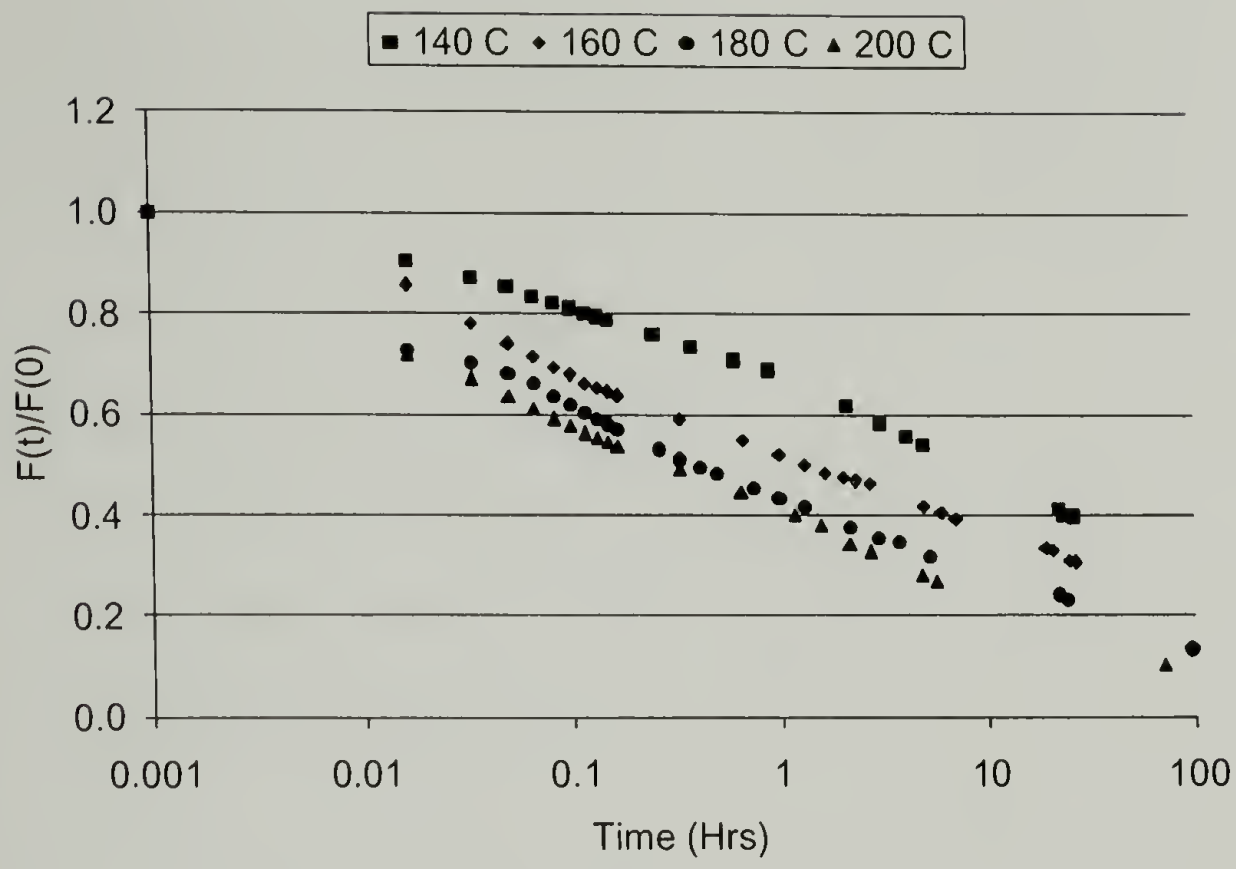

Figure 6.15. Continuous stress relaxation results for sulfur cured, carbon black-filled NR/S-SBR physical blend.

$$\frac{f(t)}{f(0)} = 0.400 = e^{-k't}$$

Equation 6.4

$$\ln(0.400) = \ln(e^{-k't})$$

Equation 6.5

$$k' = \frac{0.9162}{t}$$

Equation 6.6

Table 6.3. Superposition calculations for sulfur cured, carbon black-filled NR/S-SBR physical blend.

Time (hrs)	K'	1/k'	Temp C	(1/T)*10^3
22.5	0.04	24.56	140	2.42
6	0.15	6.55	160	2.31
1.7	0.54	1.86	180	2.21
1.18	0.78	1.29	200	2.11

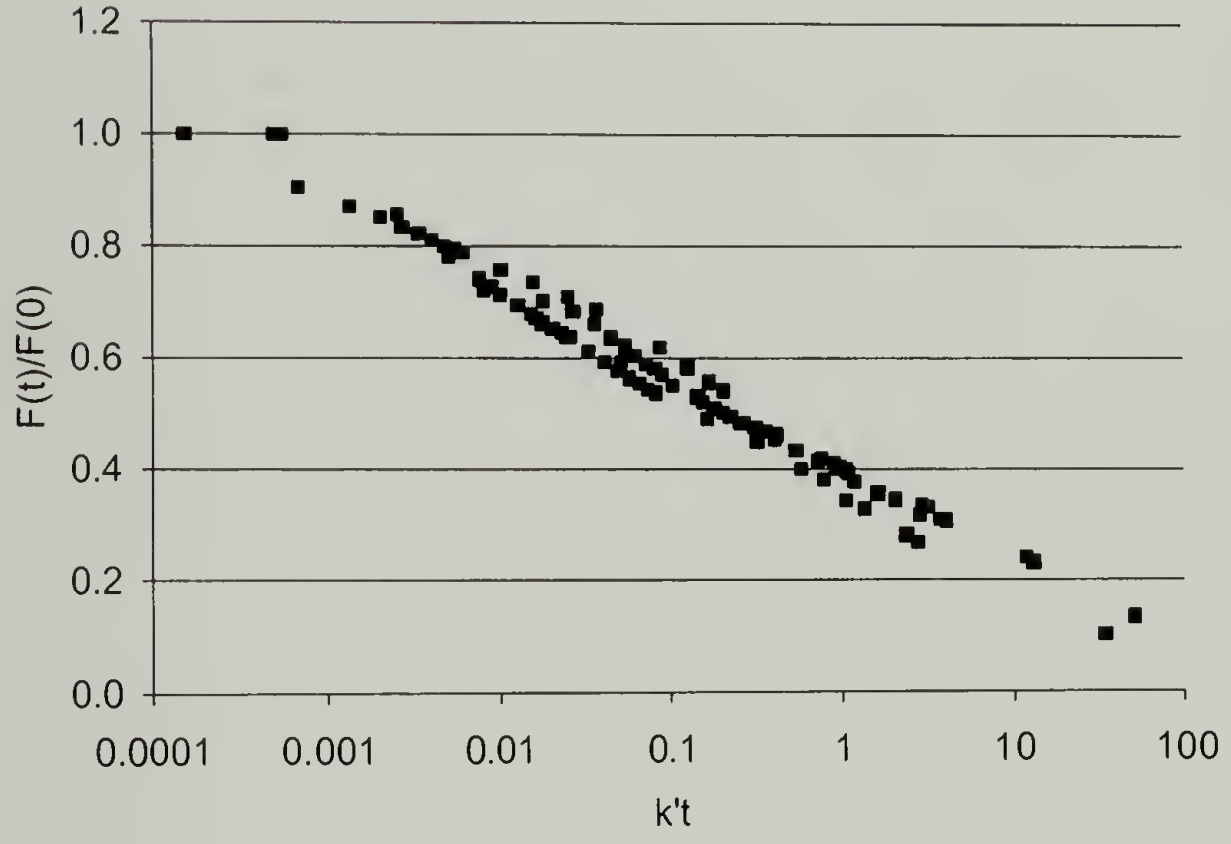

Figure 6.16. Superimposed continuous stress relaxation results for sulfur cured, carbon black-filled NR/S-SBR physical blend.

The influence of temperature on the intermittent stress relaxation of NR/S-SBR is shown in Figure 6.17 again utilizing the Instron compression relaxation apparatus of Figure 3.5. Similar to SBR, as the temperature of the experiment is increased, the intermittent stress relaxation value becomes greater than 1. This is indicative of overcrosslinking and is consistent with the data obtained in the previous HPHTS section for NR/S-SBR.

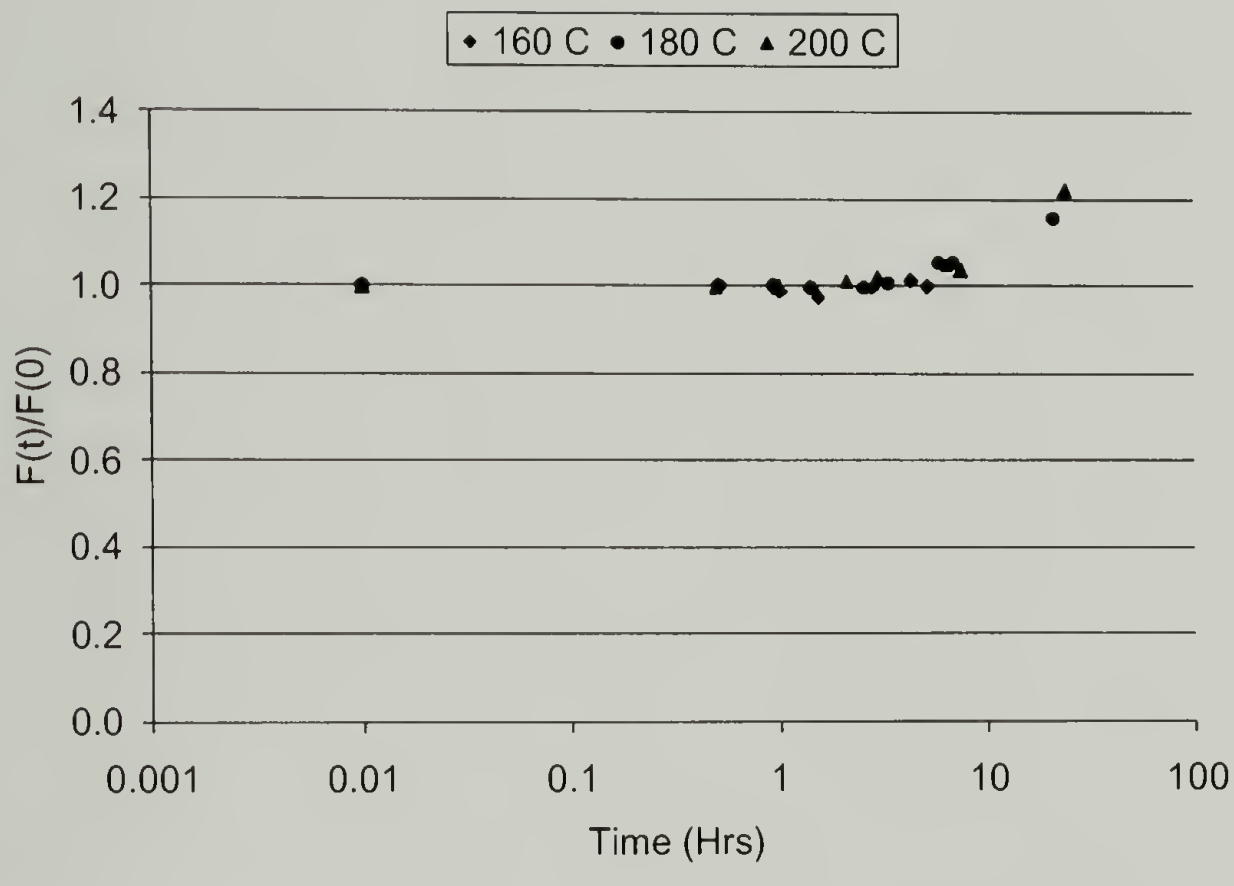

Figure 6.17. Intermittent stress relaxation results for sulfur cured, carbon black-filled NR/S-SBR physical blend.

Superposition of the data through the time-temperature superposition described in the continuous section for NR/S-SBR is shown for the intermittent stress relaxation in Figure 6.18. This graph illustrates how the NR/S-SBR is gaining crosslink density when exposed to the extreme temperatures of HPHTS. Again, the continuous and intermittent

stress relaxation results can be used to predict HPHTS results. First, the intermittent stress relaxation is reflected through 1 (Figure 6.19) as described previously in Chapter 4 (SBR new bond calculation). Superimposing Figure 6.16 and Figure 6.19, and using Equation 4.4 (new bond formation theory), one obtains Figure 6.20. It is apparent that the overcrosslinking (portrayed as a diminishing intermittent stress relaxation in Figure 6.20) is directly responsible for the new bond formation curve not reaching 100%. In fact, as a result of a decreasing intermittent curve, the highest new bond formation potential generated from the CSR data is around 60%.

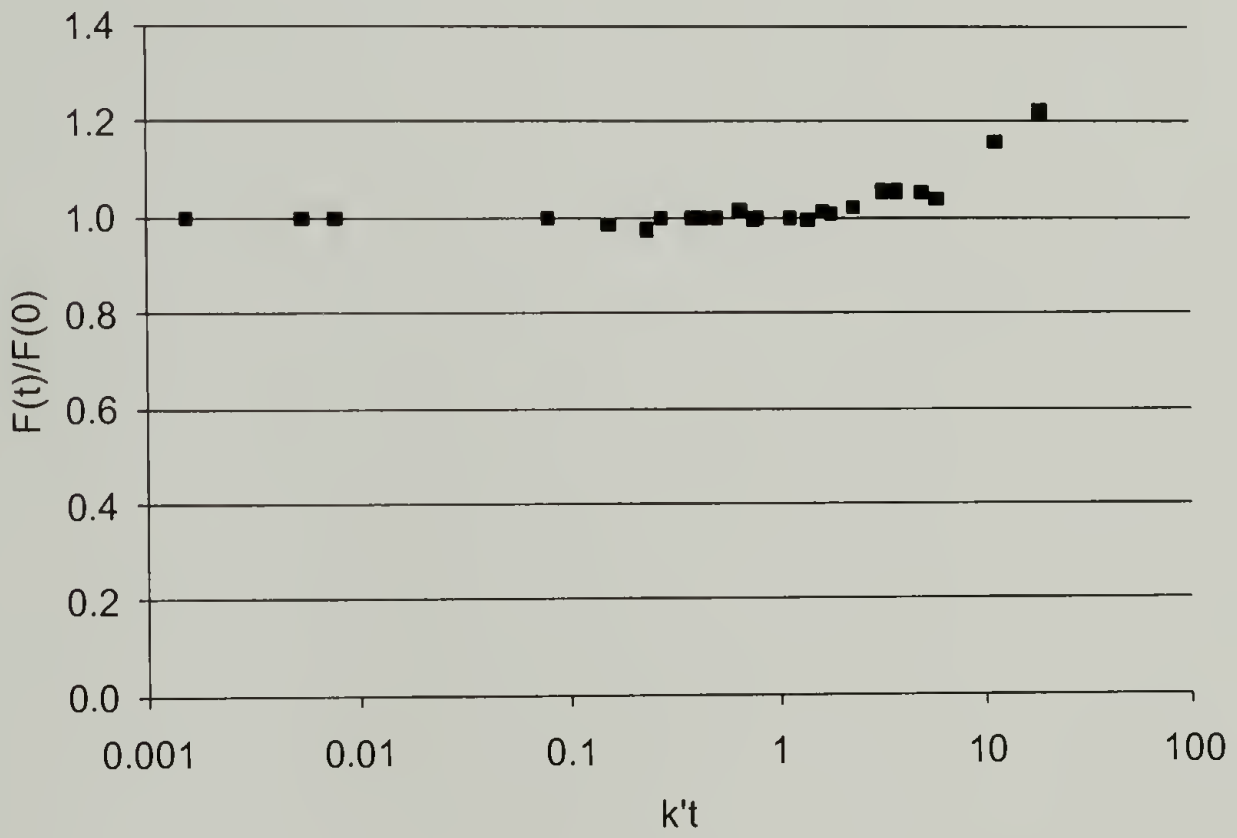

Figure 6.18. Superimposed intermittent stress relaxation results for sulfur cured, carbon black-filled NR/S-SBR physical blend.

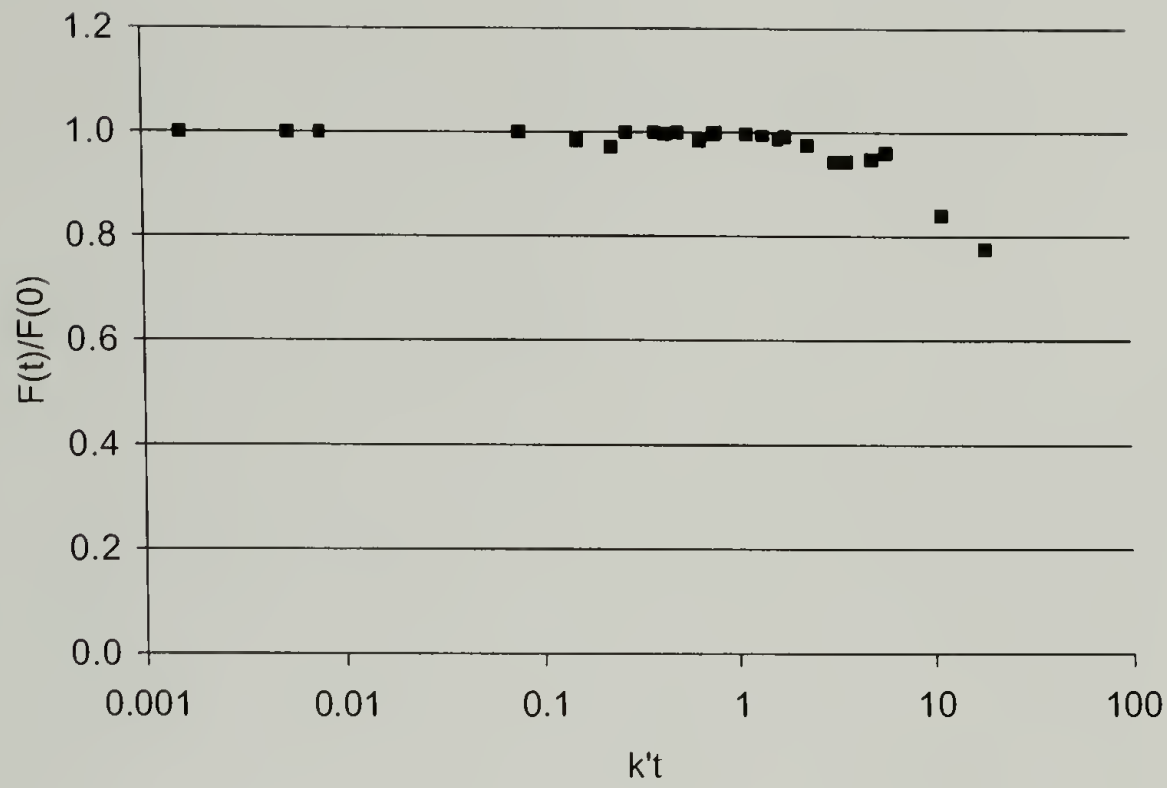

Figure 6.19. Reflected superimposed intermittent stress relaxation results for sulfur cured, carbon black-filled NR/S-SBR physical blend.

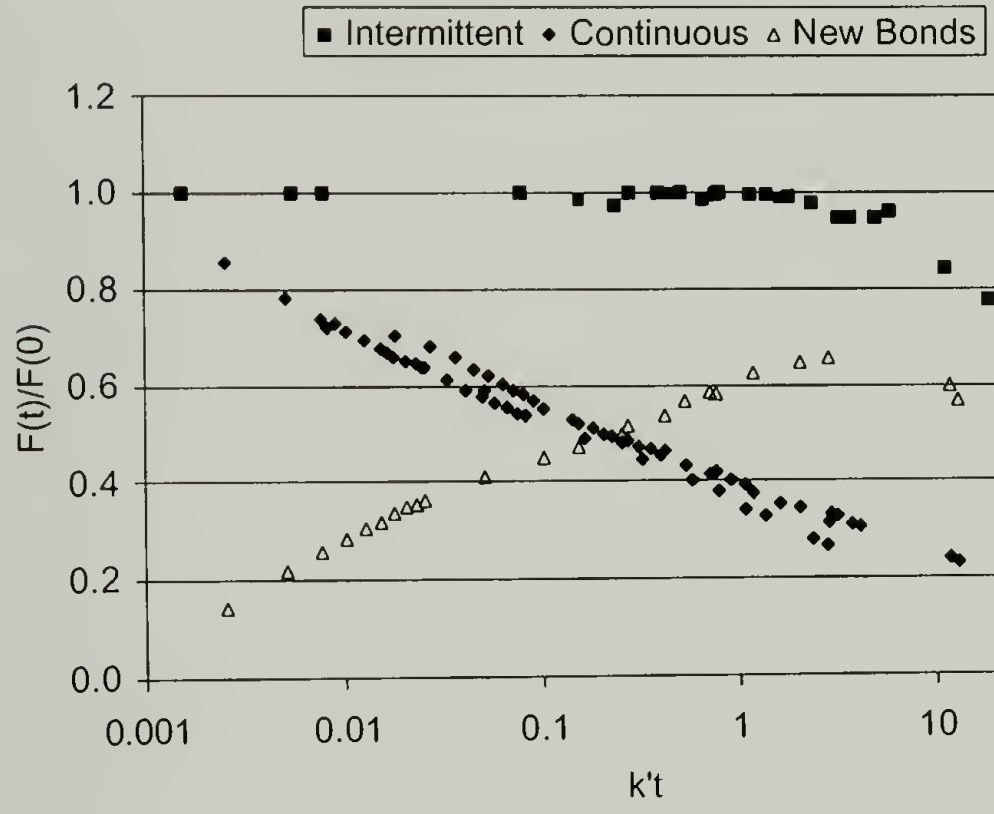

Figure 6.20. Superimposed continuous and intermittent stress relaxation results and calculated new bond formation for NR/S-SBR physical blend.

Table 6.4 shows the corresponding k' values for temperature from the NR/S-SBR CSR. Figure 6.21 highlights the extrapolation equation necessary to get values of k' at temperatures beyond those of CSR experiments. Again using the value of 1 for time (as all HPHTS experiments were conducted at 1 hour), one is able to generate the predicted retention of sintering values for NR/S-SBR from Figure 6.20 by using the k' values of Table 6.4.

Table 6.5 summarizes these results, along with showing the actual HPHTS retention data from Figure 6.14. Overall, the values of HPHTS are slightly below those predicted, however the results do follow the same general trend. One possibility for the discrepancy is the quick drop in the continuous relaxation noted in Figure 6.20. If this relaxation was shifted to slightly higher k't values, the data would be closer to retained HPHTS values.

Table 6.4. Extrapolation of shift factor correlation with temperature for NR/S-SBR physical blend (extrapolation in italics).

Time (hrs)	K'	1/k'	Temp C	(1/T)*10^3
22.50	0.04	24.56	140	2.42
6.00	0.15	6.55	160	2.31
1.70	0.54	1.86	180	2.21
1.18	0.78	1.29	200	2.11
	1.27	*0.79*	*220*	*2.03*
	2.55	*0.39*	*240*	*1.95*
	4.86	*0.21*	*260*	*1.88*

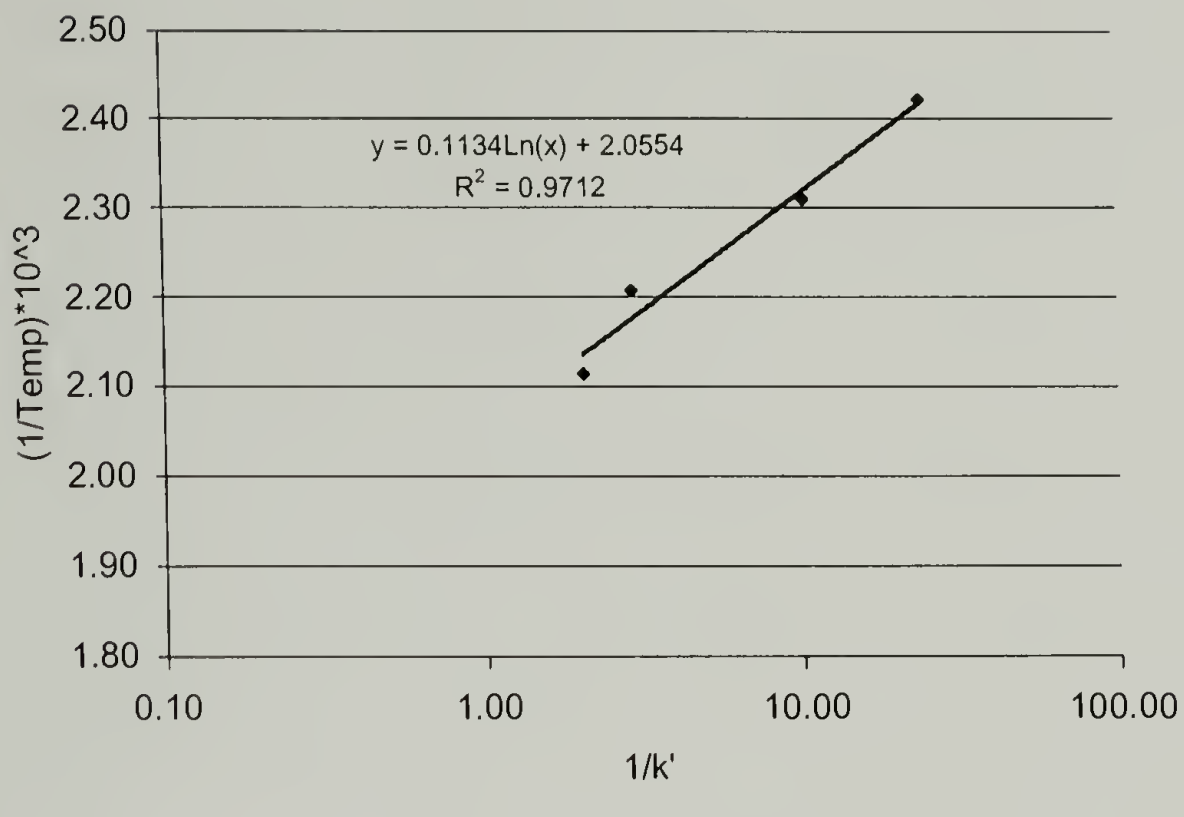

Figure 6.21. Relationship of temperature to shift factor k' for NR/S-SBR physical blend (with correlation equation).

Table 6.5. Strength % retention predicted by new bond formation theory and actual HPHTS strength retention results as a function of temperature for NR/S-SBR physical blend.

K'	Temp C	% Predicted	HPHTS Actual
0.04	140	30	N/A
0.15	160	45	30
0.54	180	55	40
0.78	200	60	45
1.27	220	65	50
2.55	240	65	40
4.86	260	60	35

6.4 Natural Rubber/ Emulsion-Styrene-Butadiene Rubber Blends

The last "engineered" rubber investigated was a natural rubber/emulsion-polymerized styrene-butadiene rubber. The emulsion polymerization of SBR results in a much lower vinyl content along the backbone of the rubber (less 1,2 insertion during polymerization).

6.4.1 HPHTS Results

Figure 6.22, Figure 6.23 and Figure 6.24 give the HPHTS results for strength at break, elongation at break and 100% modulus, respectively. In comparison with the NR/S-SBR blend, the NR/E-SBR blend behaves completely different. While the critical temperature value is still 220°C, the 100% modulus data indicates that reversion is taking place. However, this is countered by a drop at higher sintering temperatures of the elongation at break, a trend that is typically common of overcrosslinking rubbers. Figure 6.25 summarizes the retention of original mechanical properties for HPHTS sheets of NR/E-SBR. The retention of mechanical properties is very similar for that of the NR/S-SBR blend, although the mechanism of property loss is not 100% clear (reversion or overcrosslinking) as it was with the NR/S-SBR blend.

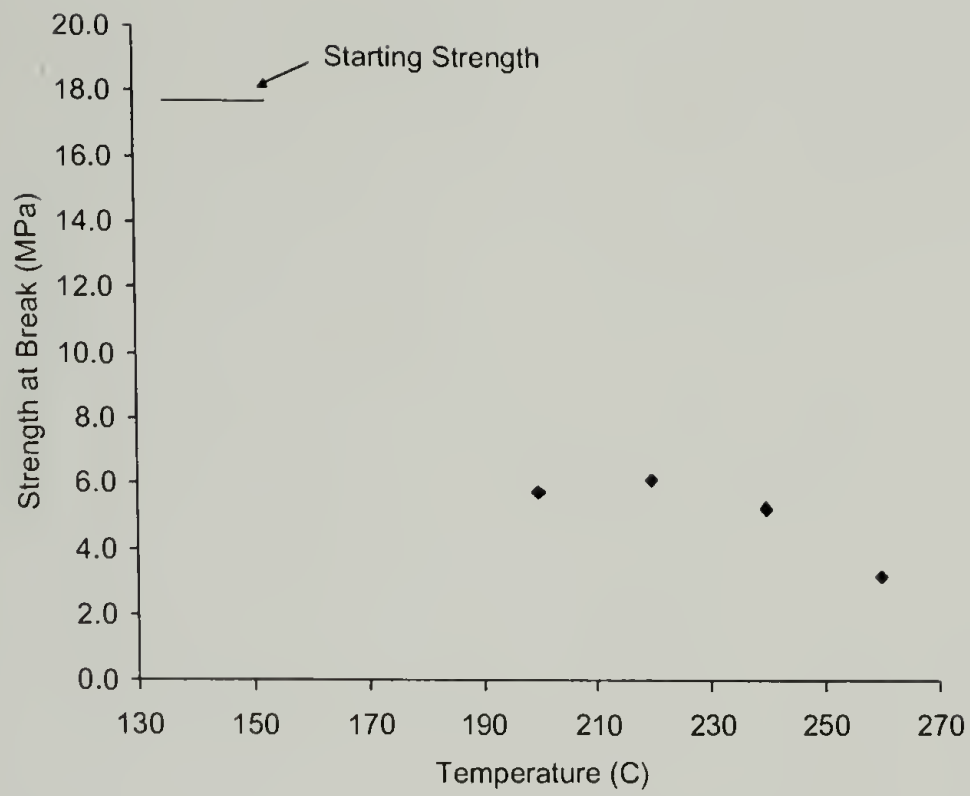

Figure 6.22. HPHTS results of strength at break vs. temperature for carbon black-filled NR/E-SBR sintered at 8.6 MPa for 1 hour.

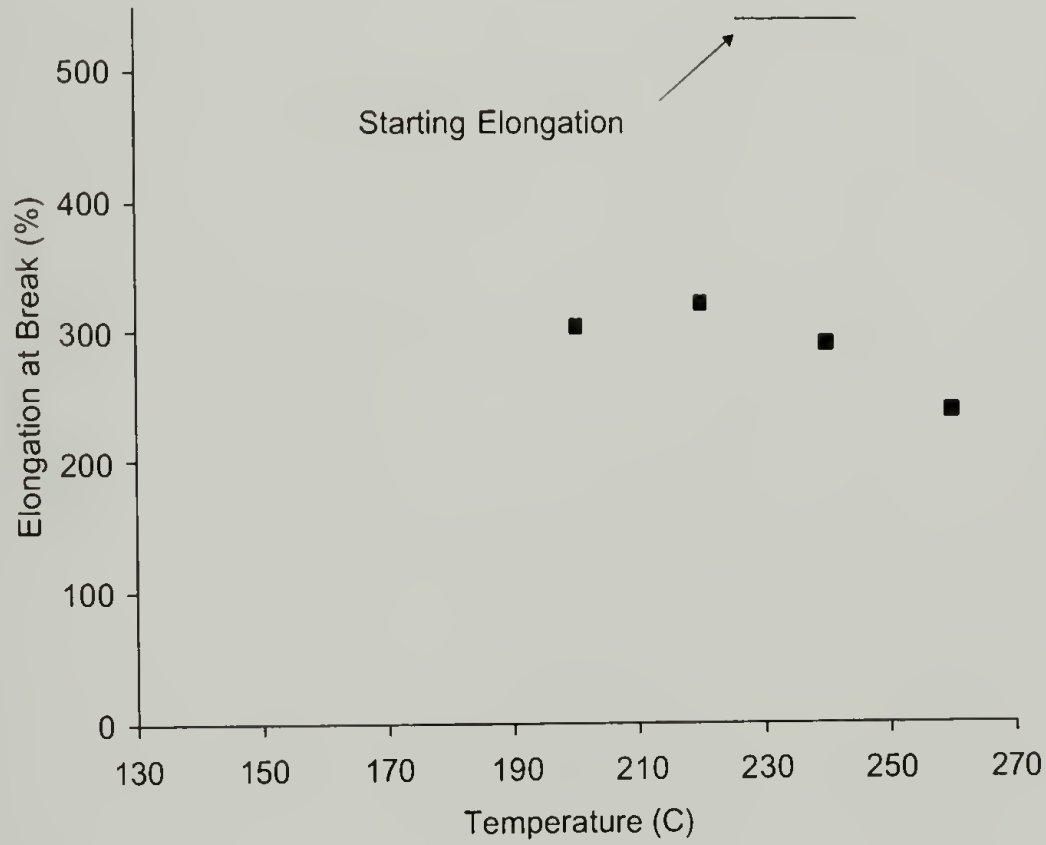

Figure 6.23. HPHTS results of elongation at break vs. temperature for carbon black-filled NR/E-SBR sintered at 8.6 MPa for 1 hour.

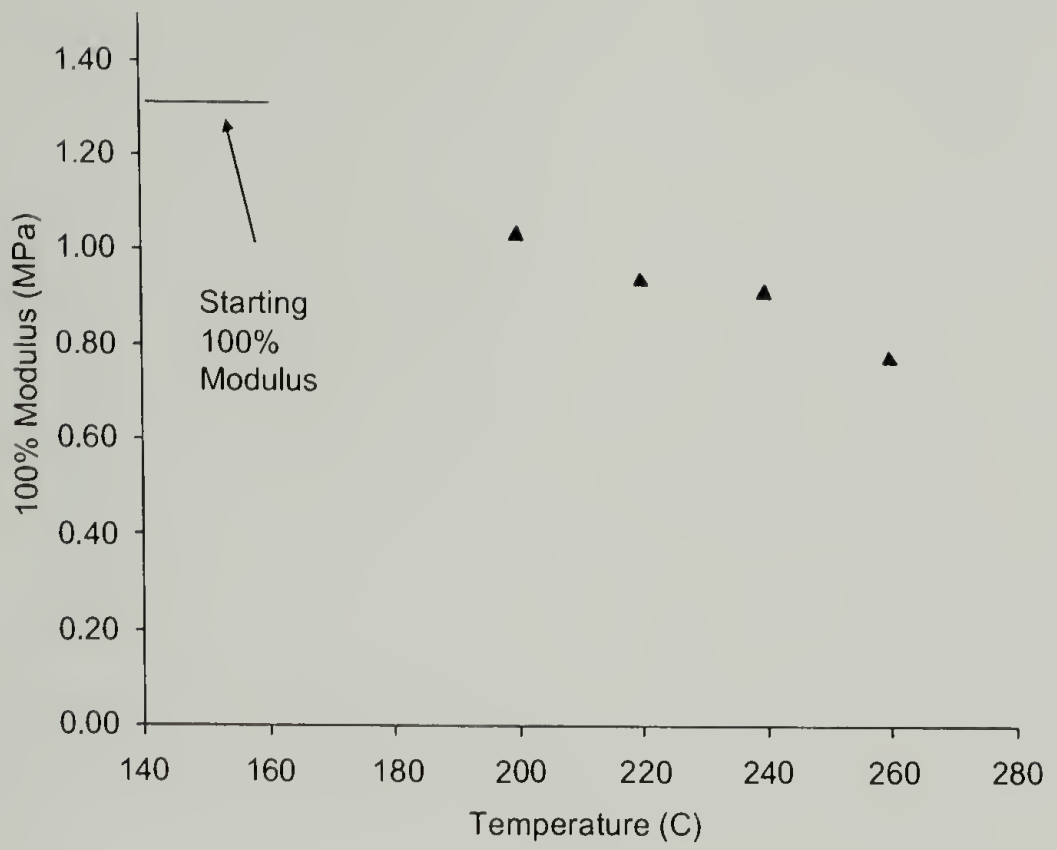

Figure 6.24. HPHTS results of 100% modulus vs. temperature for carbon black-filled NR/E-SBR sintered at 8.6 MPa for 1 hour.

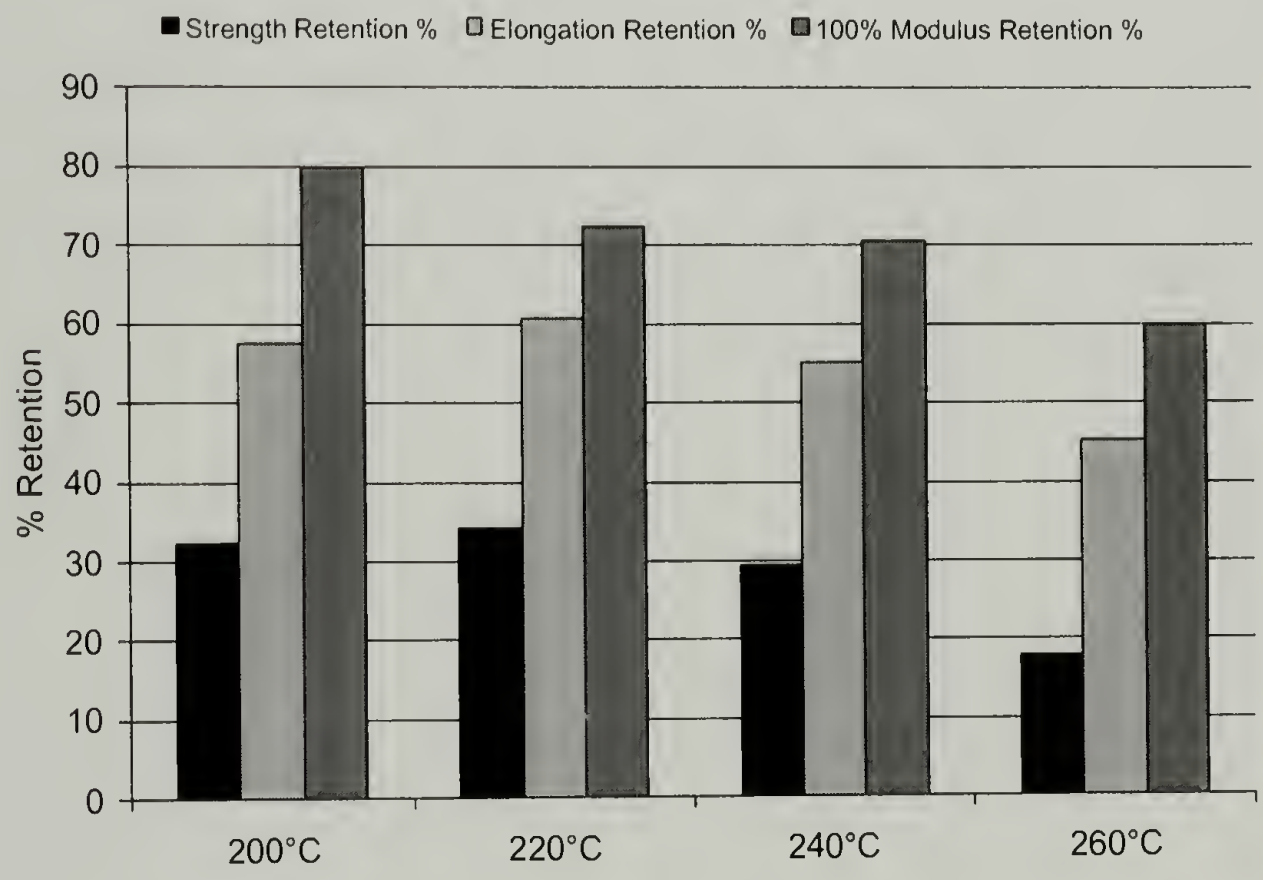

Figure 6.25. Mechanical property retention summary for carbon black-filled NR/E-SBR sintered at 8.6 MPa for 1 hour.

6.5 Conclusions

Overall, the terpolymer blend of styrene, isoprene, and butadiene appears to recycle slightly better than either NR or SBR. However, it may be possible to increase the retention of SIBR by changing the proportions of styrene, butadiene and isoprene, as the terpolymer appears to revert at its critical temperature. Unlike the chemically bonded blend, the physical blends did not perform as well. This is likely due to the larger domain sizes of the blend, resulting in areas overcrosslinking, while other areas revert. The S-SBR/NR blend does retain a higher percentage of properties in comparison to the E-SBR/NR blend, suggesting that higher vinyl content in the SBR region may improve property retention.

As with Chapter 4, CSR again proves to be a useful technique in predicting HPHTS data. SIBR and NR/S-SBR CSR data superimpose well and offer master curves for HPHTS prediction. Both SIBR and NR/S-SBR are predicted to retain around 60% of their original mechanical properties. The next logical step is to procure additional SIBR rubbers of different compositions and evaluate their CSR behavior.

CHAPTER 7

DEGRADED RUBBER

7.1 Background

There are numerous patents and papers discussing the degradation/ devulcanization of rubber and the subsequent recompounding or revulcanization of the resulting material. The patent and journal literature is filled with techniques describing microwave, ultrasonic and chemical methods as means to degrade/devulcanize crosslinked rubber. In the 1990's alone there are over 100 patents and papers discussing them. The overall objective of these papers and patents was to turn waste rubber into a usable form either as filler to virgin rubber, or as a new material through revulcanization. However, despite the extensive amount of research in this area, all the techniques employ more than the necessary steps to produce degraded/devulcanized rubber.

The United States patent literature details extensive work aimed at degrading/devulcanizing rubber and subsequent recompounding and revulcanization. Some examples include patent # 4,104,205 [46] and # 5,578,700 [47] in which the inventors claim microwave devulcanization of rubber, yielding materials "capable of recompounding and revulcanization". Patents # 5,258,413 [48], # 5,284,625 [49], and # 6,095,440 [50] detail work done involving the ultrasonic devulcanization of rubber and subsequent reforming of new parts in a manner similar to that of uncrosslinked rubber. Patent # 4,161,464 [51] claims devulcanization via a phase transfer catalyst, to produce a "recyclable rubber." Patent # 5,798,394 [52] involves swelling the rubber in a suitable solvent and then exposing the swollen rubber to an alkali metal. The devulcanized rubber can then be revulcanized by adding the appropriate curing chemicals. Patent # 5,891,926

[53] exposes cured rubber to high temperatures and pressures in the presence of 2-butanol to achieve devulcanization. It also describes how the produced devulcanized rubber can be recompounded and recurred. Similarly, patent # 6,380,269 [54] describes surface devulcanization of cured rubber crumb at high temperatures and pressures in the presence of 2-butanol. Patent # 6,133,413 [55] also incorporates high temperatures as well as shearing pressure to devulcanize the rubber. It further describes molding and revulcanizing said devulcanized rubber into new parts comprised only of devulcanized rubber. Finally, patent # 6,387,966 [56] utilizes mechanical and chemical means to devulcanize rubber.

The journal literature also has numerous references to the devulcanization of waste rubber, many stemming from the initial patented work. Fix [57] further describes work conducted at Goodyear involving the microwave devulcanization of rubber waste. Isayev et al. [58] details recent work carried out regarding the devulcanization of carbon black filled natural rubber, and also lists numerous references involving ultrasonic devulcanization. Nicholas [59] and Milani [60] highlight work involving the phase transfer catalyst path to rubber devulcanization. Crane and Kay discuss degradation of scrap tire rubber at high temperatures in an oil media, [61] as does Henry [62] regarding silicone rubber in silicone oil. Finally, Padella [63] and Magini [64] describe mechano-chemical methods for devulcanization. Warner [65] provides an excellent review of the methods of devulcanization.

7.2 Motivation

In the quest to find a suitable method for the recycling of rubber, degrading rubber to a viscous "liquid" and then blending it back in to virgin rubber appears to be a viable option. To date, the viscous "liquid" produced using the Parr reactor (Figure 7.3) has been shown to be compatible with unvulcanized rubber over a large range of loadings and has been revulcanized back to the elastomeric state through the addition of sulfur. To obtain this material, vulcanized rubber is placed in the Parr reactor and the reactor is filled with either a nitrogen or air environment. The temperature is then raised and the material is allowed to degrade for a given time period in either an open (volatiles escape) or closed (volatiles remain in material) bomb. The resulting material is a viscous, pseudo-liquid due to the breakdown of the rubber network and backbone. Variables to be explored include the temperature of degradation, the environment (air or inert, open or closed) and the time allowed.

Herein, it is shown that replacing oil with the degraded rubber allows one to produce a material with a high recycle content, while not sacrificing any mechanical properties. One major limitation to regrind blending is that mechanical property retention is impacted by two factors, the amount of regrind incorporated, and its particle size. Figure 7.1 and Figure 7.2 after Krekic [66] and other authors highlight these occurrences. [67,68,69,70,71,72,73]

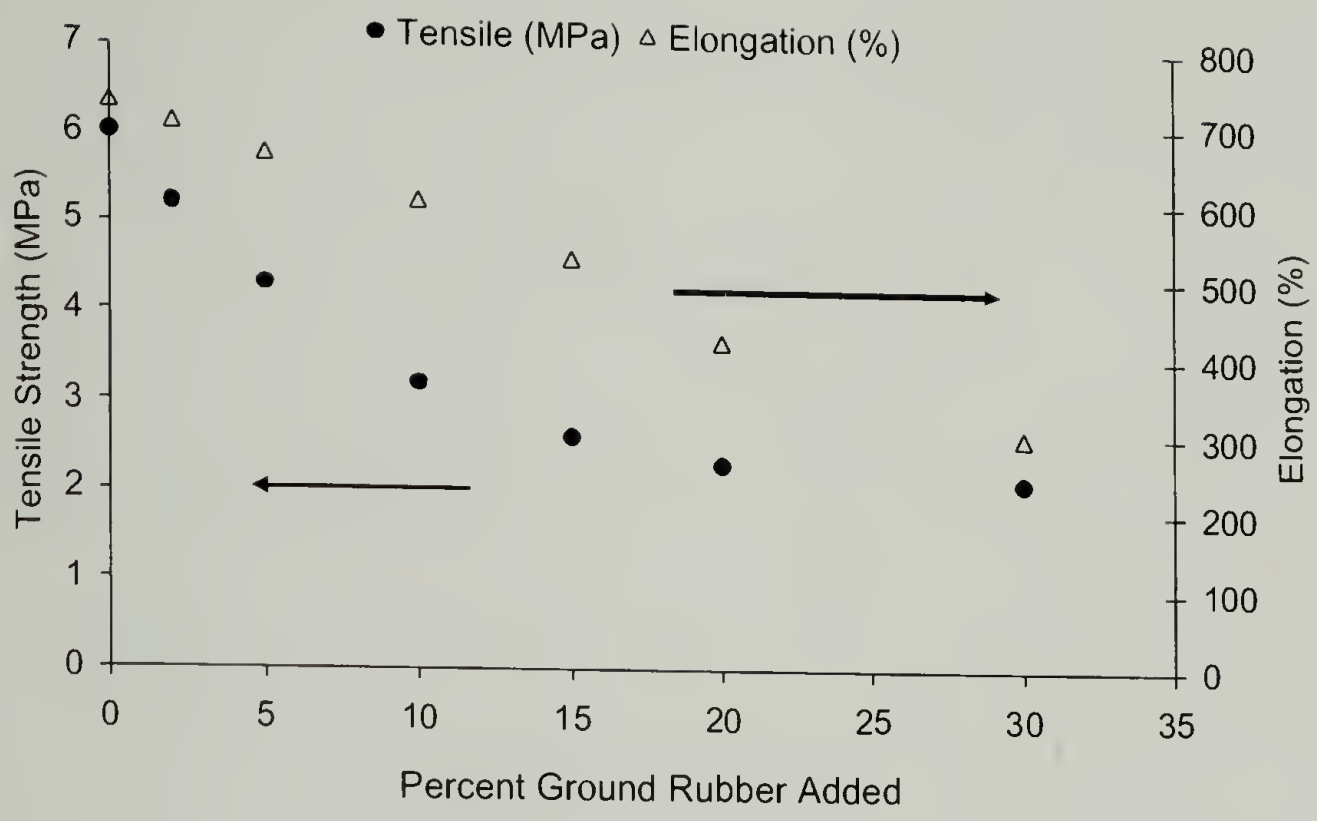

Figure 7.1. Tensile and elongation decrease versus amount of ground rubber added for a natural rubber system.

Economically, the degraded/devulcanized material no longer needs to be ground into a powder to be reincorporated into the virgin rubber. Also, there is the potential for completely eliminating the size reduction step as it should be possible to turn large parts directly into degraded/devulcanized material. This is advantageous as grinding rubber to powder can be an expensive process. In addition, as one goes to smaller particle sizes, the cost of the process increases. As such, it is easy to see that there is a tradeoff of mechanical properties and cost when incorporating regrind into virgin rubber. However, as degraded/devulcanized rubber does not have these limitations it is conceivable that adding degraded rubber to virgin rubber as a replacement for oil might be not only be an environmentally friendly alternative, but an economic one as well.

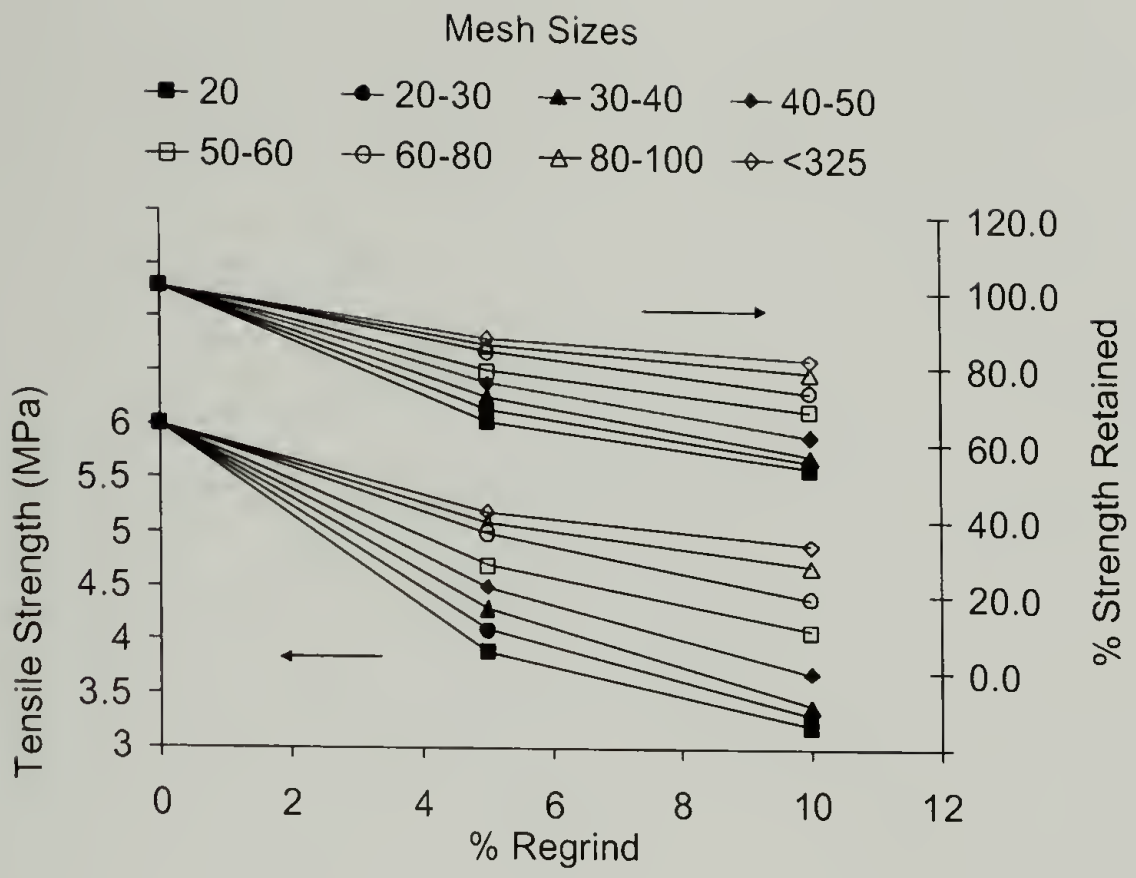

Figure 7.2. Decrease in tensile strength versus amount and size of regrind.

7.3 Proposed Work

The work to be attempted aims at first degrading/devulcanizing rubber under high temperatures, and subsequently using the produced viscous material in a variety of applications, most specifically as a plasticizer/extender to replace leachable oils in rubber compounding. As is shown in Table 7.1, oils and other chemicals are important agents in rubber as they enhance its workability, flexibility and/or distensibility. Plasticizers and extenders also help incorporate carbon black into the rubber during compounding. Oils and other agents used for extending are inherently less expensive than virgin rubber and thus help to reduce the cost as well as increase its processability. Addition of plasticizers during mixing can reduce hot melt viscosity and retard chain cleavage. However, retention of plasticizer inside the rubber matrix is one of the key issues in ensuring

consistent mechanical properties over time. As elastomers are comprised of long crosslinked hydrocarbon chains, replacing oil by a reactive polymeric plasticizer would be an obvious choice to help alleviate the oozing of the oil to the rubber surface, and leaching of the oil when rubber products come in contact with solvents. This should improve the aging of the rubber. For all of these reasons, it is believed that degraded rubber, if able to mimic processing parameters and mechanical properties when replacing oil, should serve as an excellent, low cost extender/plasticizer.

Table 7.1. Uses of plasticizers/extenders in typical rubber compounds.

Truck Tread Compounds[1]		**Steam Hose Compounds**[2]		**Shoe Sole Compounds**[3]	
Natural rubber	100	EPDM	100	Nitrile Rubber	100
Peptizer	0.10	FEF Carbon Black	110	Carbon Black	60
HAF Carbon Black	50	***Paraffinic oil***	***70***	***DOP****	***16***
Aromatic oil	***12***	***Factice***	***20***	ZnO	5.0
ZnO	5.0	ZnO	5.0	Stearic Acid	1.5
Stearic Acid	1.5	Stearic Acid	1.0	Antioxidant	1.0
Antioxidant	1.0	Antioxidant	1.0	Antiozonant	1.0
Antiozonant	1.0	Antiozonant	1.0	Accelerators	3.0
Accelerator-MOZ	0.45	Accelerators	1.5	Sulfur	1.5
Sulfur	2.5	Sulfur	1.5		

* DOP = Dioctyl phthalate

[1,2] Bayer Rubber Chemical Handbook

[3] Nippon Zeon Company Limited Formulary

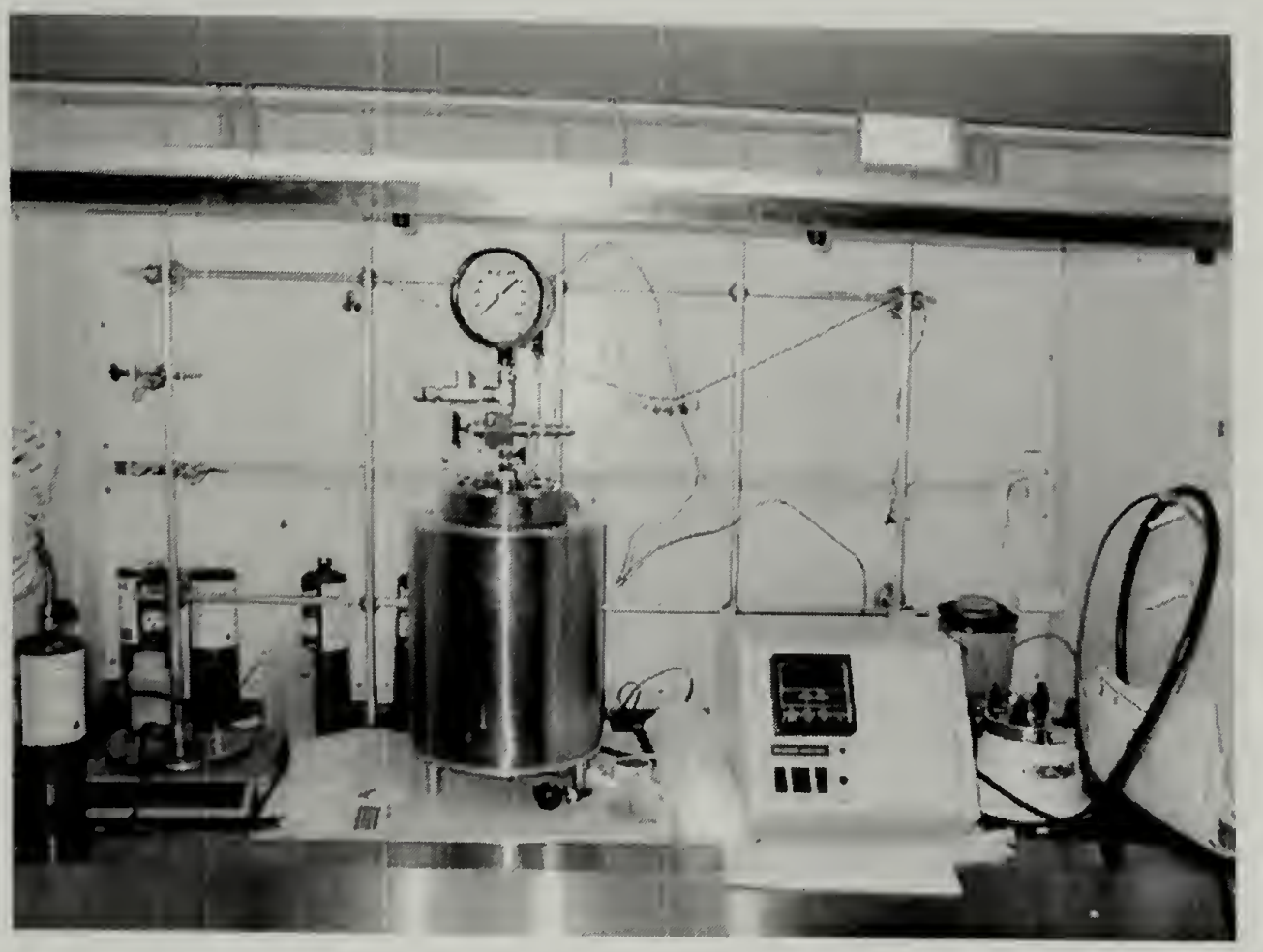

Figure 7.3. Parr reactor used for the degradation/devulcanization of rubber.

7.4 Experimental

7.4.1 Degradation

A Parr Reactor was used to supply high temperature during the degradation/devulcanization of rubber. Up to 500 grams of rubber could be degraded at a time in a batch process. The reactor could reach temperatures in excess of 300°C in a controlled manner. It also had pressure rated tubing, thus allowing for the control of the reaction environment (air, N_2, Ar, etc.). All of the degradation herein were conducted under a closed, high pressure N_2 environment (around 4.1 MPa), restricting the volatilization of oils present in the degrading rubber (w/out pressure, over 20% of the original starting weight can be volatilized and lost).

7.4.2 Differential Scanning Calorimetry (DSC)

Differential Scanning Calorimetry (DSC) was conducted on a TA 2910 Modulated DSC with supported liquid nitrogen cooling accessory (LCNA) head to reach sub-ambient temperatures. Its main use was to explore the state of the rubbers after degradation. DSC is an excellent analytical tool to explore glass transitions of polymers. Specifically, DSC was used to measure changes in heat flow as a function of temperature as the rubbers were heated from below -80°C to room temperature Rubbers typically show glass transitions around -60°C.

7.4.3 T-90 Experiments

Torque experiments were run on a Rheometrics rheometer for the compounded rubbers. The time at 90% of the maximum torque (T-90) at a set temperature of 160°C was used as the vulcanization time.

7.4.4 Rubber Compounding

A Braybender mixer was used to mix virgin, unvulcanized rubbers for later vulcanization. These rubbers contained various amounts of plasticizers (oil or degraded rubber), along with other fillers (carbon black) and vulcanizing agents (sulfur, accelerators, etc.) The Braybender allowed for sufficient mixing to occur and the aim of dispersing the various components evenly throughout the rubber was achieved. The temperature of the mixing was roughly 60°C to reduce the viscosity of the uncrosslinked natural rubber and help with the mixing. Components were added step wise starting with virgin rubber, followed by sulfur and other accelerators, and finally the carbon black and

oil/degraded rubber portion, as is established in the rubber industry. According to Mooney viscosity studies, the viscosities of the oil and degraded rubber compounded rubbers were comparable over all loadings.

7.4.5 Vulcanization of Compounded Rubbers

A Carver model C melt press and a Phi model B230-C were used to supply pressure and temperature during the vulcanization of the compounded rubbers. Average vulcanization temperatures were around 150-160°C, and were easily obtained and controlled with the melt presses.

7.4.6 Thermal Gravimetric Analysis (TGA)

Thermogravimetric Analysis (TGA) was conducted on the rubbers after vulcanization. TGA allows one to explore the temperature at which degradation occurs by monitoring the weight loss of a sample as a function of temperature. It also yields information about the charring characteristics of a material, which can correlate to a materials fire resistance (higher char yields indicate less material available for burning and usually perform better in flame testing). As oils and other low molecular weight additives are extremely volatile, it is likely that rubbers compounded with them will show a lower degradation onset temperature (weight loss). Rubbers compounded with degraded rubber however have the benefit of potentially being polymeric in nature and should show better stability and higher char yield due to their lower volatility and the additional carbon black present in them (will show up in the char yield as carbon black will not be lost during the experiment).

7.4.7 Acetone Extraction

Acetone was used in attempts to extract the plasticizer (oil or degraded rubber) after vulcanization. As mentioned previously, it is important for plasticizers to remain within rubbers after vulcanization, even when exposed to solvents. As degraded rubber is higher in molecular weight, more similar in nature to natural rubber, and has the ability to react with matrix (natural rubber) during vulcanization, it is believed that less will be extracted in comparison to an oil plasticized sample.

7.4.8 Tensile Testing

Stress-strain curves were obtained on ring samples with average diameters of 20.0 mm, 2.5 mm thick and 2 mm wide, using an Instron 4468 at test rates of 10 mm/min, following ASTM D 412.

7.4.9 Aging Experiments

Studies to measure the aging properties of the compounded rubbers were also conducted. Circular rings cut from vulcanized sheets of the DR compounded rubbers were subjected to 100°C in an oven for various times. The rings were then removed and tested at room temperature as described above on an Instron 4468. It is believed that the DR compounded rubbers will show better aging properties as they should retain a greater percentage of their plasticizer (DR) compared to a similarly procured oil extended rubber.

7.5 Natural Rubber with Degraded Natural Rubber

7.5.1 Tensile Results

Figure 7.4, Figure 7.5 and Figure 7.6 exhibit the mechanical properties of strength at break, elongation at break and 100% modulus, respectively, versus the amount of oil or degraded natural rubber (DNR) added to the compounding formulations (Table 7.2). As expected, the natural rubber vulcanizates compounded with oil show a decrease in the strength at break, a gradual increase in the elongation at break and a reduction in the 100% modulus with increasing amounts of oil. On the contrary, natural rubber vulcanizates (Table 7.2) over a range from 10 to 40 phr (parts per 100 parts rubber) loading of DNR, maintain a constant strength at break (Figure 7.4) while exhibiting an increase in the elongation at break (Figure 7.5) and a decrease in the 100% modulus (Figure 7.6). However, the 100% modulus values in the DNR loaded samples, show higher values than the corresponding oil compounded vulcanizates and they (DNR loaded samples) do not decrease as much as in the oil added samples, especially at the higher loading levels.

Table 7.2. Compositions of NR vulcanizates in the presence of DNR and oil.

	DNR[a] Recipe	Oil Recipe
NR (SMR CV)	100	100
ZnO	5	5
Stearic Acid	1.0	1.0
Carbon Black	40	40
Oil (Sundex 8825)	-	10 - 40
DNR[a]	10 - 40	-
Sulfur	1.5	1.5
CBS[b]	1.5	1.5
TMTD[c]	0.2	0.2

[a] Degraded vulcanized natural rubber (DNR)
[b] N-cyclohexylbenzothiazole-2-sulfenamide
[c] Tetramethylthiuram disulfide

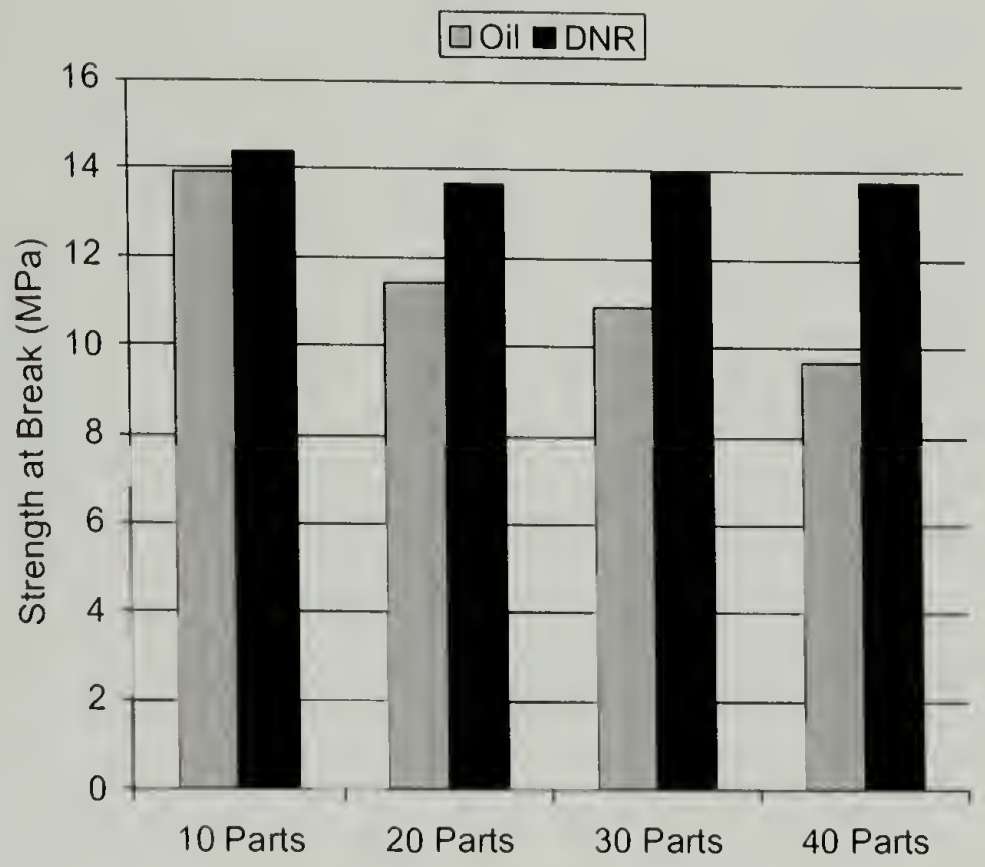

Figure 7.4. Strength at break (before aging) of natural rubber vulcanizates vs. the amount of degraded natural rubber/oil.

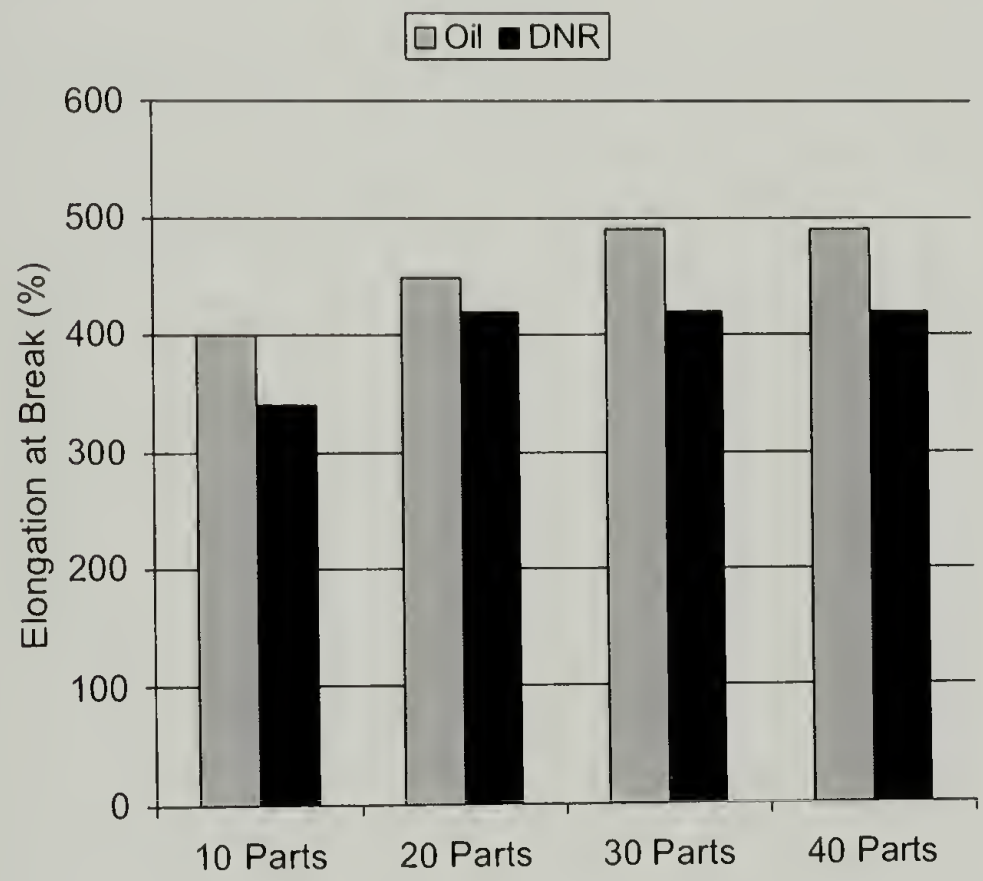

Figure 7.5. Elongation at break (before aging) of natural rubber vulcanizates vs. the amount of degraded natural rubber/oil.

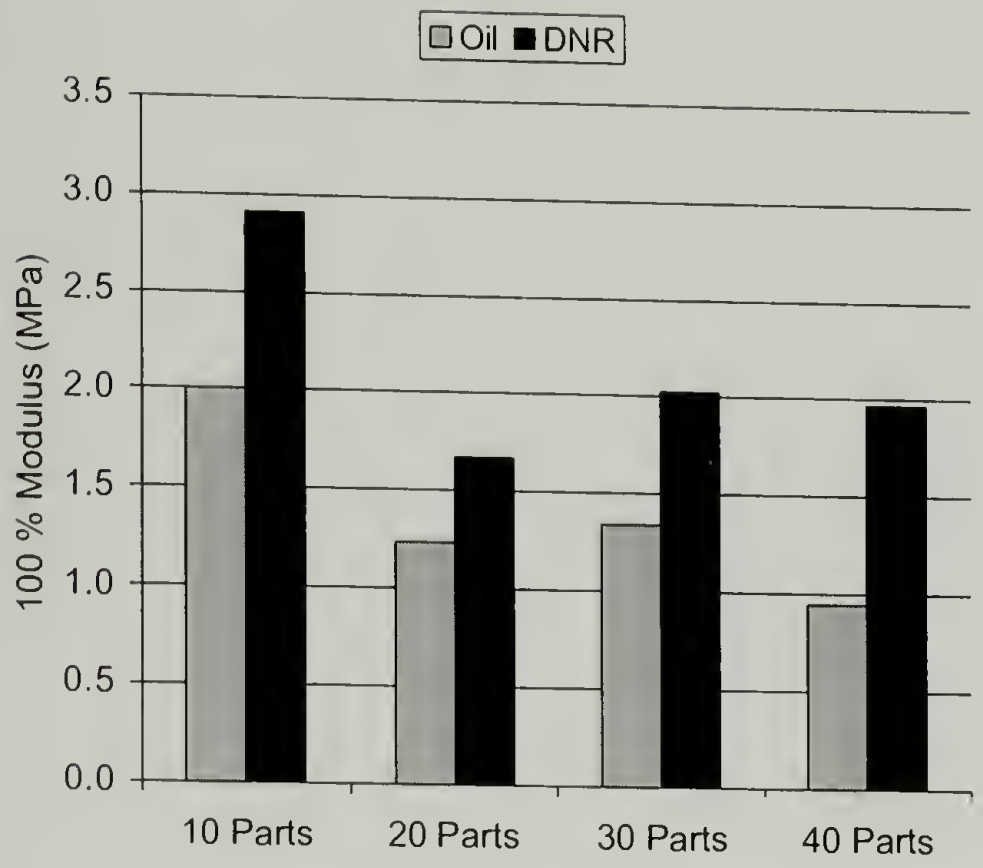

Figure 7.6. 100% Modulus (before aging) of natural rubber vulcanizates vs. the amount of degraded natural rubber/oil.

According to Krekic et al.,[66] even adding low concentrations of ground scrap rubber (30 – 40 mesh) to virgin rubber compounds results in a 15% reduction in the tensile strength (Figure 7.1 and Figure 7.2). Interestingly, even with adding over 40% DNR to the virgin natural rubber vulcanizate one still maintains a constant strength at break. Figure 7.7 and Figure 7.8 illustrate the effect on mechanical properties of adding 40 mesh cryoground scrap rubber to virgin rubber (Table 7.3), following the same compounding formulations as Table 7.2. As is clear in Figure 7.7 and Figure 7.8, the mechanical properties of are reduced as the amount of scrap rubber powder is increased in the formulation. The observations are in full agreement with the results obtained by Krekic et al. (Figure 7.1 and Figure 7.2) and others.[14,74]

Table 7.3. Compositions of NR Vulcanizates in the Presence of Ground Vulcanized Natural Rubber (40 mesh) and 10 phr of Oil.

	A	B	C	D
NR (SMR CV)	100	100	100	100
ZnO	5	5	5	5
Stearic Acid	1.0	1.0	1.0	1.0
Carbon Black	40	40	40	40
Oil (Sundex 8825)	10	10	10	10
GVNR[a] – 40 mesh	-	10	20	30
Sulfur	1.5	1.5	1.5	1.5
CBS	1.5	1.5	1.5	1.5
TMTD	0.2	0.2	0.2	0.2

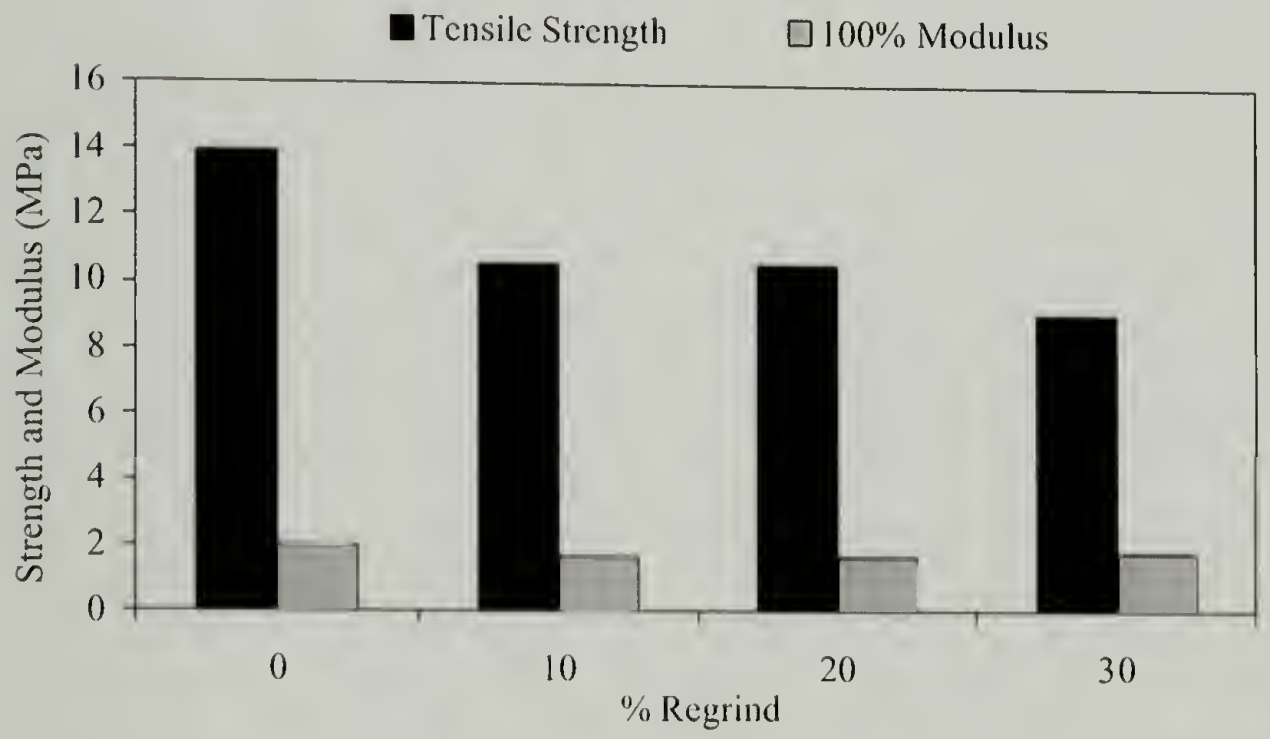

Figure 7.7. Strength at break and 100% modulus of natural rubber vulcanizates vs. the % of regrind.

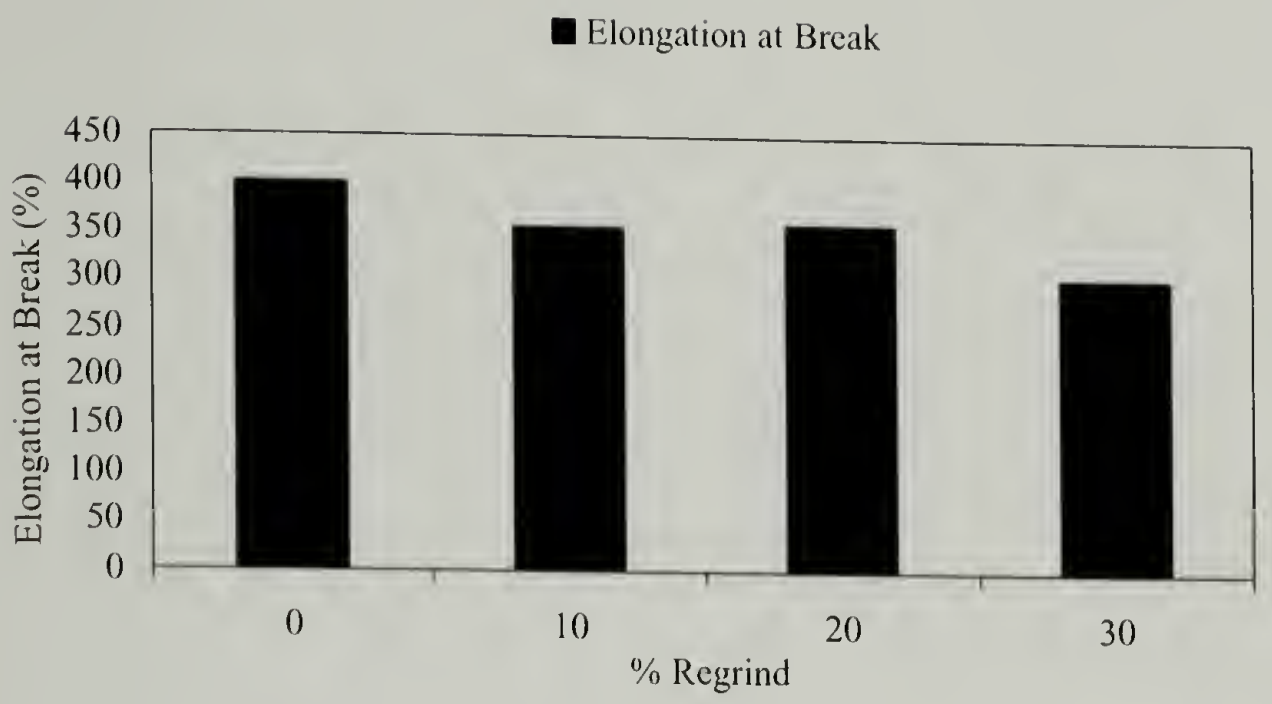

Figure 7.8. Elongation at break of natural rubber vulcanizates vs. the % of regrind.

7.5.2 Aging Experiments

Figure 7.9, Figure 7.10 and Figure 7.11 show the strength at break, elongation at break and 100% modulus, respectively, of the natural rubber vulcanizates (Table 7.2), after aging at 100 ^{0}C for 48 hrs. Although all of the mechanical properties are reduced compared to the unaged properties, the materials compounded with DNR show better property retention than those compounded with oil. At 40 phr loading of DNR, the materials retain over 80% of their original strength value, compared to just over 60% for materials compounded with oil. Elongation retention is equal for both systems at the 40 phr loading. The DNR loaded materials show slightly higher modulus retention at the 40 phr loading.

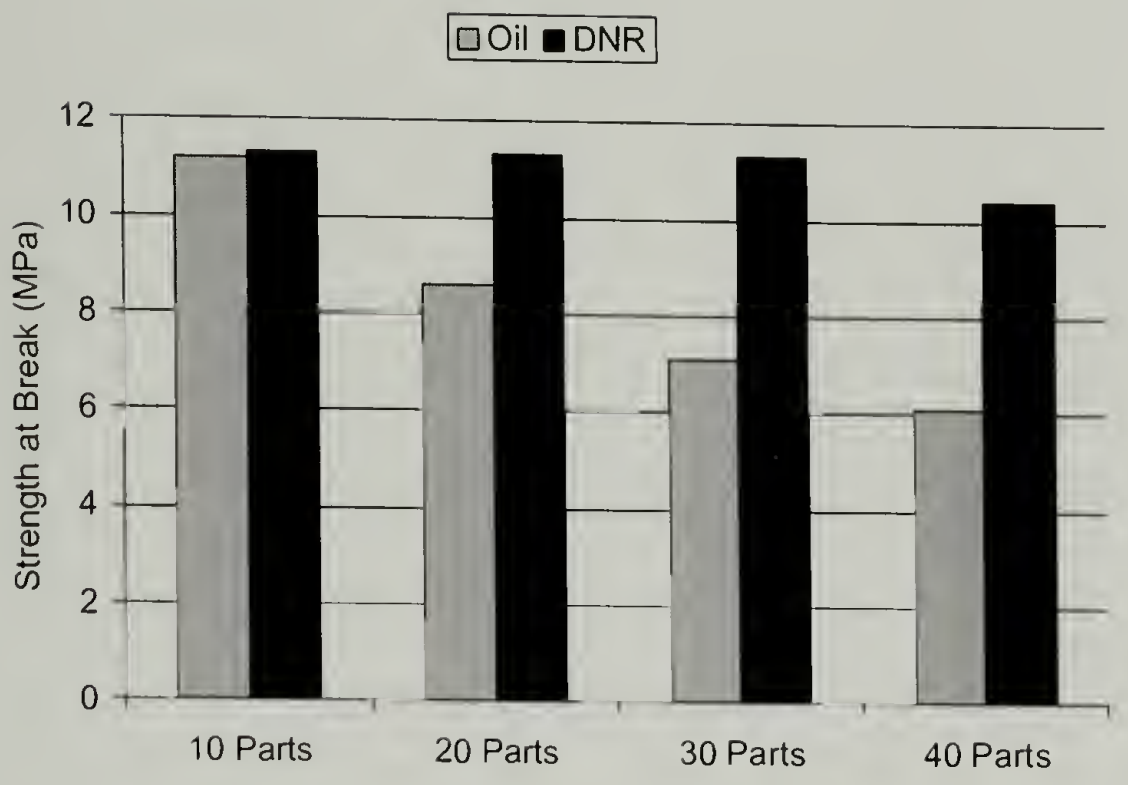

Figure 7.9. Strength at break (after aging) of natural rubber vulcanizates vs. the amount of degraded natural rubber/oil.

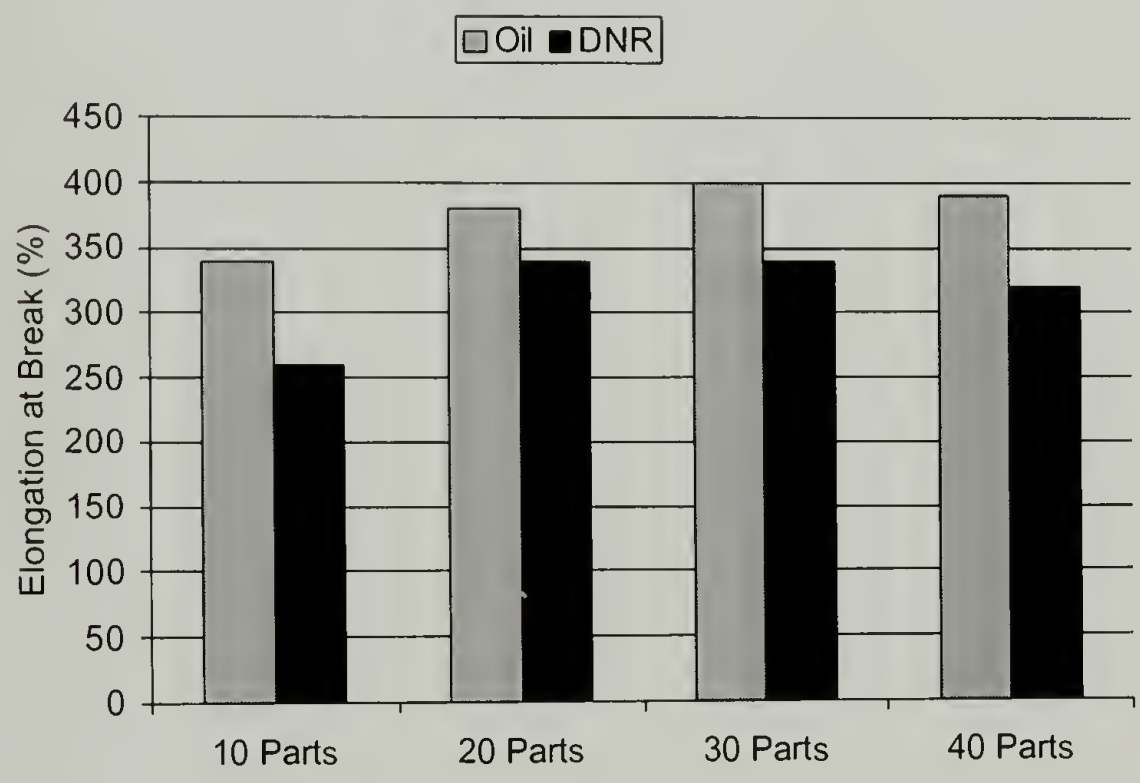

Figure 7.10. Elongation at break (after aging) of natural rubber vulcanizates vs. the amount of degraded natural rubber/oil.

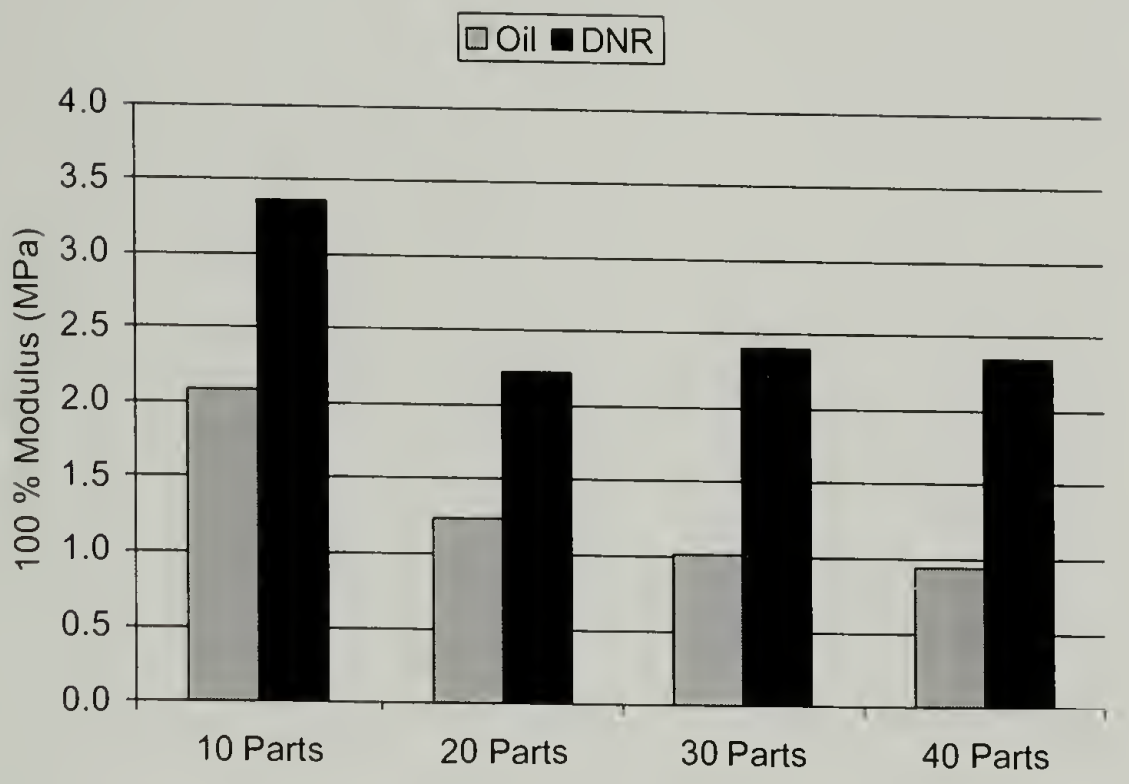

Figure 7.11. 100% Modulus (after aging) of natural rubber vulcanizates vs. the amount of degraded natural rubber/oil.

7.5.3 Polymeric Nature of DNR

The improvement in aging properties with the addition of DNR can be accounted for from the fact that DNR is a degraded/devulcanized, but still polymeric form of natural rubber. DNR acts as extra rubber capable of further vulcanization, along with incorporating a higher loading of carbon black into the NR vulcanizate (as carbon black is present in DNR). The DSC curves (Figure 7.12) for scrap NR rubber before and after degradation show how the T_g of DNR (at -51^0C) is only slightly higher than the original scrap rubber (T_g of scrap natural rubber at -58^0C). This supports the idea of DNR retaining its polymeric structure. The Gel Permeation Chromatography (GPC) results (Table 7.4) of DNR, confirm this observation that DNR is a highly degraded form of NR (original unvulcanized molecular weight of NR is > 1,000,000). The two peaks present

show that backbone degradation must be occurring and that there is a very small molecular weight fraction along with a significantly larger molecular weight fraction in approximately even proportions (It is possible that a large molecular weight fraction exists as well, but does not make it into the column due to solubility issues. To date however, this has not been substantiated.) Therefore, DNR can be treated as a polymeric plasticizer and this is why DNR has been able to provide better mechanical properties than the corresponding oil loaded samples before and after aging.

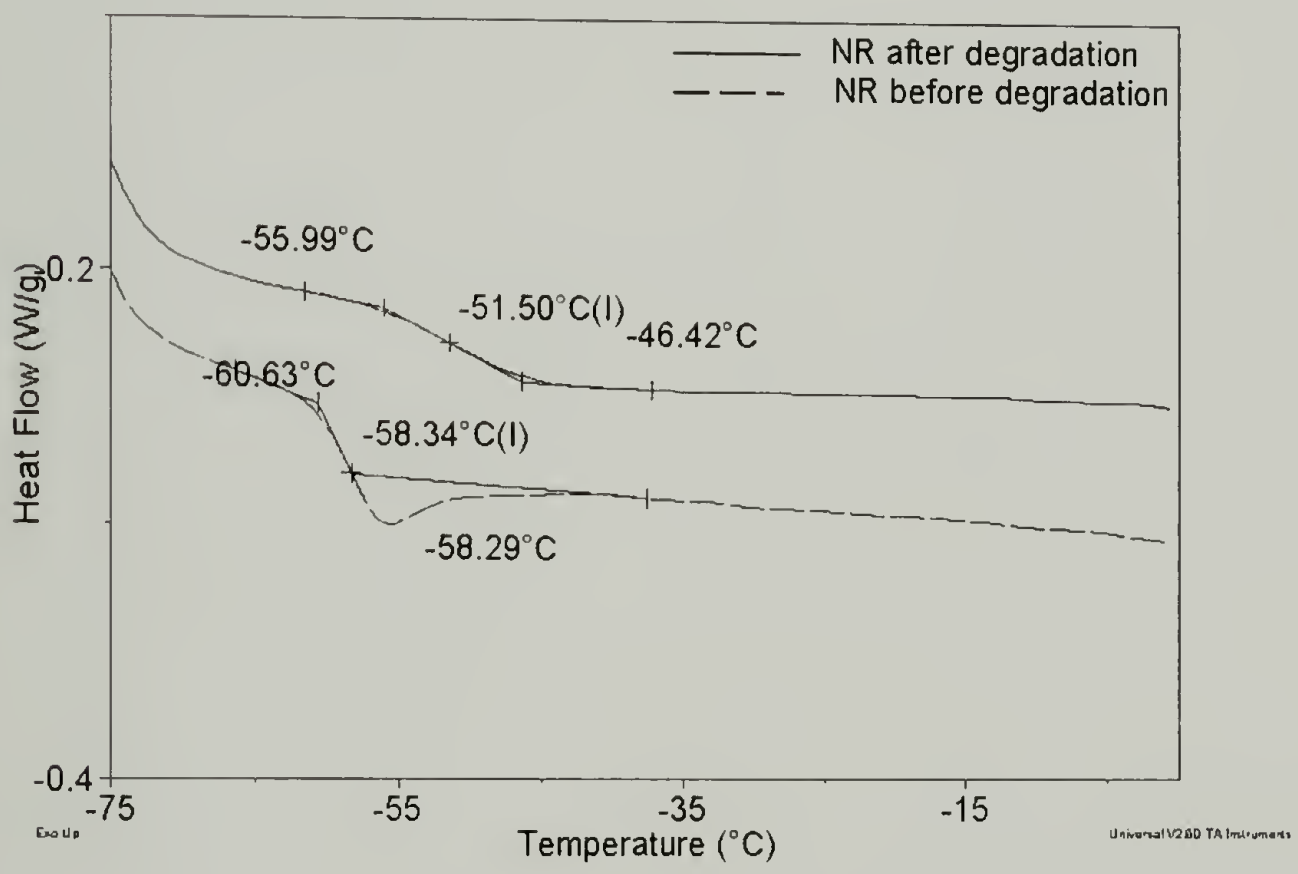

Figure 7.12. DSC thermogram of vulcanized natural rubber before and after degradation.

Table 7.4. GPC Data of Degraded Natural Rubber.

GPC	DNR[a]
M_n	36,000 and 6,000
Polydispersity index (PDI)	~2.3

[a] Degraded (at 310^0C) natural rubber

7.5.4 Extraction Experiments

Figure 7.13 shows the results for the acetone extraction of NR samples compounded with oil and DNR. As is evident, the materials compounded with oil show a much higher extractable level than those compounded with DNR. The results support the hypothesis that materials procured with DNR as the plasticizer enable less leaching of the plasticizer (DNR). Again, it is believed this is due to the polymeric nature of DNR and its higher compatibility with the rubber matrix. Nevertheless, DNR, being a degraded/devulcanized form of natural rubber, may also partake in the crosslinking reactions occurring during vulcanization and consequently this might be restricting the extraction in acetone, as the plasticizer (DNR) becomes part of the rubber network. A conversion of weight percent extracted into phr shows that all of the oil is removed during acetone extraction. On the contrary, only about 30% of the DNR is extracted in a similar conversion. This is likely a low molecular weight fraction present either in the oil already in DNR, or chains that are severely degraded during the high temperature degradation.

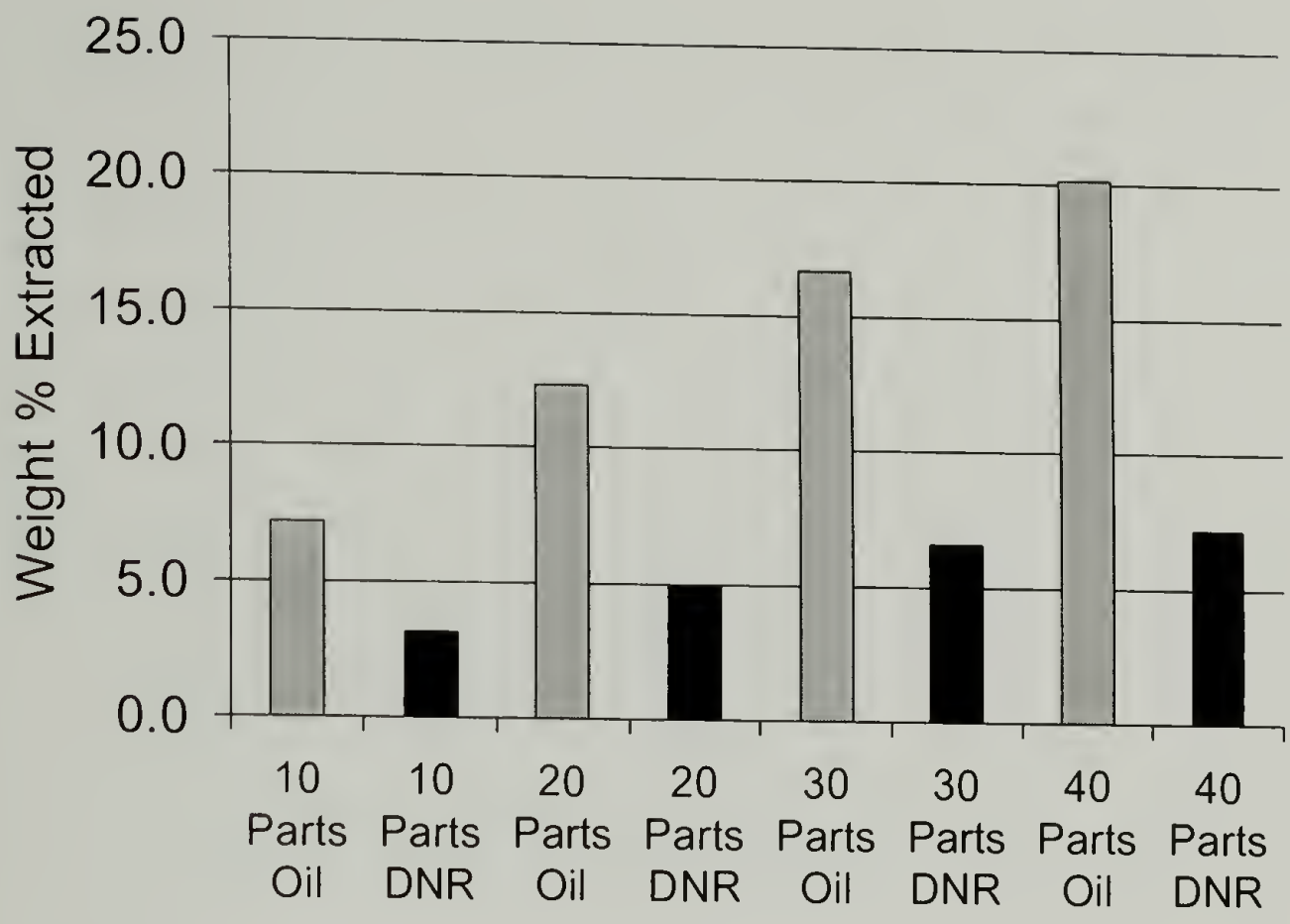

Figure 7.13. Weight % extracted vs. amount and type of plasticizer.

7.5.5 Thermogravimetric Analysis

Unlike DNR samples, the oil compounded samples are subject to oozing of oil to the rubber surface due to the diffusion of the comparatively low molecular weight materials (oil) in the rubber matrix. This is especially prevalent when these materials are subjected to aging or extraction conditions. This is the most common reason for the observed lowering of the mechanical properties after aging. The TGA curves (

Figure 7.14) of the NR vulcanizates compounded with 40 phr oil and 40 phr DNR, respectively, clearly indicate higher char content in the DNR loaded systems along with a higher onset temperature of weight loss.

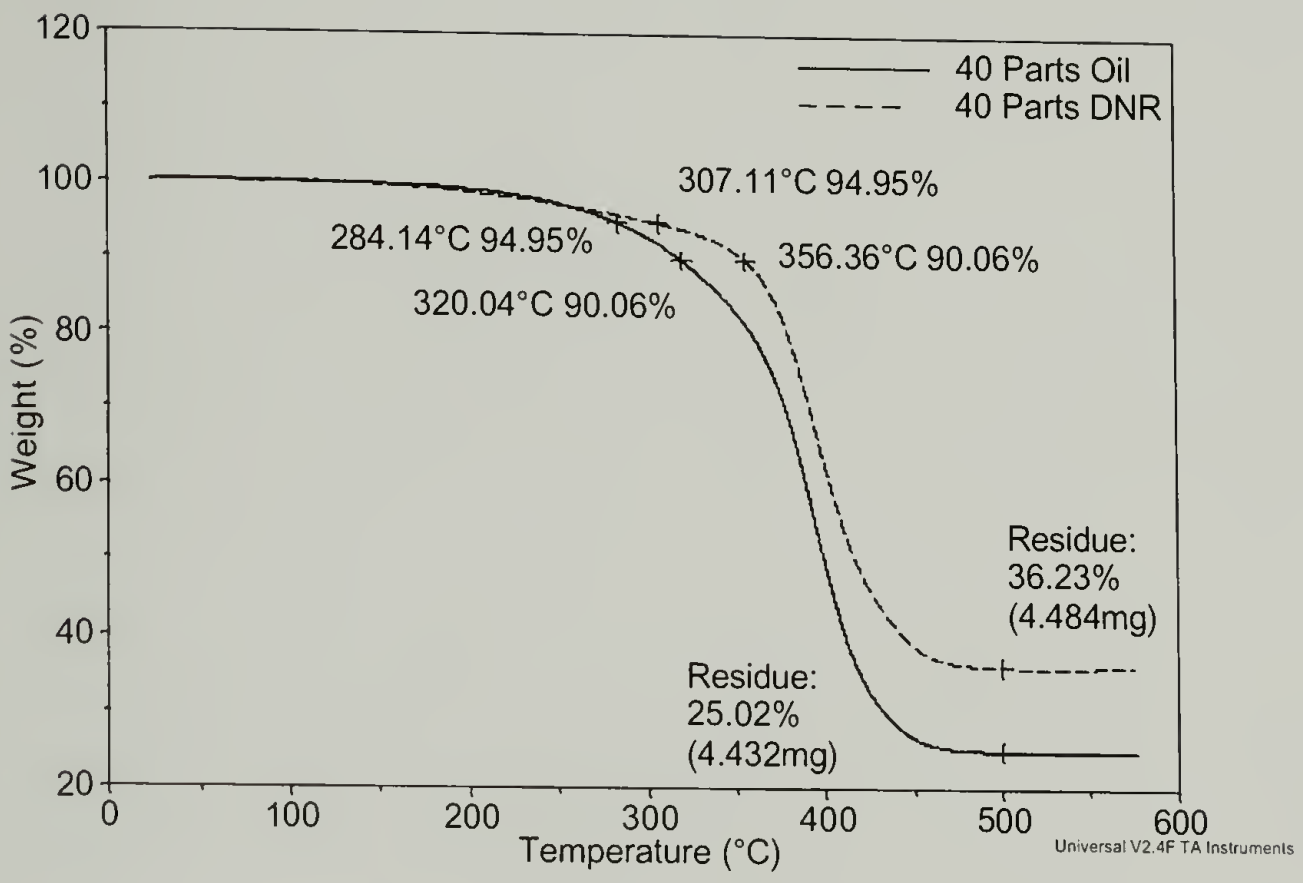

Figure 7.14. TGA thermogram of weight loss of plasticizer vs. temperature.

7.5.6 Swelling

Figure 7.15 shows the percentage swelling in toluene and the 100% modulus against the amount of DNR and oil added. As uncrosslinked natural rubber is soluble in toluene, the swelling of the NR vulcanizate in toluene can reasonably predict the crosslink densities in the context of network structure determination.[75,76] Specifically, if interfacial bonds are formed between the matrix (rubber) and the added dispersed phase (plasticizers: degraded rubber or oil), the dispersed phase will restrict the swelling of the highly swollen continuous phase.[77] As degraded rubber behaves like a polymeric plasticizer and has the ability for further crossliking, the percentage swelling in toluene should be less than that of corresponding oil incorporated samples. As we see Figure

7.15, natural rubber compounded with DNR yields lower swelling than the comparable oil added samples. Although the percentage of swelling increases as the loading of the oil or DNR is increased from 10 to 40 phr in the NR vulcanizate, the swelling of DNR loaded samples remains much lower when compared to oil added samples of similar compositions. Therefore, it appears that DNR contributes to the phase adhesion of the plasticizer (DNR) with the rubber matrix through some mechanism.

DNR loaded NR vulcanizates with extra curatives (not shown) did not show any improvement in the percentage swelling in toluene in comparison with the unmodified samples. Thus it appears that degraded rubber does not participate in crosslinkings reaction with virgin rubber. On the contrary, oil added NR vulcanizates loaded with extra carbon black (not shown) provided lower swelling measurements than those of oil added samples without extra carbon black. This suggests that reinforcing carbon black in the oil added NR vulcanizates gives a mere phase adhesion with unsaturated cis-polyisoprene (natural rubber), as confirmed by Krause[78] and others.[79,80] As DNR contains extra particulate carbon black, this may be one reason why less swelling is observed in the DNR loaded samples.

The lower part of the Figure 7.15 shows the 100% modulus value of the DNR and oil added samples. As the 100% modulus relates to the crosslink density,[28] a lower modulus value indicates a lower crosslink density as well as a high percentage of swelling. As expected, whenever the percentage swelling increases, the 100% modulus value decreases for Figure 7.15. Modified samples with extra curatives (not shown) did not show any improvement in 100% modulus in comparison with the corresponding unmodified samples. This again verifies that DNR has hardly any contribution to the

crosslinking reactions occurring during vulcanization. On the other hand, extra carbon black modified samples (not shown) showed higher modulus values. This finding helps confirm the role of reinforcing carbon black in the NR vulcanizates, especially in the DNR added materials.

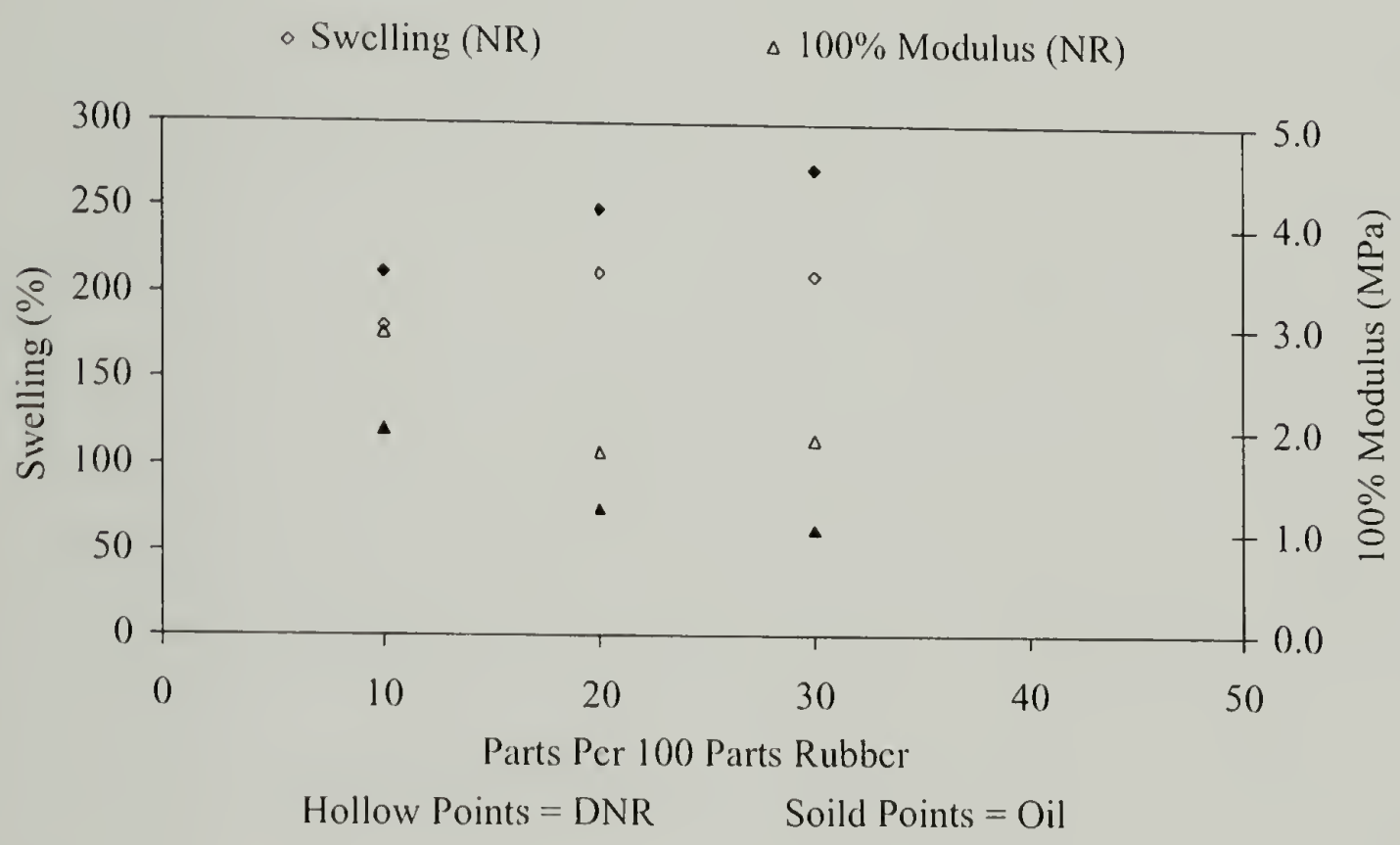

Figure 7.15. Swelling and 100% modulus results for NR compounded with DNR and Oil.

7.6 Styrene-Butadiene Rubber with Degraded Natural Rubber

7.6.1 Tensile Results

The before aging mechanical properties of DNR incorporated into virgin SBR (as per formulations shown in table 1 except SBR in place of NR) are shown in Figure 7.16, Figure 7.17 and Figure 7.18. Unlike the DNR in NR systems the SBR vulcanizates loaded with both DNR and oil have nearly same tensile strength at all respective loading

ratios, and decreases in strength with increasing loadings is evidenced. The individual elongation at break values increase as the amount of oil and DNR is increased separately in the SBR vulcanizates, however, the DNR values remain below those of the oil compounded samples. The 100% modulus decreases as the oil or DNR percentage is increased over the range of 10 to 30 phr loading in SBR.

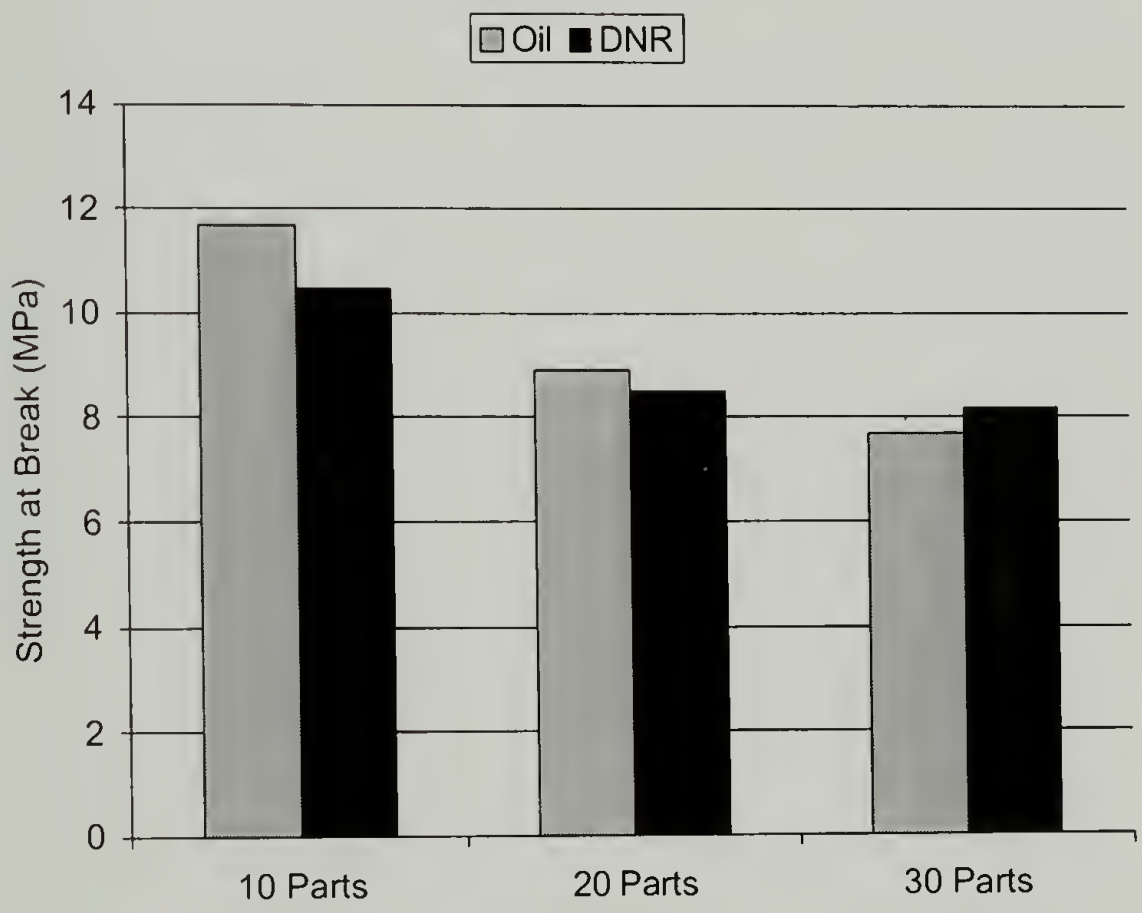

Figure 7.16. Strength at break (before aging) of styrene-butadiene rubber vulcanizates vs. the amount of degraded natural rubber/oil.

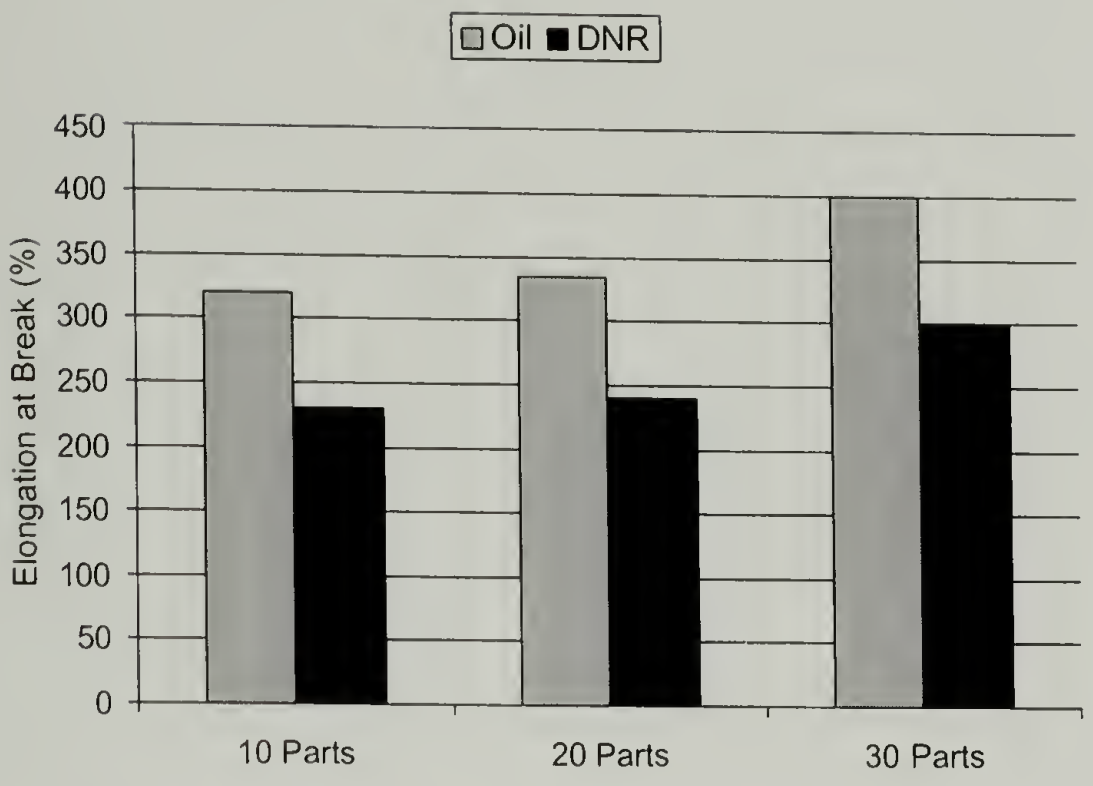

Figure 7.17. Elongation at break (before aging) of styrene-butadiene rubber vulcanizates vs. the amount of degraded natural rubber/oil.

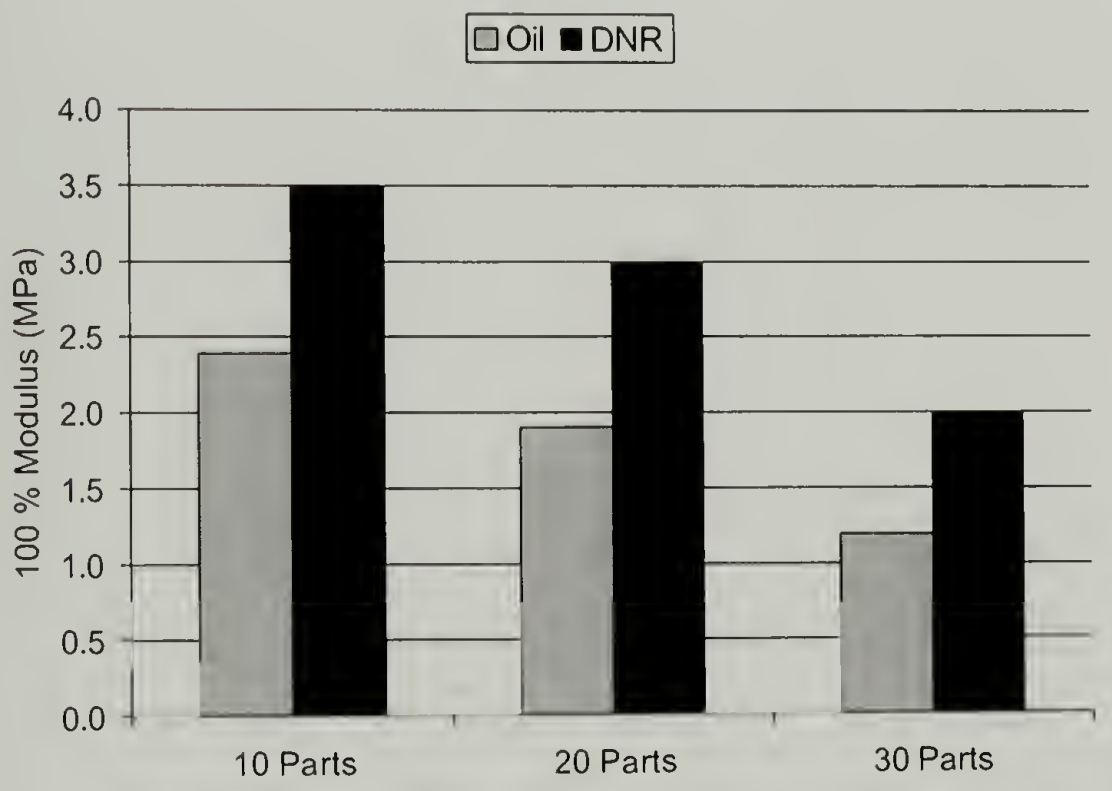

Figure 7.18. 100% Modulus (before aging) of styrene-butadiene rubber vulcanizates vs. the amount of degraded natural rubber/oil.

7.6.2 Extraction Experiments

Similar results to the DNR in NR have been obtained for DNR in SBR (Figure 7.19). Almost all incorporated oil has been extracted in the oil extended samples when compared with the degraded rubber loaded samples, which show much lower extraction levels. This means that DNR is again acting like a polymeric plasticizer in the SBR compounds. Furthermore, there is hardly any difference in the extractable levels for the DNR in SBR. The DNR in SBR vulcanizates provide less than 10% extractable level even at 30 parts loadings.

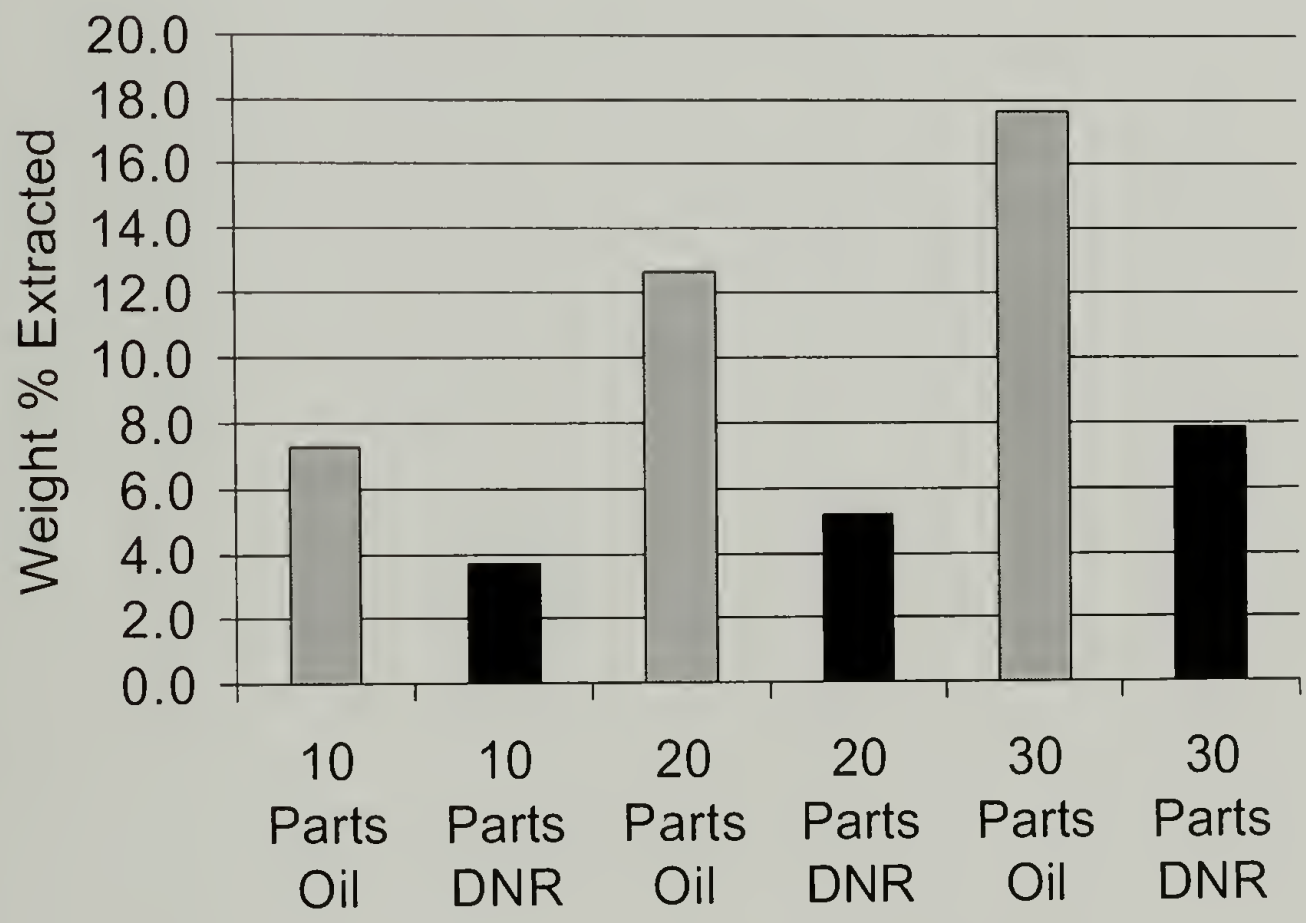

Figure 7.19. Extraction weight (%) in acetone vs. the amount of degraded natural rubber/oil in styrene-butadiene rubber vulcanizates.

7.6.3 Aging Experiments

Similar trends of better retention in tensile strength and elongation at break in the aged samples have been noticed in the DNR loaded in SBR vulcanizates (Figure 7.20, Figure 7.21 and Figure 7.22). Most importantly, the tensile strength, especially in the higher percentage of degraded rubber loading, remains persistently higher in value than those of corresponding oil extended SBR samples at higher loadings.

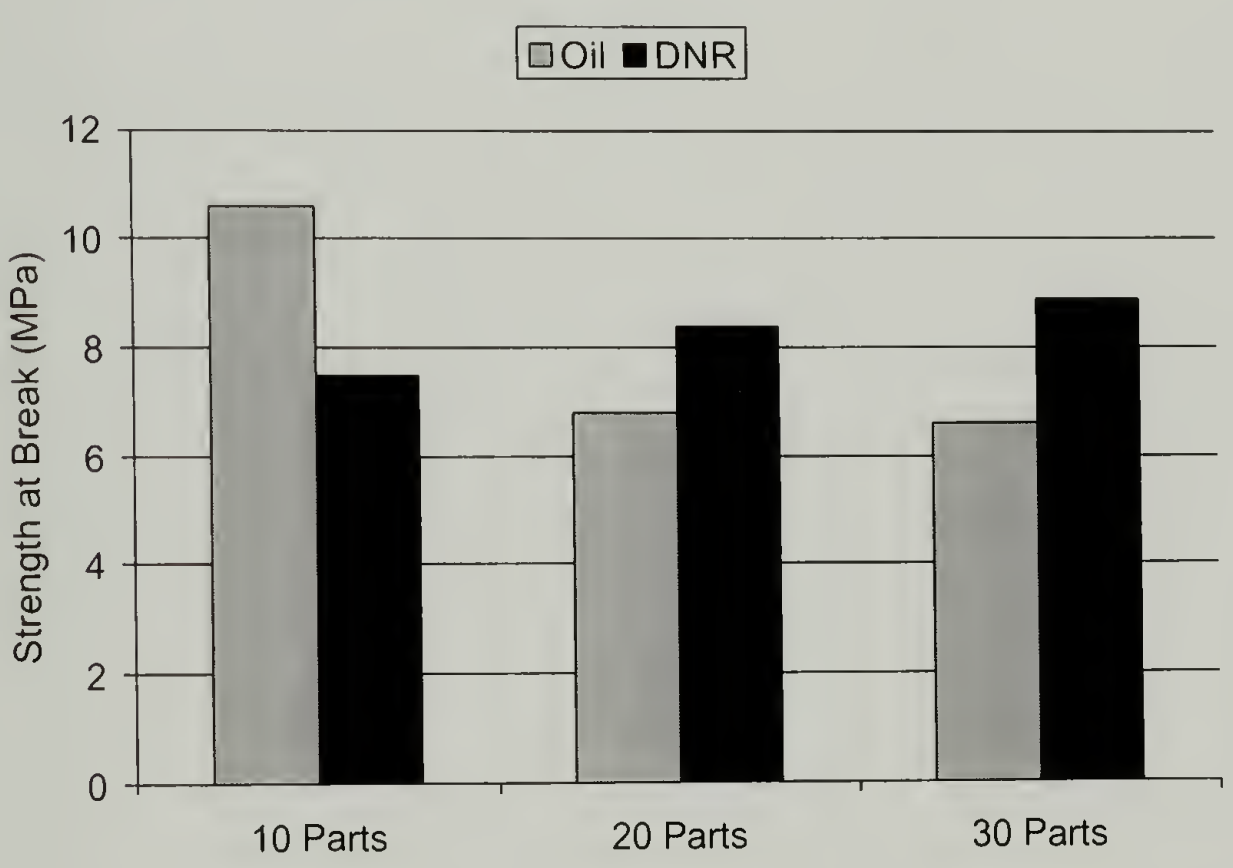

Figure 7.20. Strength at break (after aging) of styrene-butadiene rubber vulcanizates vs. the amount of degraded natural rubber/oil.

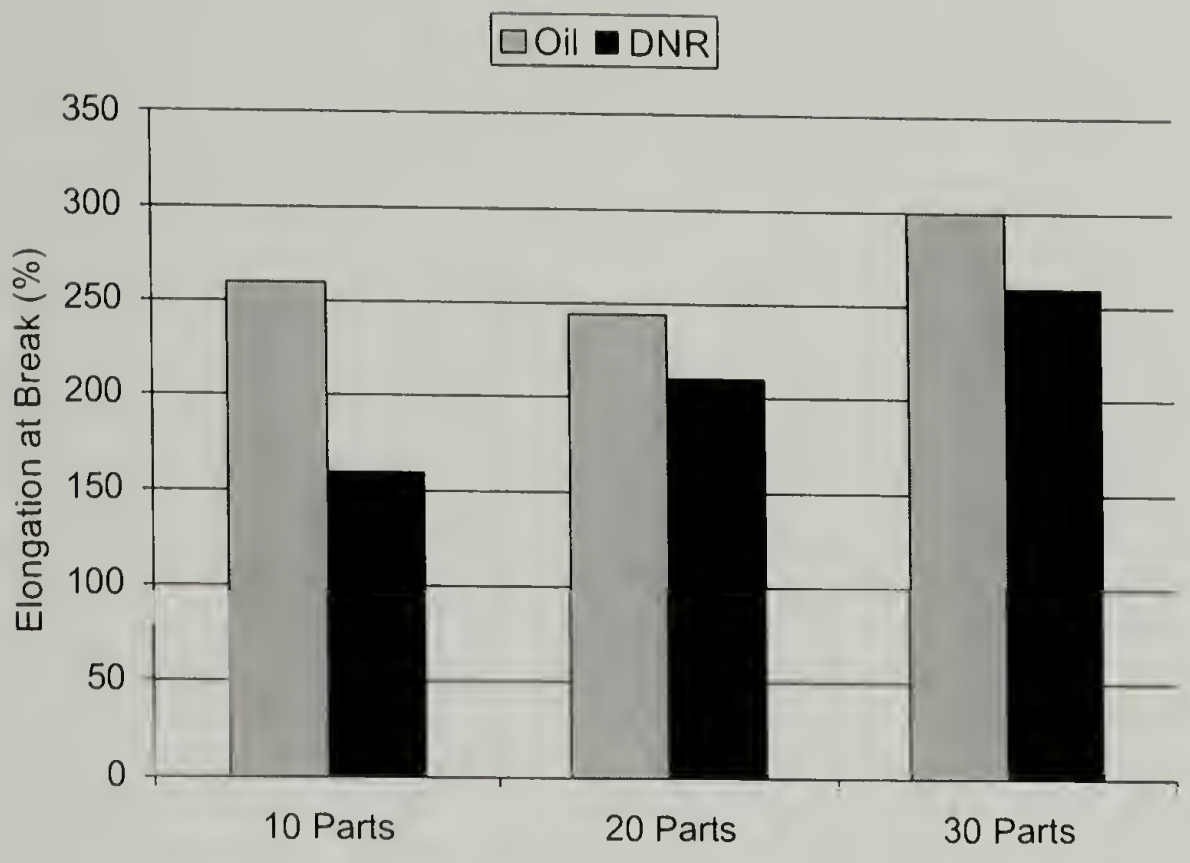

Figure 7.21. Elongation at break (after aging) of styrene-butadiene rubber vulcanizates vs. the amount of degraded natural rubber/oil.

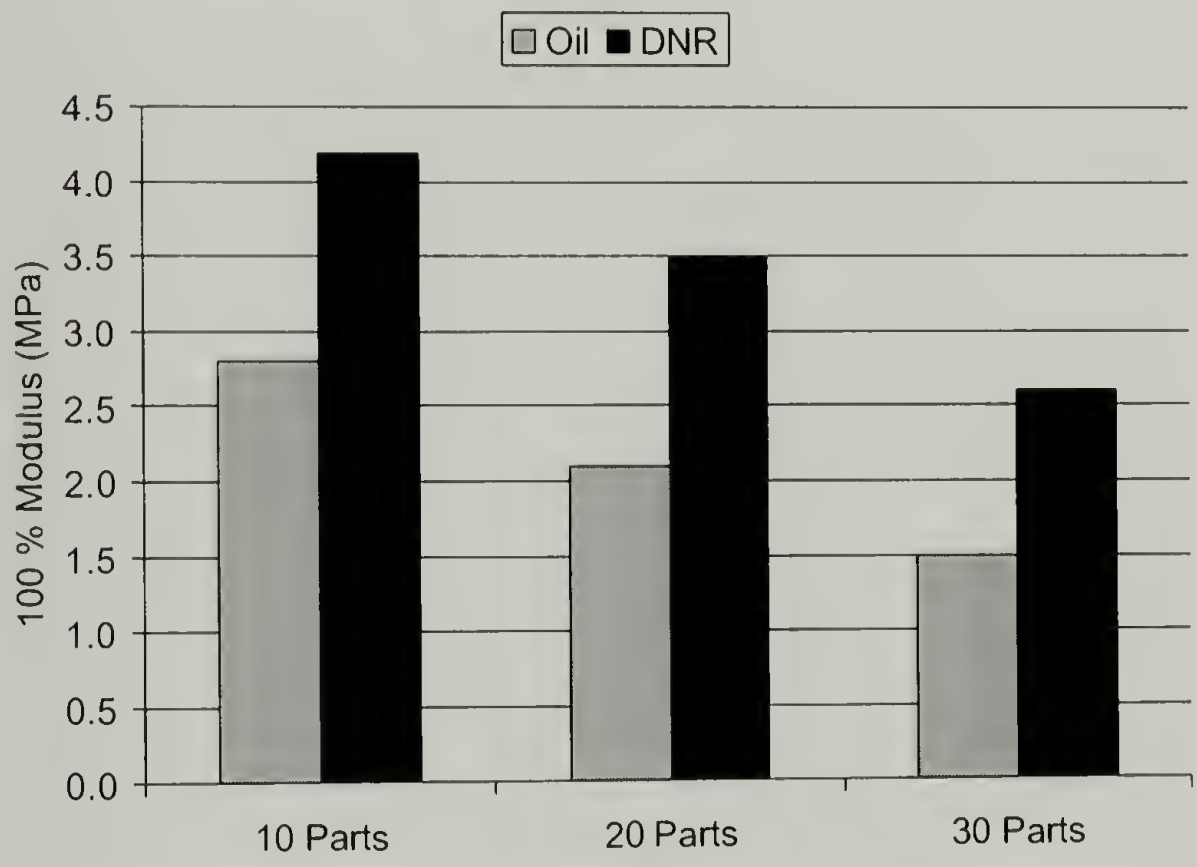

Figure 7.22. 100% Modulus (after aging) of styrene-butadiene rubber vulcanizates vs. the amount of degraded natural rubber/oil.

7.6.4 Swelling

Figure 7.23 exhibits the percentage swelling in toluene along with the 100% modulus versus the amount of DNR and oil loaded into the SBR samples. As expected, whenever the percentage of swelling becomes high, the 100% modulus remains low. The increase in the percentage of swelling and the decrease in the 100% modulus with increased amounts of DNR in the SBR vulcanizates remain small in comparison with the respective oil incorporated SBR samples. However, the percentage of swelling and 100% modulus of the oil added SBR samples remain significantly higher and lower, respectively, than those of DNR loaded SBR vulcanizates (figure 16).

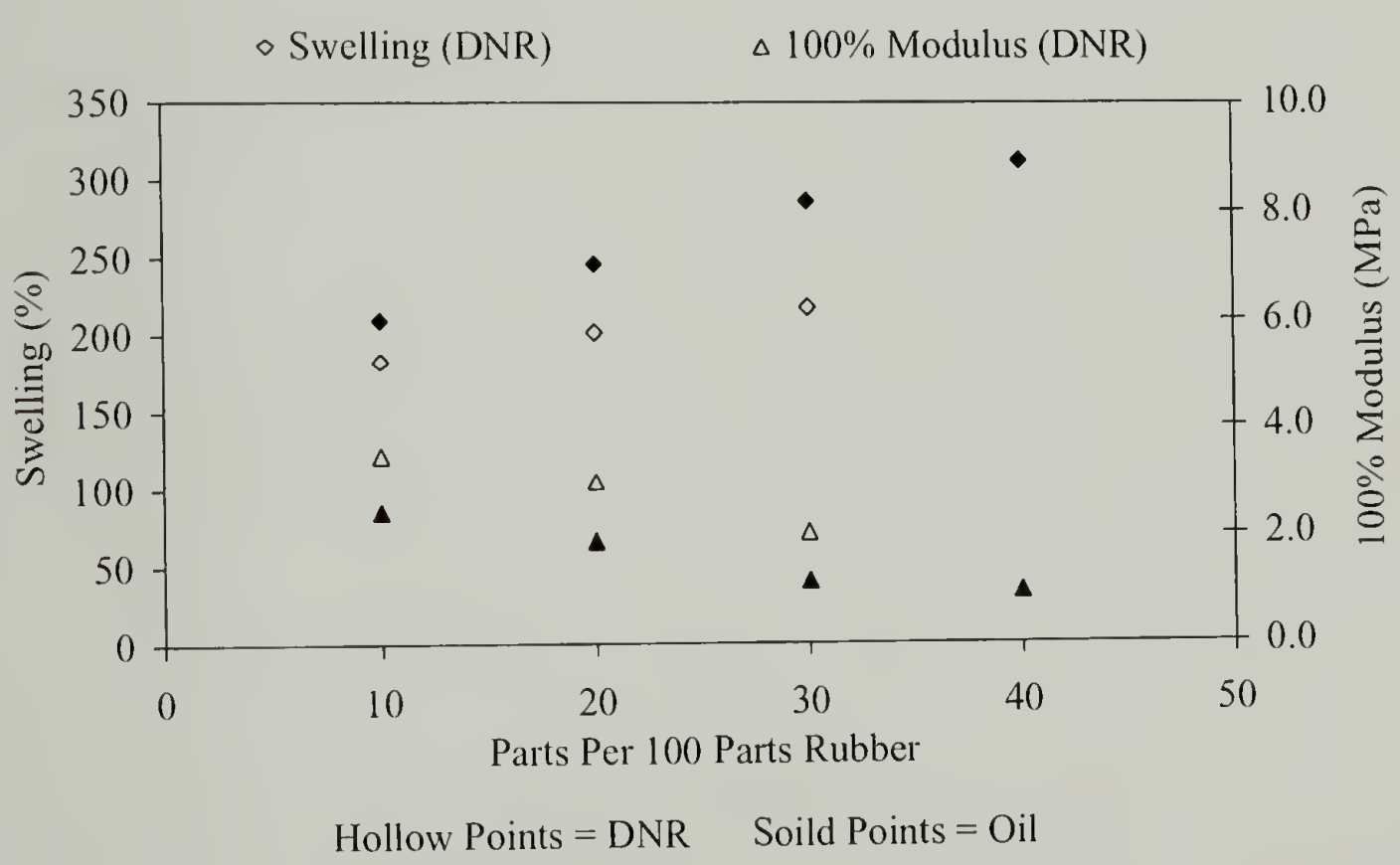

Figure 7.23. Swelling and 100% modulus results for SBR compounded with DNR and Oil.

7.7 Styrene-Butadiene Rubber with Degraded Styrene-Butadiene Rubber

7.7.1 Tensile Results

The before aging mechanical properties of DSBR incorporated into virgin SBR (as per formulations shown in table 1 except SBR in place of NR) are shown in Figure 7.24, Figure 7.25 and Figure 7.26. Unlike the DNR in NR systems the SBR vulcanizates loaded with both DSBR and oil have nearly same tensile strength at all respective loading ratios, and decrease in strength with increasing loadings is evidenced. The individual elongation at break values increase as the amount of oil and DSBR is increased separately in the SBR vulcanizates. The 100% modulus decreases as the oil or DSBR is increased over the range of 10 to 40 phr loading in SBR. However, the 100% modulus in DSBR added systems is superior to the oil extended samples in all ratios.

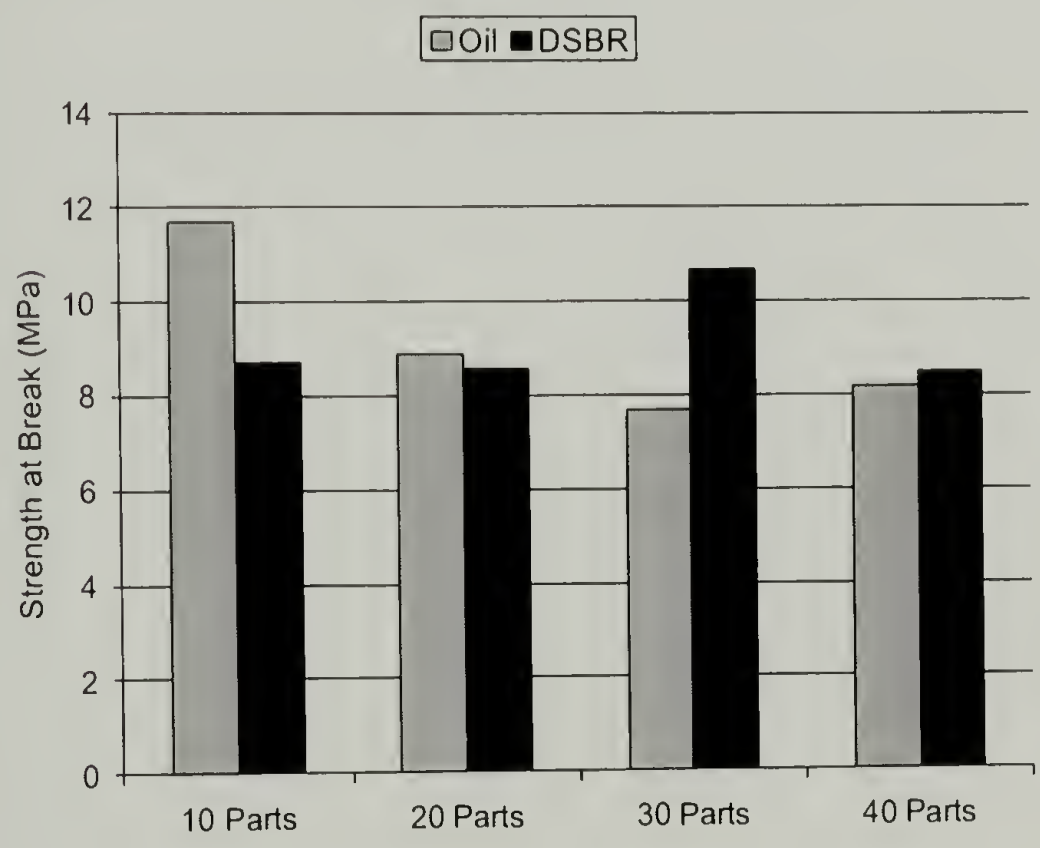

Figure 7.24. Strength at break (before aging) of styrene-butadiene rubber vulcanizates vs. the amount of degraded styrene butadiene rubber/oil.

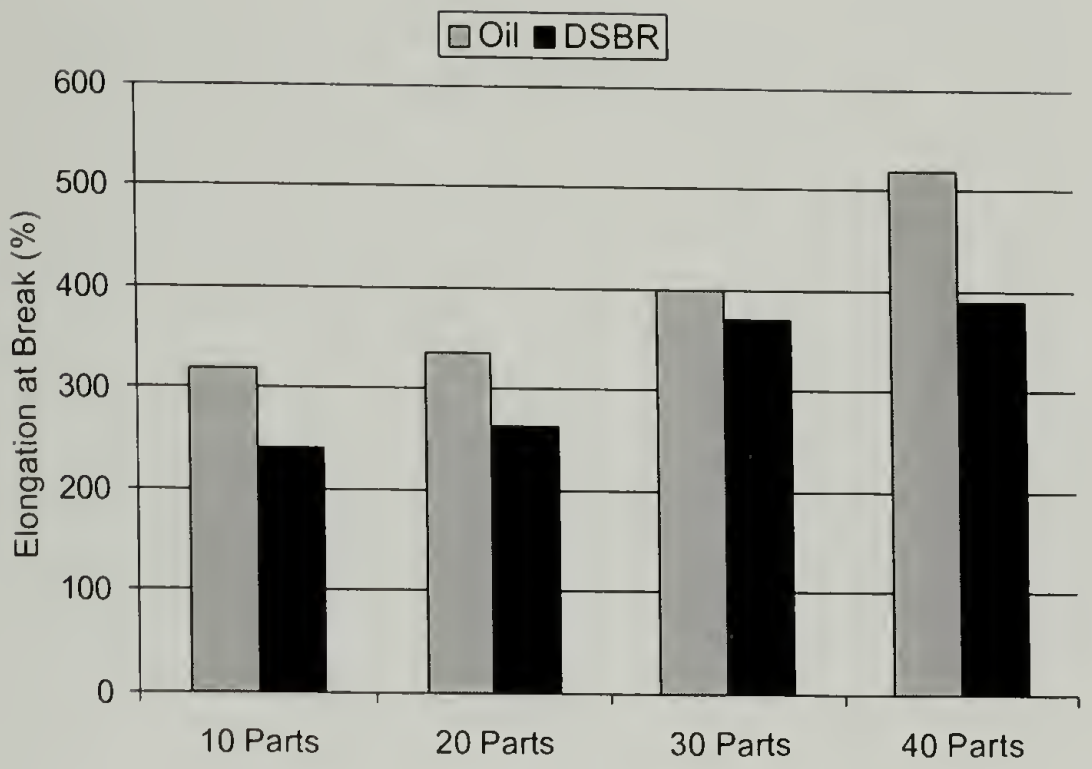

Figure 7.25. Elongation at break (before aging) of styrene-butadiene rubber vulcanizates vs. the amount of degraded styrene butadiene rubber/oil.

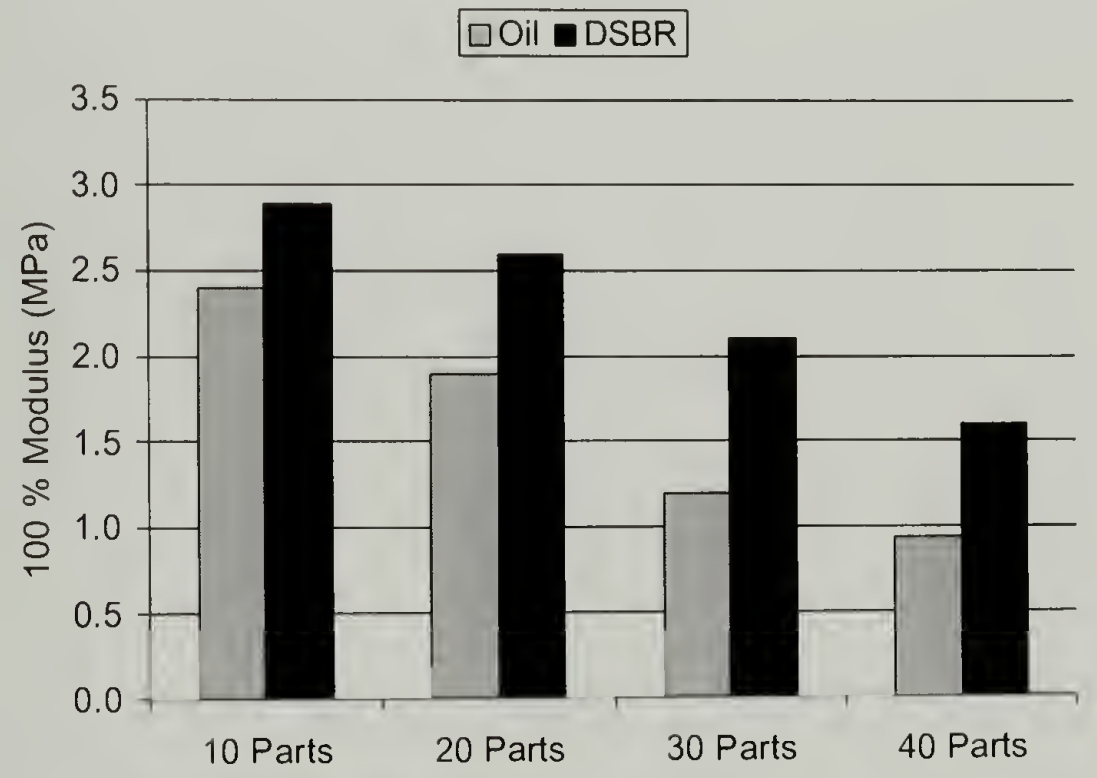

Figure 7.26. 100% Modulus (before aging) of styrene-butadiene rubber vulcanizates vs. the amount of degraded styrene butadiene rubber/oil.

7.7.2 Extraction Experiments

Similar results to the DNR in NR and DNR in SBR have been obtained for DSBR in SBR (Figure 7.27). Almost all incorporated oil has been extracted in the oil extended samples when compared with the degraded rubber loaded samples, which show much lower extraction levels. This means that DSBR is again acting like a polymeric plasticizer. The DSBR in SBR vulcanizates provide less than 10% extractable level even at 40 parts loadings compared to over 20% extractables for the oil loaded compound.

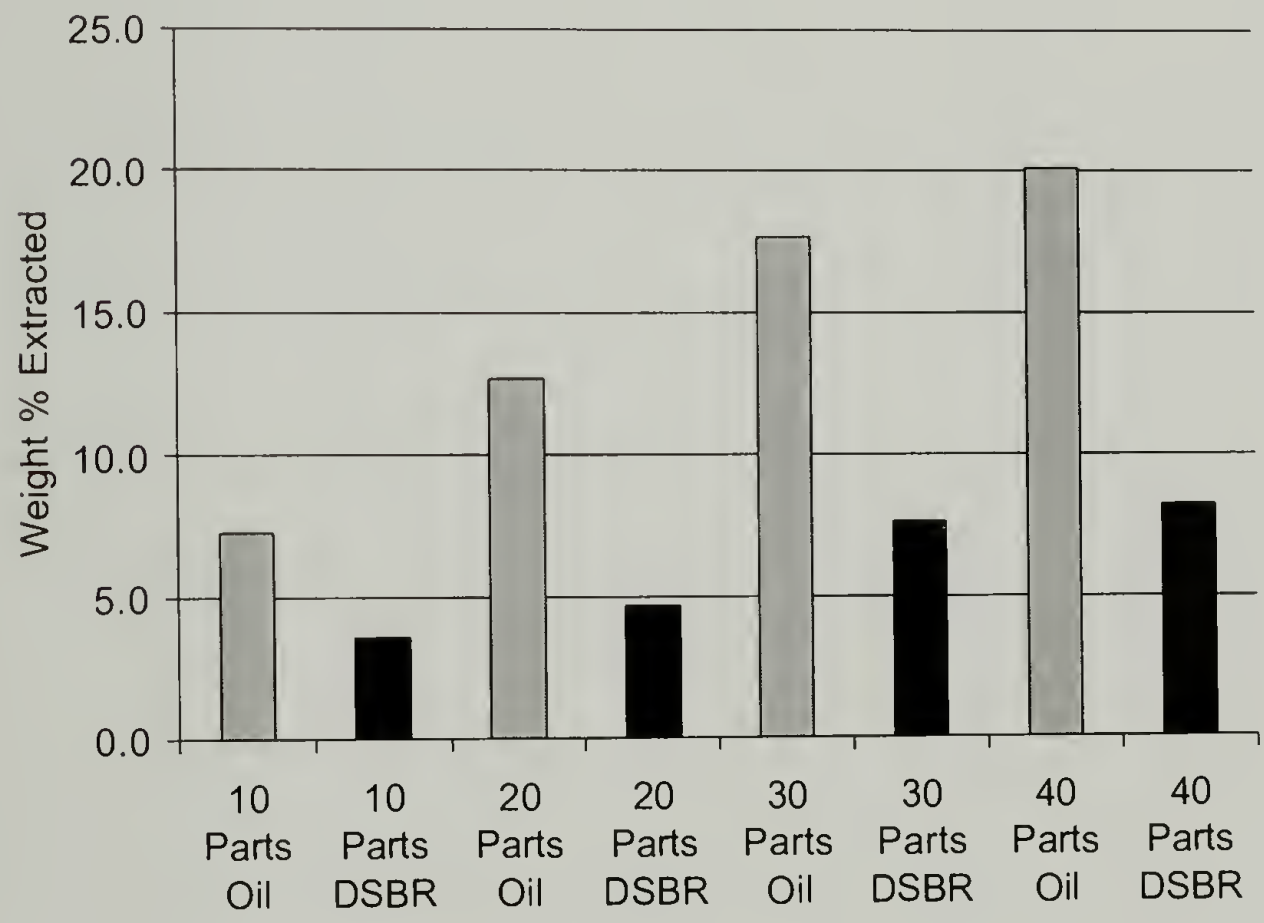

Figure 7.27. Extraction weight (%) in acetone vs. the amount of degraded styrene butadiene rubber /oil styrene-butadiene rubber vulcanizates.

7.7.3 Aging Experiments

Similar trends of better retention in tensile strength and elongation at break in the aged samples have been noticed in the DSBR loaded SBR vulcanizates (Figure 7.28, Figure 7.29 and Figure 7.30). Most importantly, the tensile strength, especially in the higher percentage of degraded rubber loading, remains persistently higher in value than those of corresponding oil extended SBR samples at higher loadings.

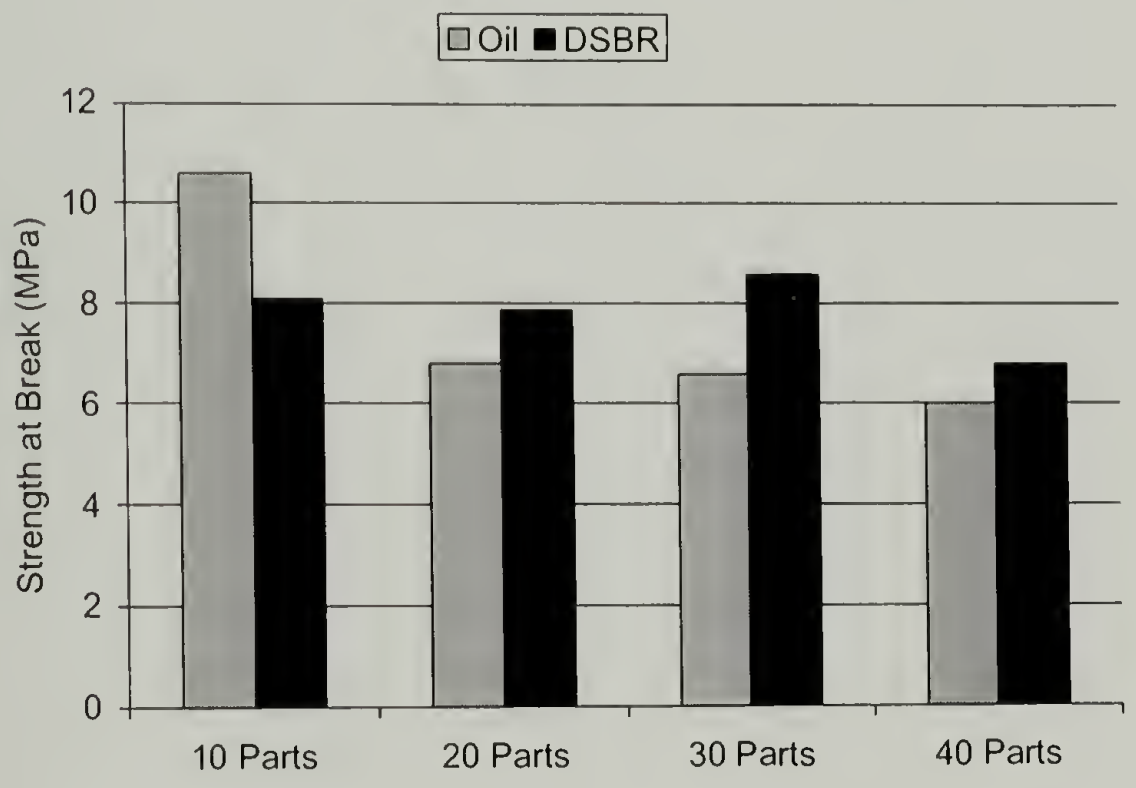

Figure 7.28. Strength at break (after aging) of styrene-butadiene rubber vulcanizates vs. the amount of degraded styrene butadiene rubber/oil.

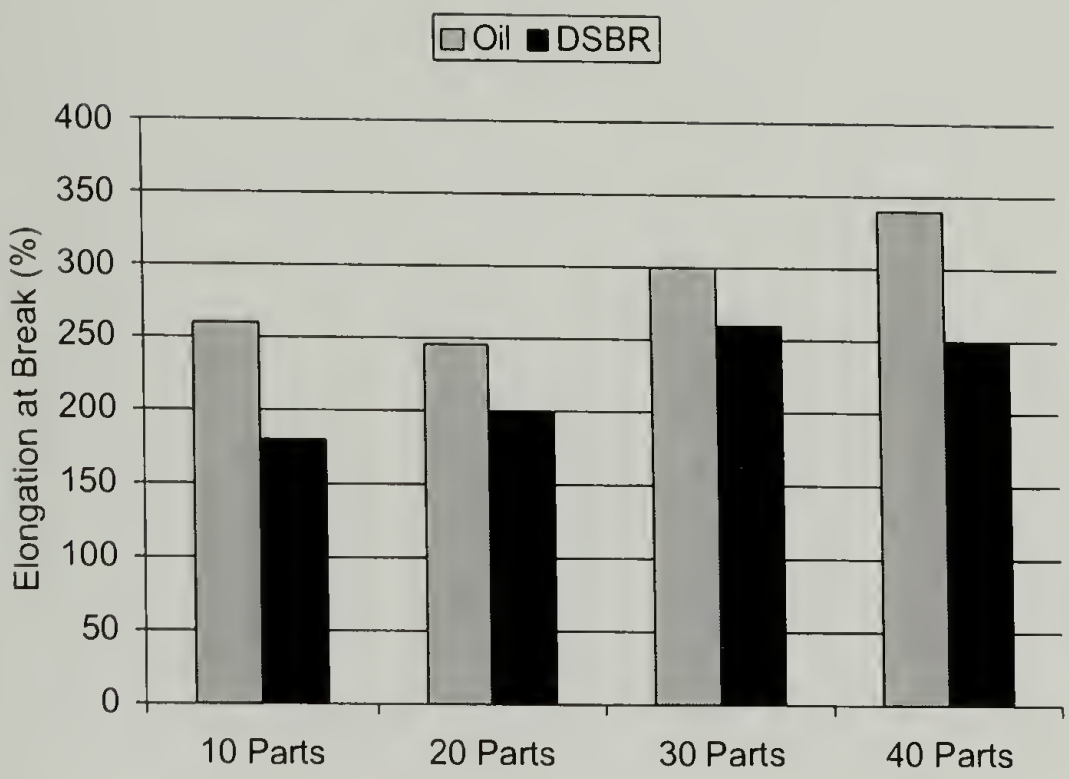

Figure 7.29. Elongation at break (after aging) of styrene-butadiene rubber vulcanizates vs. the amount of degraded styrene butadiene rubber/oil.

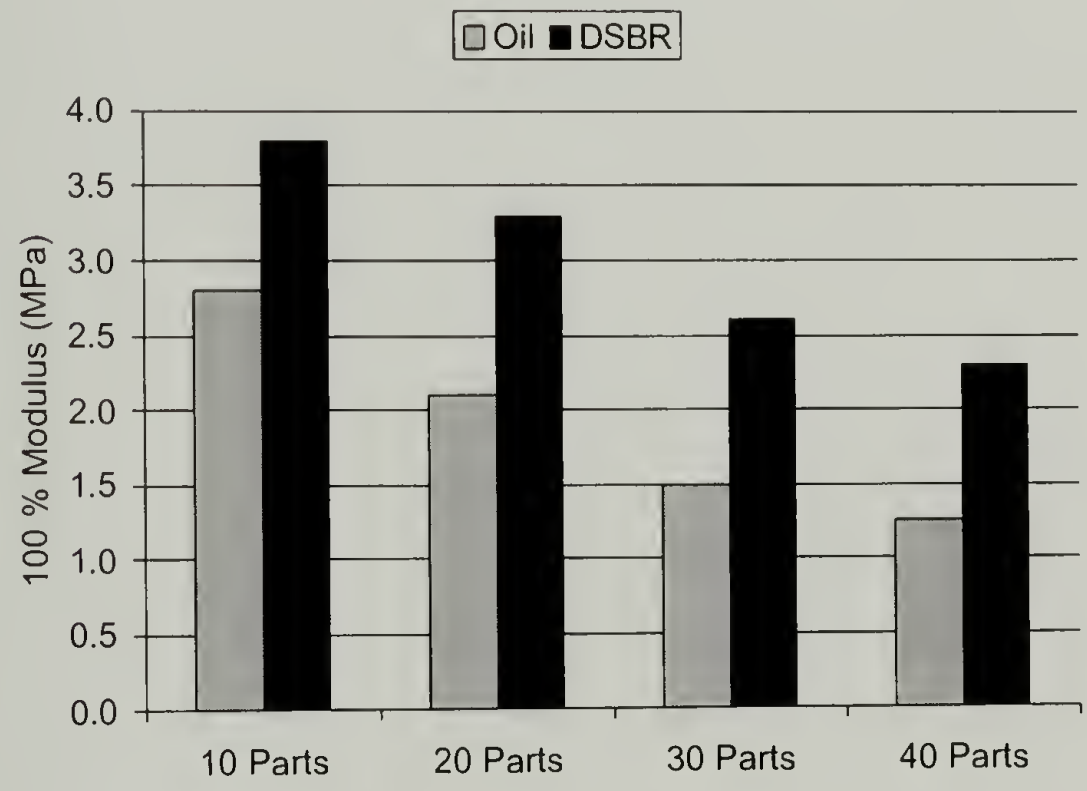

Figure 7.30. 100% Modulus (after aging) of styrene-butadiene rubber vulcanizates vs. the amount of degraded styrene butadiene rubber/oil.

7.7.4 Swelling

Figure 7.31 exhibits the percentage swelling in toluene along with the 100% modulus versus the amount of DSBR and oil loaded into the SBR samples. As expected, whenever the percentage of swelling becomes high, the 100% modulus remains low. The increase in the percentage of swelling and the decrease in the 100% modulus with increased amounts DSBR in the SBR vulcanizates remain small in comparison with the respective oil incorporated SBR samples. However, the percentage of swelling and 100% modulus of the oil added SBR samples remain significantly higher and lower, respectively, than those of the DSBR loaded SBR vulcanizates.

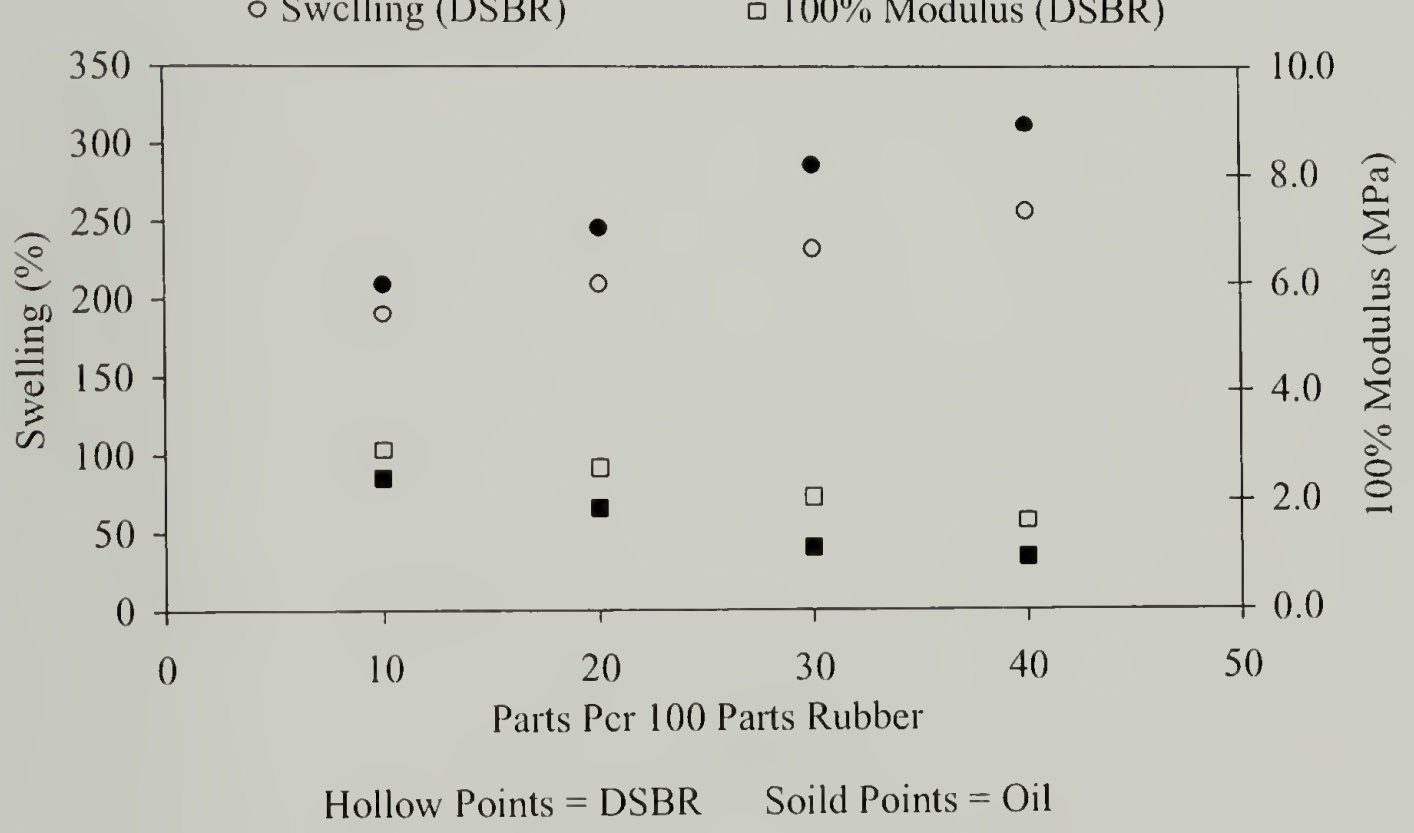

Figure 7.31. Swelling and 100% modulus results for SBR compounded with DSBR and Oil.

7.8 Economics

As a consequence of the range and variety of recycling techniques, each has its own pros and cons. Use of regrind does not require any change in the process condition, but its maximum loading has been restricted to approximately 10% of the rubber weight in order to maintain mechanical properties. It is noted that having a smaller particle size for the powder allows one to invoke higher loadings and maintain better retention of properties at the higher loadings. However, decreasing particle size of the recycled rubber powder is not cost effective as the smaller particle sizes are more expensive to obtain.

On the other hand, HPHTS integrates 100% scrap rubber without incorporating any virgin rubber or binder with at least 60% recovery of the original mechanical properties irrespective of rubber types. However, applying high pressure and high temperature in HPHTS requires modification in the processing conditions of current processing techniques, especially when concerning powder handling and molding.

Degradation/devulcanization, on the contrary, does not need any powder source or grinding. Rubber scrap can be degraded into a paste just through high temperature in a reactor or extruder. The paste is compatible with the rubber compounds and has the capability to plasticize the rubber compounds during mixing. Even with a 40-50% loading of the degraded rubber in virgin rubber compounds one is able to maintain almost all of the original properties of the rubber compound. Rubber vulcanizates, compounded with degraded rubber swell less in organic solvents and have less extractables in acetone in comparison to the rubber compounded with a corresponding amount of regrind or oil.

7.9 Degraded Rubber Summary and Future Work

Degraded natural rubber has been shown to be an excellent replacement for oil in natural rubber compounds. Natural rubber compounded with degraded natural rubber maintains excellent mechanical properties even up to 40 phr loading. As degraded rubber remains in a polymeric form, the retention of the after aging mechanical properties is superior to the respective oil added samples. Replacing oil by a polymeric plasticizer like degraded rubber in rubber compounds greatly reduces the amount of extractables (as confirmed by acetone extraction). Solvent swelling in toluene indicates that degraded rubber incorporated samples have more crosslink density than those of corresponding oil incorporated samples irrespective of rubber kinds. It seems that degraded rubber remains grafted or entangled in the rubber matrix and this helps to enhance the mechanical properties, especially after aging. Finally, adding degraded rubber to virgin rubber as a replacement for oil is not only an economic alternative, but an environmentally friendly one as well as much higher loadings of recycled materials in virgin compounds has been achieved.

Future work should aim at further increasing the loading of degraded rubber in virgin rubber. A comprehensive study of the impact of degraded material on the rubber compounding and molding should also be conducted. Continuing work in this area is highly recommended as initial results have been very positive. Other studies might include other difficult to process materials such as polytetrafluoroethylene (PTFE), as degraded PTFE may serve as an excellent plasticizer for PTFE.

BIBLIOGRAPHY

[1] Goodyear, C., U.S. Patent 240, 1837.

[2] Bradford, K. and Pierce, D.D., *Trials of an Inventor, Life and Discoveries of Charles Goodyear*, Phillips Hunt Publishers, New York, 1866.

[3] Hayward, N., U.S. Patent 1,090, 1839.

[4] Goodyear, C., U.S. Patent 3,633, 1844.

[5] Hancock, T., *Personal Narrative of the Origin and Progress of the Caoutchouc or India-Rubber Manufacture in England,* Longman, London, 1857.

[6] http://www.plastiquarian.com/hancock.htm

[7] http://www.rma.org/scraptires/facts_figures.html

[8] http://www.polyurethane.org

[9] Goodyear, C., British Patent 2,933, 1853.

[10] Morey, C., U.S. Patent 12,212, 1855.

[11] Accetta, A., Vergnaud, J.M., *Rubber Chem. Tech.*, **54**, 302, 1981.

[12] Accetta, A., Vergnaud, J.M., *Rubber Chem. Tech.*, **55,** 961, 1982.

[13] Phadke, A.A. and De, S.K., *Kautschuk + Gummi Kunststoffe*, **37** (9), 776, 1984.

[14] Phadke, A.A., Chakraborty, S.K. and De, S.K., *Rubber Chem. Tech.*, **57**, 19, 1984.

[15] Law, W.K., Patel, T., Swisher, K. and Shutov, F., *Polymer Recycling* **3,** 269, 1998.

[16] James, O., *Proceedings of the Annual Technical Conference (ANTEC) 1997*, paper no. 275, 3076, 1997.

[17] Corbett, G.E. and Wadie, B.J., *Journal of Cellular Plastics*, **10**(1), 26, 1974.

[18] Arastoopour, H., et al., U.S. Patent 5,904,885, 1999.

[19] Adhikari, B., De, D. and Maiti, S., *Prog. Polym. Sci.* **25**, 909, 2000.

[20] Beckman, J.A., Crane, G., Kay, E.L. and Laman, J.R., *Rubber Chem. Tech.*, **47**, 597, 1974.

[21] Paul, J, Rubber reclaiming, in *Encyclopedia of Polymer Science and Engineering*, **14**, 787, 1988.

[22] Morin, J.E., Williams, D.E. and Farris, R.J., , *Rubb. Chem. Tech.*, 75, 955, 2002.

[23] Morin, J.E., Thermoset recycling via high-pressure high-temperature sintering: revisiting the effect of interchange chemistry, Ph.D. thesis, University of Massachusetts Amherst, Amherst, MA, 2002.

[24] Farris, R.J., Williams, D.E. and Tripathy, A.R., "Recycling Crosslinked Networks via High-Pressure High-Temperature Sintering (HPHTS)" CRC Press, Boca Raton, FL, to be published in 2004.

[25] Kraus, G., Reinforcement of elastomers by particulate fillers, in *Science and Technology of Rubber*, Eirich, F.R., Academic Press, New York, 1978, Chap. 8.

[26] Law, W.K. et al., *Polymer Recycling*, 3, 269, 1998.

[27] Anderson, L., A predictive model for the mechanical behavior of particulate composites, Ph.D. thesis, University of Massachusetts Amherst, Amherst, MA, 1989.

[28] Ahagon, A., Extensibility of black-filled elastomers, *Rubb. Chem. Tech.*, 59, 187, 1986.

[29] Bellander, M., Stenberg, B. and Persson, S., Crosslinking of polybutadiene without any vulcanizing agent, *Polym. Eng. and Sci.*, 38, 1254, 1998.

[30] Gent, A.N., Strength of elastomers, in *Science and Technology of Rubber*, Eirich, F.R, Academic Press, New York, 1978, Chap. 10.

[31] Tobolsky, A.V., *Properties and Structures of Polymers,* John Wiley and Son, New York, 1960.

[32] Ahagon, A., *Rubber Chem. Tech.*, **59**, 187, 1986.

[33] Decker, G.E., Wise, R.W. and Guerry, D., *Rubber Chem. Tech.*, **36**, 451, 1963.

[34] Eller, S.A., *Rubber Chem. Tech.*, **29**, 263, 1956.

[35] Armah, J.C., et al., *Rubber Chem. Tech.*, **59**, 765 1986.

[36] Stern, M.D. and Tobolsky, A.V., *J. Chem. Phys.*, **14**, 93, 1946.

[37] Offenbach, J.A. and Tobolsky, A.V., *J. Colloid Sci.*, **11**, 39, 1956.

[38] Nieuwenhuizen, P. J., et al., *Rubber Chem. Tech.*, **72**, 27, 1999.

[39] Nieuwenhuizen, P. J., et al., *Rubber Chem. Tech.*, **72**, 43, 1999.

[40] Nieuwenhuizen, P.J., Haasnoot, J.G. and Reeduk, J., *Rubber Chem. Tech.*, **72**, 15, 1999.

[41] Datta, R.N., et al., *Rubber Chem. Tech.*, **70**, 129, 1997.

[42] Datta, R.N. and Wagenmakers, J.C., *J. Polym. Mat.*, **15**, 379, 1998.

[43] Datta, R. N., *Rubber Chem. Tech.*, **72**, 15, 1999.

[44] Tripathy, A.R., Morin, J.E., Williams, D.E., Eyles, S.J. and Farris, R.J., *Macromolecules*, **35**, 4616, 2002.

[45] Abouzahr, S., Mohajer, Y., Wilkes, G.L. and McGrath, J.E., *Polymer*, **23**, 1519, 1982.

[46] Novotny, D.S., et al., US Patent 4,104,205, 1978.

[47] Hunt, J.R., et al., US Patent 5,578,700, 1996.

[48] Isayev, A.I., US Patent 5,258,413, 1993.

[49] Isayev, A.I., US Patent 5,284,625, 1994.

[50] Roberson, P.R., US Patent 6,095,440, 2000.

[51] Nicholas, P.P., US Patent 4,161,464, 1979.

[52] Myers, R.D., et al, US Patent 5,798,394, 1998.

[53] Hunt, J.R., et al, US Patent 5,891,926, 1999.

[54] Benko, D.A., et al, US Patent 6,380,269, 2002.

[55] Mouri, M., et al, US Patent 6,133,413, 2000.

[56] Goldshtein, V., et al, US Patent 6,387,966, 2002.

[57] Fix, S.R., *Elastomerics*, **112**, 38, 1980.

[58] Isayev, A.I., Hong, C.K., *J. Appl. Polym. Sci.*, **79**, 2340, 2001.

[59] Nicholas, P.P., *Rubber Chem. Tech.*, **55**, 1499, 1982.

[60] Milani, M., *Polym. React. Eng.*, **9**, 19, 2001.

[61] Crane, G. and Kay, E.L., *Rubber Chem. Tech.*, **48**, 50, 1975.

[62] Henry, A.W., *Rubber Chem. Tech.*, **56**, 83, 1983.

[63] Padella, F., *Polym. Recycling*, **6** (1), 11, 2001.

[64] Magini, M., *Proceedings of the International Symposium on Metastabel, Mechanically Alloyed and Noncrystalline Materials* (ISMANAM), Ann Arbor, MI, 263, June 24-29 2001.

[65] Warner, W.C., *Rubber Chem. Tech.*, **67**, 559, 1994.

[66] Krekic et al., *Rubber Chem. Tech.*, 49, pp. 375-378 (1976)

[67] Hilyard, N., Tong, S., and Harrison, K., *Plast. Rubber Process. Appl.*, 3, 315, 1983.

[68] Strak, F., *Rubber India*, 43 (11), 17, 1991.

[69] Grebenkina, Z., Zakharov, N., and Volkova, E., *Int. Polym. Sci. Tech.*, 5, T/2, 1978.

[70] Fesus, E. and Eggleton, R., *Rubber World*, 203 (6), 23, 1991.

[71] Gibala, D. and Hamed, G.R., *Rubber Chem. Tech.*, 67, 636, 1994.

[72] Burford, R. and Pittolo, M., *Rubber Chem. Tech.*, 55, 1233, 1982.

[73] Larsen, J.W. and Chang, B., *Rubber Chem. Tech.*, 49, 1120, 1976.

[74] Swor, R., Jensen, L., and Budzol, M., *Rubber Chem. Tech.*, 53, 1215, 1980.

[75] Moore, C.G. and Trego, B.R., *J. Appl. Polym. Sci.*, 8, 1957, 1964.

[76] Butenuth, G., *Rubber Chem. Tech.*, 37, 326, 1964.

[77] Zapp, R.L., *Rubber Chem. Tech.*, 46, 25, 1973.

[78] Krause, G., *J. Appl. Polym. Sci.*, 7, 861, 1963.

[79] Mullins, L. and Tobin, N., *J. Appl. Polym. Sci.*, 9, 2993, 1965.

[80] Boonstra B.B. and Taylor, G.L., *Rubber Chem. Tech.*, 38, 943, 1965.